ARL TECHNICAL REPORT 60-305

VISCOELASTIC BEHAVIOR OF SURFACES OF REVOLTION UNDER COMBINED MECHANICAL AND THERMAL LOADS

L. ALBERT SCIPIO II
SZE-FOO CHIEN
JAMES A. MOSES
MANSA SINGH

UNIVERSITY OF MINNESOTA
MINNEAPOLIS, MINNESOTA

MAY 1961

CONTRACT AF 33(616)-5723

AERONAUTICAL RESEARCH LABORATORY
OFFICE OF AEROSPACE RESEARCH
UNITED STATES AIR FORCE

ARL TECHNICAL REPORT 60-305

VISCOELASTIC BEHAVIOR OF SURFACES OF REVOLUTION UNDER COMBINED MECHANICAL AND THERMAL LOADS

L. ALBERT SCIPIO II
SZE-FOO CHIEN
JAMES A. MOSES
MANSA SINGH

UNIVERSITY OF MINNESOTA
MINNEAPOLIS, MINNESOTA

MAY 1961

CONTRACT No. AF 33(616)-5723
PROJECT 7063
TASK 70524

AERONAUTICAL RESEARCH LABORATORY
OFFICE OF AEROSPACE RESEARCH
UNITED STATES AIR FORCE
WRIGHT-PATTERSON AIR FORCE BASE, OHIO

McGregor & Werner, Inc., Dayton, O.
200 - October 1961 - 6-148 & 149

FOREWORD

This report was prepared by the University of Minnesota, Minneapolis, Minnesota, under Air Force Contract No. AF 33(616)-5723. The research program was initiated by the Aeronautical Research Laboratory, Directorate of Laboratories, Air Force Research Division, Wright-Patterson Air Force Base, Ohio, under Project 7063, "Mechanics of Flight", and Task 70524, "Structures Research at Elevated Temperatures". Dr. Robert Mayerjak represented ARL as task scientist.

The work was done under direction Dr. L. Albert Scipio and experimental study was supervised by Mr. James A. Moses.

The authors wish to acknowledge the assistance of Messrs. Thomas W. Hughes, William J. Astleford, Robert F. Nepper, Robin E. Schaller, Sze-Ting Chien, and Kesava Rao Yalamanchili for their work in conducting the tests and performing the numerical calculations. Mr. Edward Zembergs and Miss Beverly Broers for preparing the manuscript. The comments of Dr. Toma Riabokin in connection with certain aspects of the theoretical analysis are acknowledged.

ABSTRACT

This paper presents the results of an analytical and experimental study of thin conical and hemispherical shells subjected to combined mechanical and thermal loads.

The analytical solutions are applicable for shells constructed from a linear viscoelastic material with temperature dependent properties.

Experimental models were subjected to various constant radiant heating rates to various steady-state temperatures. In some cases a constant normal pressure was combined with the thermal load.

Theoretical values for the meridional and circumferential stress distributions based on a viscoelastic analysis (both temperature independent and temperature dependent material properties) and the elastic analysis are compared with experimental results for typical time intervals during the transient and steady-state periods.

TABLE OF CONTENTS

TABLE OF CONTENTS (Cont'd)

LIST OF ILLUSTRATIONS

LIST OF ILLUSTRATIONS (Cont'd)

LIST OF ILLUSTRATIONS (Cont'd)

LIST OF TABLES

LIST OF TABLES (cont'd)

LIST OF SYMBOLS

α Thermal expansion coefficient

β Rate of variation of the shear modulus of elasticity with respect to temperature evaluated between a datum temperature and a prescribed temperature

γ Angle between axis of the conical shell and an element of the cone, i.e., half-angle

δ Thickness of the shell

δ_{ij} Kronecker delta

θ Angle measured about axis of shell in a plane normal to axis

ϕ Angle between axis of the shell and a normal to a meridian

η Viscosity

η_o Viscosity at a datum temperature

ϵ_{ij} Components of strain tensor

$\epsilon_{\phi M}$ Strain component in ϕ direction at the shell middle-surface

$\epsilon_{\theta M}$ Strain component in θ direction at the shell middle-surface

σ_{ij} Components of stress tensor

ξ Distance from the shell middle-surface, positive inward; displacement

ρ_1 Radius of meridian curvature

ρ_2 Distance from the shell to axis of rotation

κ Temperature - viscosity coefficient, evaluated between a datum temperature and a prescribed temperature

ν Poisson's ratio

ν_i Poisson's ratio at the initial time

ψ Change of curvature

ℓ Distance along cone element, measured from vertex

ℓ_o Slant height of cone

p Pressure, positive inward

r Radius of parallel circle

t Time

v Component of displacement along the meridian, positive in the direction of increasing ϕ

w Component of displacement perpendicular to the surface, positive inward

E Modulus of elasticity

E_i Modulus of elasticity at initial time

E_{ij} Strain deviator

F_i Components of body force

G Modulus of elasticity in shear

G_o Modulus of elasticity in shear at a datum temperature

M_ϕ Bending moment in meridian plane per unit length of parallel circle

M_θ Bending moment in plane perpendicular to meridian plane per unit length of meridional section

N_θ Membrane force per unit length of shell section

N_ϕ Membrane force tangent to a parallel circle per unit length of the meridian

Q_ϕ Shearing force per unit in plane perpendicular to meridian plane

Q_θ Shearing force per unit length tangent to a parallel circle

T Amount of temperature above that of datum temperature

T_M Amount of temperature at shell middle surface above that of datum temperature

T_o Amount of temperature at shell outer surface above that of datum temperature

T_t Amount of temperature at the tip of the shell outer surface above that of datum temperature

T_i Temperature of the shell inner surface

S_{ij} Stress deviator

I. INTRODUCTION

In recent years there has been considerable interest in the class of aircraft problems commonly known as aerodynamic heating. The effects of aerodynamic heating on the structure are: (1) thermal stresses induced in the structure, (2) creep and/or relaxation effects, and (3) development of inhomogenity since the material properties vary with the temperature distribution.

At elevated temperatures, the thermal stress problem (Condition 1) is but the first of several related problems. The phenomenon of creep (Condition 2) becomes of importance if the temperatures are high enough, even if the exposure times are short. In addition, creep buckling can take place since the stresses are compressive as well as tensile.

The deformational response[10 *] of structural metals at elevated temperatures is a combination of elastic, viscous, and plastic components. The three mechanical constants associated with these components of deformation: the elastic modulus, the coefficient of viscosity, and the yield stress; and the thermal constants which govern the level of the thermal stresses: the coefficients of linear expansion and of thermal conductivity, are temperature dependent (Condition 3).

Classical thermoelasticity[24] does not take Conditions 2 and 3 into account and therefore gives only crude approximations at elevated temperatures when these effects are known to be pronounced. A viscoelastic material[1] will satisfy Condition 2, and if in addition its material properties are taken as temperature dependent, then true aerodynamic heating effects are approached. A viscoelastic response, that is, one which exhibits relaxation and heredity effects, can be assumed to represent approximately the behavior of metals either at relatively low stresses or at very high temperatures. If this viscoelastic response is produced by temperatures, the term <u>thermoviscoelasticity</u> has been used. It includes the general theory of heat conduction, thermal stresses, and deformations produced by thermal flow in the viscoelastic media and the reverse effect of temperature distribution produced by the elastic and viscous deformation.

The first concern, therefore, is with the heat conduction in the structure itself. The usual procedure of thermoelastic analysis is to determine the stresses on the assumption that the thermal and the elastic fields are uncoupled and that the temperature field is given. Although the assumption of uncoupled thermal and elastic fields has practical truth in structural problems, the two fields are coupled by the

---

Manuscript was released by the authors on Nov. 1960, for publication as a ARF Technical Report.

* Numbers refer to entries in the bibliography. The bibliography includes references for background information in addition to those references noted in the text.

second law of thermodynamics. The heat conduction equation will contain elastic terms and the equations of elasticity will contain temperature gradients. The conventional formulation in thermoelasticity simply assumes that the thermal field does not contain the small elastic terms but that the temperature gradients are included in the equations of elasticity.

The equations of the classical theory of elasticity may be immediately extended to viscoelasticity by simply replacing the elastic moduli by their corresponding operators[3]. As in the case of thermoelasticity, the reciprocal coupling between the temperature and deformations is neglected. Classical thermodynamics shows that one effect cannot occur without the other but in the theory of structures, its order of magnitude is not significant.

The objective of the program reported herein which has been conducted at the University of Minnesota under Contract No. AF 33(616)-5723, Task 70524, Project 7063, can be stated in general terms as "Development of Analytical Methods to Predict the Structural Behavior of Curved Surfaces Subject to an Environment that Simultaneously Imposes High Heating Rates, Temperatures, Loading and Accelerations".

Specifically, the investigation is planned to study the stress and strain distributions, and buckling characteristics of surfaces of revolution subjected to external pressure and various temperature conditions.

The methods of analysis take into account the influence of time and temperature upon surfaces of revolution with temperature dependent properties. Conical and hemispherical shells are selected for the verification specimens for analytical and experimental simplicity.

The methods of analysis and their verification by experiments are summarized in the body of this report. Items of a secondary nature such as details of the experimental program, are presented in the appendices.

II. FUNDAMENTAL EQUATIONS OF THERMOVISCOELASTICITY

The mathematical formulation of the response of a viscoelastic body to combined mechanical and thermal loads can be approximately represented by the following set of differential equations:

Equations of Equilibrium $\sigma_{ij,j} + F_i = 0$

Compatibility Equations $\epsilon_{ij,kl} + \epsilon_{kl,ij} - \epsilon_{ik,jl} - \epsilon_{jl,ik} = 0$

Equations of State $P\{S_{ij}\} = 2Q\{E_{ij}\}$, $\epsilon = \alpha T$

where P and Q are linear operators representing different viscoelastic materials and $E_{ij} = \epsilon_{ij} - \frac{1}{3}\epsilon_{kk}\delta_{ij}$, $S_{ij} = \sigma_{ij} - \frac{1}{3}\sigma_{kk}\delta_{ij}$, $\epsilon_{ij} = \frac{1}{2}(\xi_{i,j} + \xi_{j,i})$ Subject to the boundary conditions, the system of nine equations on the set of nine unknown field variables σ_{ij}, ξ_i is complete in the sense that solution of the system is unique, if the solution exists.

2.1 The Model and the Equations of Equilibrium

The model of this analysis, as shown in Fig 2.1-1, is a thin shell of revolution generated by any arbitrary curve. By thin, it is implied that the shell thickness is of small order of magnitude as compared with other dimensions. The shell is further assumed to be of uniform thickness. No restrictions are placed on the manner by which the edge is supported. However, the load system is assumed to be axial-symmetric, having both mechanical and thermal origins.

For a shell of revolution, the shear stress tangent to a parallel circle is equal to zero, or $Q_\theta = 0$ [25]. Furthermore, the moment and the tensile stress in θ - direction will be independent of θ. The stresses and moments on a small element a b c d defined by two meridian planes and two paralleled circles, are shown in Fig 2.1 - 1.

Three equations of equilibrium[25] can be established by equating the force components in the direction tangent to the meridian and normal to meridian to zero and by setting the moment about cd to zero.

$$\frac{\partial (N_\phi r)}{\partial \phi} - N_\theta \rho_1 \cos\phi - Q_\phi r = 0 \qquad (2.1 - 1)$$

$$N_\phi r + N_\theta \rho_1 \sin\phi + \frac{\partial (Q_\phi r)}{\partial \phi} + p \rho_1 r = 0 \qquad (2.1 - 2)$$

$$\frac{\partial (M_\phi r)}{\partial \phi} - M_\phi \rho_1 \cos\phi - Q_\phi r \rho_1 = 0 \qquad (2.1 - 3)$$

Partial differentiations are being used because the independent variables are also functions of time.

In addition to the three equations shown above, one may also establish another equilibrium condition by considering the equilibrium of the portion of the shell above a parallel circle

$$2\pi r N_\phi \sin\phi + 2\pi r Q_\phi \cos\phi + \pi r^2 p = 0$$

from which

$$N_\phi = -Q_\phi \cot\phi - \frac{pr}{2\sin\phi} \qquad (2.1 -4)$$

One way to simplify the equations of equilibrium is to use equations (2.1 -2), (2.1 - 3), and (2.1 - 4) and introducing new variables $W = Q_\phi \rho_2$ and $\chi = \frac{1}{\rho_1}(v + \frac{\partial w}{\partial \phi})$ as described in Timoshenko[25], or to preceed by eliminating $Q_\phi r$ from the equations (2.1 -1), (2.1 - 2), and (2.1 - 3) to obtain two fundamental equations of equilibrium. This procedure of approach had been used by Stodola[23], Keller[17], and Frankhauser[9] in their elastic analysis. A brief derivation will be as follows:

From equation (2.1 - 3) one may write:

$$Q_\phi r = \frac{\partial(M_\phi r)}{\rho_1 \partial\phi} - M_\theta \cos\phi \qquad (2.1 - 5)$$

Differentiation with respect to ϕ yields

$$\frac{\partial(Q_\phi r)}{\partial\phi} = \frac{\partial}{\partial\phi}\left[\frac{1}{\rho_1}\frac{\partial(M_\phi r)}{\partial\phi}\right] - \cos\phi\,\frac{\partial M_\theta}{\partial\phi} + M_\theta \sin\phi \qquad (2.1 - 6)$$

Introducing equations (2.1 - 5) and (2.1 - 6) into equations (2.1 - 1) and (2.1 - 2) gives

$$\frac{\partial(N_\phi r)}{\partial\phi} - N_\theta \rho_1 \cos\phi + M_\theta \cos\phi - \frac{1}{\rho_1}\frac{(M_\phi r)}{\partial\phi} = 0 \qquad (2.1 - 7)$$

$$\frac{1}{\rho_1}\frac{\partial}{\partial\phi}\left[\frac{1}{\rho_1}\frac{\partial(M_\phi r)}{\partial\phi}\right] - \frac{\cos\phi}{\rho_1}\frac{\partial M_\theta}{\partial\phi} + \frac{M_\theta \sin\phi}{\rho_1} + \frac{N_\phi r}{\rho_1} + N_\theta \sin\phi + p_r = 0 \qquad (2.1 - 8)$$

Equations (2.1 - 7) and (2.1 - 8) are now the equations of equilibrium.

2.2 Equations of State

As this analysis deals with linear viscoelastic material, the relation between the stress and strain may be taken as

$$\{S_{ij}\} = 2\left(\eta \frac{\partial}{\partial t} + G\right)\{E_{ij}\} \qquad (2.2 - 1)$$

Upon introduction of the stress and strain deviators, equations (2.2 - 1) take the following form

$$\left.\begin{aligned} \tfrac{2}{3}\sigma_{\phi\phi} - \tfrac{1}{3}\sigma_{\theta\theta} &= 2\left(\eta \frac{\partial}{\partial t} + G\right)\left(\epsilon_{\phi\phi} - \alpha T\right) \\ \tfrac{2}{3}\sigma_{\theta\theta} - \tfrac{1}{3}\sigma_{\phi\phi} &= 2\left(\eta \frac{\partial}{\partial t} + G\right)\left(\epsilon_{\theta\theta} - \alpha T\right) \end{aligned}\right\} \qquad (2.2 - 2)$$

The components of stress may be written as

$$\left.\begin{aligned} \sigma_{\phi\phi} &= 2\left(\eta \frac{\partial}{\partial t} + G\right)\left(2\epsilon_{\phi\phi} + \epsilon_{\theta\theta} - 3\alpha T\right) \\ \sigma_{\theta\theta} &= 2\left(\eta \frac{\partial}{\partial t} + G\right)\left(2\epsilon_{\theta\theta} + \epsilon_{\phi\phi} - 3\alpha T\right) \end{aligned}\right\} \qquad (2.2 - 3)$$

Obviously, both $\sigma_{\phi\phi}$ and $\sigma_{\theta\theta}$ are functions of the physical properties, strains, time and temperature. It will be discussed later in paragraph 2.6 that the physical properties involved here are functions of temperature. Since the temperature may vary across.the shell thickness as well as along the surface meridian, and since, the deformations for viscoelastic material are functions of load and time, the resulting stress pattern is extremely complicated. It is therefore necessary to make reasonable assumptions to simplify the problem as the analysis proceeds.

With values of $\sigma_{\phi\phi}$ and $\sigma_{\theta\theta}$ it is possible to write the expression for membrane forces and moments. Taking the shell middle surface as a reference surface for integration, one may express the membrane forces and moments as follows

$$\left.\begin{aligned} N_\phi &= \int_{-\frac{\delta}{2}}^{\frac{\delta}{2}} \sigma_{\phi\phi}\left(1-\frac{\xi}{\rho_1}\right)d\xi \;, & M_\phi &= \int_{-\frac{\delta}{2}}^{\frac{\delta}{2}} \sigma_{\phi\phi}\,\xi\left(1-\frac{\xi}{\rho_1}\right)d\xi \\ N_\theta &= \int_{-\frac{\delta}{2}}^{\frac{\delta}{2}} \sigma_{\theta\theta}\left(1-\frac{\xi}{\rho_2}\right)d\xi \;, & M_\theta &= \int_{-\frac{\delta}{2}}^{\frac{\delta}{2}} \sigma_{\theta\theta}\,\xi\left(1-\frac{\xi}{\rho_2}\right)d\xi \end{aligned}\right\} \qquad (2.2 - 4)$$

But for thin shells, the small quantities $\frac{\xi}{\rho_1}$ and $\frac{\xi}{\rho_2}$ can be neglected. Thus,

$$\left.\begin{aligned} N_\phi &= \int_{-\frac{\delta}{2}}^{\frac{\delta}{2}} \sigma_{\phi\phi}\,d\xi \;, & M_\phi &= \int_{-\frac{\delta}{2}}^{\frac{\delta}{2}} \sigma_{\phi\phi}\,\xi\,d\xi \\ N_\theta &= \int_{-\frac{\delta}{2}}^{\frac{\delta}{2}} \sigma_{\theta\theta}\,d\xi \;, & M_\theta &= \int_{-\frac{\delta}{2}}^{\frac{\delta}{2}} \sigma_{\theta\theta}\,\xi\,d\xi \end{aligned}\right\} \qquad (2.2 - 5)$$

These integrations and the values of $\sigma_{\phi\phi}$ and $\sigma_{\theta\theta}$ in equation (2.2 - 3) reveal the importance of simplification in all variables involved in these equations.

2.3 Strains as Functions of Displacement

Considering the shell middle surface, the strain or deformation along the meridian is

$$\epsilon_{\phi M} = \frac{1}{\rho_1}\left(\frac{\partial v}{\partial \phi} - w\right) \qquad (2.3 - 1)$$

and the corresponding strain in the circumferential direction of the parallel circle is

$$\epsilon_{\theta M} = \frac{1}{\rho_2}\left(\frac{v}{\tan\phi} - w\right) \qquad (2.3 - 2)$$

Partial derivatives are being used in (2.3 - 1) and (2.3 - 2) instead of ordinary derivatives in order to consider displacements as function of both ϕ and time. If the variation of strains across the shell thickness has to be considered, the strain will be a function of distance, ξ , from the shell middle surface.

$$\left.\begin{aligned} \epsilon_{\phi\phi} &= \frac{1}{\rho_1}\left(\frac{\partial v}{\partial \phi} - w\right) - \frac{1}{\rho_1}\frac{\partial}{\partial \phi}\left(\frac{v}{\rho_1} + \frac{\partial w}{\rho_1 \partial \phi}\right)\xi \\ \epsilon_{\theta\theta} &= \frac{1}{\rho_2}\left(v\cot\phi - w\right) - \frac{\cot\phi}{\rho_2}\left(\frac{v}{\rho_1} + \frac{1}{\rho_1}\frac{\partial w}{\partial \phi}\right)\xi \end{aligned}\right\} \qquad (2.3 - 3)$$

Obviously, the strains in the form of equations (2.3 - 3) will add complication in the derivation of basic differential equations. In the treatment of thin shells, however, the variation of deformation across the shell is neglected. Appendix AI also shows the justification of this approximation by the order of magnitude consideration. With this approximation, equation (2.2 - 3) may be written

$$\left.\begin{aligned} \sigma_{\theta\theta} &= 2\left(\eta \frac{\partial}{\partial t} + G\right)\left(2\epsilon_{\phi M} + \epsilon_{\theta M} - 3\alpha T\right) \\ \sigma_{\phi\phi} &= 2\left(\eta \frac{\partial}{\partial t} + G\right)\left(2\epsilon_{\theta M} + \epsilon_{\phi M} - 3\alpha T\right) \end{aligned}\right\} \qquad (2.3 - 4)$$

In other words, in these stress equations, we take the strain of the shell middle-surface as the mean value of the strain across the shell thickness.

2.4 Pressure and Temperature of the Shell

At any point, the shell is subjected to a pressure load p, which could be taken as a function of time or a constant depending upon the status of the loading, steady or transit. In the case of a flight vehicle, the pressure is of dynamic type. The boundary layer immediately outside the body surface and the phenomena of separation[8] result in a variation of pressure along the meridian of a shell. The pressure is maximum at the stagnation point and varies as one moves downstream on the body. Furthermore, if the angle of attack is not zero, the pressure distribution will be unsymmetrical. However, this analysis is restricted to bodies of zero angle of attack so that the pressure load will be axial-symmetric. Fig 2.4 - 1 shows the pressure distribution along a meridian.

In the case of high speed vehicles, aerodynamic heating effects are experienced in addition to the surface pressure distribution. The resulting surface temperature distribution normally varies along the body surface. The manner of variation depends upon the flight Mach number and the heat transfer conditions. In this analysis, the body has a constant inner surface temperature, with heat conduction on the edge. Thus the resulting outer surface temperature will be shown as in Fig 2.4 - 2. In some cases, the mathematical complication arising from the variation of temperature along the meridian forces one to assume a uniform outer surface temperature. This assumption deviates quite seriously from the actual problem. However, excellent approximation can be made by taking a number of uniform temperatures as shown in Fig 2.4 - 3.

This analysis is primarily concerned with the temperature variation within the shell thickness. For steady state condition, the temperature gradient across the shell thickness is a constant (based on the assumption of constant inner surface temperature and thickness). For the transient state, the temperature gradient varies with the outer surface temperature and with the distance, ξ, from the middle-surface.

2.5 Boundary Conditions

With the pressure and temperature prescribed in Paragraph 2.4, the boundary conditions can be derived. Depending on the choice of the initial conditions, one of the following catagories of boundary conditions should apply:

a) Stress boundary conditions,

b) Strain boundary conditions,

c) Temperature boundary conditions,

d) Displacement and rotational boundary conditions.

It is not intended that a detailed discussion of all possible boundary conditions be presented here. However, in the subsequent methods of analysis, selection of appropriate boundary conditions are illustrated.

For the problem under discussion, the following diagram summarizes the principal boundary conditions applicable for desired solutions:

(see page 8)

BOUNDARY CONDITIONS DIAGRAM

Fixed-supported Edge

Simple-supported Edge

At t = 0, the shell is at uniform temperature. The initial stress and strain will be that resulting from the pressure load alone

At t = 0, a steady temperature gradient exists across the shell thickness. The initial stress and strain will be that resulting from both pressure and thermal loads

At t=0, the temperature gradient across the shell thickness is a function of time. The initial stress and strain will be that resulting from both pressure and thermal loads corresponding to t=0

At t = 0

p = 0

At t = 0

p ≠ 0

At t = 0

Material is Elastic

At t = 0

Material is Viscoelastic

2.6 Physical Properties

The physical properties of shell material involved in this analysis are: viscosity, shear modulus of elasticity and thermal expansion coefficient. For the most metals, viscosity and shear modulus of elasticity decrease with an increase in temperature, while the thermal expansion coefficient increases with temperature. Since we are concerned with the effects of aerodynamic heating on viscoelastic bodies, the variation of material properties with temperature has to be taken into consideration.

Fig 2.6 - 1 (Reference 4) shows the variation of the mean coefficient of thermal expansion with temperature for several typical materials. It

is obvious a linear relationship will closely approximate the actual variation. However, for some materials, the temperature effect on the thermal expansion coefficient is small as compared with other properties. For example, in case of aluminum, the value of thermal expansion coefficient is increased by 8% for a temperature variation from 250°F to 600°F. However, for the same temperature variation, the shear modulus may decrease as much as 50%. In the subsequent analysis, therefore, the thermal expansion coefficient is assumed to be constant.

The shear modulus of elasticity takes a similar trend of variation with temperature as the modulus of elasticity. The value of shear modulus of elasticity sometimes can be approximated by taking one third that of modulus of elasticity. The variation of modulus of elasticity is shown in Fig 2.6 - 2[4]. Similar to the coefficient of thermal expansion, a linear variation may be assumed. The following relationship is used

$$G = G_0(1-\beta T)$$

where G_0 is the shear modulus at some datum temperature

G is the shear modulus at T degrees above the datum temperature

β is the average rate of change of G with respect to the temperature for a specific temperature range.

The information of the viscosity for metals is very limited. Most liquids follow the Newtonian Law, that is, the viscosity decreases exponentially with the inverse of the absolute temperature. One may use a similar function for metals but the integration of viscosity with respect to temperature T will be extremely difficult. To retain the exponential property of viscosity on one hand and to take the advantage of less definite viscosity theory of metal on the other hand, it is assumed that the viscosity varies according to

$$\eta = \eta_0 e^{-KT}$$

where η_0 is viscosity at some datum temperature

η is viscosity at a temperature T degrees above the datum temperature

K is evaluated between the datum temperature and a prespecified temperature.

2.7 Methods of Analysis

In paragraph 2.1 it is shown that there are two ways of combining the equations of equilibrium which suggest there are different ways of solving the problem. Paragraph 2.3 indicates that the strain-displace-

ment relation may take a more simplified form. The physical properties may betaken as functions of temperature, or they may be evaluated at some appropriate mean temperature in which case the problem is treated as being independent of temperature. All of these choices suggest that there are many ways to arrive at a solution. In Section III the conical shell is analyzed by three different approaches. However, from a mathematical point of view, for a given shell geometry one method may be more efficient than the other.

The general procedure of analysis is:

1. To procede with the given temperature profile which leads to the physical properties and thermal stresses.

2. To make a choice of strain-displacement relation for substitution into the equation of state.

3. To find the values of membrane forces and moments from the stress components and express them in terms of displacements, material properties, and independent variables. In some cases, the use of appropriately chosen new variables may be useful.

4. To introduce the values of membrane forces and moments into the equations of equilibrium to obtain the governing equations. In some cases, instead of using membrane forces as obtained from 3 a fourth equation of equilibrium may be used.

5. To solve the governing equations the boundary conditions are inserted to evaluate arbitrary constants that arise from the integration of the differential equations.

The process of analysis may be summarized with the following diagram

PROCESS OF ANALYSIS DIAGRAM

Temperature Profile → Equations of State ← Strain-Displacement Relations

Temperature Profile ↓ Physical Properties

Equations of State
↓
Membrane Forces and Moments
↓
Equations of Equilibrium
↓
Governing Equations
↓ ← Boundary Conditions
Solutions

III. ANALYSIS OF CONICAL SHELL

The critical section of many space flight vehicles is of conical geometry. The conical shell therefore, is taken as one of the examples for demonstrating the analysis.

Three different methods of analysis are used to attack this problem and solutions are illustrated for specific conditions.

3.1 Simplified Strain-Displacement Relation Method

3.1.1 The Governing Equations

For the conical shell, it is convenient to use the shell element length l as an independent variable which is measured from the tip of the shell. The principal radius ρ_1 approaches infinity with $\rho_1 d\phi$ approaching $d\ell$ and $\rho_2 = \ell \tan\gamma,\ r = \ell \sin\gamma,\ \gamma$ being half of the apex angle.

The equations of equilibrium are now written as

$$\left.\begin{aligned} &\frac{\partial(M_\phi \ell)}{\partial \ell} - M_\theta - Q_\phi \ell = 0 \\ &\frac{\partial(N_\phi \ell)}{\partial \ell} = N_\theta \\ &\frac{\partial(Q_\phi \ell)}{\partial \ell} + N_\theta \cot\gamma + p\ell = 0 \end{aligned}\right\} \qquad (3.1.1 - 1)$$

which may be combined into two equations

$$\left.\begin{aligned} &\frac{\partial(N_\phi \ell)}{\partial \ell} = N_\theta \\ &\frac{\partial^2(M_\phi \ell)}{\partial \ell^2} - \frac{\partial M_\theta}{\partial \ell} + N_\theta \cot\gamma + p\ell = 0 \end{aligned}\right\} \qquad (3.1.1 - 1a)$$

For the strain-displacement relations, the simplified functions discussed in paragraph 2.3 and also shown in Appendix AI are used

$$\epsilon_{\phi\zeta} \doteq \epsilon_{\phi M} = \frac{\partial v}{\partial \ell}$$

$$\epsilon_{\theta\zeta} \doteq \epsilon_{\theta M} = \frac{v - w\cot\gamma}{\ell}$$

A uniform outer surface temperature is assumed to be T_t degrees above the inner surface temperature. However, T_t may be considered as a function of time, if desired. The steady-state temperature gradient across the shell thickness will be (T_t/δ) and the temperature at a distance ζ from the middle surface will be T degrees above that of the inner surface temperature, or

$$T = T_t\left(\frac{1}{2} - \frac{\zeta}{\delta}\right) \qquad (3.1.1 - 2)$$

The temperature dependent properties are written as

$$\left.\begin{aligned} \eta &= \eta_o e^{-KT_t\left(\frac{1}{2}-\frac{\xi}{\delta}\right)} \\ G &= G_o\left[1-\beta\left(\frac{1}{2}-\frac{\xi}{\delta}\right)T_t\right] \\ \alpha &= \alpha_o \end{aligned}\right\} \qquad (3.1.1 - 3)$$

Introducing (3.1.1 - 3) into equation (2.3 - 4), one finds for the stress components

$$\left.\begin{aligned} \sigma_{\phi\phi} &= 2\left\{\eta_o e^{-KT_t\left(\frac{1}{2}-\frac{\xi}{\delta}\right)}\frac{\partial}{\partial t}+G_o\left[1-\beta T_t\left(\frac{1}{2}-\frac{\xi}{\delta}\right)\right]\right\}\left[2\epsilon_{\phi M}+\epsilon_{\theta M}-3\alpha T_t\left(\frac{1}{2}-\frac{\xi}{\delta}\right)\right] \\ \sigma_{\theta\theta} &= 2\left\{\eta_o e^{-KT_t\left(\frac{1}{2}-\frac{\xi}{\delta}\right)}\frac{\partial}{\partial t}+G_o\left[1-\beta T_t\left(\frac{1}{2}-\frac{\xi}{\delta}\right)\right]\right\}\left[2\epsilon_{\theta M}+\epsilon_{\phi M}-3\alpha T_t\left(\frac{1}{2}-\frac{\xi}{\delta}\right)\right] \end{aligned}\right\} \qquad (3.1.1 - 4)$$

Thus the membrane forces and the moments can be integrated as required by equations (2.2 - 5). For example

$$\begin{aligned} N_\theta = \int_{-\frac{\delta}{2}}^{\frac{\delta}{2}}\sigma_{\theta\theta}\,d\xi &= 4\eta_o\frac{\delta}{KT_t}e^{-\frac{KT_t}{2}}\sinh\frac{KT_t}{2}\frac{\partial}{\partial t}\left(2\epsilon_{\theta M}+\epsilon_{\phi M}\right)+2G_o\delta\left(1-\frac{\beta T_t}{2}\right)\left(2\epsilon_{\theta M}+\epsilon_{\phi M}\right)- \\ &- 6\eta_o\alpha e^{-\frac{KT_t}{2}}\frac{\delta}{KT_t}\left[\sinh\frac{KT_t}{2}+\frac{1}{KT_t}\left(2\sinh\frac{KT_t}{2}-KT_t\cosh\frac{KT_t}{2}\right)\right]\frac{\partial T_t}{\partial t}- \\ &- \left(3-2\beta T_t\right)G_o\alpha T_t\delta \end{aligned} \qquad (3.1.1 - 5)$$

$$\begin{aligned} M_\theta = 2\eta_o e^{-\frac{KT_t}{2}}\left(\frac{\delta}{KT_t}\right)^2&\left(KT_t\cosh\frac{KT_t}{2}-2\sinh\frac{KT_t}{2}\right)\frac{\partial\left(2\epsilon_{\theta M}+\epsilon_{\phi M}\right)}{\partial t}+\frac{G_o\delta^2\beta T_t}{6}\left(2\epsilon_{\theta M}+\epsilon_{\phi M}\right)- \\ &-3\eta_o\alpha e^{-\frac{KT_t}{2}}\delta^2\left\{\left[\left(\frac{1}{KT_t}\right)^2+\frac{4}{\left(KT_t\right)^3}\right]\left(KT_t\cosh\frac{KT_t}{2}-2\sinh\frac{KT_t}{2}\right)-\frac{\sinh\frac{KT_t}{2}}{KT_t}\right\}\frac{\partial T_t}{\partial t}+ \\ &+\frac{G_o\alpha T_t\delta^2}{2}\left(1-\beta T_t\right) \end{aligned} \qquad (3.1.1 - 6)$$

Introducing equations (3.1.1 - 5) and (3.1.1 - 6) and the corresponding expressions for N_ϕ and M_ϕ into the equation of equilibrium (3.1.1 - 1a) one obtains

$$\begin{aligned} 2\eta_o\frac{1}{KT_t}\left(1-e^{-KT_t}\right)&\left[\ell\,\frac{\partial^2\left(2\epsilon_{\phi M}+\epsilon_{\theta M}\right)}{\partial t\,\partial\ell}+\frac{\partial\left(\epsilon_{\phi M}-\epsilon_{\theta M}\right)}{\partial t}\right]+ \\ &+2G_o\left(1-\frac{\beta T_t}{2}\right)\left[\ell\,\frac{\partial\left(2\epsilon_{\phi M}+\epsilon_{\theta M}\right)}{\partial\ell}+\left(\epsilon_{\phi M}-\epsilon_{\theta M}\right)\right]=0 \end{aligned} \qquad (3.1.1 - 7)$$

and

$$2\eta_o e^{-\frac{KT_t}{2}}\left\{\left(\frac{\delta}{KT_t}\right)^2\left(KT_t \cosh\frac{KT_t}{2}-2\sinh\frac{KT_t}{2}\right)\left[\ell\frac{\partial^3(2\epsilon_{\phi M}+\epsilon_{\theta M})}{\partial t\,\partial \ell^2}+3\frac{\partial^2\epsilon_{\phi M}}{\partial t\,\partial \ell}\right]+\right.$$

$$\left.+\frac{2\delta}{KT_t}\cot\gamma\sinh\frac{KT_t}{2}\,\frac{\partial(2\epsilon_{\theta M}+\epsilon_{\phi M})}{\partial t}\right\}+\frac{G_o\delta^2\beta T_t}{6}\left[\ell\frac{\partial^2(2\epsilon_{\phi M}+\epsilon_{\theta M})}{\partial \ell^2}+3\frac{\partial\epsilon_{\phi M}}{\partial \ell}\right]+$$

$$+2G_o\delta\left(1-\frac{\beta T_t}{2}\right)\cot\gamma\left(2\epsilon_{\theta M}+\epsilon_{\phi M}\right)+p\ell=$$

$$=\cot\gamma\left\{6\eta_o\alpha e^{-\frac{KT_t}{2}}\frac{\partial T_t}{\partial t}\frac{\delta}{KT_t}\left[\sinh\frac{KT_t}{2}-\frac{1}{KT_t}\left(KT_t\cosh\frac{KT_t}{2}-\right.\right.\right.$$

$$\left.\left.\left.-2\sinh\frac{KT_t}{2}\right)\right]+\left(3-2\beta T_t\right)G_o\alpha\delta T_t\right\} \qquad (3.1.1 - 8)$$

3.1.2 <u>Method of Solving the Governing Equations</u>

First of all, introducing new variables $U=2\epsilon_{\phi M}+\epsilon_{\theta M}$ and $V=\epsilon_{\phi M}$ to replace terms involving $\epsilon_{\phi M}$ and $\epsilon_{\theta M}$, results in the following form for the governing equations

$$\frac{2\eta_o}{KT_t}\left(1-e^{-KT_t}\right)\frac{\partial}{\partial t}\left(\ell\frac{\partial U}{\partial \ell}+3V-U\right)+G_o\left(2-\beta T_t\right)\left(\ell\frac{\partial U}{\partial \ell}+3V-U\right)=0 \qquad (3.1.2 - 1)$$

and

$$\eta_o\left(\frac{\delta}{KT_t}\right)^2\left[KT_t\left(1+e^{-KT_t}\right)-2\left(1-e^{-KT_t}\right)\right]\frac{\partial}{\partial t}\left(\ell\frac{\partial^2 U}{\partial \ell^2}+3\frac{\partial V}{\partial \ell}\right)+2\eta_o\frac{\delta}{KT_t}\cot\gamma\left(1-e^{-KT_t}\right)\frac{\partial}{\partial t}\left(2U-3V\right)+$$

$$+\frac{G_o\delta^2\beta T_t}{6}\left(\ell\frac{\partial^2 U}{\partial \ell^2}+3\frac{\partial V}{\partial \ell}\right)+G_o\delta\left(2-\beta T_t\right)\cot\gamma\left(2U-3V\right)+p\ell=$$

$$=6\eta_o\frac{\alpha\delta}{KT_t}\left(-e^{-KT_t}+\frac{1-e^{-KT_t}}{KT_t}\right)\cot\gamma\,\frac{\partial T_t}{\partial t}+G_o\delta\alpha T_t\left(3-2\beta T_t\right)\cot\gamma \qquad (3.1.2 - 2)$$

From equation (3.1.2 - 1) $\frac{\partial}{\partial t}\left(\ell\frac{\partial U}{\partial \ell}+3V-U\right)=-\frac{G_o(2-\beta T_t)KT_t}{2\eta_o(1-e^{-KT_t})}\left(\ell\frac{\partial U}{\partial \ell}+3V-U\right)$

and for smoothly continuous functions of U and V with respect to ℓ and t , it can be written that

$$\ell\frac{\partial^3 U}{\partial t\,\partial \ell^2}+3\frac{\partial^2 V}{\partial t\,\partial \ell}=\frac{\partial}{\partial \ell}\left(\ell\frac{\partial^2 U}{\partial t\,\partial \ell}-\frac{\partial U}{\partial t}+3\frac{\partial V}{\partial t}\right)$$

and

$$\frac{\partial}{\partial \ell}\left(\ell\frac{\partial U}{\partial \ell}+3V-U\right)=\ell\frac{\partial^2 U}{\partial \ell^2}+3\frac{\partial V}{\partial \ell}$$

Hence

$$\ell \frac{\partial^3 U}{\partial t \partial \ell^2} + 3\frac{\partial^2 V}{\partial t \partial \ell} = -\frac{G_o(2-\beta T_t)\kappa T_t}{2\eta_o(1-e^{-\kappa T_t})}\left(\ell\frac{\partial^2 U}{\partial \ell^2} + 3\frac{\partial V}{\partial \ell}\right) \quad (3.1.2 - 3)$$

Using equations (3.1.2 - 1), (3.1.2 - 2), and (3.1.2 - 3), the new governing equations become

$$\frac{\partial}{\partial t}\left(\ell\frac{\partial U}{\partial \ell} + 3V - U\right) + F_1\left(\ell\frac{\partial U}{\partial \ell} + 3V - U\right) = 0 \quad (3.1.2 - 1a)$$

$$F_2\left(\ell\frac{\partial^2 U}{\partial \ell^2} + 3\frac{\partial V}{\partial \ell}\right) + \frac{\partial}{\partial t}\left(\ell\frac{\partial U}{\partial \ell} + U\right) + F_1\left(\ell\frac{\partial U}{\partial \ell} + U\right) + F_3 p \ell = F_4 \quad (3.1.2 - 4)$$

where

$$F_1 = \frac{G_o \kappa T_t (2-\beta T_t)}{2\eta_o(1-e^{-\kappa T_t})}$$

$$F_2 = \frac{G_o \delta \kappa T_t \tan\gamma}{4\eta_o(1-e^{-\kappa T_t})}\left[\frac{\beta T_t}{3} - (2-\beta T_t)\left(\frac{1+e^{-\kappa T_t}}{1-e^{-\kappa T_t}} - \frac{2}{\kappa T_t}\right)\right]$$

$$F_3 = \frac{\kappa T_t \tan\gamma}{2\delta\eta_o(1-e^{-\kappa T_t})}$$

$$F_4 = \frac{\kappa T_t}{2\eta_o(1-e^{-\kappa T_t})}\left[6\eta_o\frac{\alpha}{\kappa T_t}\left(\frac{1-e^{-\kappa T_t}}{\kappa T_t} - e^{-\kappa T_t}\right)\frac{\partial T_t}{\partial t} + G_o \alpha T_t(3-2\beta T_t)\right]$$

For cases where T_t is a function of time, then F_1, F_2, F_3, and F_4 are all functions of time. The method of separation of variables are used to solve the governing equations. By trying a solution $(\ell\, \partial U/\partial \ell + 3V - U)$ of equation (3.1.2 - 1a) in the form $L_1(\ell)T_1(t)$, one obtains

$$\left(\ell\frac{\partial U}{\partial \ell} + 3V - U\right) = L_1(\ell)T_1(0)\, e^{-\int_0^t F_1 dt} \quad (3.1.2 - 5)$$

The values of $L_1(\ell)T_1(0)$ may be obtained from the boundary conditions, i.e., the value of $(\ell\, \partial U/\partial \ell - U + 3V)_{\ell=\ell,\, t=0}$ at a point ℓ and at an arbitrarily chosen initial time. It is, therefore, the choice of boundary conditions which has an influence on whether the solution of the problem can be obtained. For this example, the boundary conditions are chosen such that

a) A uniform and constant pressure is exerted on the shell at all times.

b) T_t is a function of time, equal to zero, at $t = 0$; increasing to a constant value when a steady state condition is reached. For simplification it is assumed that $T_t = Ct$ for $0 \leq t \leq t_c$ and $T_t = \bar{T}_t$ for $t > t_c$, where C and $\bar{T}_t$ are constants and t_c is the transition period.

c) The edge of the shell is fixed.

These boundary conditions imply that at $t = 0$ the shell has a deformation which is caused by the pressure load alone. The next question is the state of the material conditions at $t = 0$, whether elastic or viscoelastic. This depends on the type of material and the temperature to which the material is subjected at the initial time. In the elastic case, one may evaluate $(\ell \, \partial U/\partial \ell + 3V - U)_{\ell=\ell, t=0}$ from results of elastic analysis as discussed in most applied elasticity textbooks. A simplified version of the elastic analysis of a conical shell with thermal stress is discussed in Appendix A2. For the present application, we will use the results of Appendix A2 but omit the contributions from thermal effects. However, if the boundary conditions are specified as an elastic material with thermal stress at the initial moment, then the complete results should be used.

For elastic analysis

$$V\Big|_{\substack{\ell=\ell \\ t=0}} = \frac{1}{E_i \delta}\left(N_\phi - \nu_i N_\theta\right)_{EL.} \qquad , \qquad U\Big|_{\substack{\ell=\ell \\ t=0}} = \frac{1}{E_i \delta}\left[(2-\nu_i)N_\phi + (1-2\nu_i)N_\theta\right]_{EL.}$$

and

$$\left(\ell \frac{\partial U}{\partial \ell} + 3V - U\right)_{\substack{\ell=\ell \\ t=0}} = \left(\ell \frac{\partial U}{\partial \ell} + 3V - U\right)_{EL.} = \frac{1}{E_i \delta}(1-2\nu_i)\,\ell \frac{\partial}{\partial \ell}\left(N_\phi + N_\theta\right)_{EL.} =$$

$$= \frac{(1-2\nu_i)}{E_i \delta}\left\{E_i \delta \cot\gamma \left[A_1\left(-Z_1 - \frac{2Z_2'}{y}\right) + A_2\left(-Z_2 + \frac{2Z_1'}{y}\right)\right] - \frac{3}{2} p \ell \tan\gamma\right\} \qquad (3.1.2 - 6)$$

A_1 and A_2 are to be evaluated from the edge conditions.

The equation (3.1.2 - 5) may be written

$$\left(\ell \frac{\partial U}{\partial \ell} + 3V - U\right) = \frac{1}{E_i \delta}(1-2\nu_i)\,\ell \frac{\partial}{\partial \ell}\left(N_\phi + N_\theta\right)_{EL.} e^{-\int_0^t F_1 dt} \qquad (3.1.2 - 7)$$

From (3.1.2 - 7), the values of $\partial V/\partial \ell$ can be expressed in the derivatives of U and the known initial values

$$\frac{\partial V}{\partial \ell} = -\frac{\ell}{3}\frac{\partial^2 U}{\partial \ell^2} + \frac{1}{3} e^{-\int_0^t F_1 dt} \frac{(1-2\nu_i)}{E_i \delta}\frac{\partial}{\partial \ell}\left[\ell \frac{\partial}{\partial \ell}\left(N_\phi + N_\theta\right)\right]_{EL.} \qquad (3.1.2 - 8)$$

where

$$\frac{\partial}{\partial \ell}\left[\ell \frac{\partial}{\partial \ell}\left(N_\phi + N_\theta\right)\right]_{EL.} = 4E_i \cot^2\gamma \sqrt{3(1-\nu_i)^2}\left[A_1\left(-\frac{Z_1'}{y} + \frac{2Z_1}{y^2} + \frac{4Z_2'}{y^3}\right) + A_2\left(-\frac{Z_2'}{y} + \frac{2Z_2}{y^2} - \frac{4Z_1'}{y^3}\right)\right] - \frac{3}{2} p \tan\gamma$$

substitution of $\partial V/\partial \ell$ from equation (3.1.2 - 8) into equation (3.1.2 - 4) reduces it to a single dependent variable equation.

$$\frac{\partial}{\partial t}\left(\ell \frac{\partial U}{\partial \ell} + U\right) + F_1\left(\ell \frac{\partial U}{\partial \ell} + U\right) = -F_3 p \ell + F_4 - F_2 e^{-\int_0^t F_1 dt}\frac{(1-2\nu_i)}{E_i \delta}\frac{\partial}{\partial \ell}\left[\ell \frac{\partial}{\partial \ell}\left(N_\phi + N_\theta\right)\right]_{EL.} \qquad (3.1.2 - 9)$$

Again using the method of separation of variables and boundary conditions, one finds for $\mathcal{U}$

$$\mathcal{U}=\frac{e^{-\int_0^t F_1 dt}}{\ell}\left(\int_0^{\ell}\int_0^{t}\left\{(F_4-F_3\rho\ell)e^{\int_0^t F_1 dt}-\frac{F_2(1-2\nu_i)}{E_i\delta}\frac{\partial}{\partial\ell}\left[\ell\frac{\partial}{\partial\ell}(N_\phi+N_\theta)_{EL}\right]\right\}dt\,d\ell+\right.$$
$$\left.+\frac{1}{E_i\delta}\int_0^{\ell}\left[3(1-\nu_i)N_\theta+(1-2\nu_i)\ell\frac{\partial N_\theta}{\partial\ell}\right]_{EL}d\ell\right) \qquad (3.1.2 - 10)$$

From equation (3.1.2 - 7) the corresponding value of $\mathcal{V}$ is found to be

$$\mathcal{V}=\frac{e^{-\int_0^t F_1 dt}}{3}\left(\frac{2}{\ell}\int_0^{\ell}\int_0^{t}\left\{(F_4-F_3\rho\ell)e^{\int_0^t F_1 dt}-\frac{F_2(1-2\nu_i)}{E_i\delta}\frac{\partial}{\partial\ell}\left[\ell\frac{\partial}{\partial\ell}(N_\phi+N_\theta)_{EL}\right]\right\}dt\,d\ell+\right.$$
$$+\frac{2}{E_i\delta\ell}\int_0^{\ell}\left[3(1-\nu_i)N_\theta+(1-2\nu_i)\ell\frac{\partial N_\theta}{\partial\ell}\right]_{EL}d\ell-\int_0^t\left\{(F_4-F_3\rho\ell)e^{\int_0^t F_1 dt}-\right.$$
$$\left.-\frac{F_2(1-2\nu_i)}{E_i\delta}\frac{\partial}{\partial\ell}\left[\ell\frac{\partial}{\partial\ell}(N_\phi+N_\theta)_{EL}\right]\right\}dt-\frac{1}{E_i\delta}\left[3(1-\nu_i)N_\theta+(1-2\nu_i)\ell\frac{\partial N_\theta}{\partial\ell}\right]_{EL}+$$
$$\left.+\frac{(1-2\nu_i)}{E_i\delta}\ell\frac{\partial}{\partial\ell}(N_\phi+N_\theta)_{EL}\right) \qquad (3.1.2 - 11)$$

With values of $\mathcal{U}$ and $\mathcal{V}$ the subsequent values of $2\epsilon_{\phi M}+\epsilon_{\theta M}$ and $2\epsilon_{\theta M}+\epsilon_{\phi M}$ their time derivatives, and the membrane forces and moments can be readily determined. The values of N_θ and M_θ are illustrated as follows

$$N_{\theta(\ell,t)}=2\delta\left[G_0\left(1-\frac{\beta T_t}{2}\right)-\frac{F_1\eta_0}{KT_t}\left(1-e^{-KT_t}\right)\right]e^{-\int_0^t F_1 dt}\left(\int_0^t\left\{(F_4-F_3\rho\ell)e^{\int_0^t F_1 dt}-\frac{F_2(1-2\nu_i)}{E_i\delta}\frac{\partial}{\partial t}\left[\ell\frac{\partial}{\partial\ell}(N_\phi+N_\theta)_{EL}\right]\right\}dt-\right.$$
$$\left.-\frac{(1-2\nu_i)}{E_i\delta}\ell\frac{\partial}{\partial\ell}(N_\phi+N_\theta)_{EL}+\frac{1}{E_i\delta}\left[3(1-\nu_i)N_\theta+(1-2\nu_i)\ell\frac{\partial N_\theta}{\partial\ell}\right]_{EL}\right)+$$
$$+\frac{2\delta\eta_0}{KT_t}\left(1-e^{-KT_t}\right)\left\{(F_4-F_3\rho\ell)e^{-\int_0^t F_1 dt}-\frac{F_2(1-2\nu_i)}{E_i\delta}\frac{\partial}{\partial\ell}\left[\ell\frac{\partial}{\partial\ell}(N_\phi+N_\theta)_{EL}\right]\right\}-$$
$$-\frac{2\delta\eta_0\left(1-e^{-KT_t}\right)}{KT_t}F_4 \qquad (3.1.2 - 12)$$

and

$$M_{\theta(\ell,t)} = \delta^2 e^{-\int_0^t F_1 dt}\left\{\frac{G_0\beta T_t}{6} - \frac{F_1\eta_0}{(KT_t)^2}\left[KT_t\left(1+e^{-KT_t}\right)-2\left(1-e^{-KT_t}\right)\right]\right\}\left(\int_0^t\left[(F_4-F_3 p\ell)e^{\int_0^t F_1 dt} - \right.\right.$$

$$\left. - \frac{F_2(1-2\nu_i)}{E_i\delta}\frac{\partial}{\partial\ell}\left[\ell\frac{\partial}{\partial\ell}(N_\phi+N_\theta)_{EL}\right]\right\}dt - \frac{(1-2\nu_i)}{E_i\delta}\ell\frac{\partial}{\partial\ell}(N_\phi+N_\theta)_{EL} +$$

$$\left. + \frac{1}{E_i\delta}\left[3(1-\nu_i)N_\theta + (1-2\nu_i)\ell\frac{\partial N_\theta}{\partial\ell}\right]_{EL}\right) + \eta_0\left(\frac{\delta}{KT_t}\right)^2\left[KT_t\left(1+e^{-KT_t}\right) - \right.$$

$$\left. - 2\left(1-e^{-KT_t}\right)\right]\left\{(F_4-F_3 p\ell)e^{-\int_0^t F_1 dt} - \frac{F_2(1-2\nu_i)}{E_i\delta}\frac{\partial}{\partial\ell}\left[\ell\frac{\partial}{\partial\ell}(N_\phi+N_\theta)_{EL}\right]\right\} -$$

$$- 3\eta_0\alpha\delta^2\left\{\left[\frac{1}{(KT_t)^2} + \frac{4}{(KT_t)^3}\right]\left[KT_t\frac{(1+e^{-KT_t})}{2} - \left(1-e^{-KT_t}\right)\right] - \frac{1-e^{-KT_t}}{2KT_t}\right\}\frac{\partial T_t}{\partial t} +$$

$$+ \frac{G_0\alpha T_t\delta}{2}\left(1-\beta T_t\right) \tag{3.1.2 - 13}$$

From this example, it can be seen that the method of analysis can be extended to apply to other boundary conditions; for example, if pressure is being a function of time and distance along the shell element, $p(t,\ell)$, or if an initial temperature gradient across the shell thickness exists or if the edge is simply supported.

3.2 Simplified Differential Equation Method

One of the important simplification made in paragraph 3.1.1 was the omission of terms containing ξ in the equations of $\epsilon_{\phi\phi}$ and $\epsilon_{\theta\theta}$. In doing so it was assumed that the middle surface values were the mean values and that the order of magnitude of these terms was small. In this paragraph, the basic governing equations are derived without imposing this limitation, however, v and w are assumed not to be functions of ξ.

Applying equation (2.3 - 3) to the conical shell results, one may write

$$\left.\begin{aligned} \epsilon_{\phi\xi} &= \frac{\partial v}{\partial\ell} - \frac{\partial^2 w}{\partial\ell^2}\xi \\ \epsilon_{\theta\xi} &= \frac{v - w\cot\gamma}{\ell} - \frac{\xi}{\ell}\frac{\partial w}{\partial\ell} \end{aligned}\right\} \tag{3.2 - 1}$$

Employing the same temperature profile as given in paragraph 3.1.1, the stress components may be written as

$$\sigma_{\phi\phi} = 2\left\{\eta_0 e^{-KT_t\left(\frac{1}{2}-\frac{\xi}{\delta}\right)}\frac{\partial}{\partial t} + G_0\left[1-\beta\left(\frac{1}{2}-\frac{\xi}{\delta}\right)T_t\right]\right\}\left\{2\left(\frac{\partial v}{\partial\ell} - \frac{\partial^2 w}{\partial\ell^2}\xi\right) + \frac{v-w\cot\gamma}{\ell} - \frac{\xi}{\ell}\frac{\partial w}{\partial\ell} - 3\alpha T_t\left(\frac{1}{2}-\frac{\xi}{\delta}\right)\right\} \tag{3.2 - 2}$$

$$\sigma_{\theta\theta}=2\left\{\eta_0 e^{-KT_t\left(\frac{1}{2}-\frac{\xi}{\delta}\right)}\frac{\partial}{\partial t}+G_0\left[1-\beta\left(\frac{1}{2}-\frac{\xi}{\delta}\right)T_t\right]\right\}\left\{2\left(\frac{v-w\cot\gamma}{\ell}-\frac{\xi}{\ell}\frac{\partial w}{\partial \ell}\right)+\frac{\partial v}{\partial \ell}-\xi\frac{\partial^2 w}{\partial \ell^2}-3\alpha T_t\left(\frac{1}{2}-\frac{\xi}{\delta}\right)\right\} \tag{3.2 - 3}$$

The membrane forces and moments will be

$$N_\phi=\int_{-\frac{\delta}{2}}^{\frac{\delta}{2}}\sigma_{\phi\phi}\,d\xi=$$

$$=4\eta_0 e^{-\frac{KT_t}{2}}\frac{\delta}{KT_t}\left[\sinh\frac{KT_t}{2}\frac{\partial}{\partial t}\left(2\frac{\partial v}{\partial \ell}+\frac{v-w\cot\gamma}{\ell}\right)-\frac{\delta}{KT_t}\left(\frac{KT_t}{2}\cosh\frac{KT_t}{2}-\sinh\frac{KT_t}{2}\right)\frac{\partial}{\partial t}\left(2\frac{\partial^2 w}{\partial \ell^2}+\frac{1}{\ell}\frac{\partial w}{\partial \ell}\right)\right]+$$

$$+2G_0\delta\left(1-\frac{\beta T_t}{2}\right)\left(2\frac{\partial v}{\partial \ell}+\frac{v-w\cot\gamma}{\ell}\right)-\frac{G_0\beta T_t\delta^2}{6}\left(2\frac{\partial^2 w}{\partial \ell^2}+\frac{1}{\ell}\frac{\partial w}{\partial \ell}\right)-$$

$$-\frac{6\alpha\delta\eta_0 e^{-\frac{KT_t}{2}}}{6}\left[-e^{-\frac{KT_t}{2}}+\frac{2}{KT_t}\sinh\frac{KT_t}{2}\right]\frac{\partial T_t}{\partial t}-G_0\alpha T_t\delta\left(3-2\beta T_t\right) \tag{3.2 - 4}$$

$$N_\theta=\int_{-\frac{\delta}{2}}^{\frac{\delta}{2}}\sigma_{\theta\theta}\,d\xi=$$

$$=4\eta_0 e^{-\frac{KT_t}{2}}\frac{\delta}{KT_t}\left[\sinh\frac{KT_t}{2}\frac{\partial}{\partial t}\left(2\frac{v-w\cot\gamma}{\ell}+\frac{\partial v}{\partial \ell}\right)-\frac{\delta}{KT_t}\left(\frac{KT_t}{2}\cosh\frac{KT_t}{2}-\sinh\frac{KT_t}{2}\right)\frac{\partial}{\partial t}\left(\frac{2}{\ell}\frac{\partial w}{\partial \ell}+\frac{\partial^2 w}{\partial \ell^2}\right)\right]+$$

$$+2G_0\delta\left(1-\frac{\beta T_t}{2}\right)\left(\frac{\partial v}{\partial \ell}+2\frac{v-w\cot\gamma}{\ell}\right)-\frac{G_0\beta T_t\delta^2}{6}\left(\frac{2}{\ell}\frac{\partial w}{\partial \ell}+\frac{\partial^2 w}{\partial \ell^2}\right)-$$

$$-\frac{6\alpha\delta\eta_0 e^{-\frac{KT_t}{2}}}{KT_t}\left[\frac{2}{KT_t}\sinh\frac{KT_t}{2}-e^{-\frac{KT_t}{2}}\right]\frac{\partial T_t}{\partial t}-G_0\alpha T_t\delta\left(3-2\beta T_t\right) \tag{3.2 - 5}$$

$$M_\phi = 2\eta_0 e^{-\frac{KT_t}{2}} \left\{ \left[\left(\frac{\delta}{KT_t}\right)^2 \left(KT_t \cosh \frac{KT_t}{2} - 2 \sinh \frac{KT_t}{2} \right) \frac{\partial}{\partial t} \left(2\frac{\partial v}{\partial l} + \frac{v - w\cot\gamma}{l} \right) \right] - \right.$$

$$- \left[\frac{\delta^3}{2KT_t} \sinh \frac{KT_t}{2} + 2\left(\frac{\delta}{KT_t}\right)^3 \left(2\sinh\frac{KT_t}{2} - KT_t \cosh \frac{KT_t}{2} \right) \right] \frac{\partial}{\partial t} \left. \left(2\frac{\partial^2 w}{\partial l^2} + \frac{1}{l}\frac{\partial w}{\partial l} \right) \right\} -$$

$$- \frac{G_0 \delta^3}{6} \left[\left(1 - \frac{\beta T_t}{2}\right) \left(2\frac{\partial^2 w}{\partial l^2} + \frac{1}{l}\frac{\partial w}{\partial l} \right) - \frac{\beta T_t}{\delta} \left(2\frac{\partial v}{\partial l} + \frac{v - w\cot\gamma}{l} \right) \right] +$$

$$+ \frac{3\alpha\eta_0\delta^2 e^{-\frac{KT_t}{2}}}{KT_t} \left[-e^{-\frac{KT_t}{2}} - \frac{1}{KT_t}\left(e^{\frac{KT_t}{2}} + 3e^{-\frac{KT_t}{2}} \right) + \frac{8}{(KT_t)^2} \sinh\frac{KT_t}{2} \right] \frac{\partial T_t}{\partial t} +$$

$$+ \frac{G_0 \alpha \delta^2 T_t}{2} \left(1 - \beta T_t \right) \qquad (3.2 - 6)$$

$$M_\theta = 2\eta_0 e^{-\frac{KT_t}{2}} \left\{ \left[\left(\frac{\delta}{KT_t}\right)^2 \left(KT_t \cosh \frac{KT_t}{2} - 2 \sinh \frac{KT_t}{2} \right) \frac{\partial}{\partial t} \left(2\frac{v - w\cot\gamma}{l} + \frac{\partial v}{\partial l} \right) \right] - \right.$$

$$- \left[\frac{\delta^3}{2KT_t} \sinh \frac{KT_t}{2} + 2\left(\frac{\delta}{KT_t}\right)^3 \left(2\sinh\frac{KT_t}{2} - KT_t \cosh \frac{KT_t}{2} \right) \right] \frac{\partial}{\partial t} \left. \left(\frac{2}{l}\frac{\partial w}{\partial l} + \frac{\partial^2 w}{\partial l^2} \right) \right\} -$$

$$- \frac{G_0 \delta^3}{6} \left[\left(1 - \frac{\beta T_t}{2}\right) \left(\frac{2}{l}\frac{\partial w}{\partial l} + \frac{\partial^2 w}{\partial l^2} \right) - \frac{\beta T_t}{\delta} \left(2\frac{v - w\cot\gamma}{l} + \frac{\partial v}{\partial l} \right) \right] +$$

$$+ \frac{3\alpha\eta_0\delta^2 e^{-\frac{KT_t}{2}}}{KT_t} \left[-e^{-\frac{KT_t}{2}} - \frac{1}{KT_t}\left(e^{\frac{KT_t}{2}} + 3e^{-\frac{KT_t}{2}} \right) + \frac{8}{(KT_t)^2} \sinh\frac{KT_t}{2} \right] \frac{\partial T_t}{\partial t} +$$

$$+ \frac{G_0 \alpha \delta^2 T_t}{2} \left(1 - \beta T_t \right) \qquad (3.2 - 7)$$

Introducing equations (3.2 - 4) through (3.2 - 7) into the equations of equilibrium (3.1.1 - 1a), one reduces the governing equations to two 5th order linear partial differential equations. They are

$$\frac{4\eta_0 e^{-\frac{KT_t}{2}}}{KT_t} \left\{ \sinh\frac{KT_t}{2} \frac{\partial}{\partial t} \left[-\frac{2}{l}(v - w\cot\gamma) + 2\frac{\partial v}{\partial l} + 2l\frac{\partial^2 v}{\partial l^2} - \cot\gamma\frac{\partial w}{\partial l} \right] - \right.$$

$$- \frac{2\delta}{KT_t}\left(\frac{KT_t}{2}\cosh\frac{KT_t}{2} - \sinh\frac{KT_t}{2} \right) \frac{\partial}{\partial t} \left. \left[l\frac{\partial^3 w}{\partial l^3} + \frac{\partial^2 w}{\partial l^2} - \frac{1}{l}\frac{\partial w}{\partial l} \right] \right\} +$$

$$+ 2G_0\left(1 - \frac{\beta T_t}{2}\right)\left[2l\frac{\partial^2 v}{\partial l^2} + 2\frac{\partial v}{\partial l} - \cot\gamma\frac{\partial w}{\partial l} - 2\frac{v - w\cot\gamma}{l} \right] -$$

$$- \frac{G_0 \beta T_t \delta}{3}\left[l\frac{\partial^3 w}{\partial l^3} + \frac{\partial^2 w}{\partial l^2} - \frac{1}{l}\frac{\partial w}{\partial l} \right] = 0 \qquad (3.2 - 8)$$

and

$$2\eta_0 e^{-\frac{KT_t}{2}}\Bigg\{\frac{\delta^2}{(KT_t)^2}\left(KT_t\cosh\frac{KT_t}{2}-2\sinh\frac{KT_t}{2}\right)\frac{\partial}{\partial t}\left(2l\frac{\partial^3 w}{\partial l^3}+4\frac{\partial^2 v}{\partial l^2}-\frac{2}{l}\frac{\partial v}{\partial l}+\frac{2v}{l^2}-2\cot\gamma\frac{\partial^2 w}{\partial l^2}-\frac{2w\cot\gamma}{l^2}\right)+$$

$$+\left[\frac{\delta^3}{2KT_t}\sinh\frac{KT_t}{2}+\frac{2\delta^3}{(KT_t)^3}\left(2\sinh\frac{KT_t}{2}-KT_t\cosh\frac{KT_t}{2}\right)\right]\frac{\partial}{\partial t}\left[-2l\frac{\partial^4 w}{\partial l^4}-4\frac{\partial^3 w}{\partial l^3}+\frac{1}{l}\frac{\partial^2 w}{\partial l^2}-\frac{1}{l^2}\frac{\partial w}{\partial l}\right]\Bigg\}+$$

$$+\frac{G_0\delta^3}{6}\Bigg\{-2\left(1-\frac{\beta T_t}{2}\right)\left(l\frac{\partial^4 w}{\partial l^4}+2\frac{\partial^3 w}{\partial l^3}-\frac{1}{2l}\frac{\partial^2 w}{\partial l^2}+\frac{1}{2l^2}\frac{\partial w}{\partial l}\right)+$$

$$+\frac{\beta T_t}{\delta}\left[2l\frac{\partial^3 v}{\partial l^3}+4\frac{\partial^2 v}{\partial l^2}-\frac{2}{l}\frac{\partial v}{\partial l}+\frac{2v}{l^2}-2\cot\gamma\frac{\partial^2 w}{\partial l^2}-\frac{2w\cot\gamma}{l^2}\right]\Bigg\}+$$

$$+4\eta_0 e^{-\frac{KT_t}{2}}\frac{\delta}{KT_t}\cot\gamma\left\{\sinh\frac{KT_t}{2}\frac{\partial}{\partial t}\left(\frac{\partial v}{\partial l}+2\frac{v-w\cot\gamma}{l}\right)\right\}+2G_0\delta\left(1-\frac{\beta T_t}{2}\right)\left(\frac{\partial v}{\partial l}+2\frac{v-w\cot\gamma}{l}\right)\cot\gamma+$$

$$+\frac{6\alpha\eta_0 e^{-\frac{KT_t}{2}}}{KT_t}\delta\cot\gamma\left(e^{-\frac{KT_t}{2}}-\frac{2}{KT_t}\sinh\frac{KT_t}{2}\right)\frac{\partial T_t}{\partial t}-G_0\alpha T_t\delta\cot\gamma\left(3-2\beta T_t\right)+pl=0$$

(3.2 - 9)

The order of magnitude of each terms in these two equations is investigated by a method similar to that discussed in Appendix A. With v and w having the order of magnitude of shell thickness δ, the terms involving v and w in equation (3.2 - 8) have the order of magnitude $\frac{1}{t}\left(\frac{\delta}{l}\right)$, $\frac{1}{t}\left(\frac{\delta}{l}\right)^2$, $\frac{\delta}{l}$, and $\left(\frac{\delta}{l}\right)^2$, and in equation (3.2 - 9) $\frac{\delta}{t}\left(\frac{\delta}{l}\right)$, $\frac{\delta}{t}\left(\frac{\delta}{l}\right)^2$, $\frac{\delta}{t}\left(\frac{\delta}{l}\right)^3$, $\delta\left(\frac{\delta}{l}\right)$, $\delta\left(\frac{\delta}{l}\right)^2$ and $\delta\left(\frac{\delta}{l}\right)^3$.

Neglecting the terms having the order of magnitudes of $\frac{1}{t}\left(\frac{\delta}{l}\right)^2$ and $\left(\frac{\delta}{l}\right)^2$ in equation (3.2 - 8) and $\frac{\delta}{t}\left(\frac{\delta}{l}\right)^3$, $\delta\left(\frac{\delta}{l}\right)^3$ terms in equation (3.2 - 9), the governing equations are written as follows

$$\frac{2\eta_0}{KT_t}\left(1-e^{-KT_t}\right)\frac{\partial}{\partial t}\left[2\left(\frac{\partial v}{\partial l}-\frac{v-w\cot\gamma}{l}\right)+2l\frac{\partial^2 v}{\partial l^2}-\cot\gamma\frac{\partial w}{\partial l}\right]+$$

$$+2G_0\left(1-\frac{\beta T_t}{2}\right)\left[2\left(\frac{\partial v}{\partial l}-\frac{v-w\cot\gamma}{l}\right)+2l\frac{\partial^2 v}{\partial l^2}-\cot\gamma\frac{\partial w}{\partial l}\right]=0 \qquad (3.2 - 10)$$

and

$$2\eta_0 e^{-\frac{KT_t}{2}}\left\{\left(\frac{\delta}{KT_t}\right)^2\left(KT_t\cosh\frac{KT_t}{2}-2\sinh\frac{KT_t}{2}\right)\frac{\partial}{\partial t}\left[l\frac{\partial^2}{\partial l^2}\left(2\frac{\partial v}{\partial l}+\frac{v-w\cot\gamma}{l}\right)+3\frac{\partial^2 v}{\partial l^2}-\cot\gamma\left(\frac{\partial^2 w}{\partial l^2}+\frac{2}{l}\frac{\partial w}{\partial l}\right)\right]+\right.$$

$$\left.+\frac{2\delta}{KT_t}\cot\gamma\sinh\frac{KT_t}{2}\frac{\partial}{\partial t}\left(2\frac{v-w\cot\gamma}{l}+\frac{\partial v}{\partial l}\right)\right\}+$$

$$+\frac{G_0\delta^2\beta T_t}{6}\left[\frac{\partial^2}{l\,\partial l^2}\left(2\frac{\partial v}{\partial l}+\frac{v-w\cot\gamma}{l}\right)+3\frac{\partial^2 v}{\partial l^2}-\cot\gamma\left(\frac{\partial^2 w}{\partial l^2}+\frac{2}{l}\frac{\partial w}{\partial l}\right)\right]+$$

$$+2G_0\delta\left(1-\frac{\beta T_t}{2}\right)\left(\frac{\partial v}{\partial l}+2\frac{v-w\cot\gamma}{l}\right)\cot\gamma+\frac{6\alpha\eta_0 e^{-\frac{KT_t}{2}}}{KT_t}\delta\cot\gamma\left(e^{-\frac{KT_t}{2}}-\frac{2}{KT_t}\sinh\frac{KT_t}{2}\right)\frac{\partial T_t}{\partial t}-$$

$$-G_0\delta\alpha T_t\cot\gamma\left(3-2\beta T_t\right)+pl=0 \qquad (3.2 - 11)$$

Comparing equations (3.2 - 10) and (3.2 - 11) with the corresponding equations (3.1.1 - 7) and (3.1.1 - 8) which were derived by applying the order of magnitude consideration before the derivation of the governing equations, one finds the first equations are exactly the same while the second equations differed by the terms

$$-2\eta_0 e^{-\frac{KT_t}{2}}\left(\frac{\delta}{KT_t}\right)^2\left(KT_t\cosh\frac{KT_t}{2}-2\sinh\frac{KT_t}{2}\right)\cot\gamma\frac{\partial}{\partial t}\left(\frac{\partial^2 w}{\partial l^2}+\frac{2}{l}\frac{\partial w}{\partial l}\right)-\frac{G_0\delta^2\beta T_t\cot\gamma}{6}\left(\frac{\partial^2 w}{\partial l^2}+\frac{2}{l}\frac{\partial w}{\partial l}\right)$$

From a mathematical point of view, the solutions of equations (3.2 - 10) and (3.2 - 11) will a better approximation than that of equations (3.1.1 - 7) and (3.1.1 - 8), provided that both sets of equations can be solved analytically. However, it has been found that in this case the governing equations are not as readily solvable as in the former case. Some efforts have been spent to simplify the governing equations. The results are presented here.

$$\frac{\partial}{\partial t}\left[\frac{\partial}{\partial l}(lU)-2U+3V\right]+F_1\left[\frac{\partial}{\partial l}(lU)-2U+3V\right]=0 \qquad (3.2 - 12)$$

$$F_5\frac{\partial}{\partial t}\left\{\frac{\partial}{\partial l}\left[l\frac{\partial V}{\partial l}+\frac{\partial l(U-V)}{\partial l}\right]+\frac{U-3V}{l}\right\}+F_6\left\{\frac{\partial}{\partial l}\left[l\frac{\partial V}{\partial l}+\frac{\partial l(U-V)}{\partial l}\right]+\frac{U-3V}{l}\right\}+$$

$$+\frac{\partial}{\partial t}(2U-3V)+F_1(2U-3V)+F_3\,pl=F_4 \qquad (3.2 - 13)$$

where

$$U=2\frac{\partial v}{\partial l}+\frac{1}{l}\left(v-w\cot\gamma\right)$$

$$V=\frac{\partial v}{\partial l}$$

$$F_5 = 2\delta \tan\gamma \left[\frac{1}{2}\,\frac{1+e^{-KT_t}}{1-e^{-KT_t}} - \frac{1}{KT_t}\right] \quad , \quad F_6 = \frac{G_0 \delta \beta K T_t^2 \tan\gamma}{6\eta_0 (1-e^{-KT_t})}$$

and F_1, F_3, F_4 are defined in paragraph 3.1.2.

3.3 Constant Property Method

Although the main interest of this analysis is concerned with shells which have temperature dependent material properties, a crude approximation however, can be made by assigning properties at some arbitrary constant temperature, say the middle surface temperature, and then treat the problem as a temperature-independent one.

3.3.1 Governing Equations

The equations of equilibrium will be the same as those in paragraph 3.1.1.

$$\left.\begin{aligned} &\frac{\partial(M_\phi \ell)}{\partial \ell} - M_\theta - Q_\phi \ell = 0 \\ &\frac{\partial(N_\phi \ell)}{\partial \ell} = N_\theta \\ &\frac{\partial(Q_\phi \ell)}{\partial \ell} + N_\theta \cot\gamma + p\ell = 0 \end{aligned}\right\} \qquad (3.3.1 - 1)$$

The strain components remain as

$$\left.\begin{aligned} \sigma_{\phi\xi} &= 2\left(\eta \frac{\partial}{\partial t} + G\right)\left(2\epsilon_{\phi\xi} + \epsilon_{\theta\xi} - 3\alpha T\right) \\ \sigma_{\theta\xi} &= 2\left(\eta \frac{\partial}{\partial t} + G\right)\left(2\epsilon_{\theta\xi} + \epsilon_{\phi\xi} - 3\alpha T\right) \end{aligned}\right\} \qquad (3.3.1 - 2)$$

except, here η, G, and α are constants. Temperature profile across the shell thickness is assumed to be the same as given in paragraph 3.1.1, i.e., $T = (\frac{1}{2} - \xi/\delta) T_t$.

Using the strain-displacement relations as

$$\left.\begin{aligned} \epsilon_{\phi\xi} &= \frac{\partial v}{\partial \ell} - \frac{\partial^2 w}{\partial \ell^2}\xi \\ \epsilon_{\theta\xi} &= \frac{v - w\cot\gamma}{\ell} - \frac{\xi}{\ell}\frac{\partial w}{\partial \ell} \end{aligned}\right\} \qquad (3.3.1 - 3)$$

In this method, the procedure may follow that given by Timoshenko[25].

Introducing

$$\psi = \frac{\partial w}{\partial \ell}$$

the moments can be written

$$M_\phi = -2\delta^3\left(\eta\frac{\partial}{\partial t}+G\right)\left[\frac{1}{12}\frac{\chi}{l}+\frac{1}{6}\frac{\partial\chi}{\partial l}-\frac{\alpha T_t}{4\delta}\right]$$

$$M_\theta = -2\delta^3\left(\eta\frac{\partial}{\partial t}+G\right)\left[\frac{1}{6}\frac{\chi}{l}+\frac{1}{12}\frac{\partial\chi}{\partial l}-\frac{\alpha T_t}{4\delta}\right] \qquad (3.3.1 - 4)$$

The value of N_ϕ is derived from equation (2.1 - 4) as follows

$$2\pi l \sin\gamma\, N_\phi \cot\gamma + 2\pi l\, Q_\phi \sin^2\gamma + \pi\left(l^2 \sin^2\gamma\right)p = 0$$

or

$$N_\phi = -Q_\phi \tan\gamma - \frac{pl\sin\gamma}{2\cos\gamma} = -\left(Q_\phi + \frac{pl}{2}\right)\tan\gamma \qquad (3.3.1 - 5)$$

From the third equilibrium equation of (3.3.1 - 1), N_θ is:

$$N_\theta = -\left(\frac{\partial(Q_\phi l)}{\partial l} + pl\right)\tan\gamma \qquad (3.3.1 - 6)$$

Combination of equations (3.3.1 - 4) through (3.3.1 - 6) and the introduction of the new variable $W = Q_\phi l \tan\gamma$ yields the first governing differential equation

$$\frac{\partial^3\chi}{\partial t\partial l^2}+\frac{G}{\eta}\frac{\partial^2\chi}{\partial l^2}+\frac{1}{l}\frac{\partial^2\chi}{\partial t\partial l}+\frac{G}{\eta l}\frac{\partial\chi}{\partial l}-\frac{1}{l^2}\frac{\partial\chi}{\partial t}-\frac{G}{\eta l^2}\chi = \frac{3\cot\gamma}{\eta\delta^3}\frac{W}{l}-\frac{3}{2}\frac{\alpha}{\delta}\frac{\partial^2 T_t}{\partial t\partial l}-\frac{3\alpha G}{2\eta\delta}\frac{\partial T_t}{\partial l} \qquad (3.3.1 - 7)$$

The integrated equation of state in paragraph 2.2

$$E_{ij} = \frac{e^{-\frac{G}{\eta}t}}{2\eta}\int_0^t S_{ij}\, e^{\frac{G}{\eta}t}\,dt \qquad (3.3.1 - 8)$$

may be used to derive the strain components. They are

$$\epsilon_{\phi\phi} = \frac{e^{-\frac{G}{\eta}t}}{6\eta}\int_0^t\left(2\sigma_{\phi\phi}-\sigma_{\theta\theta}\right)e^{\frac{G}{\eta}t}\,dt + \alpha T \qquad (3.3.1 - 9)$$

and

$$\epsilon_{\theta\theta} = \frac{e^{-\frac{G}{\eta}t}}{6\eta}\int_0^t\left(2\sigma_{\theta\theta}-\sigma_{\phi\phi}\right)e^{\frac{G}{\eta}t}\,dt + \alpha T \qquad (3.3.1 - 10)$$

The new variable χ may be also written in terms of the strain components.

$$\chi = \left(\epsilon_{\phi\phi}-\epsilon_{\theta\theta}\right)\tan\gamma - l\tan\gamma\,\frac{\partial\epsilon_{\theta\theta}}{\partial l} \qquad (3.3.1 - 11)$$

Combining equations (3.3.1 - 5), (3.3.1 - 6), and (3.3.1 - 9) through (3.3.1 -10), one may write the second governing differential equation as

$$\frac{\partial^2 W}{\partial l^2}+\frac{1}{l}\frac{\partial W}{\partial l}-\frac{W}{l^2}=\frac{3\eta\delta}{l}\cot\gamma\left(\frac{\partial\chi}{\partial t}+\frac{G}{\eta}\chi\right)+\frac{3\eta\delta\alpha}{2}\left(\frac{\partial^2 T_t}{\partial t\partial l}+\frac{G}{\eta}\frac{\partial T_t}{\partial l}\right)-\frac{3p\tan\gamma}{2} \qquad (3.3.1 - 12)$$

Equations (3.3.1 - 7) and (3.3.1 - 12) are now the governing equations of the thermal viscoelastic conical shell of temperature independent properties.

3.3.2 Method of Solving and Solution

From equation (3.3.1 - 7) the variable W may be expressed in terms of χ and its derivatives.

$$W=-\frac{\delta^3\eta}{3}\tan\gamma\left[l\frac{\partial^3\chi}{\partial t\partial l^2}+\frac{G}{\eta}l\frac{\partial^2\chi}{\partial l^2}+\frac{\partial^2\chi}{\partial t\partial l}+\frac{G}{\eta}\frac{\partial\chi}{\partial l}-\frac{1}{l}\frac{\partial\chi}{\partial t}+\frac{G}{\eta}\frac{\chi}{l}-\frac{3\alpha l}{2\delta}\frac{\partial^2 T_t}{\partial t\partial l}+\frac{3G\alpha l}{2\eta\delta}\frac{\partial T_t}{\partial l}\right] \qquad (3.3.2 - 1)$$

After computing derivatives of W with respect to l and substituting the results into equation (3.3.1 - 12), one obtains the fifth order partial differential equation

$$l\frac{\partial^5\chi}{\partial t\partial l^4}+4\frac{\partial^4\chi}{\partial t\partial l^3}+\frac{G}{\eta}l\frac{\partial^4\chi}{\partial l^4}+4\frac{G}{\eta}\frac{\partial^3\chi}{\partial l^3}+\frac{9\cot^2\gamma}{\delta^2 l}\left(\frac{\partial\chi}{\partial t}+\frac{G}{\eta}\chi\right)=$$

$$=\frac{9}{2}\frac{p}{\delta^3\eta}-\frac{9\alpha\cot\gamma}{2\delta^2}\left[\frac{\partial^2 T_t}{\partial t\partial l}+\frac{G}{\eta}\frac{\partial T_t}{\partial l}\right]-\frac{3}{2}\frac{\alpha l}{\delta}\frac{\partial^3}{\partial l^3}\left(\frac{\partial T_t}{\partial t}+\frac{G}{\eta}T_t\right)-\frac{9}{2}\frac{\alpha}{\delta}\frac{\partial^2}{\partial l^2}\left(\frac{\partial T_t}{\partial t}+\frac{G}{\eta}T_t\right) \qquad (3.3.2 - 2)$$

It is easily seen that T_t in this method of analysis has much more flexibility; it may vary with the time t as well as with the shell element length l; i.e., $T_t = T_t(l,t)$. For uniform outer-surface temperature $\partial T_t/\partial l = 0$; and for steady state thermal load $\partial T_t/\partial t = 0$. Method of the separation of variables may be used to separate equation (3.3.2 - 2) into two ordinary differential equations; a first order equation with respect to time, and a fourth order equation with respect to the shell element length. The complementary equation of the fourth order equation may be further separated into two Bessel equations. Their solutions are the Bessel functions of the first kind and the second kind in complex variables, which can be expressed in ber, bei, kei, ker functions. With the choice of $[(\delta/9)\tan^2\gamma l]$ as a particular solution, the complete solution for uniform and steady load condition may be readily written as follows

$$
\left.
\begin{aligned}
\psi &= \left[A_1\left(Z_1+\frac{2Z_2'}{y}\right)+A_2\left(Z_2-\frac{2Z_1'}{y}\right)+A_3\left(Z_3+\frac{2Z_4'}{y}\right)+A_4\left(Z_4-\frac{2Z_3'}{y}\right)+\frac{\delta^2}{9}\tan^2\gamma\,\ell\right]\left[A_0 e^{-\frac{G}{\eta}t}+\frac{9\rho}{2G\delta^3}\right]\\
Q_\phi &= -54\frac{\rho}{\delta^2}\cot^2\gamma\left[A_1\left(-\frac{2Z_1'}{y^3}+\frac{Z_2}{y^2}\right)+A_2\left(-\frac{2Z_2'}{y^3}-\frac{Z_1}{y^2}\right)+A_3\left(-\frac{2Z_3'}{y^3}+\frac{Z_4}{y^2}\right)+A_4\left(-\frac{2Z_4'}{y^3}-\frac{Z_3}{y^2}\right)\right]\\
N_\theta &= 27\frac{\rho}{\delta^2}\cot\gamma\left[A_1\left(\frac{4Z_1'}{y^3}-\frac{2Z_2}{y^2}+\frac{Z_2'}{y}\right)+A_2(\cdots)+A_3(\cdots)+A_4(\cdots)\right]-\rho\ell\tan\gamma\\
N_\phi &= 54\frac{\rho}{\delta^2}\cot\gamma\left[A_1\left(-\frac{2Z_1'}{y^3}+\frac{Z_2}{y^2}\right)+A_2(\cdots)+A_3(\cdots)+A_4(\cdots)\right]-\frac{\rho\ell\tan\gamma}{2}\\
M_\theta &= -\frac{9}{2}\frac{\rho}{\delta}\cot\gamma\left[A_1\left(\frac{Z_1'}{y}+\frac{2Z_1}{y^2}+\frac{4Z_2'}{y^3}\right)+A_2(\cdots)+A_3(\cdots)+A_4(\cdots)\right]-\frac{\rho\delta^2\tan^2\gamma}{4}+\frac{G\delta^2\alpha T_t}{2}\\
M_\phi &= -9\frac{\rho}{\delta}\cot\gamma\left[A_1\left(\frac{Z_1'}{y}-\frac{Z_1}{y^2}-\frac{2Z_2'}{y^3}\right)+A_2(\cdots)+A_3(\cdots)+A_4(\cdots)\right]-\frac{\rho\delta^2\tan^2\gamma}{4}+\frac{G\delta^2\alpha T_t}{2}
\end{aligned}
\right\}
$$

(3.3.2 - 3)

where

$$Z_1(y) = \mathrm{ber}\, y \qquad Z' = \frac{dZ}{dy}$$

$$Z_2(y) = -\mathrm{bei}\, y$$

$$Z_3(y) = -\frac{2}{\pi}\mathrm{kei}\, y$$

$$Z_4(y) = -\frac{2}{\pi}\mathrm{ker}\, y$$

and

$$y^2 = \frac{12\cot\gamma}{\delta}\ell$$

A_0, A_1, A_2, A_3, and A_4 are to be determined by the boundary conditions. A_0 will be determined by the load condition at the initial time, i.e., $t^o = 0$. The continuity of ψ at $\ell=0$ immediately eliminates A_3 and A_4.

The edge conditions, then, determine the values of A_1 and A_2.

IV. ANALYSIS OF HEMISPHERICAL SHELL

The analysis discussed in this chapter has greater applicability than the title suggests. It may be applied to any spherical shell having a maximum ϕ equals to or less than $\pi/2$.

The method used here is similar to that described in paragraph 3.1, i.e., the simplified strain-displacement relation method. However, it is not suggested that this is the only method, on the contrary, the other

two methods presented in Paragraphs 3.2 and 3.3 may be applied. However, the application will not be discussed to avoid repetition.

4.1 Governing Equations

The independent variable ϕ used in the equations of equilibrium (2.1 - 1 to - 3) could be retained. The values of ρ_1 and ρ_2 are the same and are equal to the radius of the sphere ρ_0. The radius of parallel circles r may be replaced by $\rho_0 \sin\phi$. Hence the equations of equilibrium

$$\frac{\partial(N_\phi \rho_0 \sin\phi)}{\partial\phi} - N_\theta \rho_0 \cos\phi - Q_\phi \rho_0 \sin\phi = 0 \qquad (4.1\text{ -1})$$

$$\sin\phi(N_\phi \rho_0) + N_\theta \rho_0 \sin\phi + \frac{\partial}{\partial\phi}(Q_\phi \rho_0 \sin\phi) + p\rho_0^2 \sin\phi = 0 \qquad (4.1 - 2)$$

$$\frac{\partial(M_\phi \rho_0 \sin\phi)}{\rho_0 \partial\phi} - M_\theta \cos\phi - Q_\phi \rho_0 \sin\phi = 0 \qquad (4.1 - 3)$$

To eliminate $Q_\phi \rho_0 \sin\phi$, (4.1 - 1) is differentiated with respect to ϕ and is added to equation (4.1 - 2). Thus

$$\frac{\partial^2 N_\phi}{\partial\phi^2} + \left(2\frac{\partial N_\phi}{\partial\phi} - \frac{\partial N_\theta}{\partial\phi}\right)\cot\phi + 2N_\theta + p\rho_0 = 0 \qquad (4.1 - 4)$$

Subtraction of equation (4.1 - 1) from equation (4.1 - 3) yields

$$\frac{\partial M_\phi}{\partial\phi} - \rho_0\frac{\partial N_\phi}{\partial\phi} + (M_\phi - M_\theta)\cot\phi + \rho_0(N_\theta - N_\phi)\cot\phi = 0 \qquad (4.1 - 5)$$

The two equations of equilibrium (4.1 - 4 and 4.1 - 5) are then used. Consequently, the expressions for N_θ, N_ϕ, M_θ and M_ϕ are the same as those of equations (3.1.1 - 5) through (3.1.1 - 8). Substitution of the latter equations into equations (4.1 - 4) and (4.1 - 5) yields two governing differential equations

$$\frac{2\eta_0}{kT_t}\left(1-e^{-kT_t}\right)\left[\frac{\partial^3(2\epsilon_{\phi m}+\epsilon_{\theta m})}{\partial^2\phi\,\partial t} + 3\cot\phi\frac{\partial^2\epsilon_{\phi m}}{\partial\phi\,\partial t} + 2\frac{\partial(2\epsilon_{\theta m}+\epsilon_{\phi m})}{\partial t}\right] +$$

$$+ 2G_0\left(1-\frac{\beta T_t}{2}\right)\left[\frac{\partial^2(2\epsilon_{\phi m}+\epsilon_{\theta m})}{\partial\phi^2} + 3\cot\phi\frac{\partial\epsilon_{\phi m}}{\partial\phi} + 2(2\epsilon_{\theta m}+\epsilon_{\phi m})\right] + \frac{p\rho_0}{\delta} =$$

$$= 2G_0\alpha T_t(3-2\beta T_t) + 12\eta_0\alpha\frac{\partial T_t}{\partial t}\left[\frac{e^{-kT_t}}{kT_t} + \frac{1-e^{-kT_t}}{(kT_t)^2}\right] \qquad (4.1 - 6)$$

and

$$\frac{\partial^2(2\epsilon_{\phi m}+\epsilon_{\theta m})}{\partial t\,\partial\phi} + \cot\phi\,\frac{\partial(\epsilon_{\phi m}-\epsilon_{\theta m})}{\partial t} + \tilde{F}_1\left[\frac{\partial(2\epsilon_{\phi m}+\epsilon_{\theta m})}{\partial\phi} + \cot\phi(\epsilon_{\phi m}-\epsilon_{\theta m})\right] = 0 \qquad (4.1 - 7)$$

where

$$\tilde{F}_1 = \frac{G_0 K T_t\left[\beta T_t\left(\rho_0+\frac{\delta}{6}\right)-2\rho_0\right]}{2\eta_0\left[\left(\rho_0+\frac{\delta}{KT_t}\right)\left(e^{-KT_t}-1\right)+\frac{\delta}{2}\left(1+e^{-KT_t}\right)\right]} \qquad (4.1 - 7a)$$

4.2 Method of Solution

Introduction of new variables $U = 2\epsilon_{\phi m}+\epsilon_{\theta m}$ and $V = \epsilon_{\phi m}$ into the governing equations (4.1 - 6) and (4.1 - 7) yields

$$\frac{2\eta_0}{KT_t}\left(1-e^{-KT_t}\right)\frac{\partial}{\partial t}\left[\frac{\partial^2 U}{\partial\phi^2}+3\cot\phi\frac{\partial U}{\partial\phi}+2(2U-3V)\right]+2G_0\left(1-\frac{\beta T_t}{2}\right)\left[\frac{\partial^2 U}{\partial\phi^2}+3\cot\phi\frac{\partial U}{\partial\phi}+2(2U-3V)\right]+\frac{p\rho_0}{\delta} =$$

$$= 2G_0\alpha T_t\left(3-2\beta T_t\right)+\frac{12\eta_0\alpha}{KT_t}\,\frac{\partial T_t}{\partial t}\left(e^{-KT_t}+\frac{1-e^{-KT_t}}{KT_t}\right) \qquad (4.2 - 1)$$

and

$$\frac{\partial}{\partial t}\left[\frac{\partial U}{\partial\phi}+\cot\phi(3V-U)\right] + \tilde{F}_1\left[\frac{\partial U}{\partial\phi}+\cot\phi(3V-U)\right] = 0 \qquad (4.2 - 2)$$

Using the method of the separation of variables in equation (4.2 - 2) one finds

$$\frac{\partial U}{\partial\phi}+\cot\phi(3V-U) = \left[\frac{\partial U}{\partial\phi}+\cot\phi(3V-U)\right]_{t=0} e^{-\int_0^t \tilde{F}_1\,dt} \qquad (4.2 - 3)$$

The value of $\left[\partial U/\partial\phi+\cot\phi(3V-U)\right]_{t=0}$ has to be evaluated from the boundary conditions at the initial time, i.e., the temperature profile, the pressure load, the properties of material and the stress and strain induced at t = 0. If it is an elastic shell under pressure load without thermal stress, the analytic solution of elastic hemispherical shell given in various mechanics textbooks can be used to evaluate the initial condition. Thus knowing

$$\left(\epsilon_{\phi m}\right)_{t=0} = \frac{1}{E_i\delta}\left(N_\phi-\nu_i N_\theta\right)_{ELASTIC}$$

and

$$\left(\epsilon_{\theta m}\right)_{t=0} = \frac{1}{E_i\delta}\left(N_\theta-\nu_i N_\phi\right)_{ELASTIC}$$

By the definition of U and V, one writes

$$\left[\frac{\partial U}{\partial \phi} + \cot\phi(3V-U)\right]_{t=0} = \left[\frac{\partial U}{\partial \phi} + \cot\phi(3V-U)\right]_{EL.}$$

$$= \frac{1}{E_i\delta}\left\{\left[(2-\nu_i)\frac{\partial N_\phi}{\partial \phi} + (1-2\nu_i)\frac{\partial N_\theta}{\partial \phi}\right]_{EL.} + (1+\nu_i)(N_\phi - N_\theta)_{EL.}\cot\phi\right\} \qquad (4.2 - 4)$$

E_i and ν_i denote values of E and ν at the initial time.

Equation (4.2 - 1) may be written

$$\frac{2\eta_o(1-e^{-KT_t})}{KT_t}\left\{\frac{\partial}{\partial t}\left[\frac{\partial^2 U}{\partial \phi^2} + 3\cot\phi\frac{\partial V}{\partial \phi} - (3V-U)\right] + \frac{\partial}{\partial t}(3U-3V)\right\} +$$

$$+ 2G_o\left(1-\frac{\beta T_t}{2}\right)\left[\frac{\partial^2 U}{\partial \phi^2} + 3\cot\phi\frac{\partial V}{\partial \phi} - (3V-U) + (3U-3V)\right] + \frac{P\rho_o}{\delta} -$$

$$- 2G_o\alpha T_t(3-2\beta T_t) - \frac{12\eta_o\alpha}{KT_t}\frac{\partial T_t}{\partial t}\left(e^{-KT_t} + \frac{1-e^{-KT_t}}{KT_t}\right) = 0 \qquad (4.2 - 5)$$

By differentiating equation (4.2 - 2) with respect to ϕ and adding to the resulting equation the product of $\cot\phi$ and equation (4.2 - 2) one obtains

$$\frac{\partial}{\partial t}\left[\frac{\partial^2 U}{\partial \phi^2} + 3\cot\phi\frac{\partial V}{\partial \phi} - (3V-U)\right] = -\tilde{F}_1\left[\frac{\partial^2 U}{\partial \phi^2} + 3\cot\phi\frac{\partial V}{\partial \phi}(3V-U)\right] \qquad (4.2 - 6)$$

Substituting equation (4.2 - 4) into equation (4.2 - 3) and then differentiating with respect to ϕ one finds that

$$\frac{\partial^2 U}{\partial \phi^2} + 3\cot\phi\frac{\partial V}{\partial \phi} - (3V-U) = \left[\frac{\partial^2 U}{\partial \phi^2} + 3\cot\phi\frac{\partial V}{\partial \phi} - (3V-U)\right]_{t=0} e^{-\int_0^t \tilde{F}_1 dt} =$$

$$= \frac{e^{-\int_0^t \tilde{F}_1 dt}}{E_i\delta}\left(\frac{\partial}{\partial \phi} + \cot\phi\right)\left\{\left[(2-\nu_i)\frac{\partial N_\phi}{\partial \phi} + (1-2\nu_i)\frac{\partial N_\theta}{\partial \phi}\right]_{EL.} + \cot\phi(1+\nu_i)(N_\phi - N_\theta)_{EL.}\right\} \qquad (4.2 - 7)$$

Substitution of (4.2 - 6) and (4.2 - 7) into equation (4.2 - 5) yields

$$\frac{\partial(U-V)}{\partial t} + \tilde{F}_3(U-V) + \tilde{F}_2 = 0 \qquad (4.2 - 8)$$

where

$$\tilde{F}_2 = \frac{KT_t}{6\eta_0(1-e^{-KT_t})}\left\{\frac{p_t}{\delta} - 2G_0\alpha T_t(3-2\beta T_t) - 12\eta_0\alpha\frac{\partial T_t}{\partial t}\left(\frac{e^{-KT_t}}{KT_t} + \frac{1-e^{-KT_t}}{(KT_t)^2}\right) + \right.$$

$$\left. + \left[-\frac{2\eta_0(1-e^{-KT_t})}{KT_t}\tilde{F}_1 + 2G_0\left(1-\frac{\beta T_t}{2}\right)\right] e^{-\int_0^t \tilde{F}_1 dt}\left(\frac{\partial}{\partial\phi} + \cot\phi\right)\left[\frac{\partial U}{\partial\phi} + \cot\phi(3V-U)\right]_{t=0}\right\}$$

$$\tilde{F}_3 = \frac{G_0\left(1-\frac{\beta T_t}{2}\right)KT_t}{\eta_0(1-e^{-KT_t})} \qquad (4.2 - 9)$$

The function $\tilde{F}_2$ contains temperature and pressure, material properties, and the strain at the initial time, hence, is a function of time and ϕ .

The first order partial differential equation (4.2 - 8) is readily solvable by the method of separation of variables.

$$U - V = e^{-\int_0^t \tilde{F}_3 dt}\left\{-\int_0^t \tilde{F}_2 e^{\int_0^t \tilde{F}_3 dt} dt + [U-V]_{t=0}\right\}$$

Employing the same techniques as used in the evaluation of $\left[\frac{\partial U}{\partial\phi} + \cot\phi(3V-U)\right]_{t=0}$ it can be shown that

$$[U-V]_{t=0} = \frac{1-\nu_i}{E_i\delta}(N_\phi + N_\theta)_{EL.}$$

Thus

$$V = U - e^{-\int_0^t \tilde{F}_3 dt}\left\{-\int_0^t \tilde{F}_2 e^{\int_0^t \tilde{F}_3 dt} dt + \frac{1-\nu_i}{E_i\delta}(N_\phi + N_\theta)_{EL.}\right\} \qquad (4.2 - 10)$$

Replacing equation (4.2 - 10) for the value of V in equation (4.2 - 3), one writes that

$$\frac{\partial U}{\partial\phi} + 2\cot\phi\, U = \tilde{F}_4 \qquad (4.2 - 11)$$

where

$$\tilde{F}_4 = \frac{e^{-\int_0^t \tilde{F}_1 dt}}{E_i\delta}\left\{(2-\nu_i)\frac{\partial N_\phi}{\partial\phi} + (1-2\nu_i)\frac{\partial N_\theta}{\partial\phi} + \cot\phi(1+\nu_i)(N_\phi + N_\theta)\right\}_{EL.} +$$

$$+ 3\cot\phi\, e^{-\int_0^t \tilde{F}_3 dt}\left\{-\int_0^t \tilde{F}_2 e^{\int_0^t \tilde{F}_3 dt} dt + \frac{1-\nu_i}{E_i\delta}(N_\phi + N_\theta)_{EL.}\right\} \qquad (4.2 - 12)$$

Using the method of separation of variables on equation (4.2 - 11) and integrating one obtains

$$U = -\frac{1}{\sin^2\phi}\int_\phi^{\phi_0} \sin^2\phi\, \tilde{F}_4\, d\phi + \frac{\sin^2\phi_0}{\sin^2\phi}[U]_{\phi=\phi_0}$$

$[U]_{\phi=\phi_0}$ is the value of U at time t and at $\phi=\phi_0$ which is the edge of the shell, consequently it is determined by the edge conditions.

For example, if the edge is of fixed support, then $[U]_{\phi=\phi_0}=0$

With value of U established V can be evaluated from equation (4.2 - 10). The membrane forces and moments are subsequently evaluated by equations (3.1.1 - 5) through (3.1.1 - 8).

V. BENDING ANALYSIS

5.1 General Shell

To more accurately describe the effects of edge conditions the following derivation includes the changes in curvature of the middle surface.

5.1.1 Governing equations

Let $\epsilon_{\phi\xi}=\epsilon_1-\xi\chi_\phi$ and $\epsilon_{\theta\xi}=\epsilon_2-\xi\chi_\theta$ where ϵ_1 and ϵ_2 are the middle surface strains and χ_ϕ and χ_θ are the changes of curvature.

$$\epsilon_1=\frac{1}{\rho_1}\left(\frac{\partial v}{\partial\phi}-w\right) \qquad (5.1.1\text{-}1)$$

$$\epsilon_2=\frac{1}{\rho_2}\left(v\cot\phi-w\right) \qquad (5.1.1\text{-}2)$$

$$\chi_\phi=\frac{1}{\rho_1}\frac{\partial}{\partial\phi}\left[\frac{1}{\rho_1}\left(v+\frac{\partial w}{\partial\phi}\right)\right] \qquad (5.1.1\text{-}3)$$

$$\chi_\theta=\frac{1}{\rho_1}\left(v+\frac{\partial w}{\partial\phi}\right)\frac{\cot\phi}{\rho_2} \qquad (5.1.1\text{-}4)$$

For the Kelvin-Voigt body, the stress-strain relationship is

$$\sigma_{x\xi}=2\left\{\eta_0 e^{-K\left(T_m-\frac{\xi}{\delta}T_t\right)}\frac{\partial(\ldots)}{\partial t}+G_0\left[1-\beta\left(T_m-\frac{\xi}{\delta}T_t\right)\right](\ldots)\right\}\left\{2\epsilon_{x\xi}+\epsilon_{y\xi}-3\alpha\left(T_m-\frac{\xi}{\delta}T_t\right)\right\}$$

Proceeding with the method outlined by Timoshenko[25] where

$$N_\phi=\int_{-\delta/2}^{\delta/2}\sigma_{\phi\xi}\,d\xi$$

$$M_\phi=\int_{-\delta/2}^{\delta/2}\sigma_{\phi\xi}\,\xi\,d\xi$$

then

$$N_\phi = \Gamma(2\epsilon_1+\epsilon_2) - \Lambda(2\chi_\phi+\chi_\theta) - \Gamma(3\alpha T_m) + \Lambda\left(3\alpha\frac{T_t}{\delta}\right)$$

$$M_\phi = \Lambda(2\epsilon_1+\epsilon_2) - \Pi(2\chi_\phi+\chi_\theta) - \Lambda(3\alpha T_m) + \Pi\left(3\alpha\frac{T_t}{\delta}\right)$$

where

$$\Gamma(\cdots) = 4\eta_0 e^{-KT_m}\frac{\delta}{KT_t}\sinh\frac{KT_t}{2}\frac{\partial(\cdots)}{\partial t} + 2G_0(1-\beta T_m)\,\delta(\cdots)$$

$$\Lambda(\cdots) = 4\eta_0 e^{-KT_m}\left(\frac{\delta}{KT_t}\right)^2\left[\frac{KT_t}{2}\cosh\frac{KT_t}{2} - \sinh\frac{KT_t}{2}\right]\frac{\partial(\cdots)}{\partial t} + \frac{1}{6}G_0\beta T_t\,\delta^2(\cdots)$$

$$\Pi(\cdots) = 4\eta_0 e^{-KT_m}\left(\frac{\delta}{KT_t}\right)^3\left\{\left[\left(\frac{KT_t}{2}\right)^2+2\right]\sinh\frac{KT_t}{2} - KT_t\cosh\frac{KT_t}{2}\right\}\frac{\partial(\cdots)}{\partial t} + \frac{1}{6}G_0(1-\beta T_m)\,\delta^3(\cdots)$$

Assuming T_m and T_t independent of ℓ then

$$3\Gamma\left(\frac{\partial v}{\partial\phi} - w\right) = \rho_1(2N_\phi - N_\theta) + \Lambda\left[\frac{\partial}{\partial\phi}\left(\frac{v}{\rho_1} + \frac{1}{\rho_1}\frac{\partial w}{\partial\phi}\right)\right] - \Gamma(3\alpha T_m) + \Lambda\left(3\alpha\frac{T_t}{\delta}\right) \qquad (5.1.1\text{-}5)$$

$$3\Gamma(v\cot\phi - w) = \rho_2(2N_\theta - N_\phi) + \Lambda\left[\left(\frac{v}{\rho_1} + \frac{1}{\rho_1}\frac{\partial w}{\partial\phi}\right)\cot\phi\right] - \Gamma(3\alpha T_m) + \Lambda\left(3\alpha\frac{T_t}{\delta}\right) \qquad (5.1.1\text{-}6)$$

Eliminating w from equations (5.1.1-5) and (5.1.1-6) we have

$$3\Gamma\left(\frac{\partial v}{\partial\phi} - v\cot\phi\right) = \rho_1(2N_\phi - N_\theta) - \rho_2(2N_\theta - N_\phi) + 3\Lambda\left[\frac{\partial}{\partial\phi}\left(\frac{v}{\rho_1} + \frac{1}{\rho_1}\frac{\partial w}{\partial\phi}\right) - \cot\phi\left(\frac{v}{\rho_1} + \frac{1}{\rho_1}\frac{\partial w}{\partial\phi}\right)\right] \qquad (5.1.1\text{-}7)$$

By differentiating equation (5.1.1-6) with respect to ϕ and using equation (5.1.1-7) to eliminate $\partial v/\partial\phi$ then

$$3\Gamma\left(v + \frac{\partial w}{\partial\phi}\right) = \rho_1\cot\phi(2N_\phi - N_\theta) - \rho_2\cot\phi(2N_\theta - N_\phi) - \\ - \frac{\partial}{\partial\phi}\left[\rho_2(2N_\theta - N_\phi)\right] + 3\Lambda\left[\frac{v}{\rho_1} + \frac{1}{\rho_1}\frac{\partial w}{\partial\phi}\right] \qquad (5.1.1\text{-}8)$$

Let $V = 1/\rho_1\left(v + \partial w/\partial\phi\right)$ and $U = Q_\phi\rho_2$ then, from the equations of equilibrium for p = 0,

$$N_\phi = -\frac{1}{\rho_2}U\cot\phi$$

$$N_\theta = -\frac{1}{\rho_1}\frac{\partial U}{\partial\phi}$$

With the above, equation (5.1.1-8) becomes the first governing equation.

$$-\frac{s}{2}\left[\Gamma(V)-\frac{1}{\rho_1}\Lambda(V)\right]=\frac{\rho_2}{\rho_1^2}\frac{\partial^2 U}{\partial\phi^2}+\frac{1}{\rho_1}\left[\frac{d}{d\phi}\left(\frac{\rho_2}{\rho_1}\right)+\frac{\rho_2}{\rho_1}\cot\phi\right]\frac{\partial U}{\partial\phi}-\frac{1}{\rho_1}\left[\frac{\rho_1}{\rho_2}\cot^2\phi-\frac{1}{2}\right]U$$

(5.1.1-9)

To obtain the second governing equation, substitute the expressions for M_ϕ and M_θ into the equation of equilibrium

$$\frac{\partial}{\partial\phi}\left(\rho_2 M_\phi \sin\phi\right)-\rho_1\cos\phi\, M_\theta-\rho_1\sin\phi\, U=0$$

then

$$-2\sin\phi\,\Pi\left\{\frac{\rho_2}{\rho_1^2}\frac{\partial^2 V}{\partial\phi^2}+\frac{1}{\rho_1}\left[\frac{\rho_2}{\rho_1}\cot\phi+\frac{d}{d\phi}\left(\frac{\rho_2}{\rho_1}\right)\right]\frac{\partial V}{\partial\phi}-\frac{1}{\rho_1}\left[\frac{\rho_1}{\rho_2}\cot^2\phi+\frac{1}{2}\right]V\right\}+$$
$$+\frac{1}{\rho_1}\Lambda\left\{\frac{\partial}{\partial\phi}\left[\rho_2\sin\phi\left(2\epsilon_1+\epsilon_2\right)-\rho_1\cos\phi\left(2\epsilon_2+\epsilon_1\right)\right]\right\}=U\sin\phi$$

(5.1.1-10)

To eliminate the middle surface strains from (5.1.1-10) consider the following equation of equilibrium

$$\frac{\partial}{\partial\phi}\left(\rho_2 N_\phi\sin\phi\right)-N_\theta\,\rho_1\cos\phi-U\sin\phi=0$$

(5.1.1-11)

Substituting the expressions for N_ϕ and N_θ into (5.1.1-11) we have

$$\frac{1}{\rho_1}\Lambda\left\{\frac{\partial}{\partial\phi}\left[\rho_2\sin\phi\left(2\epsilon_1+\epsilon_2\right)\right]-\rho_1\cos\phi\left(2\epsilon_2+\epsilon_1\right)\right\}=2\sin\phi\,\Lambda\left\{\frac{1}{\Gamma}\left[\Lambda\left(\frac{\rho_2}{\rho_1^2}\frac{\partial^2 V}{\partial\phi^2}+\right.\right.\right.$$
$$\left.\left.\left.+\frac{1}{\rho_1}\left[\frac{d}{d\phi}\left(\frac{\rho_2}{\rho_1}\right)+\frac{\rho_2}{\rho_1}\cot\phi\right]\frac{\partial V}{\partial\phi}-\frac{1}{\rho_1}\left[\frac{\rho_1}{\rho_2}\cot^2\phi+\frac{1}{2}\right]V\right)\right]\right\}+\frac{1}{\rho_1}\Lambda\left\{\frac{1}{\Gamma}\left(U\sin\phi\right)\right\}$$

(5.1.1-12)

With equations (5.1.1-10) and (5.1.1-11) we now have the second governing equation

$$-2\Pi\left\{\frac{\rho_2}{\rho_1^2}\frac{\partial^2 V}{\partial\phi^2}+\frac{1}{\rho_1}\left[\frac{d}{d\phi}\left(\frac{\rho_2}{\rho_1}\right)+\frac{\rho_2}{\rho_1}\cot\phi\right]\frac{\partial V}{\partial\phi}-\frac{1}{\rho_1}\left[\frac{\rho_1}{\rho_2}\cot^2\phi+\frac{1}{2}\right]V\right\}+$$
$$+2\Lambda\left\{\frac{1}{\Gamma}\left[\Lambda\left(\frac{\rho_2}{\rho_1^2}\frac{\partial^2 V}{\partial\phi^2}+\frac{1}{\rho_1}\left[\frac{d}{d\phi}\left(\frac{\rho_2}{\rho_1}\right)+\frac{\rho_2}{\rho_1}\cot\phi\right]\frac{\partial V}{\partial\phi}\right.\right.\right.=U-\frac{1}{\rho_1}\Lambda\left\{\frac{1}{\Gamma}\left[U\right]\right\}$$

(5.1.1-13)

Let $L(\ldots) = \frac{\rho_2}{\rho_1^2}\frac{\partial^2(\ldots)}{\partial\phi^2} + \frac{1}{\rho_1}\left[\frac{d}{d\phi}\left(\frac{\rho_2}{\rho_1}\right) + \frac{\rho_2}{\rho_1}\cot\phi\right]\frac{\partial(\ldots)}{\partial\phi} - \frac{1}{\rho_1}\left[\frac{\rho_1}{\rho_2}\cot^2\phi\right](\ldots)$

then the governing equations become

$$-2\Pi\left\{L(V) + \frac{1}{2\rho_1}V\right\} + 2\Lambda\left\{\frac{1}{\Gamma}\left[\Lambda\left(L(V) + \frac{1}{2\rho_1}V\right)\right]\right\} = U - \frac{1}{\rho_1}\Lambda\left\{\frac{1}{\Gamma}(U)\right\} \qquad (5.1.1\text{-}13a)$$

$$L(U) - \frac{1}{2\rho_1}U = \frac{3}{2}\left[\Gamma(V) - \frac{1}{\rho_1}\Lambda(V)\right] \qquad (5.1.1\text{-}9a)$$

5.2 Conical Shell

For the conical shell

$$\rho_2 = \ell \tan\gamma$$

$$\frac{1}{\rho_1} = 0$$

$$\rho_1\partial\phi = \partial\ell$$

then $L(\cdots)$ becomes $L(\cdots) = \tan\gamma\left[\ell\frac{\partial^2(\ldots)}{\partial\ell^2} + \frac{\partial(\ldots)}{\partial\ell} - \frac{1}{\ell}(\ldots)\right]$
and the governing equations are

$$-2\Pi\left\{L(V)\right\} + 2\Lambda\left\{\frac{1}{\Gamma}\left[\Lambda\left\{L(V)\right\}\right]\right\} = U\tan\gamma \qquad (5.2\text{-}1)$$

$$L(U) = \frac{3}{2}\Gamma(V) \qquad (5.2\text{-}2)$$

where U is now $Q_\phi\ell$.
Solving equations (5.2-1) and (5.2-2) for V then

$$-2\Pi\left\{LL(V)\right\} + 2\Lambda\left\{\frac{1}{\Gamma}\left(\Lambda\left[LL(V)\right]\right)\right\} = \frac{3}{2}\Gamma(V) \qquad (5.2\text{-}3)$$

Assuming a product solution $V = \Phi(\ell)T(t)$ then

$$\frac{LL(\Phi)}{\Phi} = \frac{\frac{3}{2}\Gamma(T)}{-2\Pi(T) + 2\Lambda\left\{\frac{1}{\Gamma}\left[\Lambda(T)\right]\right\}} = -\mu^4 \qquad (5.2\text{-}4)$$

where the constant μ^4 must be $\mu^4 = 12(1-\nu^2)/\delta^2$ for the solution to conform to the initial condition.

The solution as a function of l is

$$\Phi(\ell) = C_1\left[Z_1(y) + \frac{2}{y}Z_2'(y)\right] + C_2\left[Z_2(y) - \frac{2}{y}Z_1'(y)\right]$$

where $y = 2\lambda\sqrt{l}$, $\lambda^4 = \mu^4 \cot^2\gamma$, $Z_1 = \mathrm{BER}(y)$, $Z_2 = -\mathrm{BEI}(y)$, $Z' = \frac{dZ}{dy}$

The equation resulting from (5.2-3) describing the solution as a function of time is a first order differential-integral equation which, when differentiated, yields

$$\left[\frac{3}{2}+A_1-A_2\right]\frac{d^2T}{dt^2}+\left\{\left[(3-A_2)A_3-A_2A_5\right](1-\beta Rt)e^{KRt}+2A_1A_4e^{KRt}-KR\left(\frac{3}{2}+A_1-A_2\right)\right\}\frac{dT}{dt}+$$
$$+\left\{\left[\frac{3}{2}A_3^2-A_2A_3A_5\right](1-\beta Rt)^2e^{2KRt}+\left[\beta RA_2A_5-\frac{3}{2}\beta RA_3\right](1-\beta Rt)e^{KRt}+\right.$$
$$\left.+A_1A_4^2e^{2KRt}\right\}T=0 \qquad (5.2-5)$$

where

$$T_m = Rt$$
$$A_1 = 2\mu^4\left(\frac{\delta}{KT_t}\right)^2\left[\frac{KT_t}{2}\coth\frac{KT_t}{2}-1\right]^2$$
$$A_2 = 2\mu^4\left(\frac{\delta}{KT_t}\right)^2\left[\left(\frac{KT_t}{2}\right)^2+2-KT_t\coth\frac{KT_t}{2}\right]$$
$$A_3 = \frac{G_0KT_t}{2\eta_0\sinh\frac{KT_t}{2}}$$
$$A_4 = G_0\beta T_t(KT_t)^2\Big/24\eta_0\left[\frac{KT_t}{2}\cosh\frac{KT_t}{2}-\sinh\frac{KT_t}{2}\right]$$
$$A_5 = G_0(KT_t)^3\Big/24\eta_0\left\{\left[\left(\frac{KT_t}{2}\right)^2+2\right]\sinh\frac{KT_t}{2}-KT_t\cosh\frac{KT_t}{2}\right\}$$

By expressing the coefficients of T and its derivatives as Taylor series then T(t) may be expressed as a power series

$$T(t) = a_0 + a_1t + a_2t^2 + \cdots + a_nt^n + \cdots$$

where

$$a_2 = -\left(a_1\left[B_2 - KRB_1\right] + a_0\left[B_3 + \beta RB_4\right]\right)\Big/2B_1$$

$$a_3 = -\left(a_1\left[B_2 KR - \beta RA_6\right] + 2a_2\left[B_2 - KRB_1\right] + a_0\left[B_3 2KR - 2\beta RB_5 + \beta RB_4 KR - (\beta R)^2 B_4\right] + a_1\left[B_3 + \beta RB_4\right]\right)\Big/3\cdot 2\,B_1$$

$$\vdots$$

$$a_{n+2} = -\left\{a_1\left[B_2\frac{(KR)^n}{n!} - BRA_6\frac{(KR)^{n-1}}{(n-1)!} + \cdots + (n+1)a_{n+1}\left[B_2 - KRB_1\right] + \right.\right.$$

$$+ a_0\left[B_3\frac{(2KR)^n}{n!} - 2\beta RB_5\frac{(2KR)^{n-1}}{(n-1)!} + (\beta R)^2 B_5\frac{(2KR)^{n-2}}{(n-2)!} + \beta RB_4\frac{(KR)^n}{n!} - (\beta R)^2 B_4\frac{(KR)^{n-1}}{(n-1)!}\right] +$$

$$\left.+ \cdots + a_n\left[B_3 - \beta RB_4\right]\right\}\Big/n(n-1)\,B_1$$

where

$$A_6 = (3-A_2)A_3 - A_2A_5$$
$$B_1 = \tfrac{3}{2} + A_1 - A_2$$
$$B_2 = 2A_1A_4 + (3-A_2)A_3 - A_2A_5$$
$$B_3 = \tfrac{3}{2}A_3^2 - A_2A_3A_5 + A_1A_4^2$$
$$B_4 = A_2A_5 - \tfrac{3}{2}A_3$$
$$B_5 = \tfrac{3}{2}A_3^2 - A_2A_3A_5$$

The first two coefficients (a_0, a_1) are then determined from the particular boundary conditions.

5.2.1 Simplified Conical Shell

Since the programmed temperature rates in the test schedule produced a temperature difference across the thickness of less than one degree, the following analysis neglects the differential ($T_t = 0$).

The operators defined in section 5.1.1 become

$$\Gamma(\cdots) = 2\left\{\eta_0 e^{-KT_m}\frac{\partial(\ldots)}{\partial t} + G_0(1-\beta T_m)(\ldots)\right\}\delta$$
$$\Lambda(\cdots) = 0$$
$$\Pi(\cdots) = 2\left\{\eta_0 e^{-KT_m}\frac{\partial(\ldots)}{\partial t} + G_0(1-\beta T_m)(\cdots)\right\}\delta^3/12$$

Let $\Gamma(\cdots) = 2\left\{\eta_0 e^{-kT_m}\frac{\partial(\ldots)}{\partial t} + G_0(1-\beta T_m)(\cdots)\right\}$, then equation (5.2-3) becomes

$$\frac{\delta^3}{6}\Gamma\left[LL(\nabla)\right] = -\frac{3}{2}\delta\Gamma(\nabla) \tag{5.2.1-1}$$

then, with a product solution, $\nabla = \Phi(\ell)T(t)$ we have

$$\Gamma(T)\left\{LL(\nabla) + \frac{9}{\delta^2}\Phi\right\} = 0 \tag{5.2.1-2}$$

where Φ is the same as that in section 5.2 and T(t) must be determined from the boundary conditions.

5.2.2 Boundary Conditions

Consider the edge of the shell fixed against rotation and expansion, then at $\ell = \ell_0$

$$\nabla = 0 \quad \text{FOR ALL } t \tag{5.2.2-1}$$

$$\epsilon_2 = \frac{\partial \epsilon_2}{\partial t} = 0 \quad \text{FOR ALL } t \tag{5.2.2-2}$$

Then

$$\nabla_{\ell=\ell_0} = 0 = \left[Z_{10} + \frac{2}{\gamma_0}Z'_{20} + A_0\left(Z_{20} - \frac{2}{\gamma_0}Z'_{10}\right)\right]T(t)$$

so

$$A_0 = -\left(Z_{10} + \frac{2}{\gamma_0}Z'_{20}\right)\Big/\left(Z_{20} - \frac{2}{\gamma_0}Z'_{10}\right)$$

Also

$$3\delta\Gamma(\epsilon_2) = 2N_\theta - N_\phi + 3\delta\Gamma(\alpha T_m) \tag{5.2.2-3}$$

where $N_\phi = 6\delta \cot\gamma \left[\frac{Z_2}{y^2} - \frac{2Z_1'}{y^3} + A_0\left(-\frac{Z_1}{y^2} - \frac{2Z_2'}{y^3}\right)\right]\Gamma(T) - p\ell \tan\gamma/2$

$$N_\theta = 3\delta \cot\gamma \left[\frac{Z_2'}{y} - \frac{2Z_2}{y^2} + \frac{4Z_1'}{y^3} + A_0\left(-\frac{Z_1'}{y} + \frac{2Z_1}{y^2} + \frac{4Z_2'}{y^3}\right)\right]\Gamma(T) - p\ell \tan\gamma$$

Applying equation 5.2.2-2 then

$$\Gamma(T) = \frac{\frac{3}{2} p\ell_0 \tan\gamma - 6\alpha\delta\left[\eta_0 e^{-KT_m}\frac{\partial T_m}{\partial t} + G_0(1-\beta T_m)T_m\right]}{6\delta \cot\gamma\left[\frac{Z_{20}'}{y_0} - \frac{3Z_{20}}{y_0^2} + \frac{6Z_{10}'}{y_0^3} + \left(-\frac{Z_{10} + \frac{2}{y_0}Z_{20}'}{Z_{20} - \frac{2}{y_0}Z_{10}'}\right)\left(-\frac{Z_{10}'}{y_0} + \frac{3Z_{10}}{y_0^2} + \frac{6Z_{20}'}{y_0^3}\right)\right]}$$

The inner surface stresses are then written as

$$\sigma_\phi = \frac{N_\phi}{\delta} + \frac{6}{\delta^2}M_\phi = 6\cot\gamma\left[\frac{Z_2}{y^2} - \frac{2Z_1'}{y^3} + A_0\left(-\frac{Z_1'}{y^2} - \frac{2Z_2'}{y^3}\right)\right]\Gamma(T) - p\ell\tan\gamma/2 -$$

$$- 6\cot\gamma\left[\frac{Z_1'}{y} - \frac{Z_1}{y^2} - \frac{2Z_2'}{y^3} + A_0\left(\frac{Z_2'}{y} - \frac{Z_2}{y^2} + \frac{2Z_1'}{y^3}\right)\right]\Gamma(T)$$

$$\sigma_\theta = \frac{N_\theta}{\delta} + \frac{6}{\delta^2}M_\theta = 3\cot\gamma\left[\frac{Z_2'}{y} - \frac{2Z_2}{y^2} + \frac{4Z_1'}{y^3} + A_0\left(-\frac{Z'}{y} + \frac{2Z_1}{y^2} + \frac{4Z_2'}{y^3}\right)\right]\Gamma(T) -$$

$$- p\ell\tan\gamma - 3\cot\gamma\left[\frac{Z_1'}{y} + \frac{2Z_1}{y^2} + \frac{4Z_2'}{y^3} + A_0\left(\frac{Z_2'}{y} + \frac{2Z_2}{y^2} - \frac{4Z_1'}{y^3}\right)\right]\Gamma(T)$$

(5.2.2-4)

Consider, now, thehinged expansion edge; that is, an edge free to rotate completely and to expand to some degree.

Then, at $\ell = \ell_0$

$$M_\phi = 0 \quad \text{FOR ALL } t \qquad (5.2.2\text{-}5)$$

$$\epsilon_2 = \alpha_e T_c \qquad (5.2.2\text{-}6)$$

where $\alpha_e T_c$ denotes the expansion of the mount. So with

$$M_\phi = -\frac{\delta^3}{12}\left\{4\lambda^2\left[\frac{Z_1'}{y} - \frac{Z_1}{y^2} - \frac{2Z_2'}{y^3} + A_0\left(\frac{Z_2'}{y} - \frac{Z_2}{y^2} + \frac{2Z_1'}{y^3}\right)\right]\right\}\Gamma(T)$$

then with (5.2.2-6)

$$A_0 = -\frac{\frac{Z_{10}'}{y_0} - \frac{Z_{10}}{y_0^2} - \frac{2Z_{20}'}{y_0^3}}{\frac{Z_{20}'}{y_0} - \frac{Z_{20}}{y_0^2} + \frac{2Z_{10}'}{y_0^3}}$$

Applying equations (5.2.2-3) and (5.2.2-6) then

$$\Gamma(T) = \frac{\frac{3}{2} P l_0 \tan\gamma - 6\delta\left[\eta_0 e^{-KT_m}\frac{\partial}{\partial t}(\alpha T_m - \alpha_e T_e) + G_0(1-\beta T_m)(\alpha T_m - \alpha_e T_e)\right]}{6\delta_c \cot\gamma \left[\frac{Z'_{20}}{y_0} - \frac{3Z_{20}}{y_0^2} + \frac{6Z'_{10}}{y_0^3} + A_0\left(-\frac{Z'_{10}}{y_0} + \frac{3Z_{10}}{y_0^2} + \frac{6Z'_{20}}{y_0^3}\right)\right]}$$

5.3 Spherical Shell

Neglecting, again, the temperature differential, equations (5.1.1-9a) and (5.1.1-13a) become, for the spherical shell of radius a,

$$L(U) - \frac{1}{2a}U = \frac{3}{2}\delta\Gamma(V) \qquad (5.3\text{-}1)$$

$$-\frac{\delta^3}{6}\Gamma\left\{L(V) + \frac{1}{2a}V\right\} = U \qquad (5.3\text{-}2)$$

where $L(\ldots) = \frac{1}{a}\left[\frac{\partial^2(\ldots)}{\partial\phi^2} + \cot\phi\frac{\partial(\ldots)}{\partial\phi} - \cot^2\phi(\ldots)\right]$

The exact solution of equations (5.3-1) and (5.3-2) is a form of the hypergeometrical series whose convergence is unsatisfactory for $\sqrt{a/\delta} > 10$. The following solution will be an approximation developed by Timoshenko[25] for shells whose angle is not small.

Let $Q_1 = Q_\phi\sqrt{\sin\phi}$ and $V_1 = V\sqrt{\sin\phi}$ then the first derivatives in equations (5.3-1) and (5.3-2) disappear. Neglecting the quantity in comparison with its second derivative we have

$$\frac{\partial^2 Q_1}{\partial\phi^2} = \frac{3}{2}\delta\Gamma(T) \qquad (5.3\text{-}3)$$

$$\frac{\partial^2(\Gamma V_1)}{\partial\phi^2} = -\frac{6a^2}{\delta^3}Q_1 \qquad (5.3\text{-}4)$$

the solution of which is

$$Q_\phi = e^{-\lambda\psi}\left[\sin(\xi-\psi)\right]^{-\frac{1}{2}}\sin(\lambda\psi+\gamma)T(t) \qquad (5.3\text{-}5)$$

where $\psi = \xi - \phi$, ξ is the shell half angle (not small), $\lambda^4 = \frac{9a^2}{4\delta^2}$ and γ is an arbitrary constant.

Then

$$N_\phi = -e^{-\lambda\psi}\left[\sin(\varsigma-\psi)\right]^{-\frac{1}{2}}\cot(\varsigma-\psi)\sin(\lambda\psi+\gamma)T(t)-\frac{Pa}{2}$$

$$N_\theta = \frac{\lambda}{2\delta}e^{-\lambda\psi}\left[\sin(\varsigma-\psi)\right]^{-\frac{1}{2}}\left[2\cos(\lambda\psi+\gamma)-\left\{2-\frac{1}{\lambda}\cot(\varsigma-\psi)\right\}\sin(\lambda\psi+\gamma)\right]T(t)-\frac{Pa}{2}$$

$$M_\phi = \frac{a}{2\lambda}e^{-\lambda\psi}\left[\sin(\varsigma-\psi)\right]^{-\frac{1}{2}}\left[\cos(\lambda\psi+\gamma)+\sin(\lambda\psi+\gamma)\right]T(t)$$

$$M_\theta = \frac{a}{4\lambda}e^{-\lambda\psi}\left[\sin(\varsigma-\psi)\right]^{-\frac{1}{2}}\left[\left\{1+\frac{3}{2}\cot(\varsigma-\psi)\right\}\cos(\lambda\psi+\gamma)+\sin(\lambda\psi+\gamma)\right]T(t)$$

Employing the fixed edge conditions on a hemisphere the inner surface stresses are then

$$\sigma_\phi = -\frac{e^{-\lambda\psi}\cot(\frac{\pi}{2}-\psi)}{\delta\sqrt{\sin(\frac{\pi}{2}-\psi)}}\sin(\lambda\psi+\frac{\pi}{2})T(t)-\frac{Pa}{2\delta}+\frac{3a}{\delta^2\lambda}\frac{e^{-\lambda\psi}}{\sqrt{\sin(\frac{\pi}{2}-\psi)}}\left[\cos(\lambda\psi+\frac{\pi}{2})+\sin(\lambda\psi+\frac{\pi}{2})\right]T(t)$$

$$\sigma_\theta = \frac{\lambda e^{-\lambda\psi}}{2\delta\sqrt{\sin(\frac{\pi}{2}-\psi)}}\left[2\cos(\lambda\psi+\frac{\pi}{2})-\left\{2-\frac{1}{\lambda}\cot(\frac{\pi}{2}-\psi)\right\}\sin(\lambda\psi+\frac{\pi}{2})\right]T(t)-\frac{Pa}{2\delta}+$$

$$+\frac{3a}{2\delta^2\lambda}\frac{e^{-\lambda\psi}}{\sqrt{\sin(\frac{\pi}{2}-\psi)}}\left\{\left[1+\frac{3}{2}\cot(\frac{\pi}{2}-\psi)\right]\cos(\lambda\psi+\frac{\pi}{2})+\sin(\lambda\psi+\frac{\pi}{2})\right\}T(t)$$

where

$$T(t) = -\frac{1}{2\lambda}\left(\frac{3}{2}Pa-6\alpha\delta\left[\eta_0 e^{-KT_m}\frac{\partial T_m}{\partial t}+G_0(1-\beta T_m)T_m\right]\right)$$

With the hinged expansion edge, the inner surface stresses are

$$\sigma_\phi = -\frac{e^{-\lambda\psi}\cot(\frac{\pi}{2}-\psi)}{\delta\sqrt{\sin(\frac{\pi}{2}-\psi)}}\sin(\lambda\psi-\frac{\pi}{4})T(t)-\frac{Pa}{2\delta}+\frac{3a}{\delta^2\lambda}\frac{e^{-\lambda\psi}}{\sqrt{\sin(\frac{\pi}{2}-\psi)}}\left[\cos(\lambda\psi-\frac{\pi}{4})+\sin(\lambda\psi-\frac{\pi}{4})\right]T(t)$$

$$\sigma_\theta = \frac{\lambda e^{-\lambda\psi}}{2\delta\sqrt{\sin(\frac{\pi}{2}-\psi)}}\left[2\cos(\lambda\psi-\frac{\pi}{4})-\left\{2-\frac{1}{\lambda}\cot(\frac{\pi}{2}-\psi)\right\}\sin(\lambda\psi-\frac{\pi}{4})\right]T(t)-\frac{Pa}{2\delta}+$$

$$+\frac{3a}{2\delta^2\lambda}\frac{e^{-\lambda\psi}}{\sqrt{\sin(\frac{\pi}{2}-\psi)}}\left\{\left[1+\frac{3}{2}\cot(\frac{\pi}{2}-\psi)\right]\cos(\lambda\psi-\frac{\pi}{4})+\sin(\lambda\psi-\frac{\pi}{4})\right\}T(t)$$

where $T(t) = \frac{1}{2\sqrt{2}\lambda}\left[\frac{Pa}{2}-6\delta\left\{\eta_0 e^{-KT_m}\frac{\partial}{\partial t}(\alpha T_m-\alpha_e T_e)+G_0(1-\beta T_m)(\alpha T_m-\alpha_e T_e)\right\}\right]$

5.4 The Simplified Conical Shell as a Maxwell Body

For a Maxwell body

$$\frac{1}{G}\frac{\partial \sigma_x}{\partial t} + \frac{1}{\eta}\sigma_x = 2\frac{\partial}{\partial t}\left[2\epsilon_x + \epsilon_y - 3\alpha T_m\right]$$

Proceeding as in section 5.1 and with

$$\Gamma(\ldots) = \frac{1}{G}\frac{\partial(\ldots)}{\partial t} + \frac{1}{\eta}(\ldots)$$

then

$$N_\phi = 12\delta\cot\gamma\left[\frac{Z_2}{\eta^2} - \frac{2Z_1'}{\eta^3} + A_0\left(-\frac{Z_1}{\eta^2} - \frac{Z_2'}{\eta^3}\right)\right]\frac{1}{\Gamma}\left\{\frac{dT}{dt}\right\} - \frac{Pl\tan\gamma}{2}$$

$$N_\theta = 6\delta\cot\gamma\left[\frac{Z_2'}{\eta} - \frac{2Z_2}{\eta^2} + \frac{4Z_1'}{\eta^3} + A_0\left(-\frac{Z_1'}{\eta} + \frac{2Z_1}{\eta^2} + \frac{4Z_2'}{\eta^3}\right)\right]\frac{1}{\Gamma}\left\{\frac{dT}{dt}\right\} - Pl\tan\gamma$$

Applying the fixed edge conditions, then

$$A_0 = -\frac{Z_{10} + \frac{2}{\eta_0}Z_{20}'}{Z_{20} - \frac{2}{\eta_0}Z_{10}'}, \quad \frac{1}{\Gamma}\left\{\frac{dT}{dt}\right\} = \frac{\frac{3}{2}Pl_0 - 6\alpha\delta e^{-\int\frac{G_0(1-\beta T_m)dt}{\eta_0 e^{-KT_m}}}\int_0^t G_0(1-\beta T_m)\frac{dT_m}{dt}e^{\int\frac{G_0(1-\beta T_m)}{\eta_0 e^{-KT_m}}dt}\,dt}{12\delta\cot\gamma\left[\frac{Z_{20}'}{\eta_0} - \frac{3Z_{20}}{\eta_0^2} + \frac{6Z_{10}'}{\eta_0^2} + A_0\left(-\frac{Z_{10}'}{\eta_0} + \frac{3Z_{10}}{\eta_0^2} + \frac{6Z_{20}'}{\eta_0^3}\right)\right]}$$

For a constant temperature rate $T_m = Rt$. The integral then becomes

$$\int_0^t G_0(1-\beta RT)Re^{\int\frac{G_0(1-\beta Rt)e^{KRt}}{\eta_0}dt}\,dt$$

For $e^{KRt} < 0.1\frac{\eta_0}{G_0}$ the exponential is essentially unity so

$$\int_0^t G_0(1-\beta Rt)Re^{\int\frac{G_0(1-\beta Rt)}{\eta_0}e^{KRt}dt}\,dt \simeq G_0\left(1-\frac{\beta R}{2}t\right)Rt \quad ; \quad \left(t < \frac{\log 0.1\frac{\eta_0}{G_0}}{KR}\right)$$

After $t > \frac{\log 0.1\frac{\eta_0}{G_0}}{KR}$ the quantity (1- β Rt) can be considered constant compared to the exponential so

$$\int_{t'}^t G_0(1-\beta Rt)Re^{\int\frac{G_0(1-\beta Rt)e^{KRt}}{\eta_0}dt}\,dt \simeq G_0(1-\beta Rt)R\left[\bar{E}_i\left(\frac{G_0(1-\beta Rt)}{KR\eta_0 e^{-KRt}}\right) - \bar{E}_i(0.1)\right]$$

where $t' = \frac{\log 0.1\frac{\eta_0}{G_0}}{KR}$ and $\bar{E}_i(\ldots)$ is defined as

$$\bar{E}_i(\log x) = \int_0^x \frac{dy}{\log y}$$

The time function is then

$$\frac{1}{K_2}\left[K_1 - 6\alpha\delta G_0\left(1 - \frac{\beta R}{2}t\right)Rt\right] \quad \text{FOR} \quad t < t'$$

$$\frac{1}{K_2}\left[K_1 - 6\alpha\delta e^{-\frac{G_0(1-\beta Rt)}{KR\eta_0 e^{-KRt}}}\left\{G_0\left(1-\frac{\beta Rt'}{2}\right)Rt' + G_0(1-\beta Rt)R\left[\bar{E}_i\left(\frac{G_0(1-\beta Rt)}{KR\eta_0 e^{-KRt}}\right) - \bar{E}_i(0.1)\right]\right\}\right] \quad \text{FOR} \quad t > t'$$

VI. EXPERIMENTAL RESULTS AND VERIFICATION OF ANALYTICAL METHODS

6.1 Basic Approach to the Test Program

In the early stages of the current investigation, it was decided that, for experimental verification of theoretical methods of predicting the viscoelastic response of shells of revolution subjected to normal pressure and elevated temperature and thermal gradients, records of the strain as a function of time would be necessary. Accordingly, steps were taken to find appropriate means of making such elevated temperature measurements.

The objectives of the experimental investigation were as follows:

(1) To obtain strain versus time curves for normal pressures and applied temperatures and thermal rates.

(2) To determine the mode and progression of failure, and the load condition necessary to cause failure under load and transient temperatures.

(3) To verify or disprove the method of analysis.

6.1.1 Test conditions

The experimental program for verification of a method of analysis does not necessarily duplicate any specific design conditions. It is required that the tests cover the parameters included in the method of analysis. These parameters should extend over a wide range of the values.

For convenience, a uniform normal pressure of 12 psi is chosen to be applied simultaneously with various combinations of temperature. A maximum test temperature of 500°F is chosen, based on a level of temperature sufficiently high to introduce material property variation and buckling.

The tests are designed to eliminate as many extraneous variables as possible. However, in the present study it is impossible to eliminate parameters such as edge constraints, and discontinuities of temperature due to mass. These variables are difficult to evaluate. In the correlation, it is not clear whether the method of analysis is at fault or the accuracy of the experimental data is questionable. The interrelationship of the above mentioned inseparable parameters and their influence on the overall stress distributions are not satisfactorily established.

6.1.2 Number of Tests

The number of tests is an important factor in the design and cost of an experimental investigation. Usually repetition of test conditions with several specimens is made to include the effect of test scatter.

A more economical approach is to test each specimen under different conditions and to compare the test results with theoretical results over the range of the variables. This approach permits checking over a large range of values with a minimum number of tests and test specimens.

The approach employed in this investigation is designed after the latter method; however, where certain doubts existed, the test conditions are repeated with another model.

6.1.3 Test Specimen

The size of the test specimen is another important consideration particularly in elevated temperature structural research. In such investigations, large specimens are required to eliminate certain testing difficulties; for example, temperature gradients are established by temperature difference along the length of a specimen. If the specimen were too small, temperature-sensing elements would be too closely spaced along the specimen with probable disturbance of the required gradient.

The design of the specimen is based on the following specifications:

(1) Geometry - conical and hemispherical shells are used analytical and testing simplicity.

(2) Radius - a base radius of 12 inches is chosen as a convenient specimen size.

(3) Thickness- the thickness is based on a radius-to-thickness ratio corresponding to a convenient anticipated buckling stress.

(4) Material - Aluminum is chosen so that material property variation with temperature, creep, and buckling occur within a convenient temperature and load range. This is of primary importance in the design of the test facility and the instrumentation.

6.2 Test Procedure

Prior to an actual test run, an unrestrained heating of the model provided data necessary for temperature compensation of the strain gages. The difference between these data and the actual test data compensated the effects of a varying coefficient of linear thermal expansion, coefficient of resistivity of the gages, and coefficients of linear thermal expansion of the gage cement and gage material. The compensated strain data is then, in effect, the total strain minus the linear thermal expansion.

With the strain-temperature data recorded and the model cooled, the shell is bolted to the steel mounting plate. The selected time-temperature function is set on the temperature programmer.

Instead of using an ice-water bath for the cold junction of each thermocouple, a separate thermocouple employing an ice-water bath provides the temperature of the recording thermocouple input to the recorder. This temperature, which is monitored on a precision millivolt potentiometer, is the effective cold junction temperature of the recording thermocouples. The strain gage bridges are balanced and zero points of all instrumentation and reference temperatures of thermocouples are noted. The oven is placed over the model and the power controller is connected to the lamps. The model is evacuated to conform to the prescribed external load, after which the recording instruments and the temperature programmer are started.

After completion of the transient portion of the test program, the temperature programmer is placed in a "hold" condition to maintain the steady-state temperature for the desired period of time. Usually the steady-state is maintained for five minutes except for collapse studies in which case thirty minutes are provided.

When the test is completed, the power controller is shut off, the model is allowed to cool and then unbolted for the next unrestrained run.

6.3 Analysis of Test Results

The experimental results are presented in Fig. 6.5-1 through 6.5-18 and included in Appendix C.

The low thermal resistance of models requires a low gain condition on the power controller to prevent a pulsing heat input. As a result of the low gain, the steady-state temperatures are 40°F to 60°F lower than that programmed in the initial tests.

The base temperatures are considerably lower than that of the rest of the shell due to heat conduction to the steel mounting plate. In an effort to remedy the low temperature at the base, the feedback thermocouple for Zone 3 was moved closer to the base. This produces a shell

temperature 40°F to 80°F higher than the program temperature, but the temperatures near the base are from 100°F to 150°F lower than the steady-state temperature. However, the resulting temperature gradient occupies only the lower three inches of the shell.

The data from the differential thermocouples are merely qualitative. Calculations show a thermal gradient across the shell thickness of 1°F for a programmed temperature rate of 20°F/sec whereas the data indicates 30°F. The large experimental values are due to a poor thermal bond between the insultated junction and the surface of the shell.

A characteristic feature of all tests is the relaxation of stress as steady-state temperature conditions are maintained. The reduction of compressive stress is due to the expansion of the steel mounting plate and a relaxation of the material. The relative contribution of each condition depends upon the temperature of the base. To separate the two effects requires insulation of the base. However, it is felt that the major factor in the reduction of compressive stress is that of material relaxation. This conclusion is supported by some of the zonal tests. In those tests where the base temperature was relatively low, say about 120°F, in which case yielding of the base should not be a problem, the compressive stresses along the model slant height decayed although the compressive stresses near the base increased with an increasing steady-state temperature.

As is expected the stresses are compressive throughout the shell with those in the circumferential direction being of the greater magnitude. Maximum values are observed at the base, and the stress decreases rapidly along the meridian for the lower section. The upper regions of the shells experience approximately the same stress magnitude. The meridional stresses are similar to the circumferential stresses but with less pronounced maxima and minima.

Collapse was encountered in a 1/16" thick conical shell during an applied heating rate of 20°F/sec (to 500°f) with a surface pressure equivalent to 22"Hg differential pressure. The same model had experienced the same program previously. The data are presented in Table C-11. Approximately at 80% of the transient period gage 4M showed an immediate change in strain. The change is believed to be caused by a slight buckle at the support. No further buckling occurred until the transient condition had been sustained for five minutes when all gages registered an immediate jump. Thereafter gages 3M and 3P showed increasing compression to five and one-half minutes when complete collapse occurred.

The collapsed cone has five non axisymmetric nodes with the wall in the region of the base almost flat against the support. After collapse the support for instrumentation wiring interferred with progression causing a tilt of the apex toward the more seriously buckled area. See Fig. 6.3-1.

6.4 Simplified Strain-Displacement Method

Compared in Fig. 7.1-4 and 7.1-5 are the experimental data for a 1/16" thick cone for 20°F/sec to 500°F with 11.5 psi pressure and the theoretical stress calculated from the equations presented in section 3.1 for a similar program. As seen from the figures the theoretical stress behavior is opposite to that of the experimental. This behavior is believed due to neglecting the change in curvature in the strain expressions thereby relegating the analysis to a non-bending case (membrane theory).

6.5 Bending Analysis Neglecting the Temperature Differential, T_t

Compared in Fig. 6.5-1 through Fig. 6.5-18 are the theoretical and experimental data for one test on a 1/32" thick cone, five test on a 1/16" cone, one test on a 1/8" cone, and two tests on a 1/16" thick hemisphere. All theoretical data are calculated for the hinged expansion edge boundary condition, i.e., the mounting plate is considered to assume the temperature of the edge of the model and the edge offers no resistance to rotation in the merional direction. A characteristic of all theoretical data is a large stress value during the early time periods when the response should be nearly elastic. The time periods are 1/3, 1/2, and end of transient.

The Kelvin-Voigt body may be pictured as a spring and a dashpot in parallel with each element having the same displacement and the resulting force being the sum of that in each. Since the applied boundary condition of a restrained edge is essentially an applied strain rate, the large stresses are developed in the viscous member conforming to the boundary condition. At such time when the temperature is increased to cause an appreciable effect on the coefficient of viscosity (the coefficient varies inversely as the temperature) the viscous resistance becomes negligible and the response is one which is mainly elastic. From section 5.2 the thermal stress is governed by the term $\eta_0 e^{-KT_m} \frac{\partial T_m}{\partial t} + G_0(1-\beta T_m)T_m$ so with $\eta_0 \sim 10^{12}$ and $G_0 \sim 10^6$ the viscous stress is necessarily large for low temperatures.

At higher temperatures the behavior of the theoretical curves are similar to that of the experimental, that is, an increasing compressive stress toward the edte increasing also with time.

Since the stresses are calculated at the inner surface they show the effect of the bending moment close to the edge. The theoretical bending moment accounts for the majority of the stress in the meridional direction. The moment changes rapidly with distance from the edge and depends considerably upon the boundary conditions.

The experimental boundary conditions cannot be assumed ideally hinged or fixed. Due to heat conducted from the edge to the mounting plate the edge will expand but not to the extent assumed in the expansion boundary. Also the edge may rotate but is not ideally hinged.

Actual edge conditions would require an analysis investigating a flanged edge.

The comparison in Fig. 7.1-4 and 7.1-5 shows the effect of boundary conditions on the inner surface stress. The two different sets of boundary conditions should bracket the actual situation. In the fixed edge, the meridian may not rotate and the edge may not expand. For the hinged expansion edge, the meridional moment at the base vanishes and the edge may expand with the steel plate ($\alpha_{aluminum} \sim 14 \times 10^{-6}$, $\alpha_{steel} \sim 7 \times 10^{-6}$). The fixed case produces tensile stress and the hinged case compressive stress near the edge on the inner surface of the shell in the meridional direction. The effect on the middle surface is shown in the following figure.

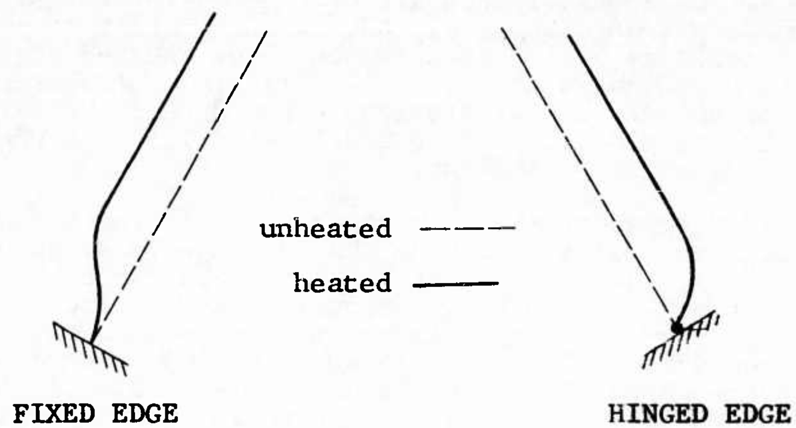

The circumferential stress depends mainly upon the degree of restraint at the edge and is proportional to the difference between the expansion of the shell and the expansion of the mount.

The experimental values compare more favorably with the theoretical stress for the hinged expansion edge. The maximum experimental circumferential stress is about 60% of that for the hinged edge while 40% of that for the fixed edge. The maximum experimental meridional stress is about 75% of that for the hinged edge while the fixed edge stress is of the same order of magnitude but of opposite sign. While the experimental stresses should fall between those of the two boundary conditions it is seen that the measured stress is still lower than either. The Kelvin-Voigt body does not consider the relaxation of stress at constant strain at high temperatures or the yielding of the material for high stress.

6.6 Comparison of the Maxwell and Kelvin-Voigt Bodies

In Fig. 6.6-1 and 6.6-2 the viscoelastic response of a 1/16" thick cone subjected to 20°F/sec to 500°F is compared for a Maxwell body and a Kelvin-Voigt body. The early response of the Kelvin-Voigt body is, again, of a highly viscous nature while the Maxwell body response is essentially elastic. At higher temperatures when the Kelvin-Voigt body becomes elastic the Maxwell response is fluidic due to the applied strain rate being absorbed in the viscous component. The theoretical stress is essentially the product of a function of slant length and a function of time. With the function of slant length being the same for both bodies the time function is presented in the following figure:

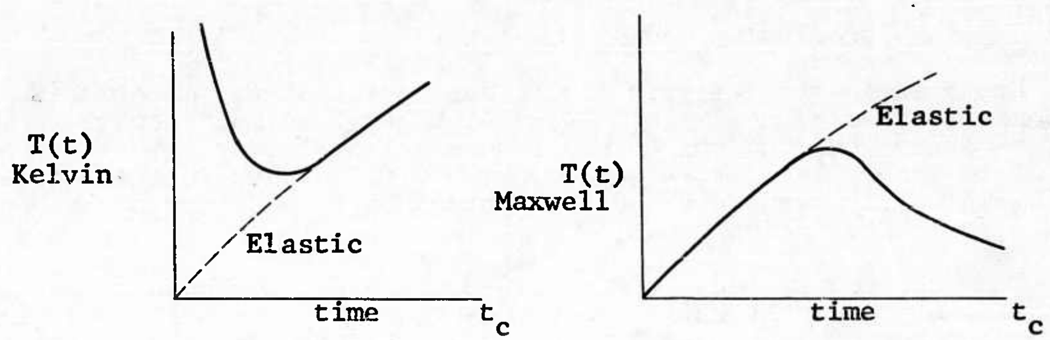

Moreover, at the steady state condition the Kelvin-Voigt body maintains a constant stress while the Maxwell body will decay exponentially.

Compared in Fig. 6.6-3 and 6.6-4 are the results of the temperature dependent properties analysis, the temperature independent properties analysis, and the temperature dependent properties elastic analysis. The property values for the temperature independent analysis were chosen at a temperature corresponding to 10 seconds. The response of the temperature independent analysis depends upon the choice of the coefficient of viscosity; if the temperature is low the response will be viscous and if the temperature is sufficiently high the response will be elastic.

The variation of the elastic solution from that of the viscoelastic solution at high temperatures is due to the choice of Poisson's ratio being 1/3 for the elastic analysis and ½ for the viscoelastic. Again the experimental stress is lower than any theoretical prediction which is believed due to the obscure boundary conditions and a yielding at the edge.

VII. SUMMARY AND CONCLUSIONS

The experimental results in some instances are in disagreement with the temperature dependent viscoelastic analysis. This is generally true for the early transient stage and the steady-state stress conditions. In an effort to explain these differences, a number of questionable elements of both the theoretical analysis and the experimental investigation were studied. These points are discussed in the following paragraphs, and when possible, recommendations to eliminate the individual effects are given.

7.1 Theoretical Analysis

7.1.1 Viscoelastic models

Employed in the analysis is the assumption of the material's response as that of a simple Kelvin-Voigt body. A much better approximation would be the development of a model consisting of a number of Kelvin-Voigt elements in series. The difficulties in the analysis during the early transient and the steady-state condition would benefit from a more descriptive model.

From the comparisons in Fig. 6.6-3 and 6.6-4 it appears that the elastic analysis would sufficiently describe the stress response in the models tested as compared to the viscoelastic analysis presented. However, neither analysis predicts the steady-state response.

7.1.2 Effect of material properties

In the present investigation, an empirical expression for was established by employing some limited data established by ALCOA at higher temperature ranges for aluminum alloys. Because the viscosity/temperature relationship is based on such limited data, three values were used in the calculations. The effect of varying η is demonstrated in Fig. 7.1-1 and 7.1-2. Changes of an order of magnitude are employed. As seen from the figures, the only effect is to advance or retard the transition from a viscous response to an elastic response.

Although some error may exist in the choice of G_o and β, it is felt that both are minor and have little effect upon the results.

RECOMMENDATION: More reliable data on the dependance of thermal properties of alloys with temperature are required for accurate analyses. In particular, viscosity/temperature data on alloys below the melting point should be established.

7.1.3 Inaccuracies in the applied boundary conditions

Agreement of the boundary conditions employed in the analysis with those acutally produced in a test program is difficult to achieve. Although such disagreement is present, it is felt that the effect is localized to the edge and apex (in the case of cones) regions as far as the stresses in the shell are concerned.

7.2 Experimental Study

Aside from the usual sources of errors encountered in experimental stress investigations and data reduction, the investigators feel that the following items are major possible contributors to the existing disagreement between theoretical and experimental results.

7.2.1 Inaccuracy in correcting strain data to eliminate temperature effects in strain gages

There is much to be done to perfect high temperature strain measuring techniques. The range of temperatures of interest is subject to a number of technical problems both in terms of model preparation and testing procedures for $T > 400^oF$. In fact, the experience gained in this investigation indicates that it requires six to eight months to develop techniques for such an investigation.

RECOMMENDATION: High temperature strain gages which require less complicated application procedures are needed. These strain gages should be temperature compensating. Since the completion of the present investigation, other hightemperature strain gages have been brought to the attention of the investigators. It would be of interest to note whether these newer developments eliminate the difficulties of application, curing, and measuring as experienced in this investigation.

7.2.2 Effect of model support on temperature distribution

The steel plate which supported the oven and the model had considerable effect on the model temperature near the support. Although steps were taken to eliminate the plate as a heat sink, its effects are evident in the experimental results. The existence of such a heat sink is perhaps the major difficulty of the equipment. It created an undesirable thermal gradient along the shell length. Otherwise the equipment performed well. The equipment was not employed to the maximum capacity.

RECOMMENDATION: For more effective use of the present equipment design, a ceramic coating should be used at the shell-support connection.

7.2.3 Imperfection of the Model

In Appendix A.3, the effect of geometrical irregularities of the initial shape are discussed.

The 1/32" thick conical shells were more likely to contain initial imperfections. This probably accounts for the poorer correlation between analytical and experimental results. However for the thicker models, not only was better correlation achieved but in several cases there was good agreement of analytical and experimental results.

On the basis of these qualitative results, the following recommendation is made:

RECOMMENDATION: Study should be made of surfaces of revolution which have unsymmetrical initial imperfections.

7.3 General Comment

In the foregoing discussion, several important aspects of the investigation are outlined. In connection therewith, the investigators feel that the results are a step in the solution of the complicated viscoelastic shell problem. Nevertheless, in addition, several other important aspects of the analysis bear further investigation; these include:

1. Extention of the theory to include the effect of internal ring- and meridional-frames, and other surface constraints.

2. Extention of the method to include viscoelastic and/or elastic layered systems of two and three layers. The use of outer liners should be investigated.

3. Future investigations might also include both unsymmetrical body forces and temperature distributions.

It is needless to say that each of these endeavors are entire subjects within themselves.

In connection with Item 2, it is felt that the present method is too complicated to be applied to layered systems. For this reason, the investigators studied the application of energy methods to the solution of viscoelastic shell problems.

REFERENCES

1. Alfrey, T., Mechanical Behavior of High Polymers, 1st Edition, Interscience Publishers, New York, N. Y., 1948.

2. Alcoa Aluminum Handbook, 1957.

3. Biot, M. A., Linear Thermodynamics and the Mechanics of Solids, Report No. SA - 787 - S - 6. Cornell Aeronautical Laboratory, Inc., Buffalo, New York, June 1958.

4. Bonney, E. A., Zucrow, M. J., and Besserer, C. W., Aerodynamics Propulsion, Structures and Design Practice, D. Van. Norstrand Co., Inc., Princeton, N. J., pp. 426 & 428, 1956.

5. Budiansky, B., "Buckling of Clamped Shallow Spherical Shells", Technical Report No. 5, Division of Engineering and Applied Physics, Harvard University, Cambridge, Massachusetts, Contract Nonn 1866(02), August, 1959.

6. Chen, W. L., "Effect of Geometrical Imperfection on the Elastic Buckling of Shallow Spherical Shells", Sc. D. Thesis, Department of Civil and Sanitary Engineering, Massachusetts Institute of Technology, January 1959.

7. Eisenhart, L. P., A Treatise on the Differential Geometry of Curved Surfaces, page 120.

8. Flachsbart, O., Handbuch der Exp. Physic, Vol. IV, Part 2, pp. 316.

9. Frankhauser, E., Dissertation, Zürich, 1913 and Vol. 58, pp. 840, 1914.

10. Freudenthal, A. M., The Inelastic Behavior of Materials And Structures, John Willey and Sons, New York, 1950.

11. Gorendown, R. F., Memorandum to NACA Subcommittee on Aircraft Loads, October 16, 1956.

12. Gray, A. & Mathews, G. B., A Treatise on Bessel Function, MacMillan & Co., London, England.

13. Huth, J. H., "Thermal Stresses in Conical Shells", Journal of the Aeronautical Sciences, Vol. 20, No. 9, pp. 613-616, September, 1953.

14. Kamke, E. S., Differentialgleichungen Lösungsmethoden und Lösungen, Chelsea Publishing Company, New York, N. Y., 1948.

15. Kaplan, A., and Fung, Y. C., A Nonlinear Theory of the Bending and Buckling of Thin Elastic Shallow Spherical Shells, NACA Technical Note 2212, August 1954.

16. KêTing-Sui, "Experimental Evidence of the Viscous Behavior of Grain Boundaries in Metal", Physics Review, Vol. 71, pp. 533-546, 1947.

17. Keller, H., Mitt. Forshungsarbeiten, Vol. 124, 1912.

18. Loria, J., Seymour, C. and Mar, J., The Effects of Thermal Radiation on Aircraft Structures, WADC Technical Report 54-384, Part III, 1954.

19. Meissner, E., "Das Elastizitätsprobleme für dünne Schalen von Ringflächen-Kugel-oder Kegelform", Physikalische Zeitschrift, Vol. 14, pp. 343-349, 1913.

20. Melan, E. and Parkus, H., Wärmespannungen, Springer, Vienna, Austria, 1953.

21. Meriam, J. L., "Stresses and Displacements in a Rotating Conical Shell", Yale University School of Engineering Publications, No. 73, November, 1942.

22. Scipio, L. A., Chien, S. F., and Moses, J. A., "Thermoviscoelastic Analysis of Thin Shells of Revolution under Constant Normal Pressure, Part I", Progress Report, University of Minnesota, Contract AF 33(616)-5723.

23. Stodola, A., Die Dampfturbinen, 4th Edition, pp. 597, 1910.

24. Timoshenko, S., Theory of Elasticity, 2nd Edition, McGraw-Hill Book Co., Inc., New York, N. Y., 1951.

25. Timoshenko, S., Theory of Plates and Shells, McGraw-Hill Book Co., Inc., New York, N. Y., 1940.

26. Watson, G. N., Bessel Functions, Cambridge University Press, London, England, 1944.

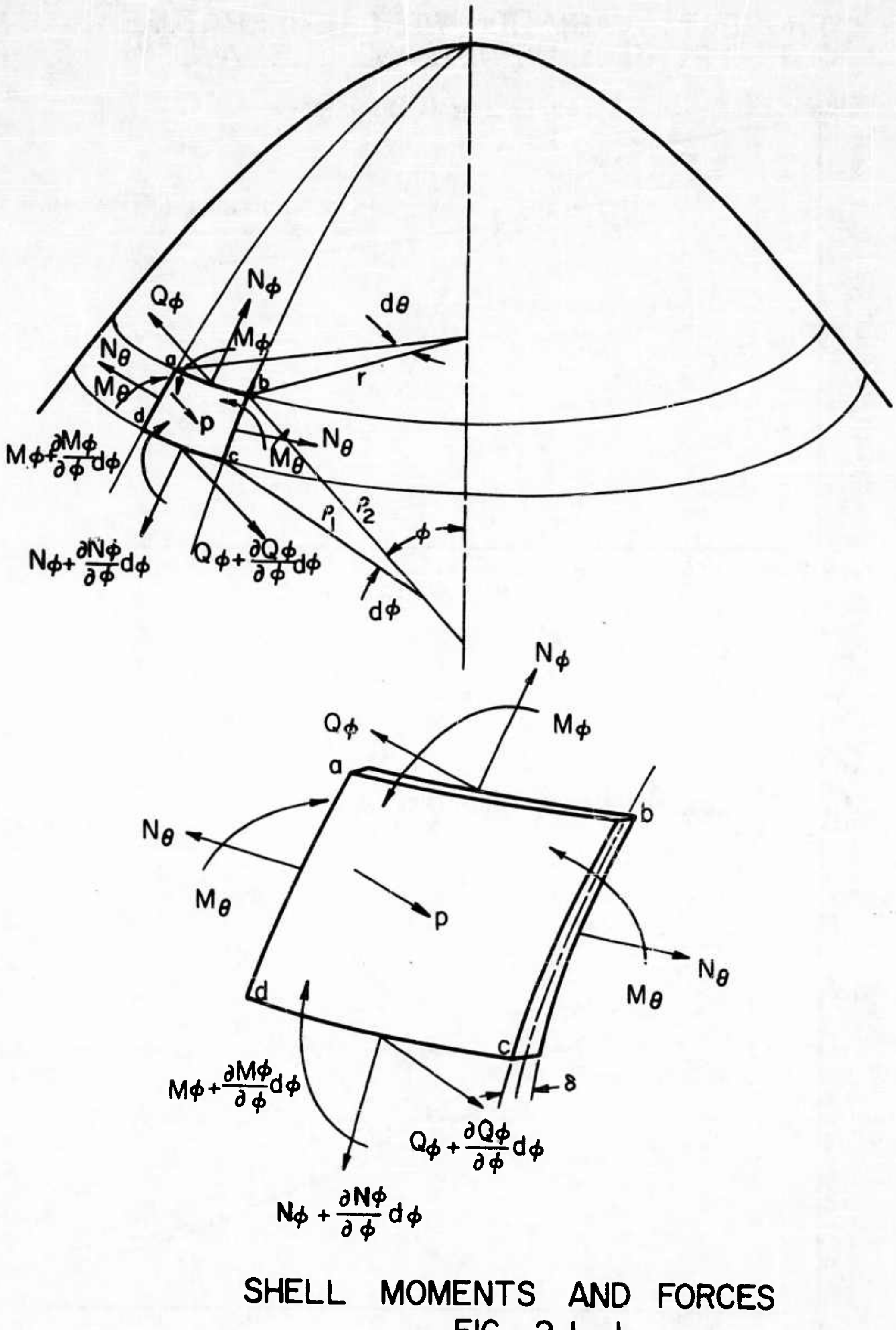

SHELL MOMENTS AND FORCES
FIG. 2.1-1

Fig. 2.1.3-1

PROPERTY VARIATION WITH TEMPERATURE FOR PURE ALUMINUM AND 6061 ALLOY

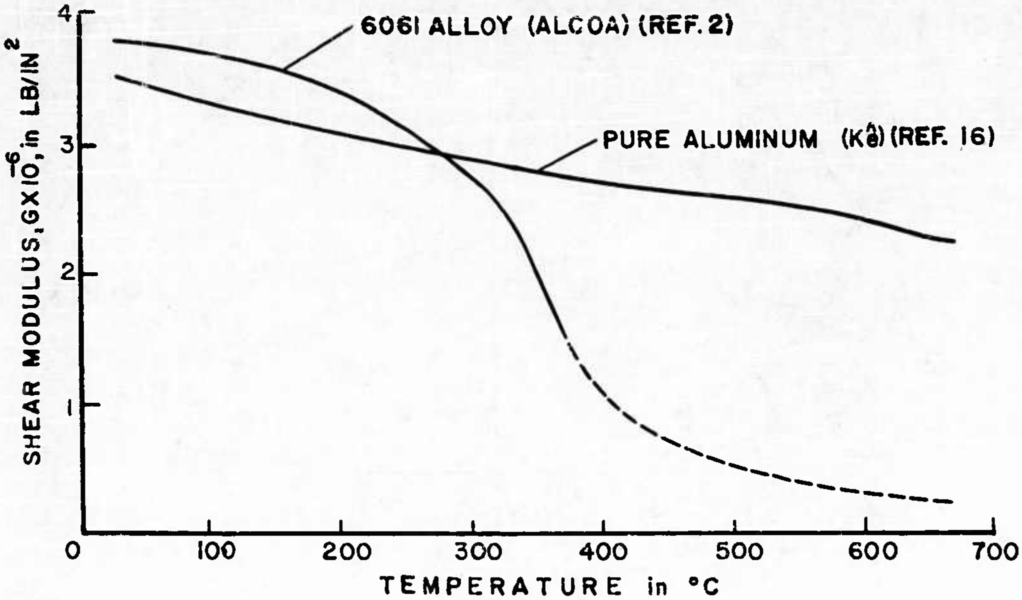

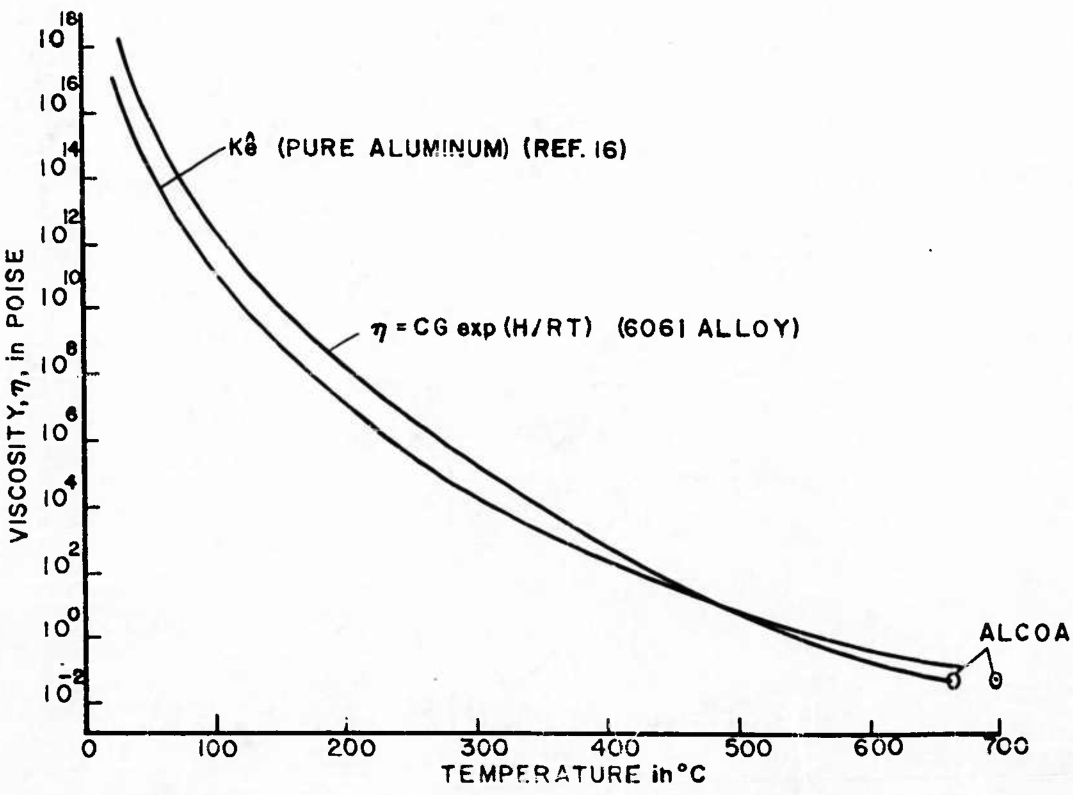

PROPERTY VARIATION WITH TEMPERATURE FOR
PURE ALUMINUM AND 6061 ALLOY

Table 2.1.3-1

T (°C)	$G \times 10^{-6}$ (psi) pure aluminum*	6061 alloy**	(poise) pure aluminum*	6061 alloy
25	3.48	3.80	2.2×10^{16}	8.15×10^{17}
100	3.34	3.78	2.1×10^{11}	4.22×10^{12}
200	3.04	3.44	1.3×10^{7}	1.45×10^{8}
285	2.90	2.85	4.8×10^{4}	3.66×10^{5}
350	2.76	2.10	2.0×10^{3}	9.30×10^{3}
450	2.61	0.65#	43.0	52.9
550	2.47	0.35#	2.2	1.38
660	2.18	0.20#	0.18	0.06**
670	2.18	--	0.14	--
700	--	--	--	0.055**

* Estimated by Kê. Refer to Kê, Ting-sui: Experimental Evidence of the Viscous Behavior of Grain Boundaries in Metal, Physical Review, Vol. 71, pp. 533-546, 1947.

** ALCOA values.

Estimated from G-T curve.

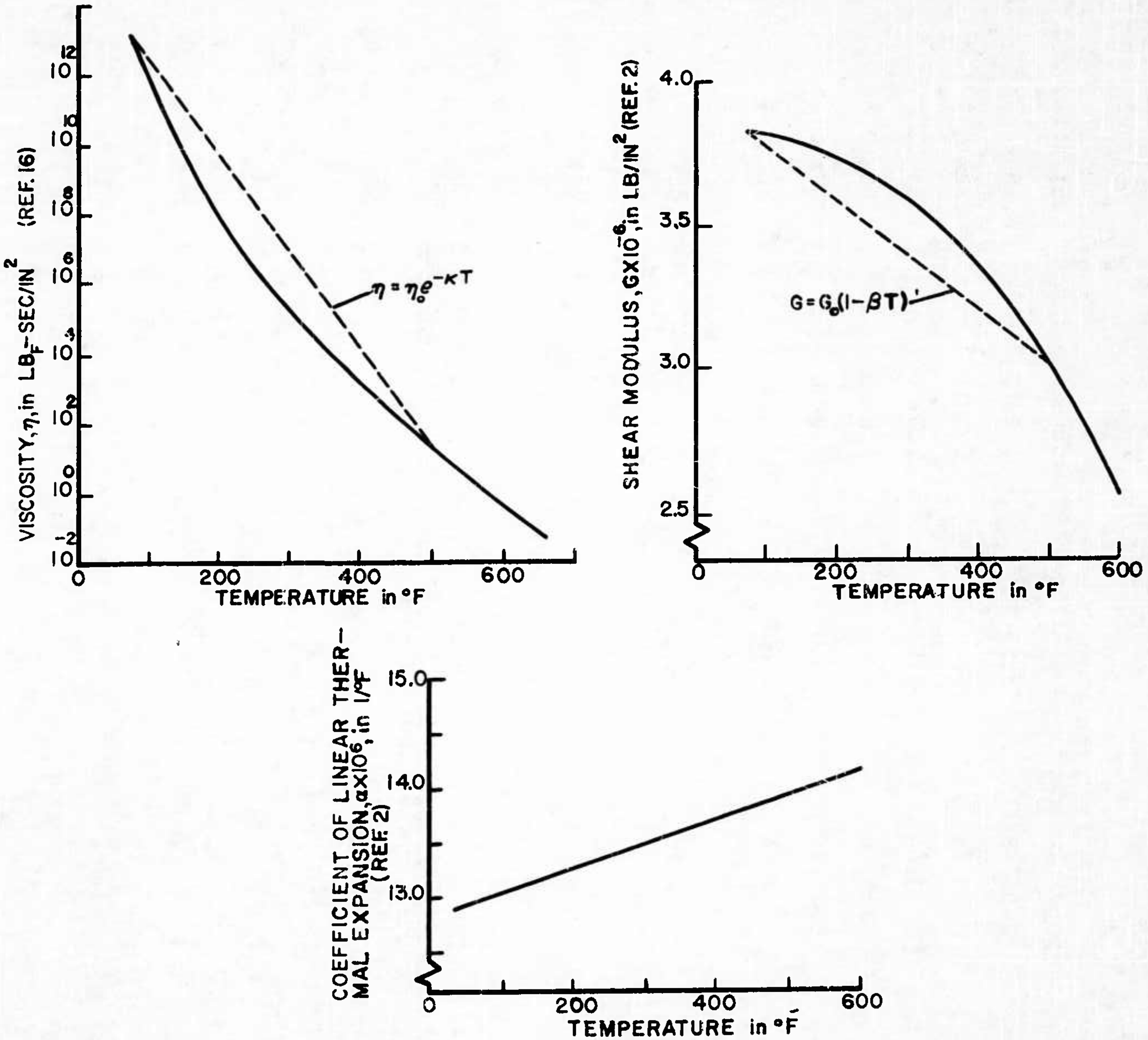

Fig. 2.1.3-2
MATERIAL PROPERTY VARIATION WITH TEMPERATURE FOR 6061 ALLOY

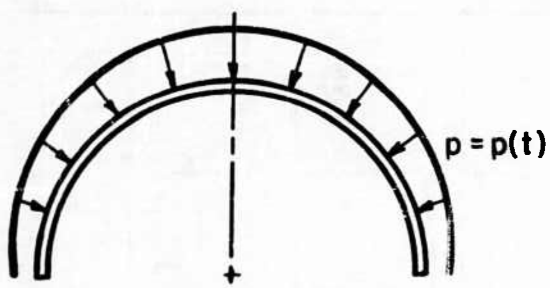

PRESSURE DISTRIBUTION

FIG. 2.4–1

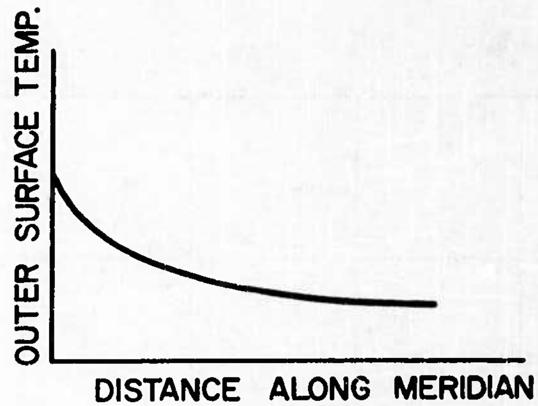

FIG. 2.4–2

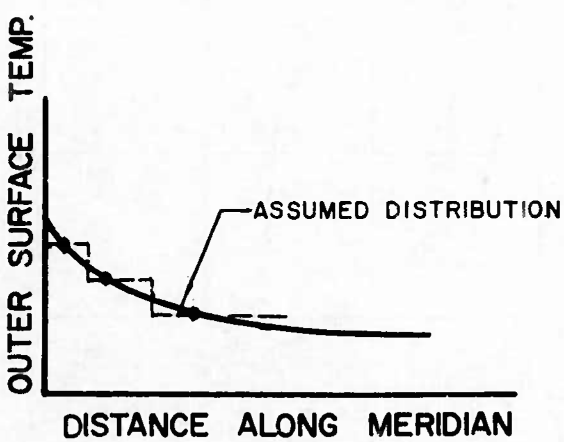

FIG. 2.4–3

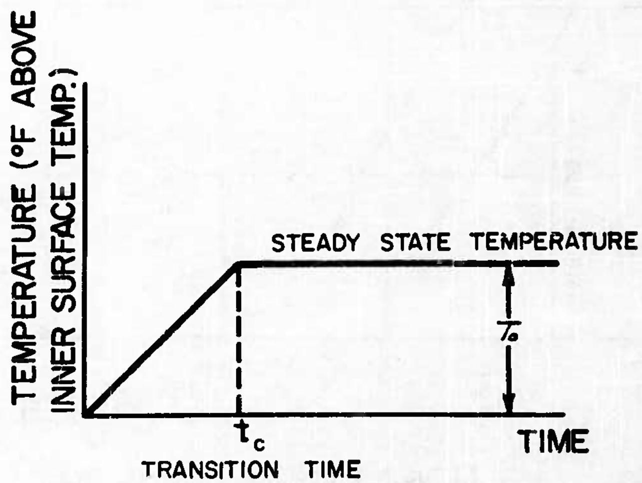

FIG. 2.4–4

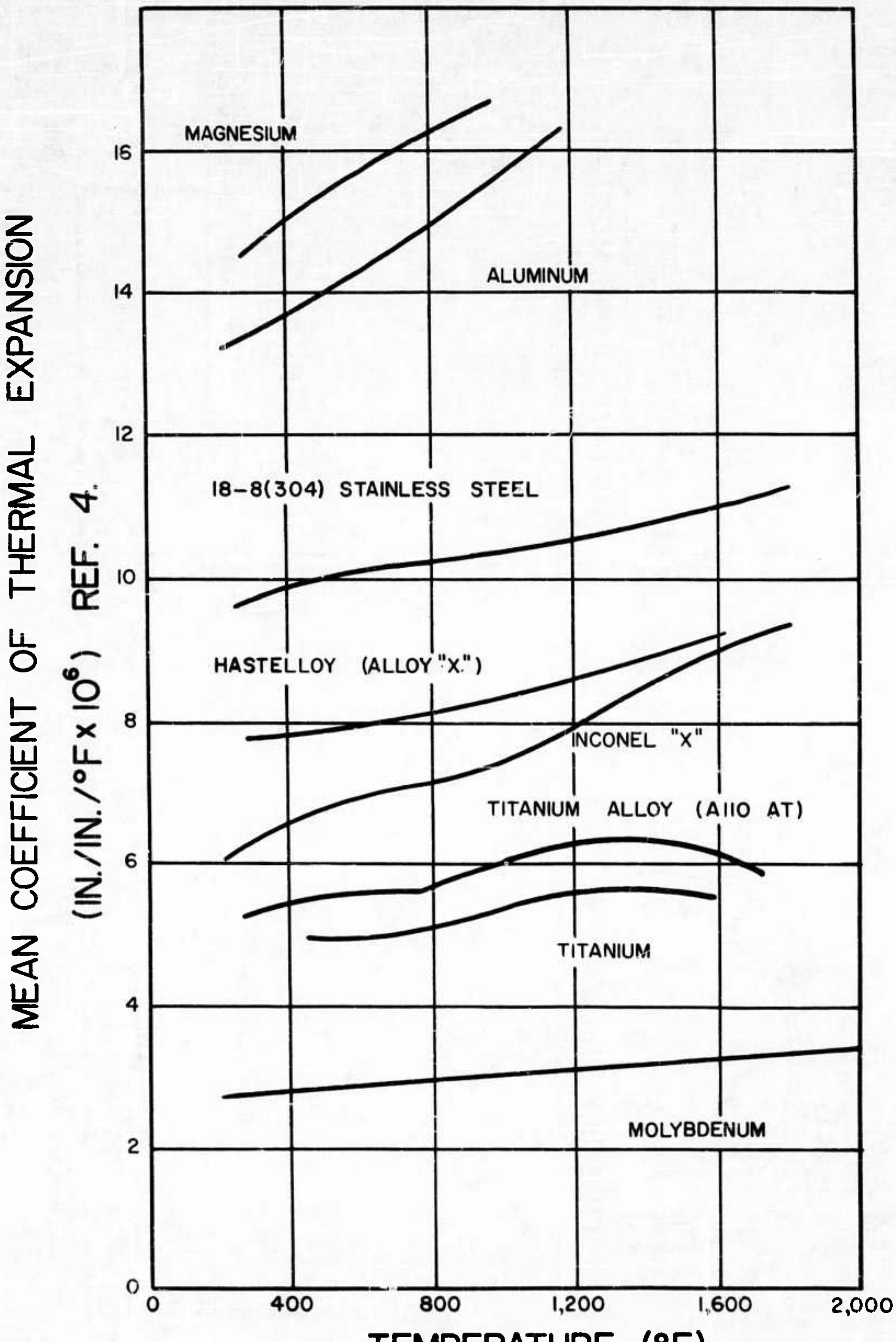
MEAN COEFFICIENT OF THERMAL EXPANSION
(IN./IN./°F x 10⁶) REF. 4.
MAGNESIUM
ALUMINUM
18-8(304) STAINLESS STEEL
HASTELLOY (ALLOY "X.")
INCONEL "X"
TITANIUM ALLOY (A110 AT)
TITANIUM
MOLYBDENUM
0
2
4
6
8
10
12
14
16
0
400
800
1,200
1,600
2,000
TEMPERATURE (°F)

FIG. 2.6-1

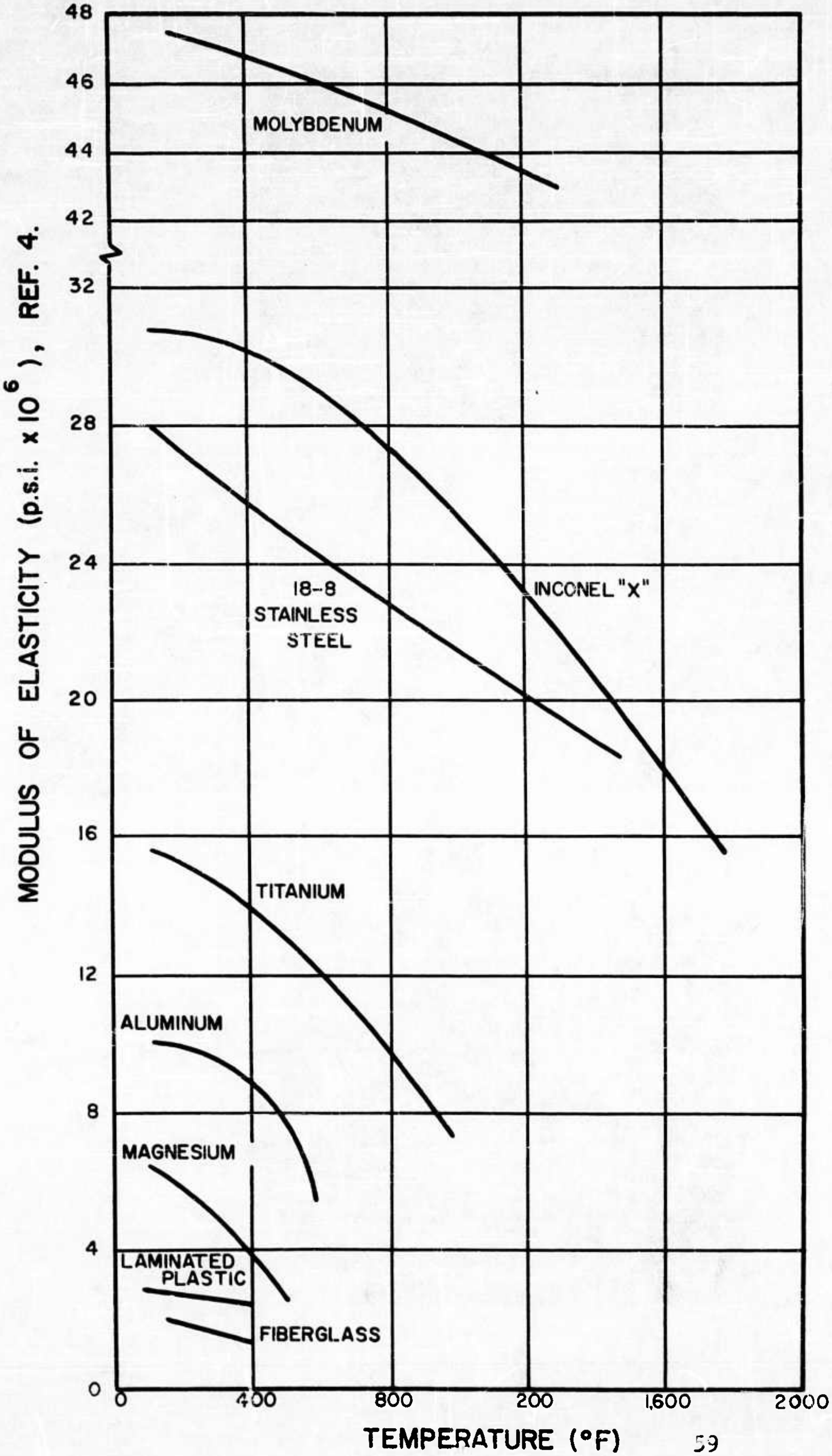

TEMPERATURE VARIATION OF MODULUS OF ELASTICITY

FIG. 2.6-2

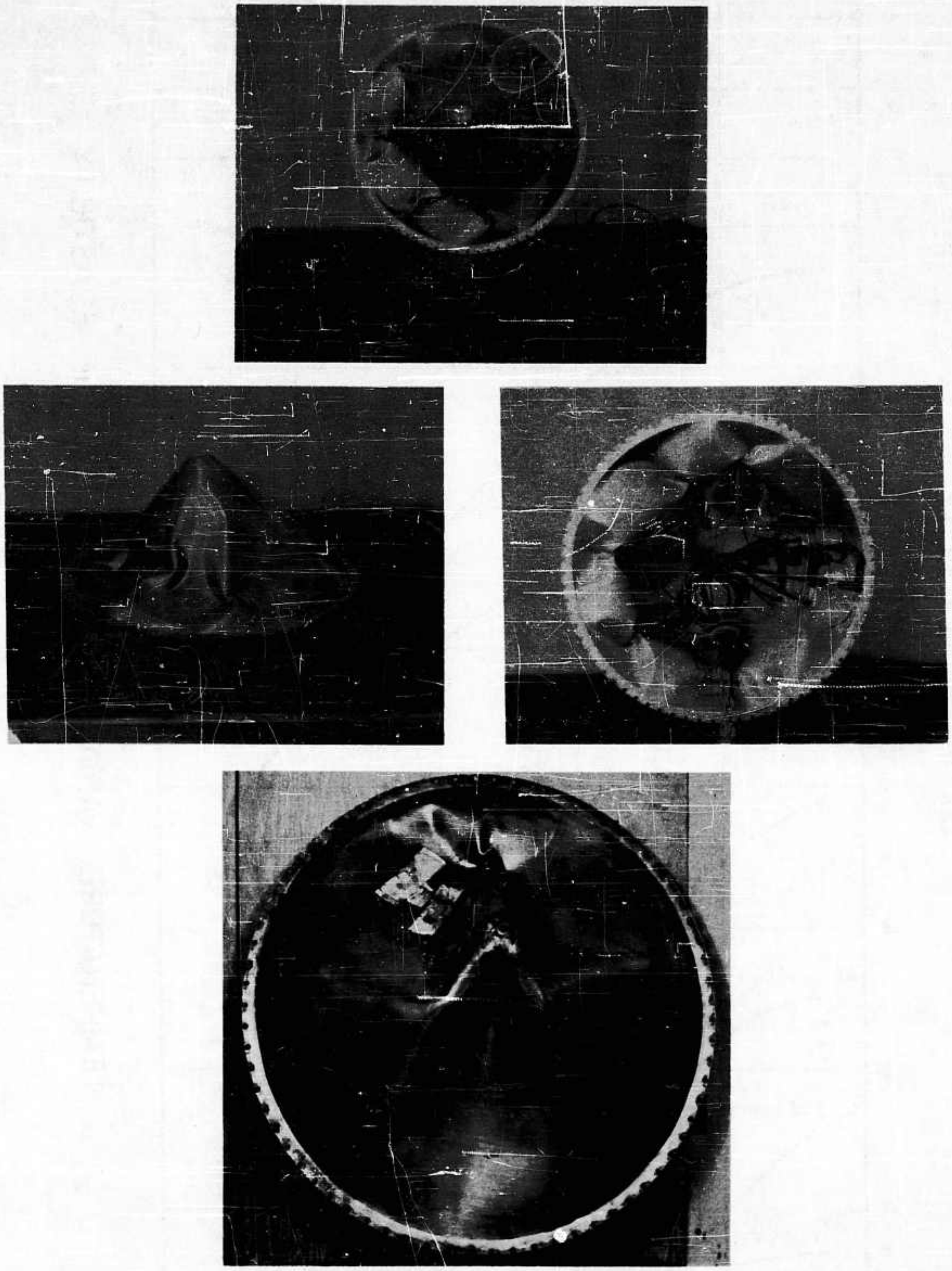

Fig. 6.3-1 Collapsed 1/16" Thick Conical Shells

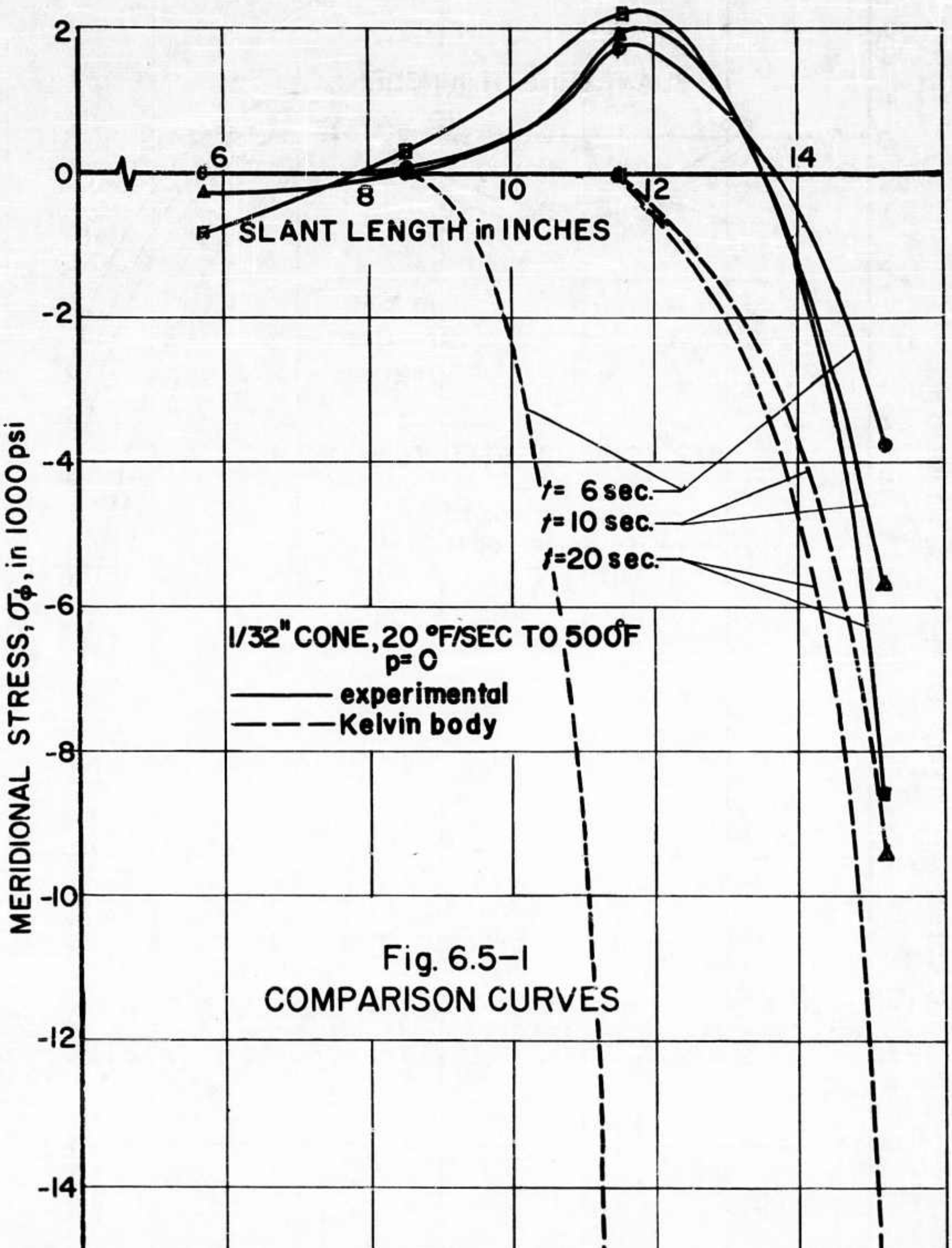

Fig. 6.5–1
COMPARISON CURVES

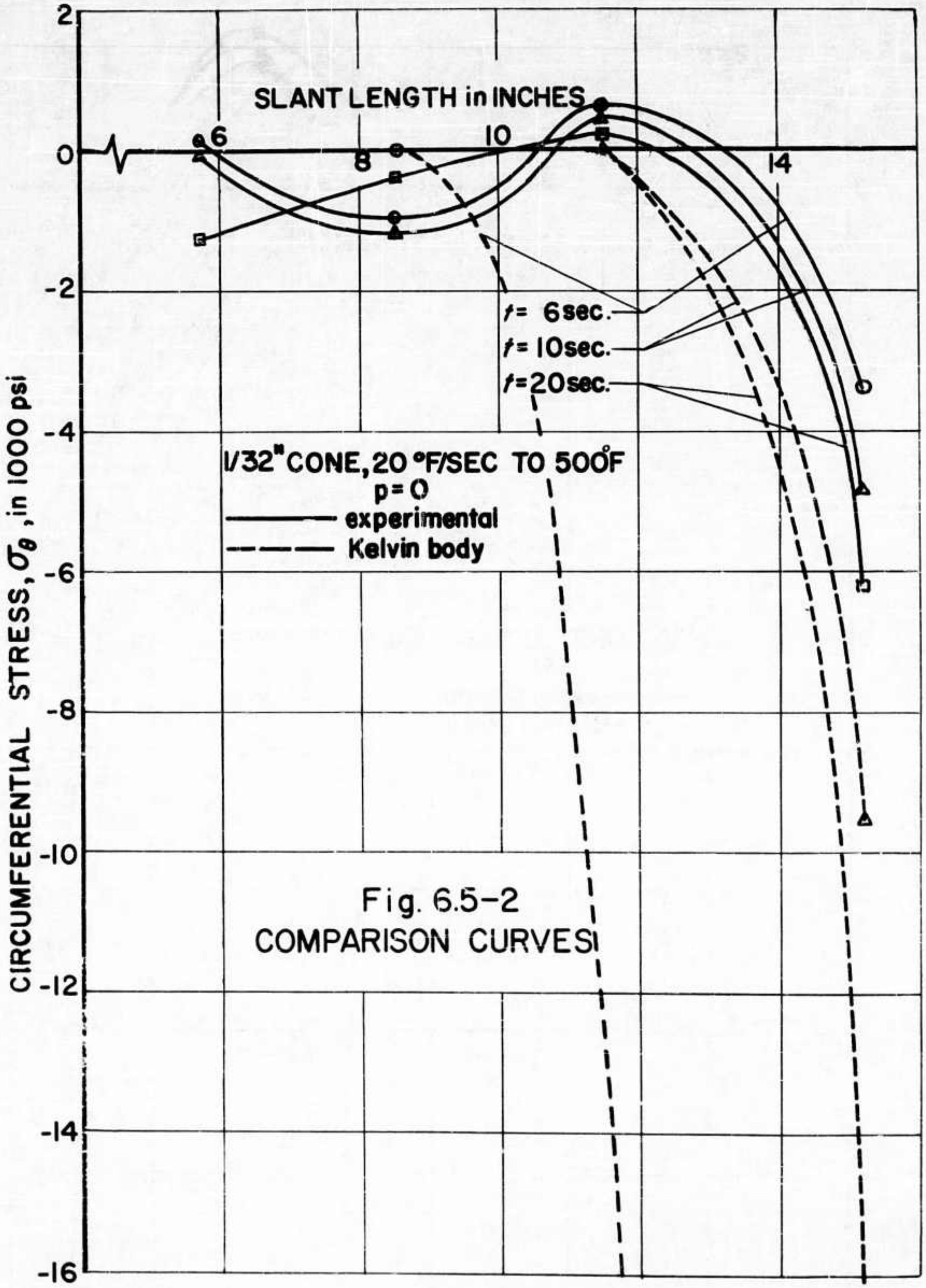

Fig. 6.5-2
COMPARISON CURVES

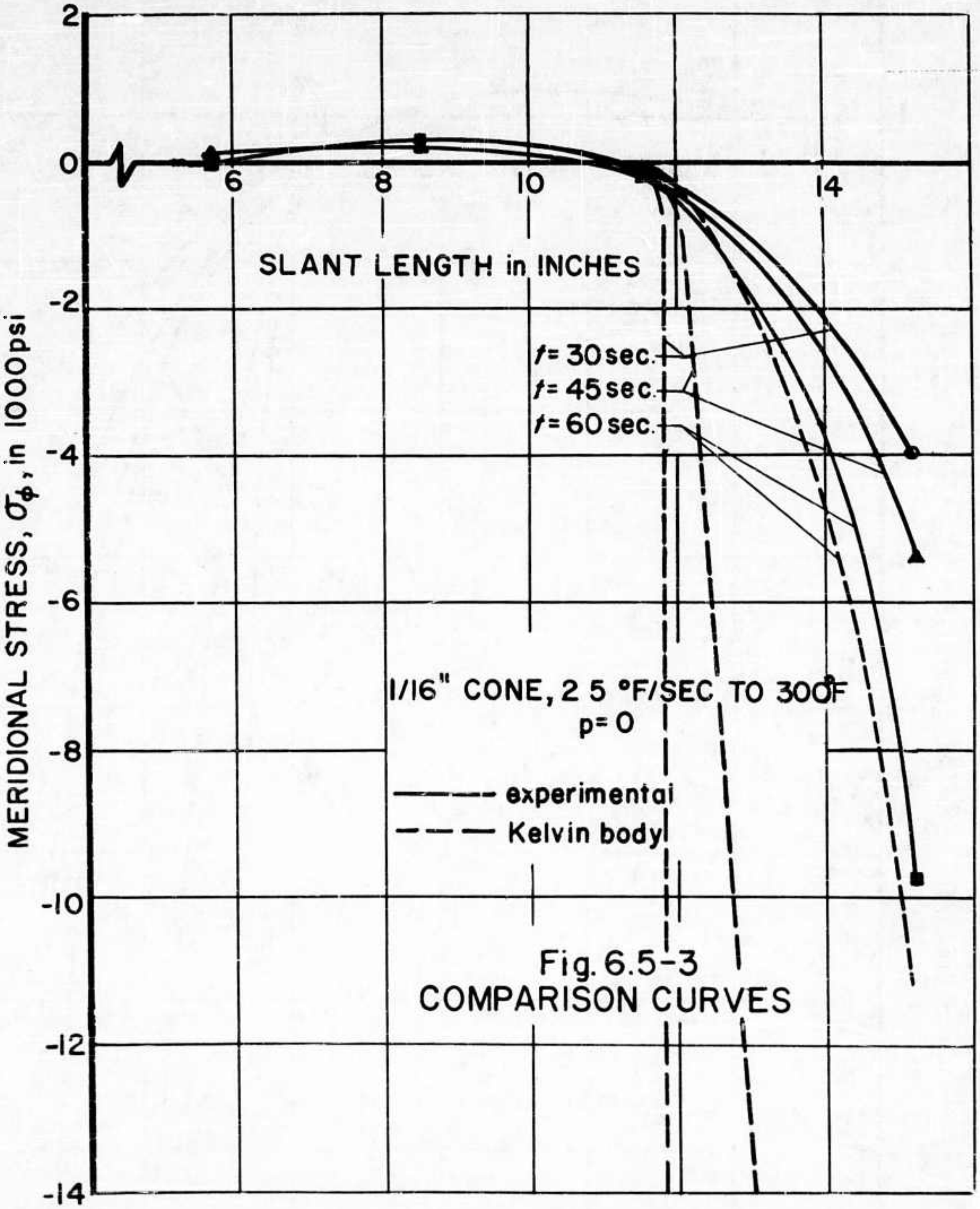

Fig. 6.5-3
COMPARISON CURVES

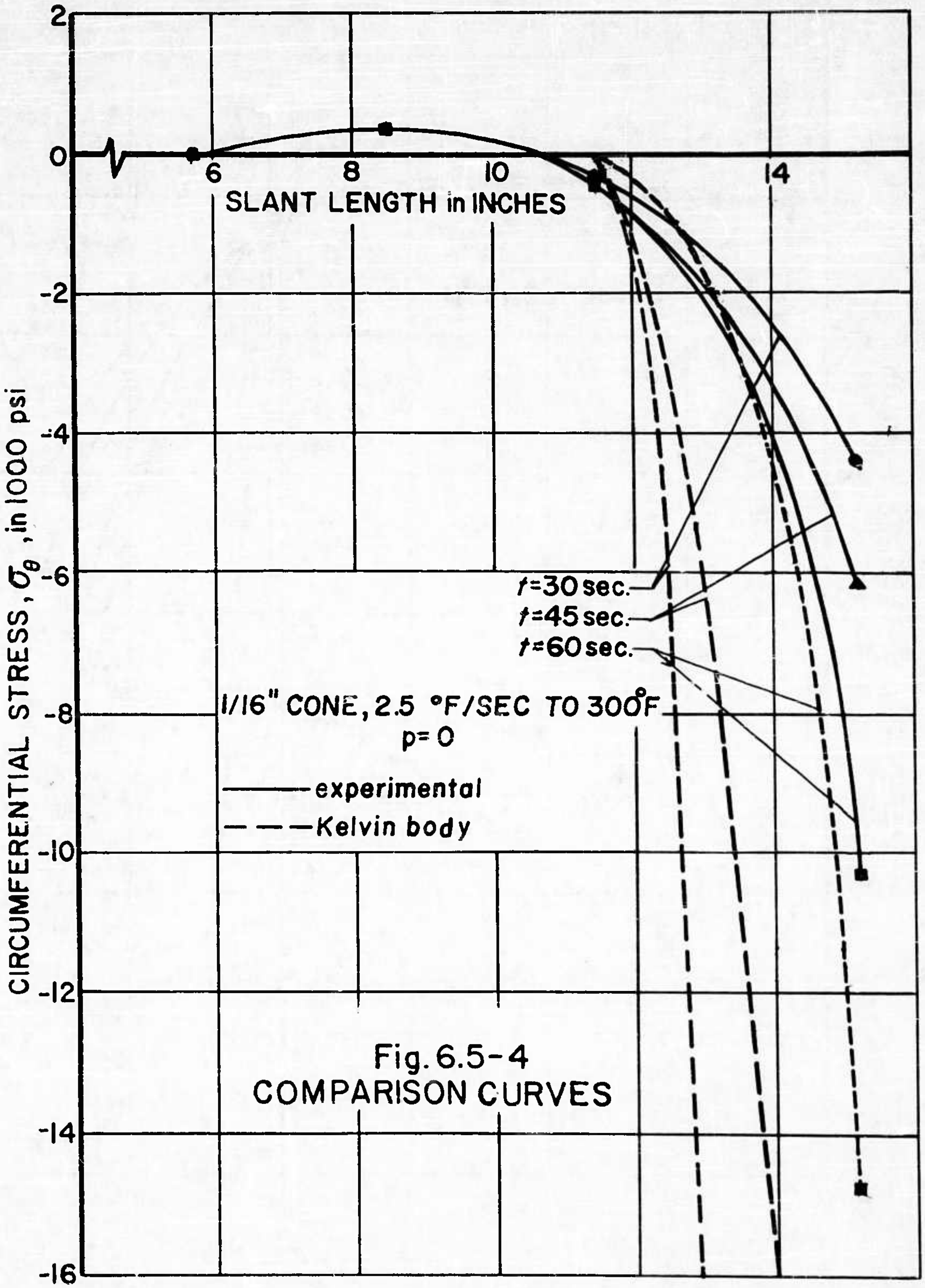

Fig. 6.5-4
COMPARISON CURVES

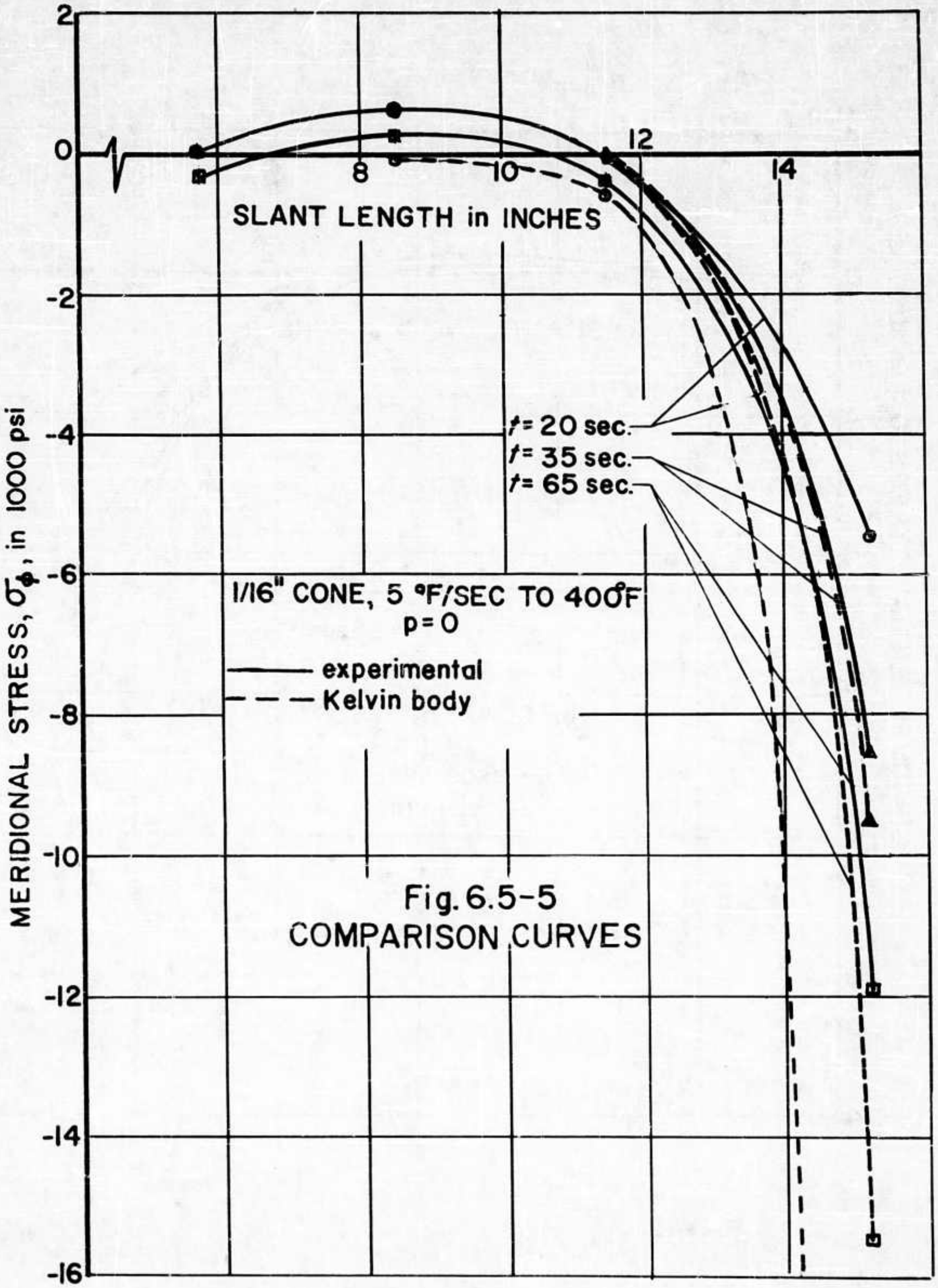

Fig. 6.5-5
COMPARISON CURVES

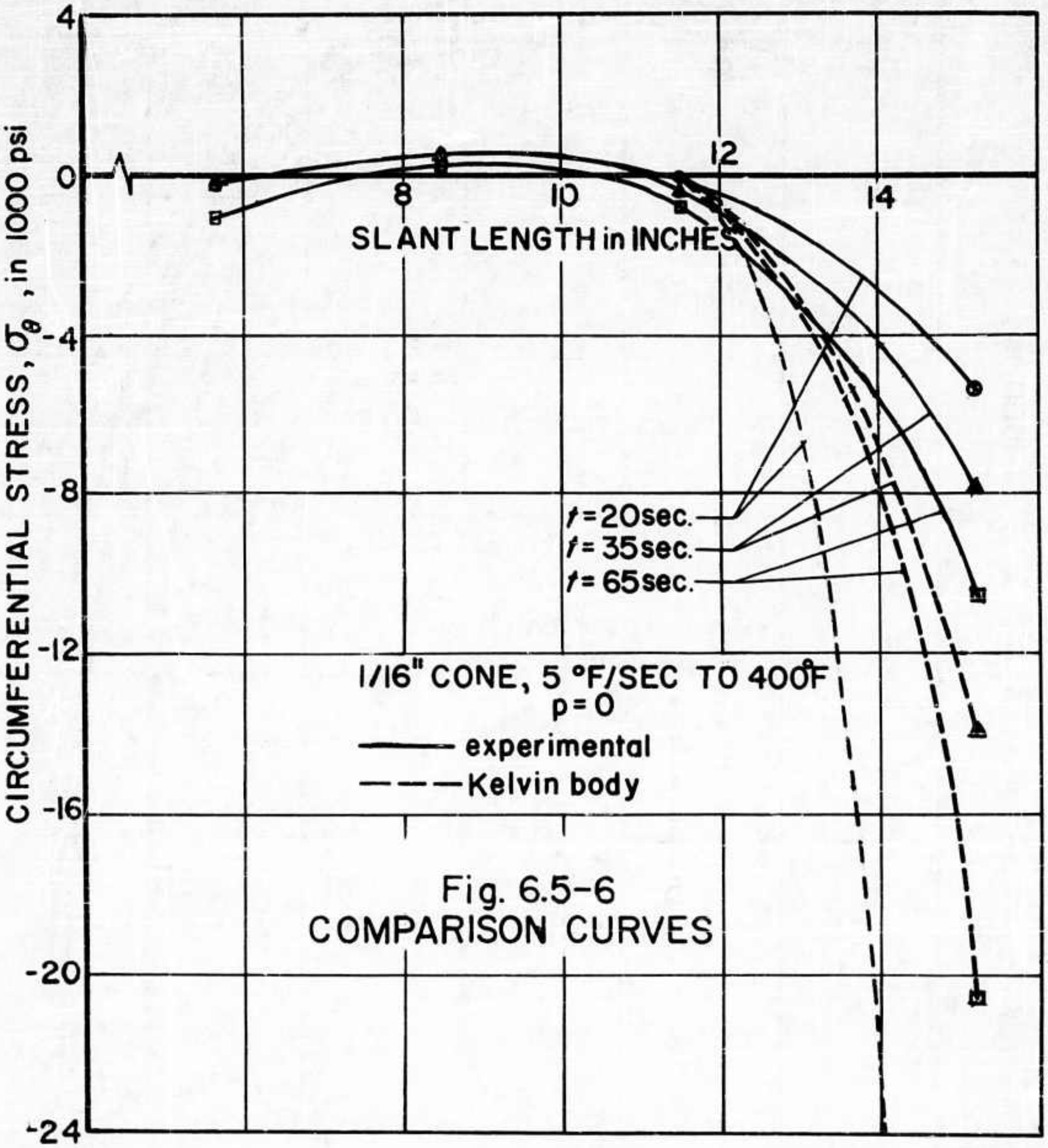

Fig. 6.5-6
COMPARISON CURVES

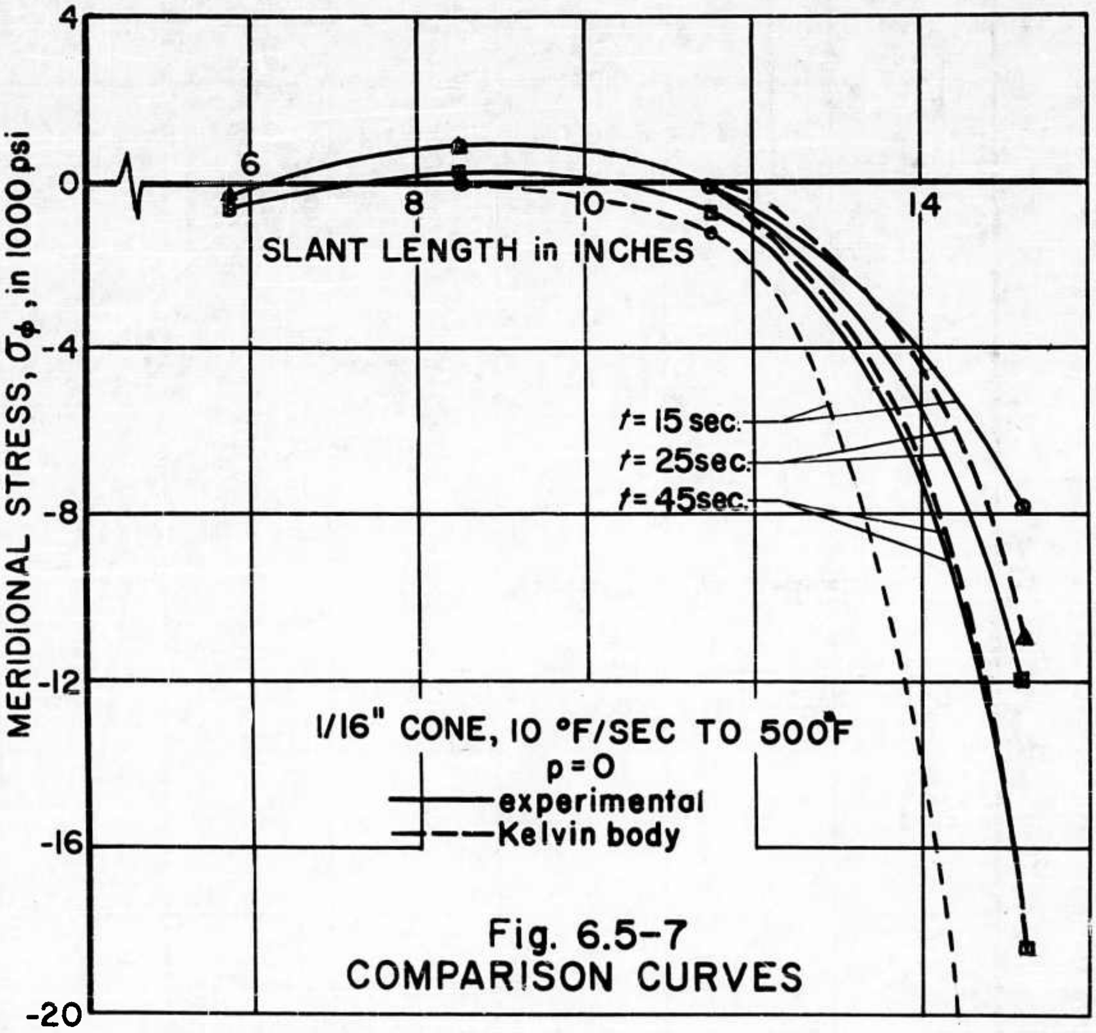

Fig. 6.5-7
COMPARISON CURVES

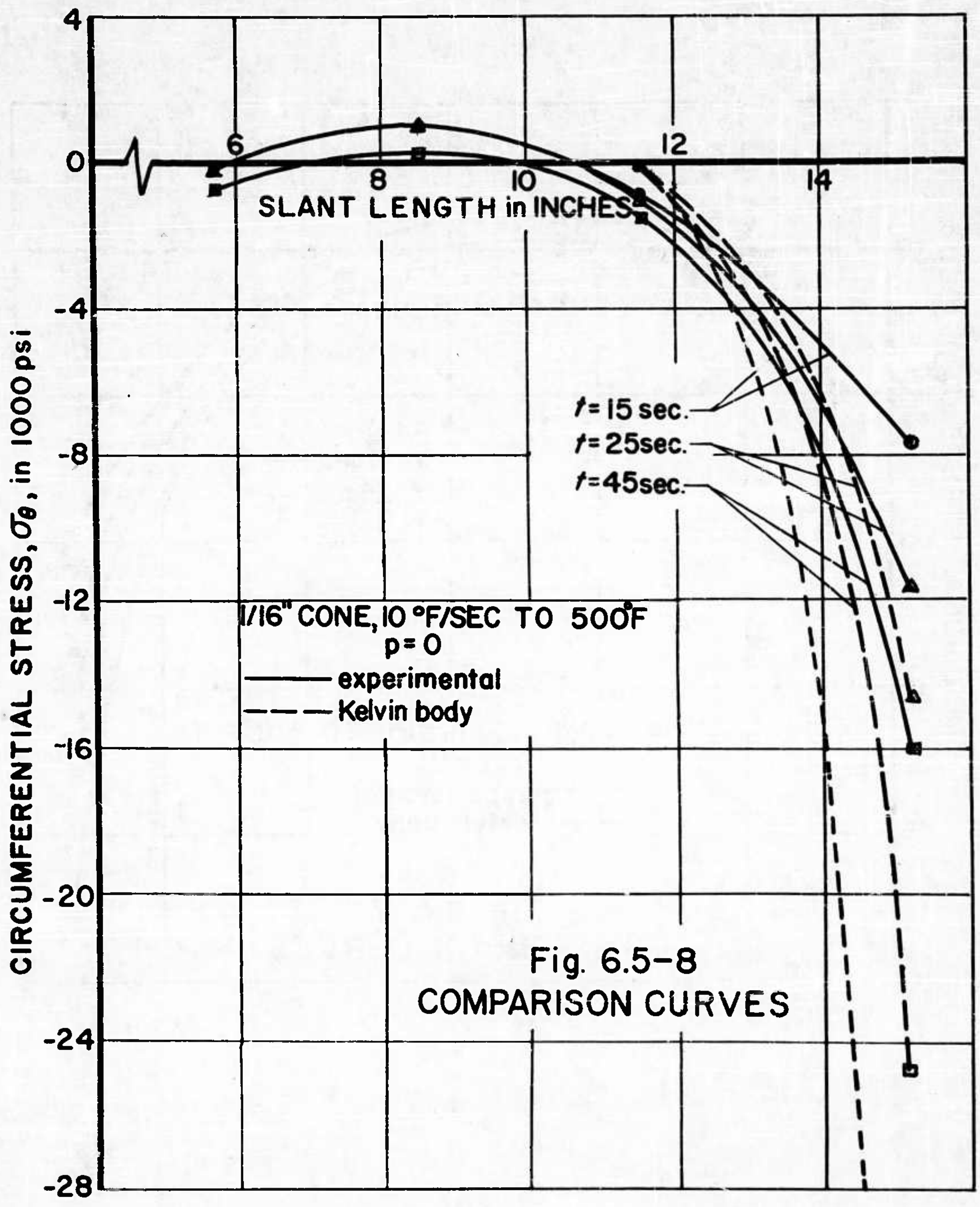

Fig. 6.5-8
COMPARISON CURVES

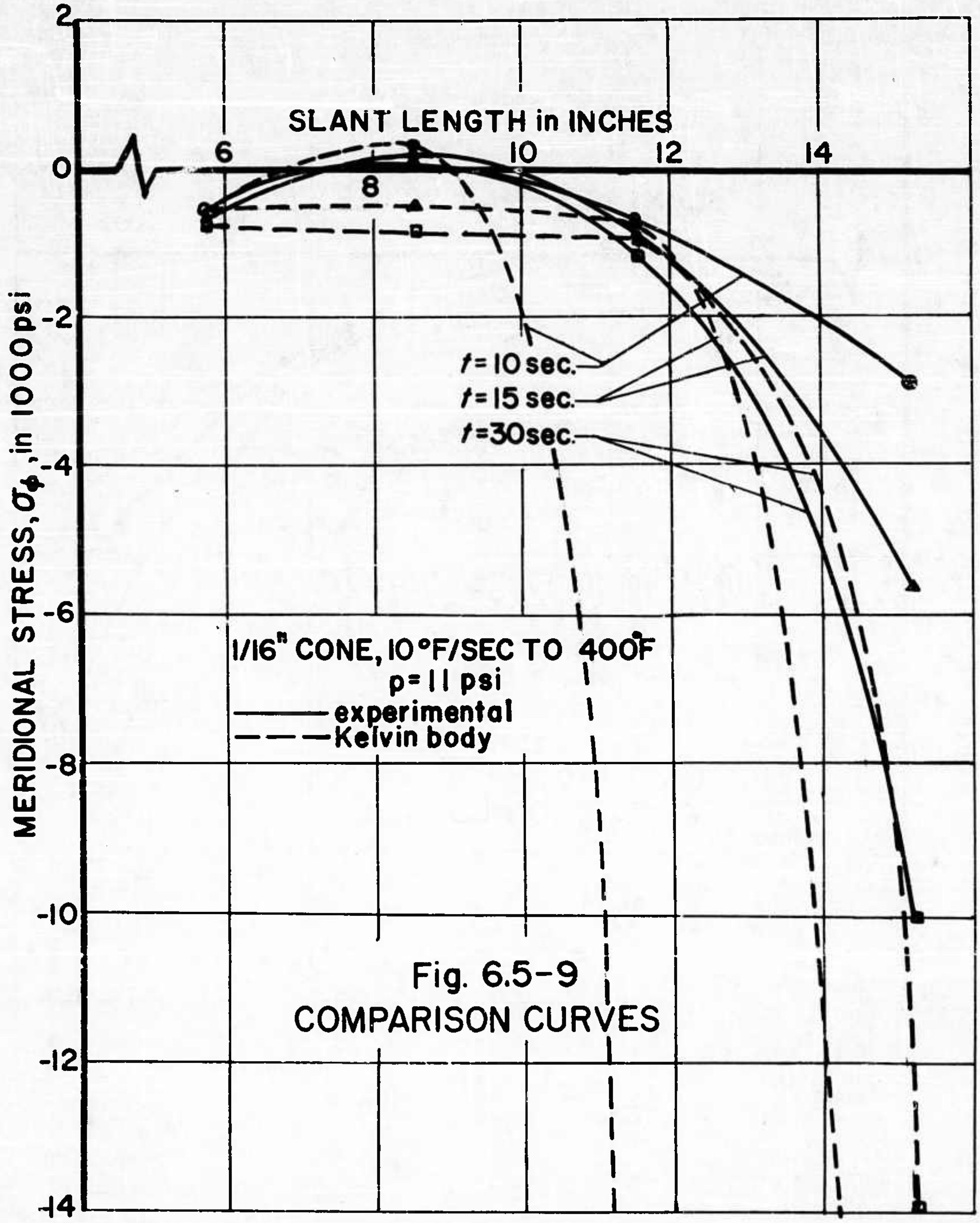

Fig. 6.5-9
COMPARISON CURVES

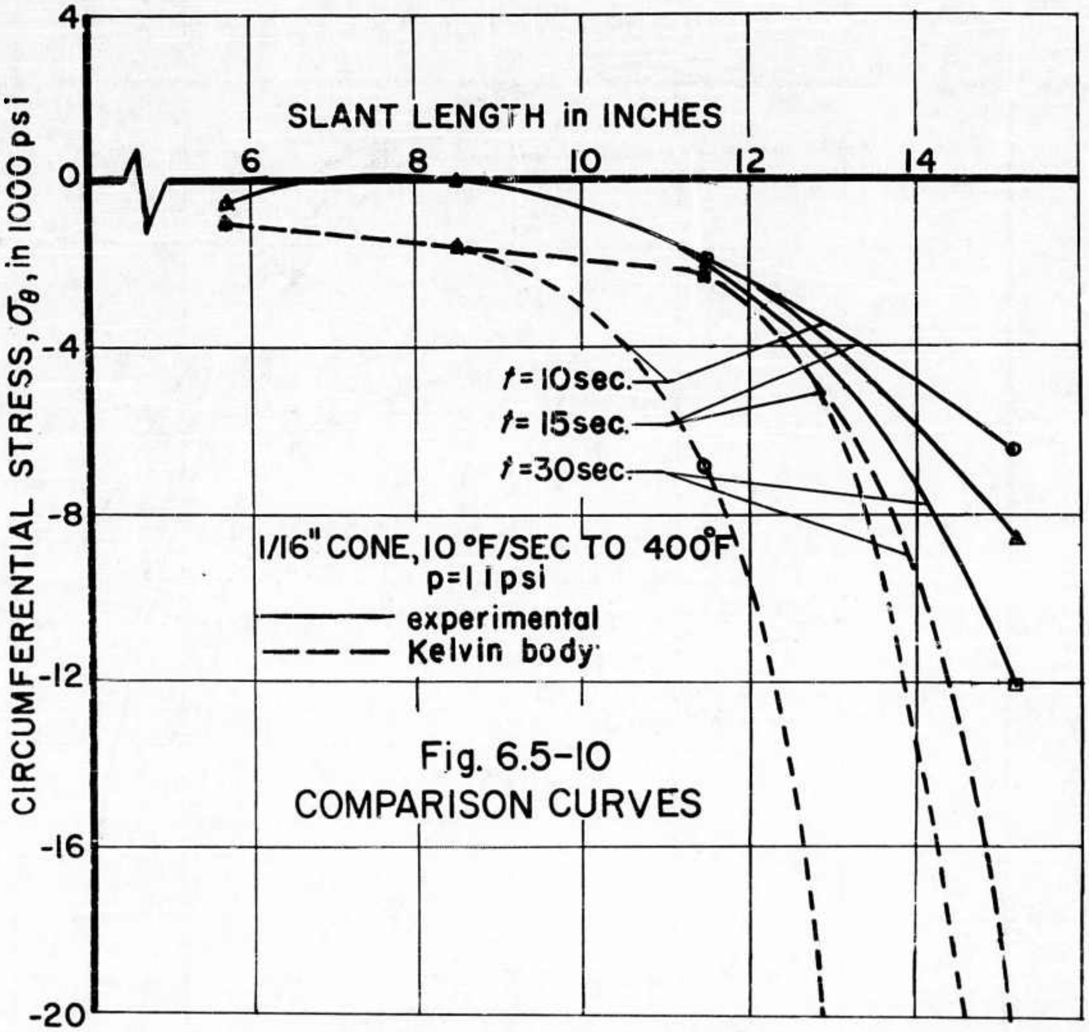

Fig. 6.5-10
COMPARISON CURVES

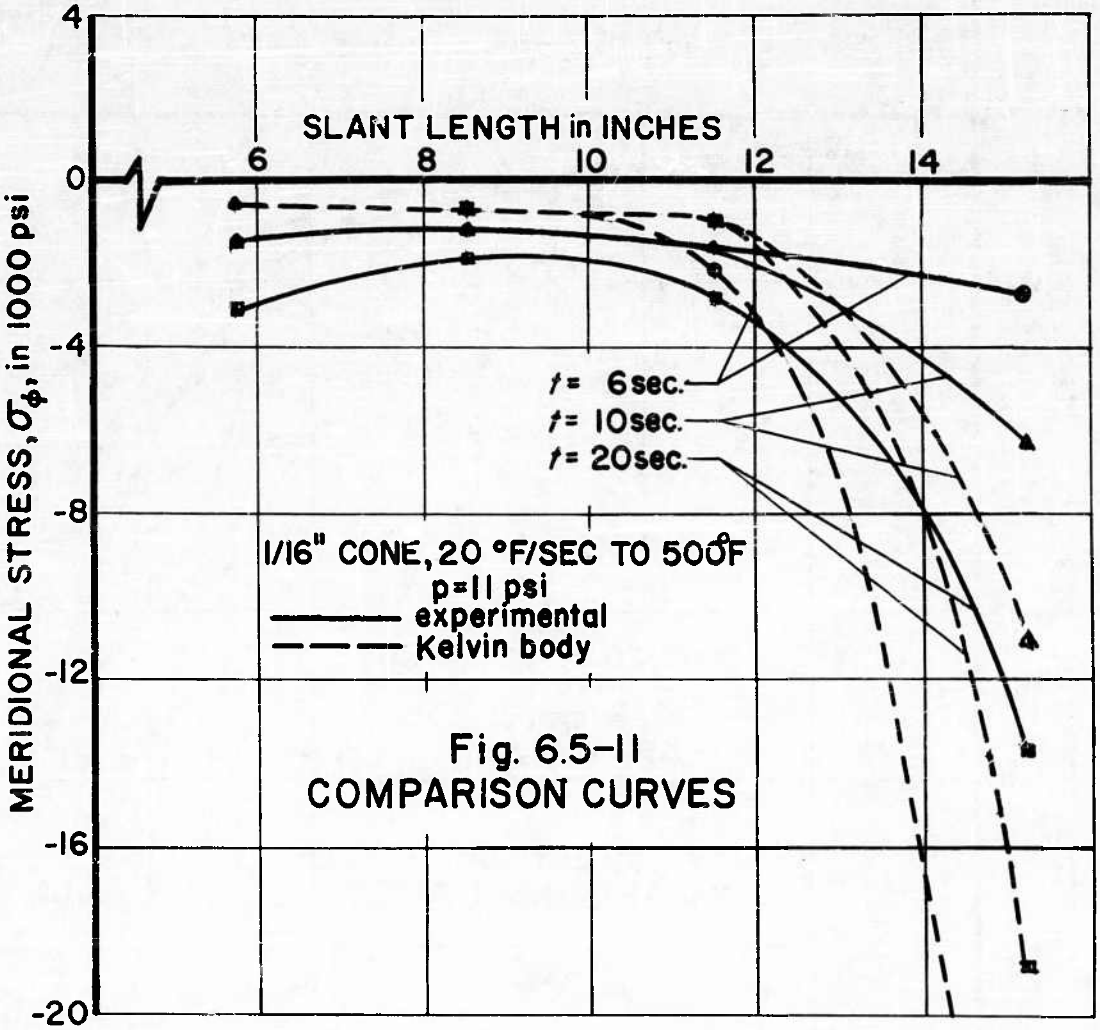

Fig. 6.5–11
COMPARISON CURVES

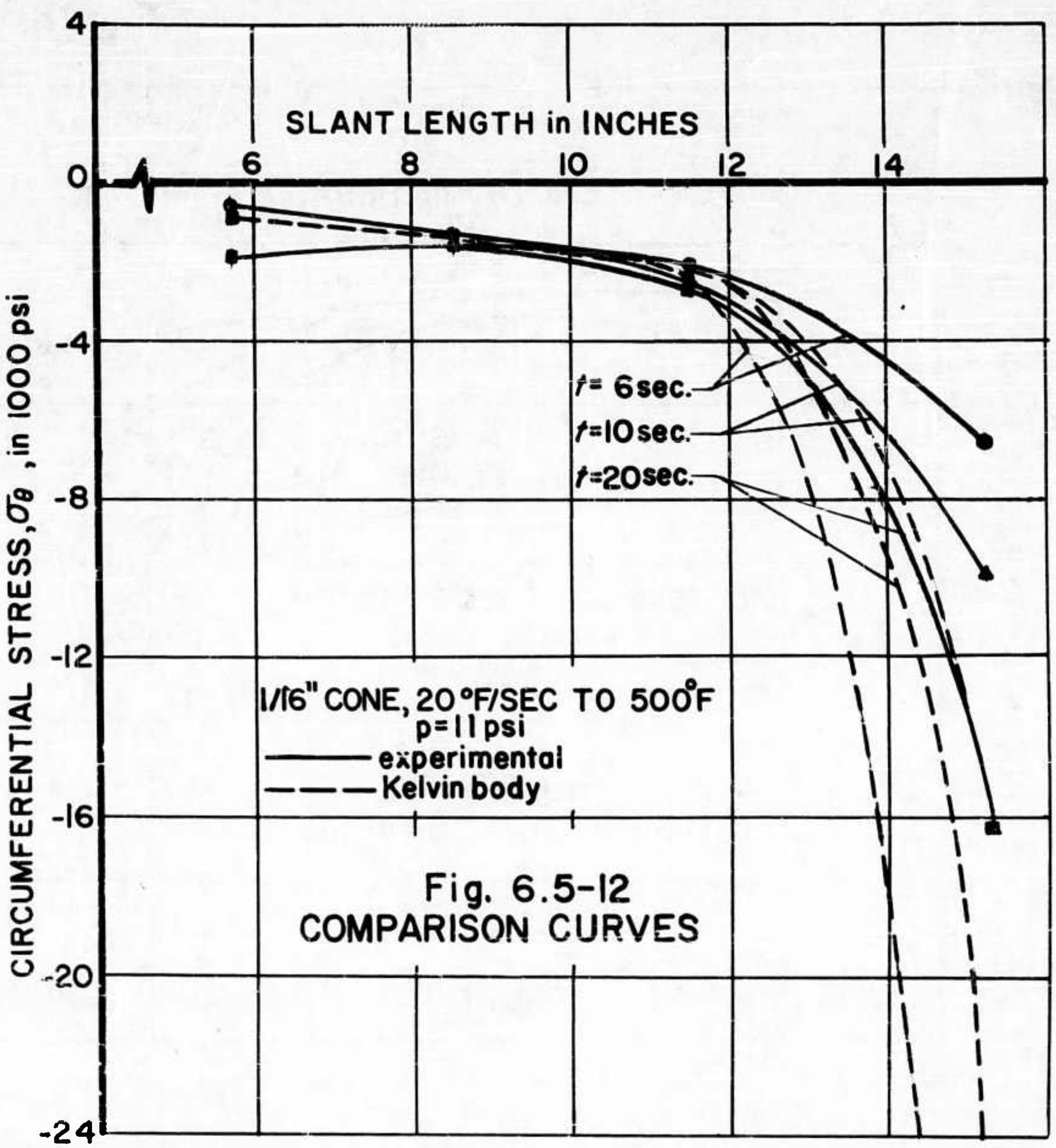

Fig. 6.5-12
COMPARISON CURVES

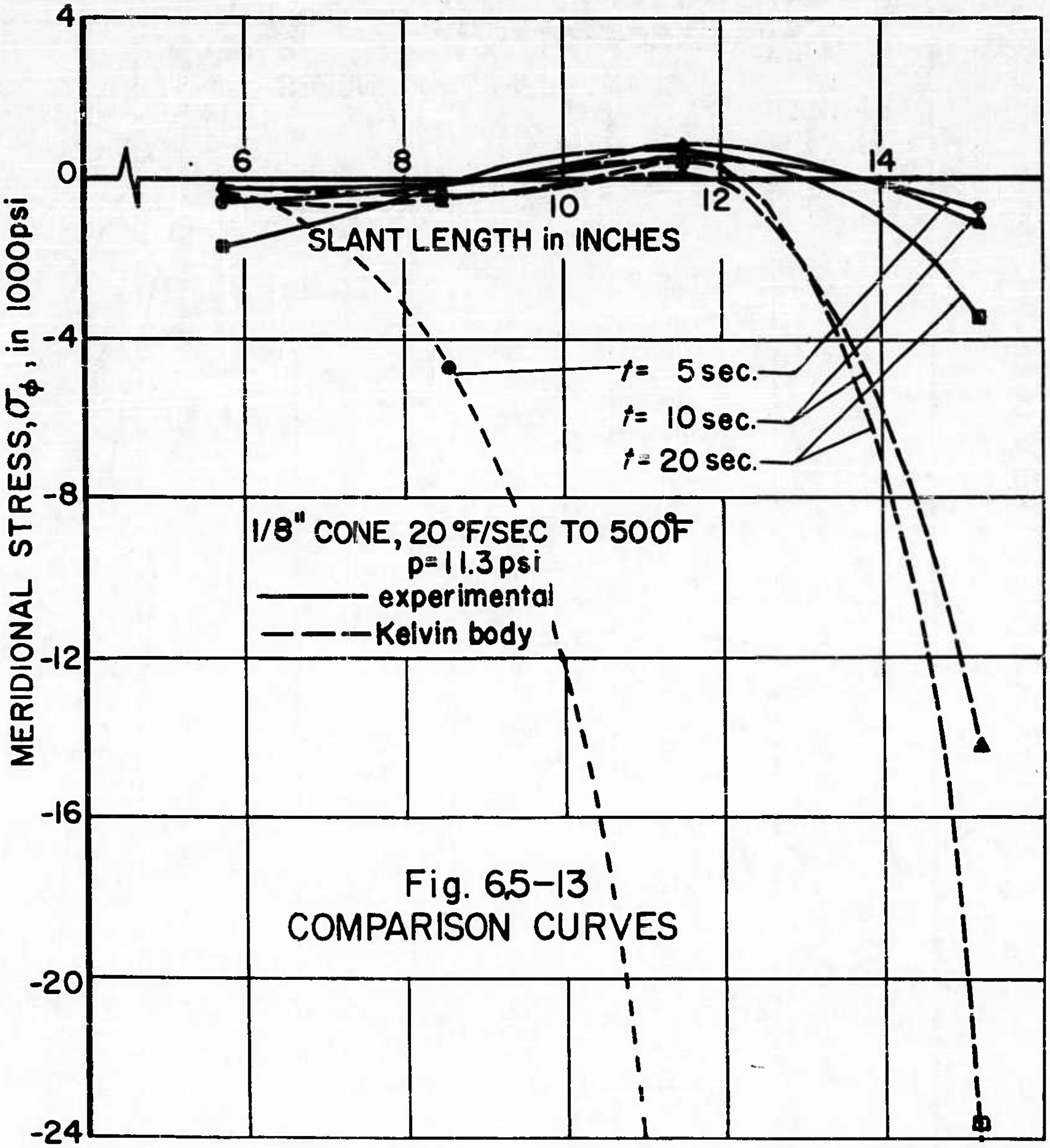

Fig. 6.5-13
COMPARISON CURVES

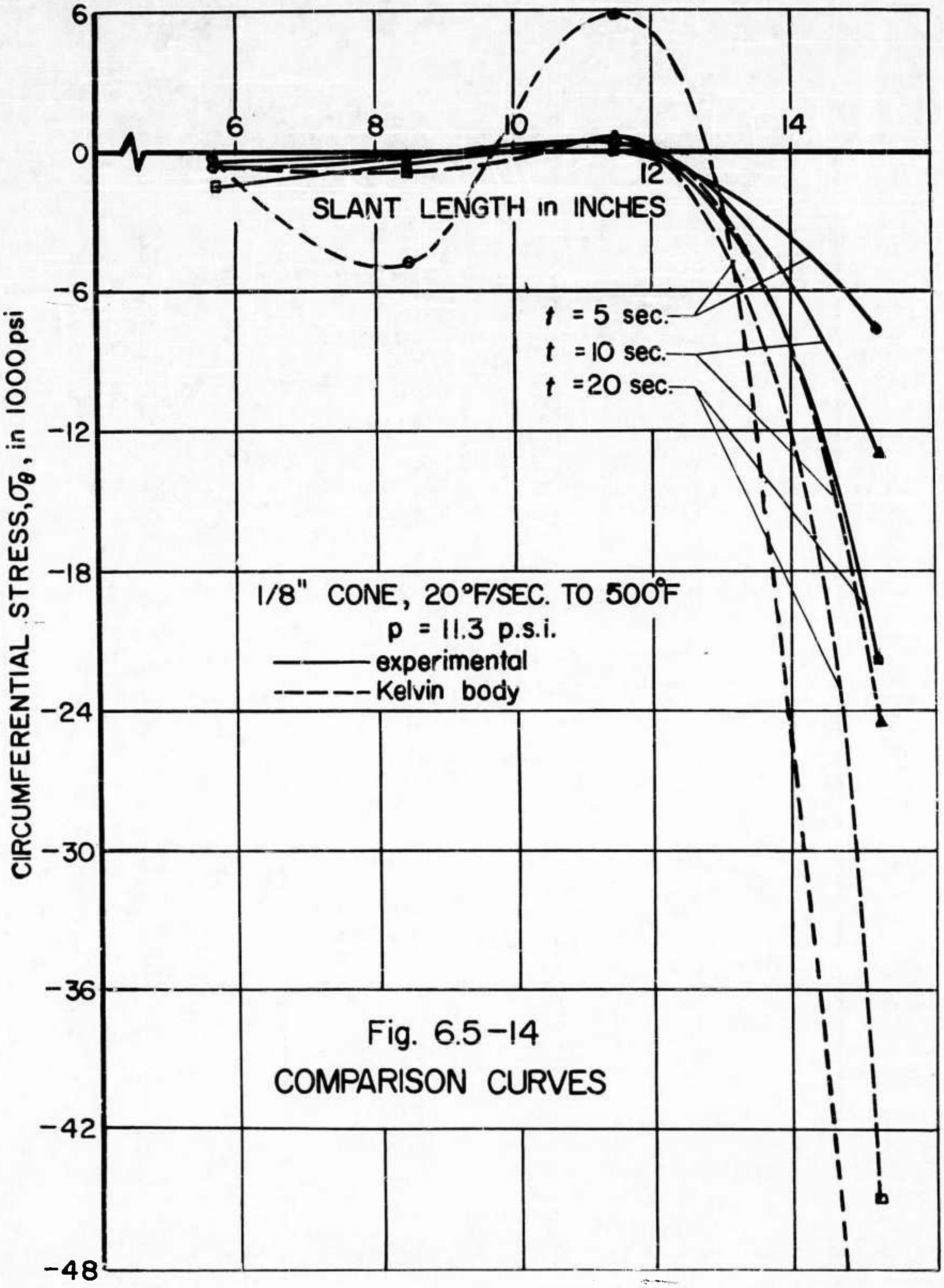

Fig. 6.5-14
COMPARISON CURVES

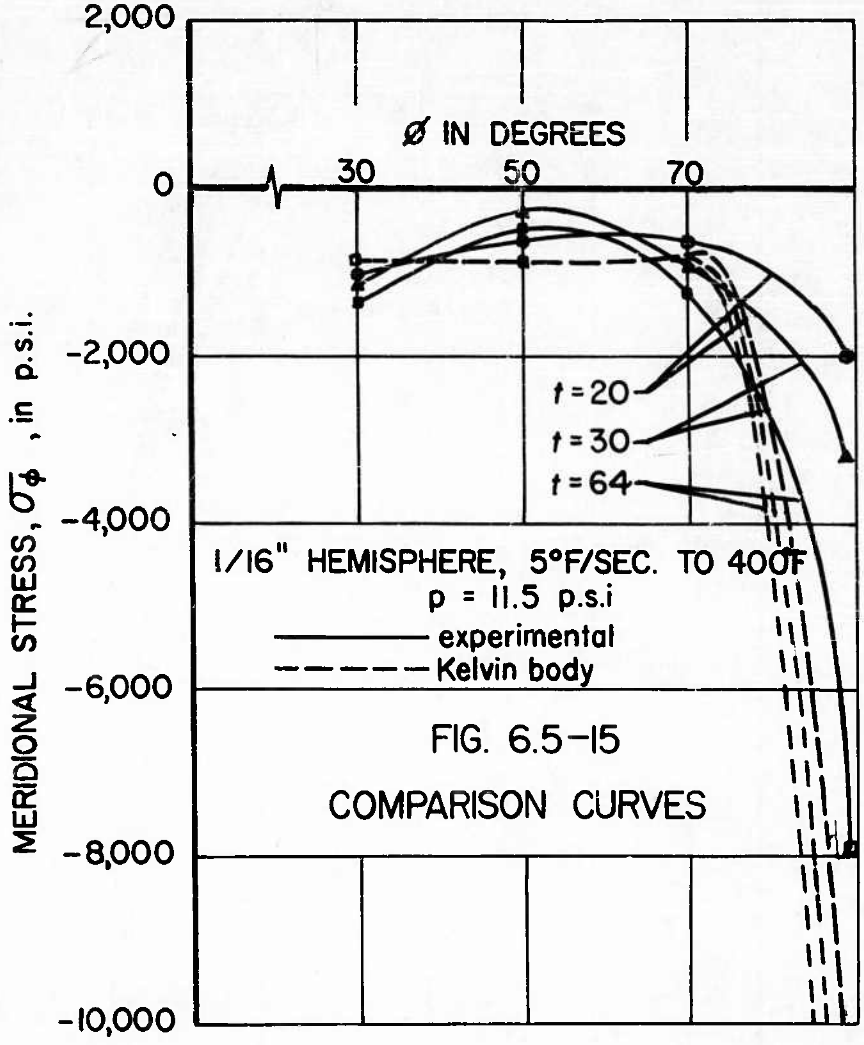

FIG. 6.5-15

COMPARISON CURVES

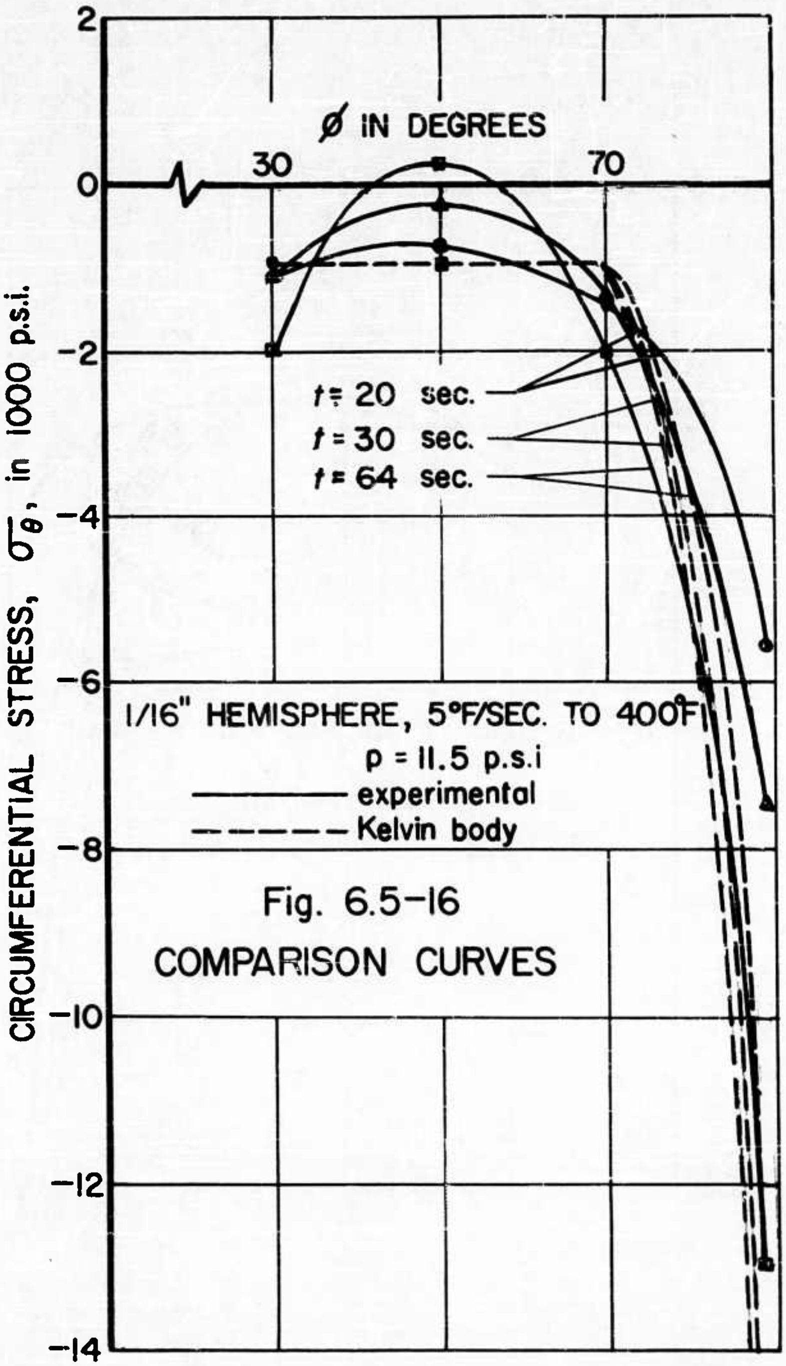

Fig. 6.5-16

COMPARISON CURVES

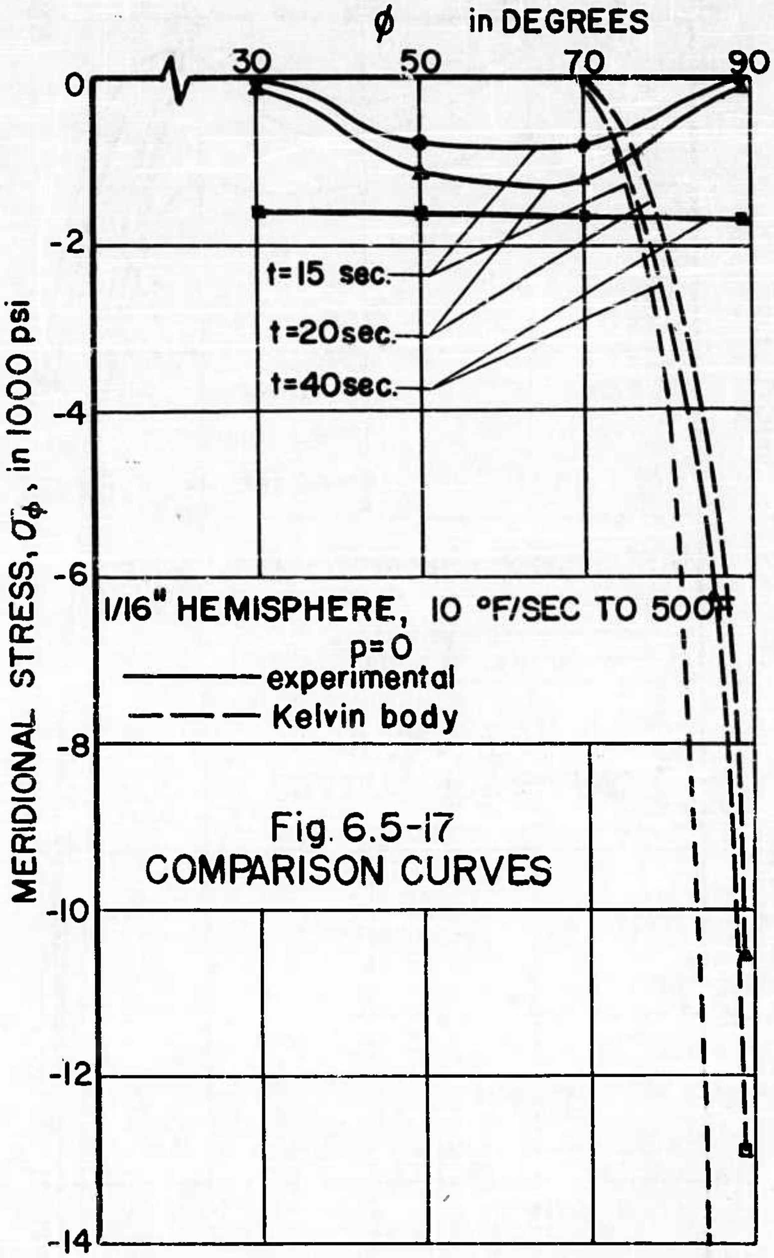

Fig. 6.5-17
COMPARISON CURVES

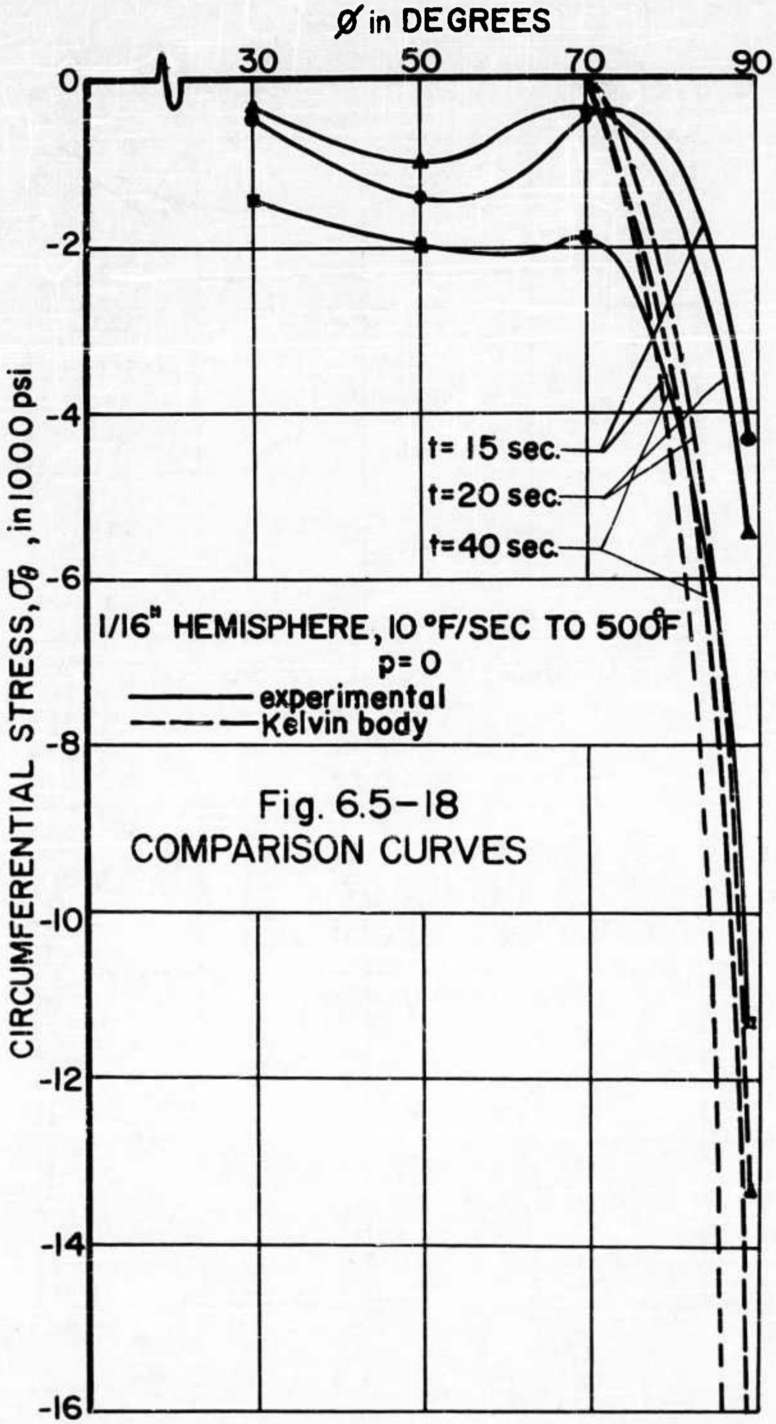

Fig. 6.5-18
COMPARISON CURVES

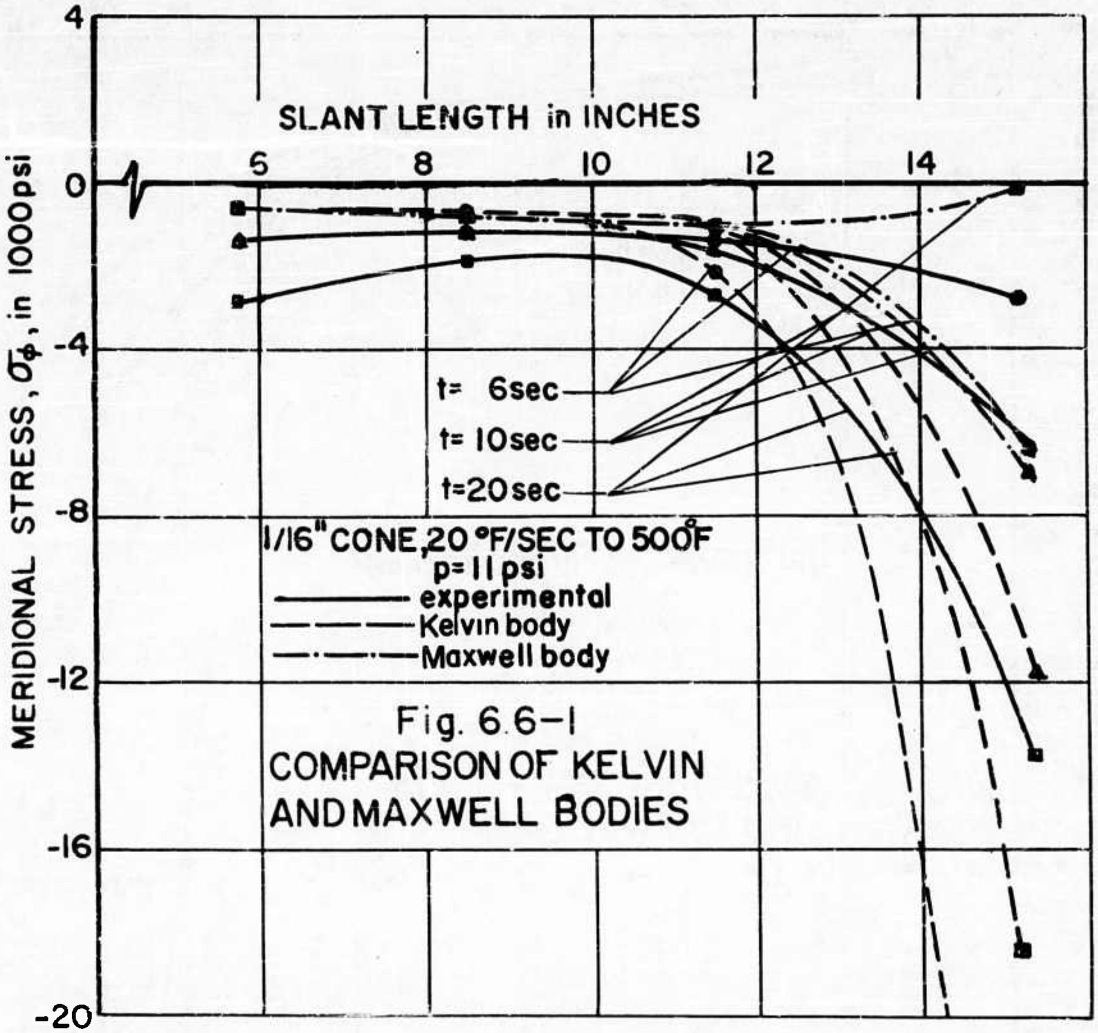

Fig. 6.6-1
COMPARISON OF KELVIN AND MAXWELL BODIES

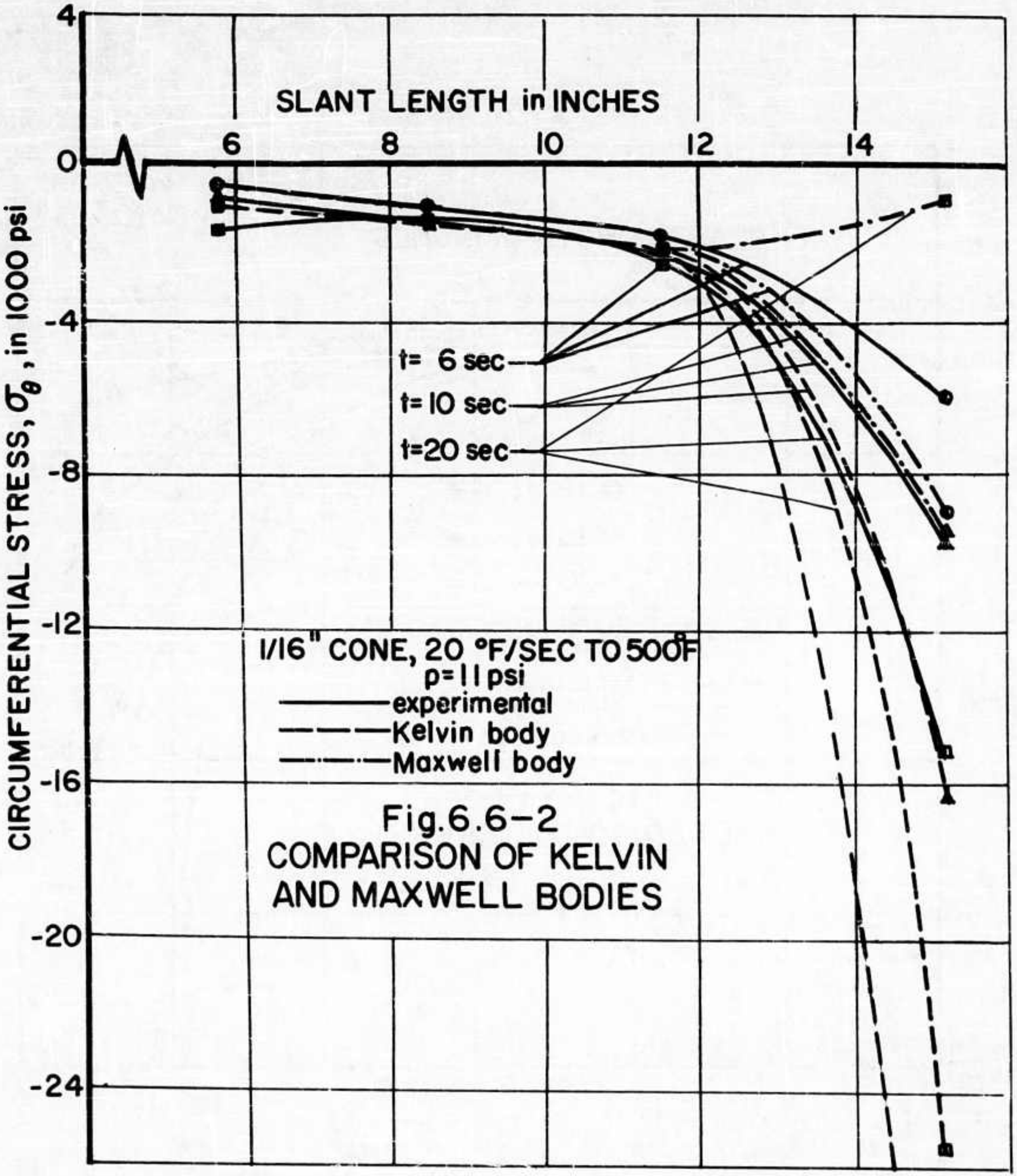

Fig.6.6-2
COMPARISON OF KELVIN AND MAXWELL BODIES

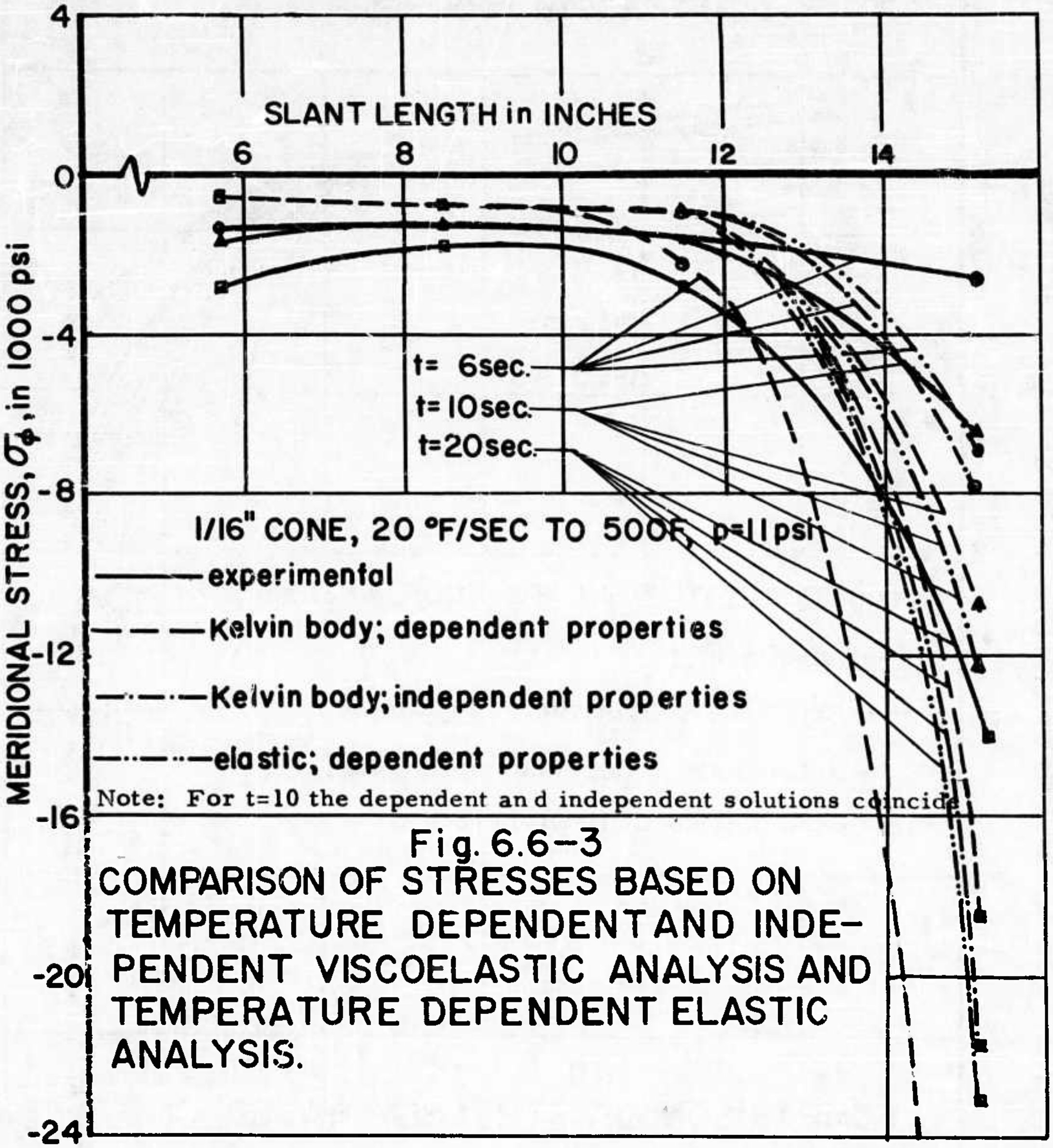

Fig. 6.6-3
COMPARISON OF STRESSES BASED ON TEMPERATURE DEPENDENT AND INDEPENDENT VISCOELASTIC ANALYSIS AND TEMPERATURE DEPENDENT ELASTIC ANALYSIS.

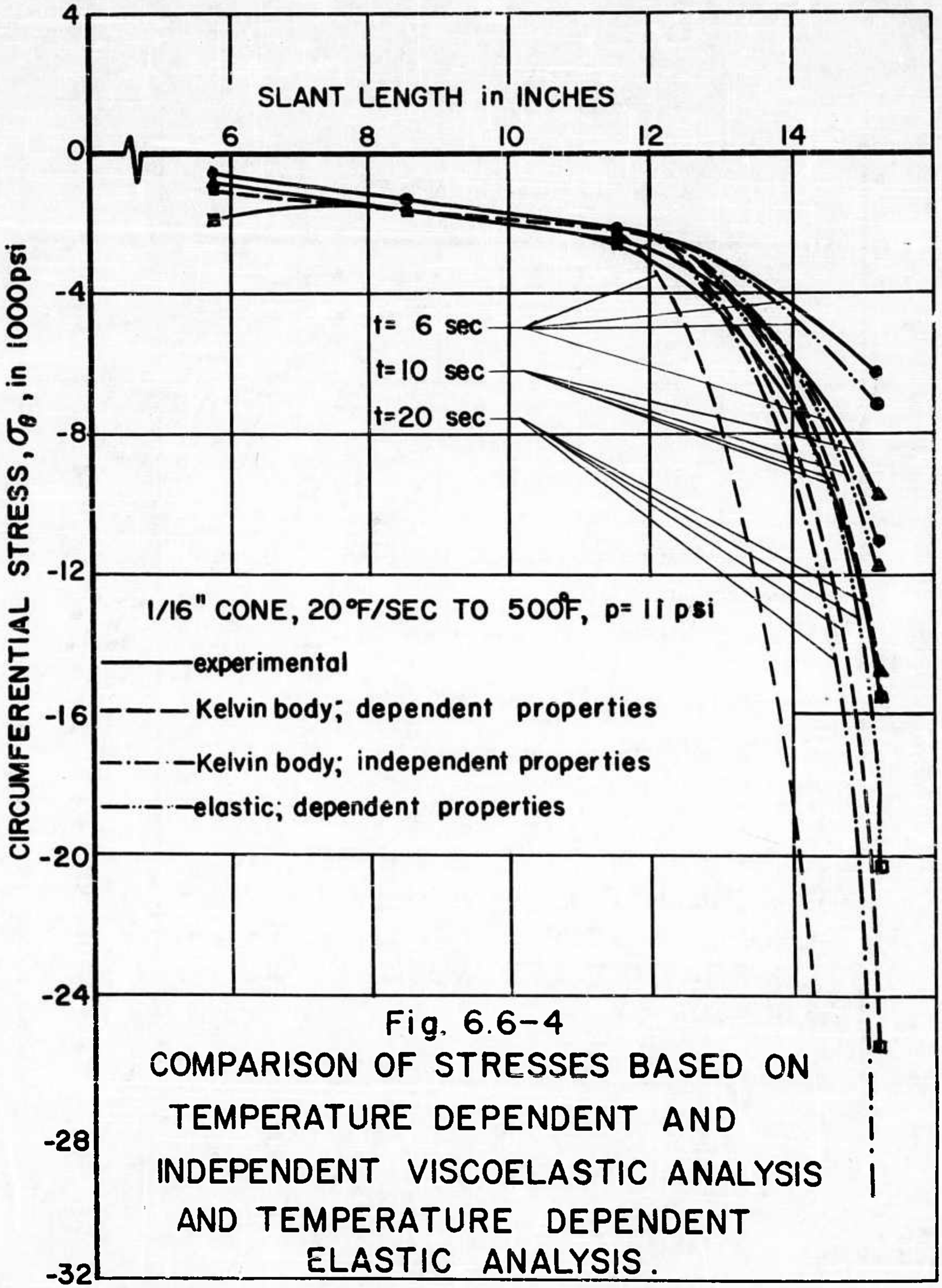

Fig. 6.6-4
COMPARISON OF STRESSES BASED ON TEMPERATURE DEPENDENT AND INDEPENDENT VISCOELASTIC ANALYSIS AND TEMPERATURE DEPENDENT ELASTIC ANALYSIS.

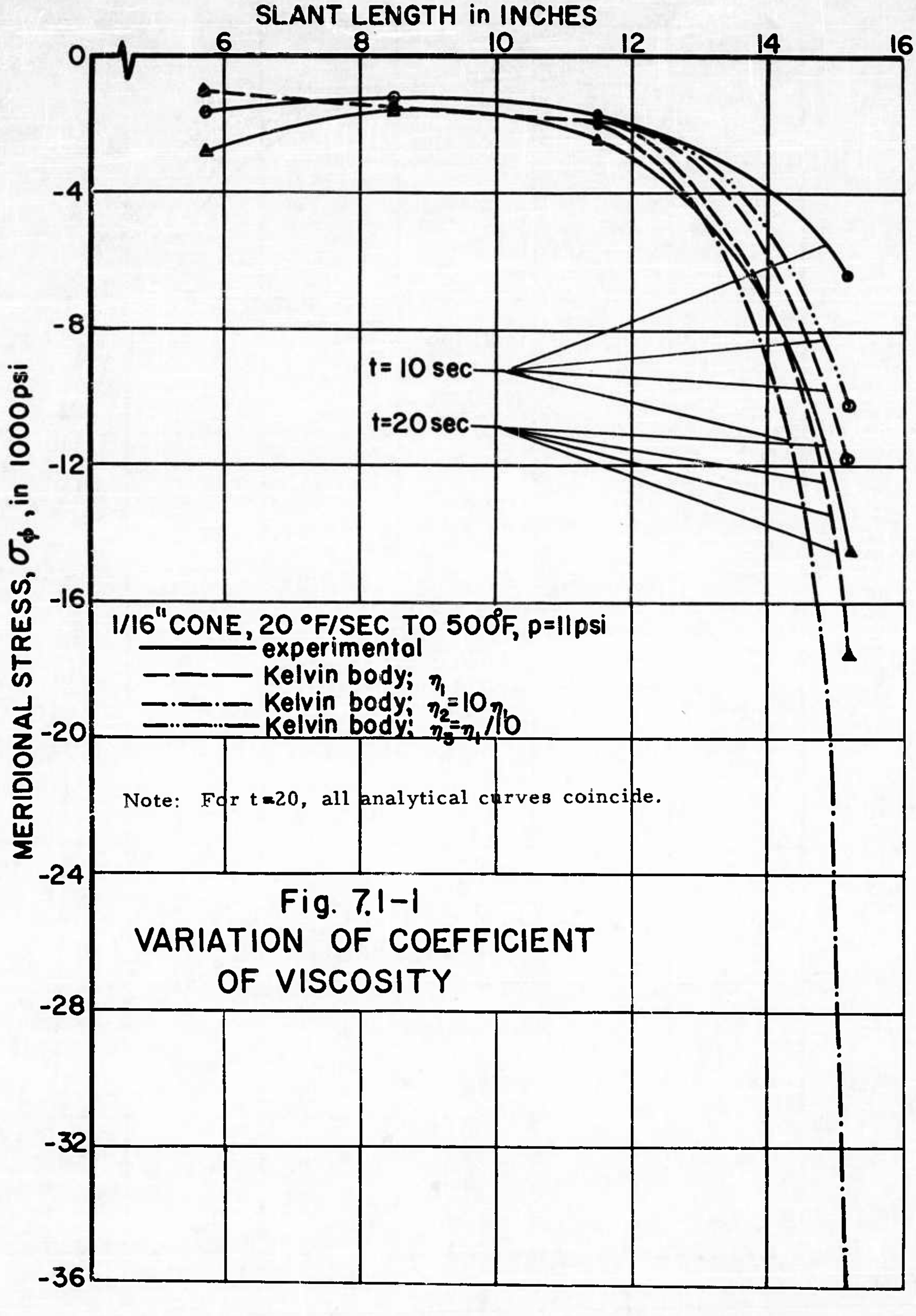

Fig. 7.1-1
VARIATION OF COEFFICIENT OF VISCOSITY

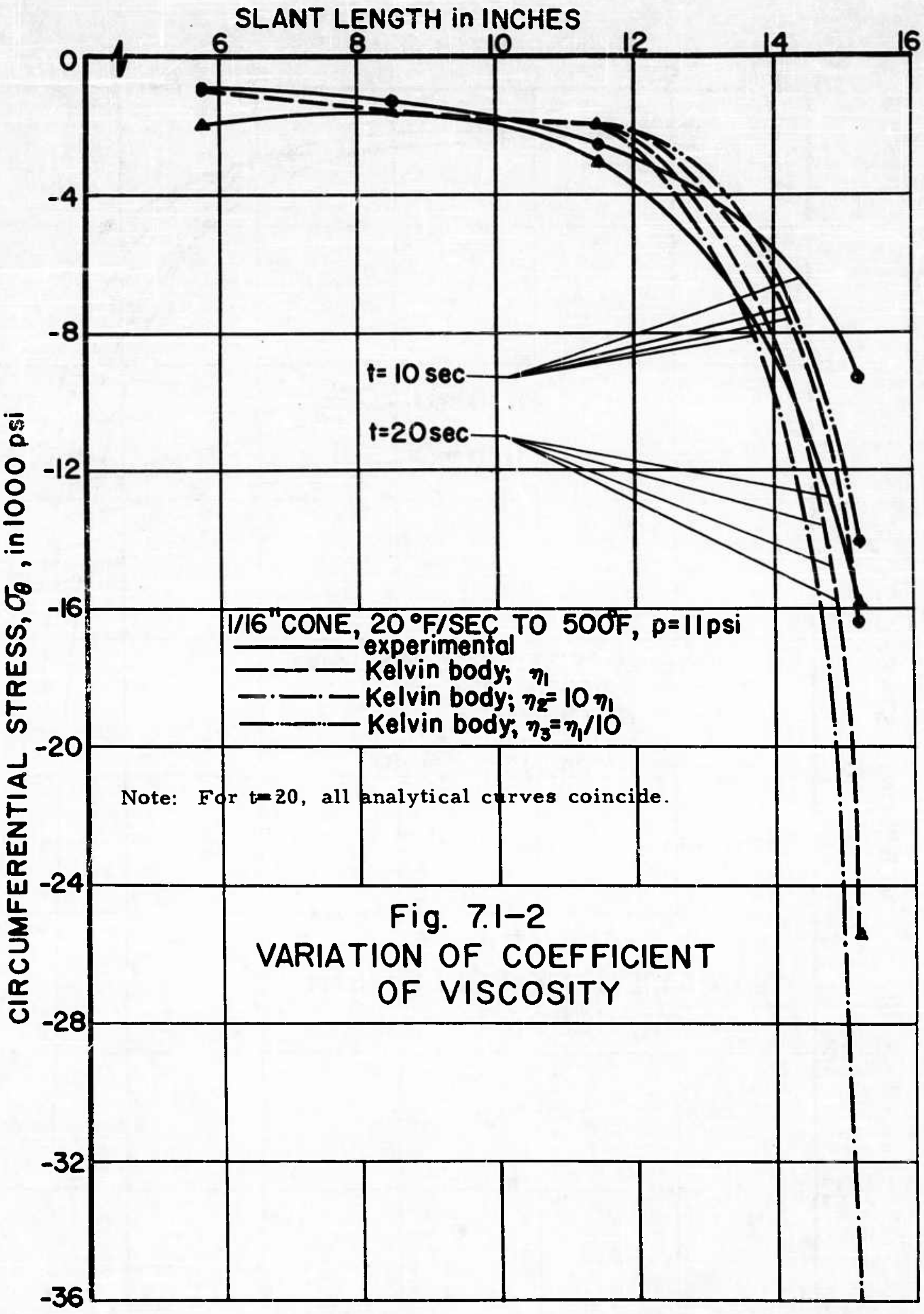

Fig. 7.1-2
VARIATION OF COEFFICIENT
OF VISCOSITY

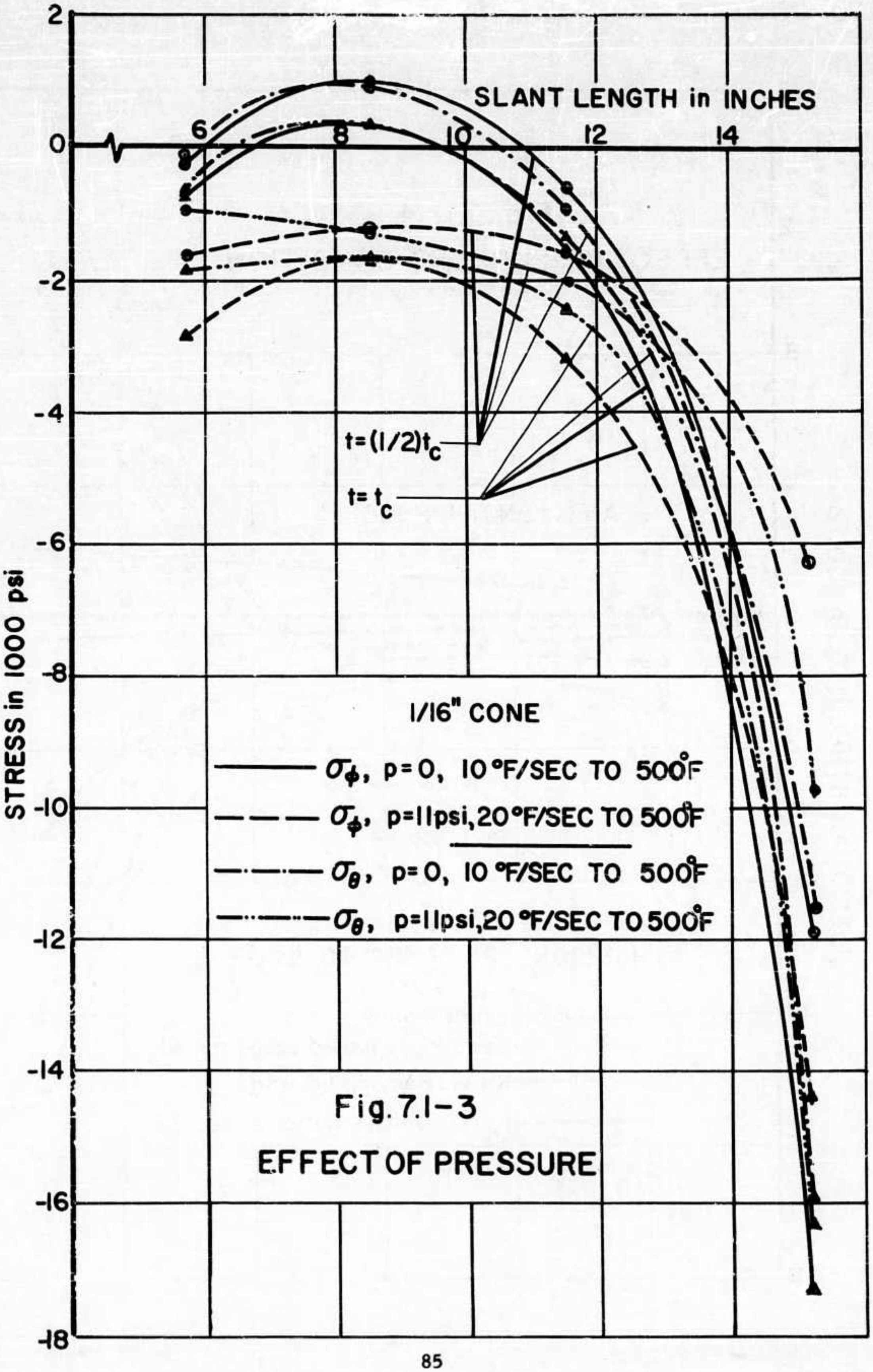

Fig. 7.1-3

EFFECT OF PRESSURE

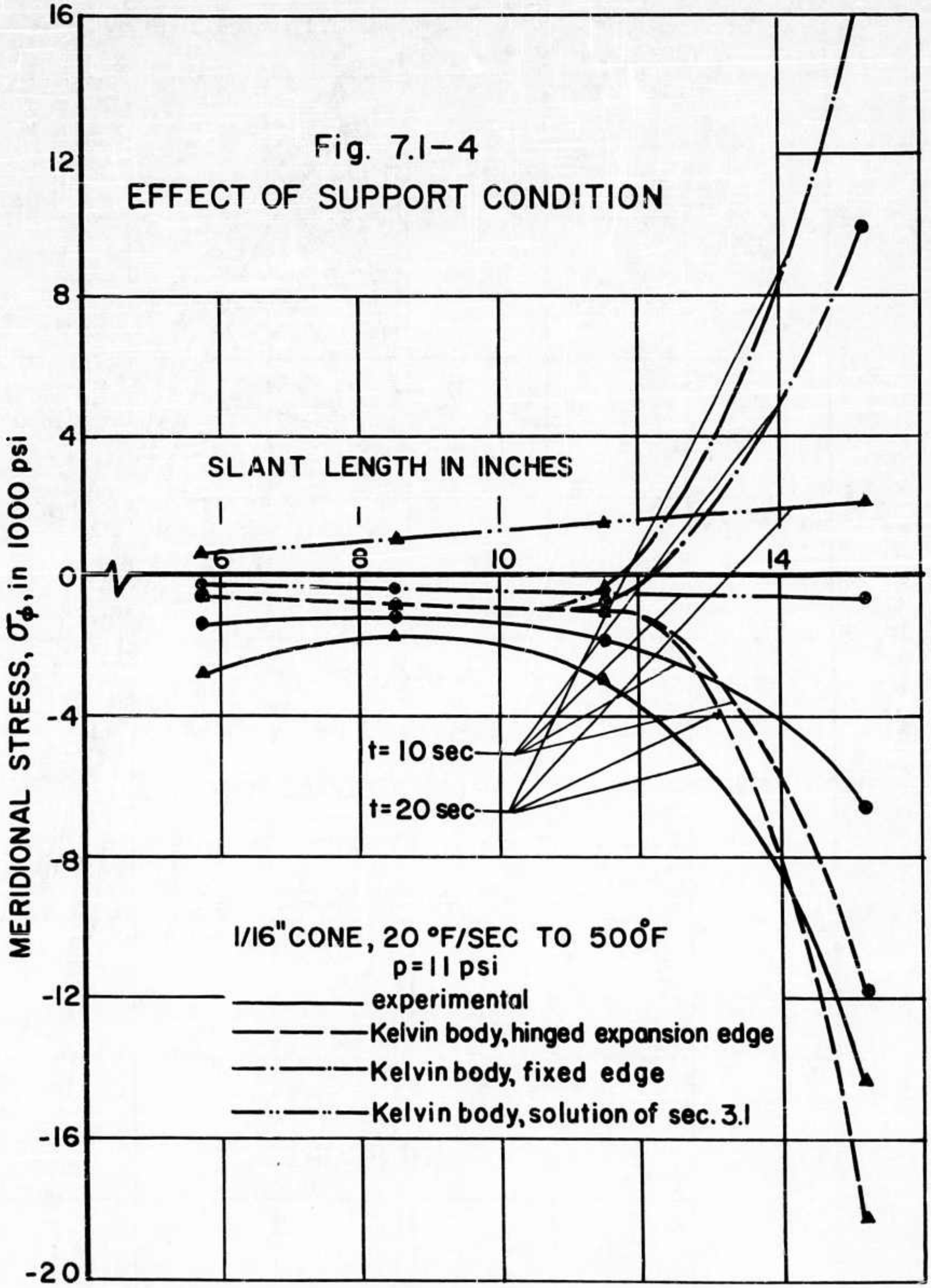

Fig. 7.1—4
EFFECT OF SUPPORT CONDITION
SLANT LENGTH IN INCHES
MERIDIONAL STRESS, σ_ϕ, in 1000 psi
16
12
8
4
0
-4
-8
-12
-16
-20
6
8
10
14
t= 10 sec
t=20 sec
1/16" CONE, 20 °F/SEC TO 500°F
p=11 psi
experimental
Kelvin body, hinged expansion edge
Kelvin body, fixed edge
Kelvin body, solution of sec. 3.1

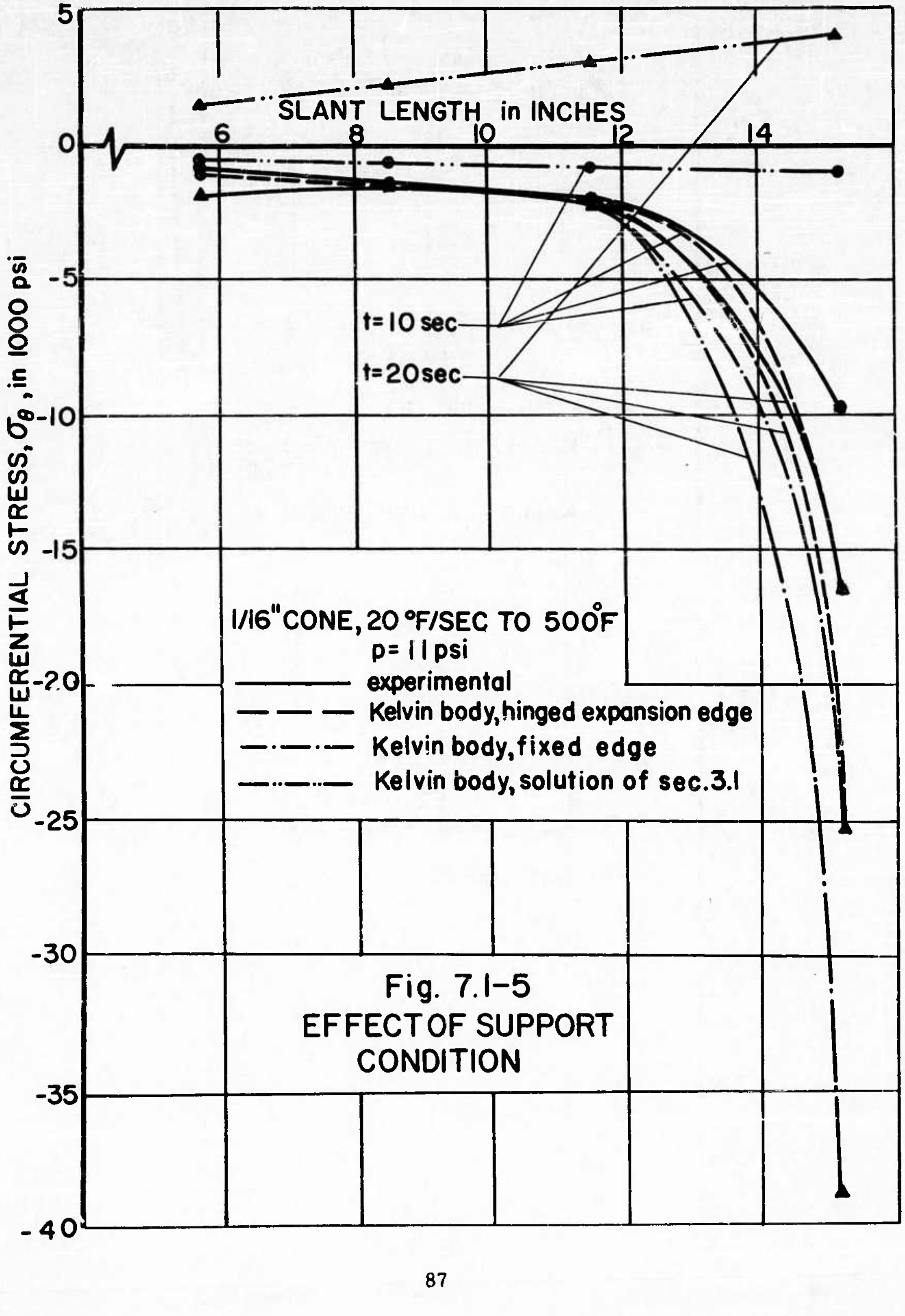

Fig. 7.1-5
EFFECT OF SUPPORT
CONDITION

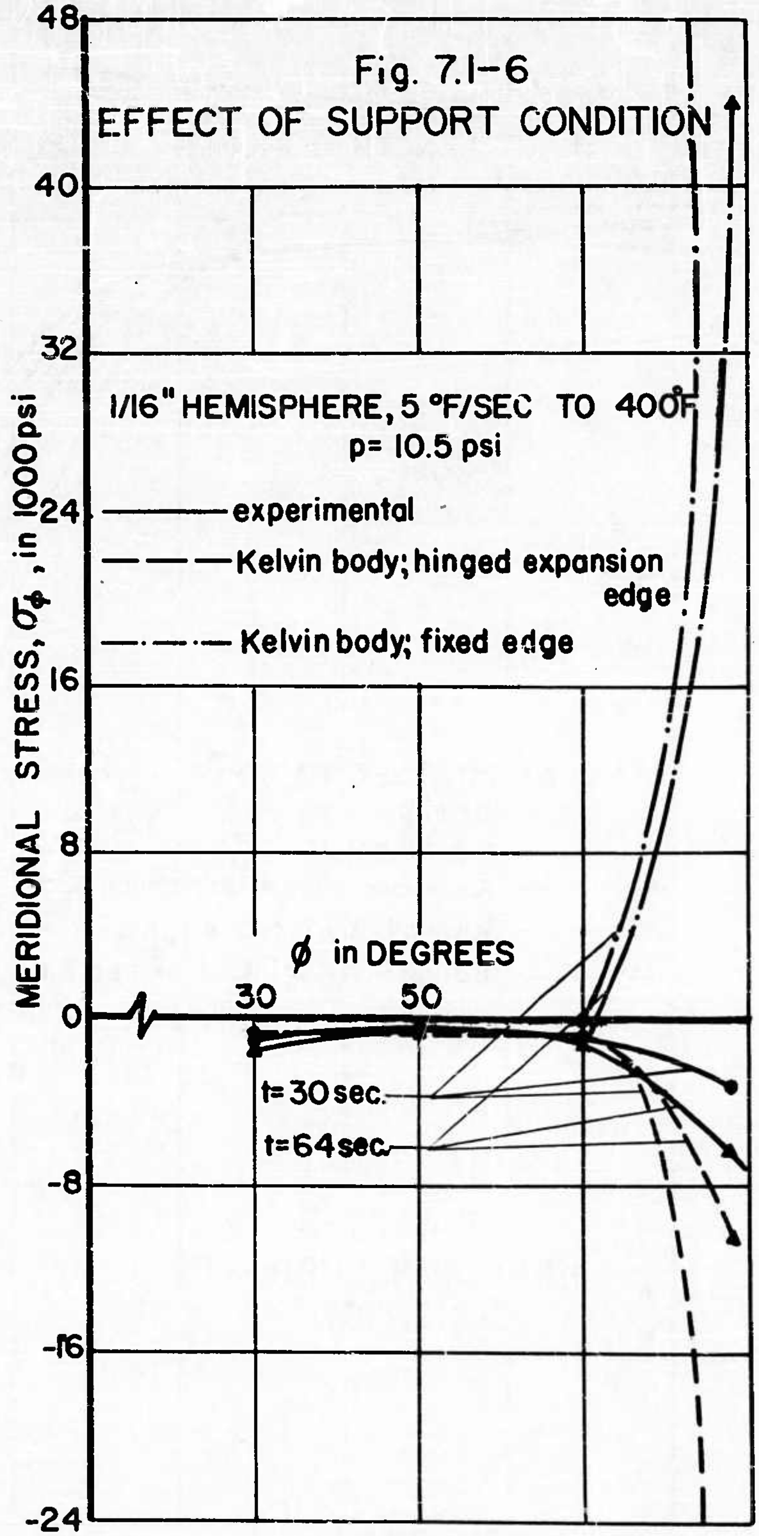
Fig. 7.1-6
EFFECT OF SUPPORT CONDITION
1/16" HEMISPHERE, 5 °F/SEC TO 400°F
p= 10.5 psi
experimental
Kelvin body; hinged expansion edge
Kelvin body; fixed edge
MERIDIONAL STRESS, σ_ϕ , in 1000psi
ϕ in DEGREES
30
50
t=30 sec.
t=64 sec.
48
40
32
24
16
8
0
-8
-16
-24

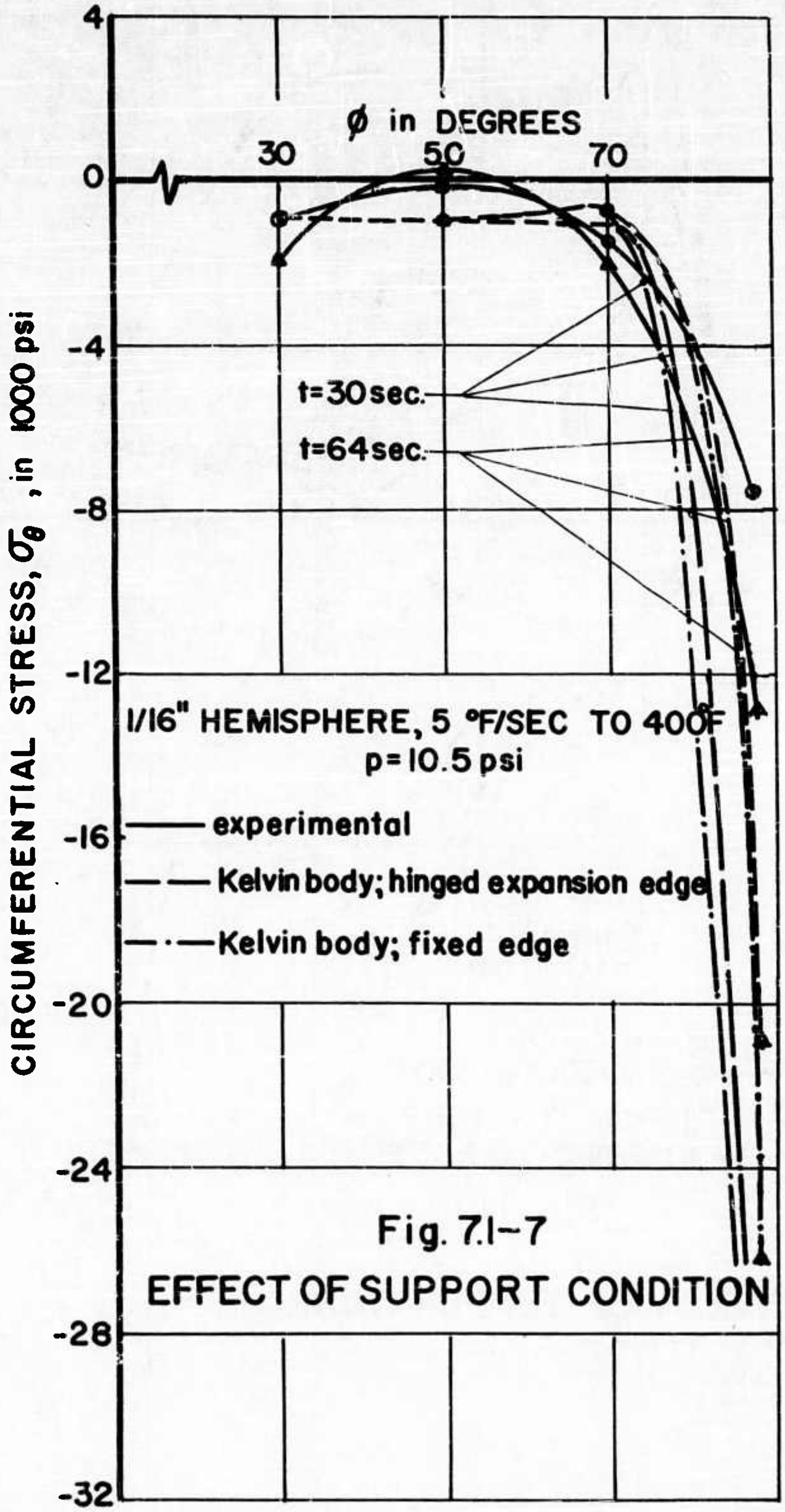

Fig. 7.1–7

EFFECT OF SUPPORT CONDITION

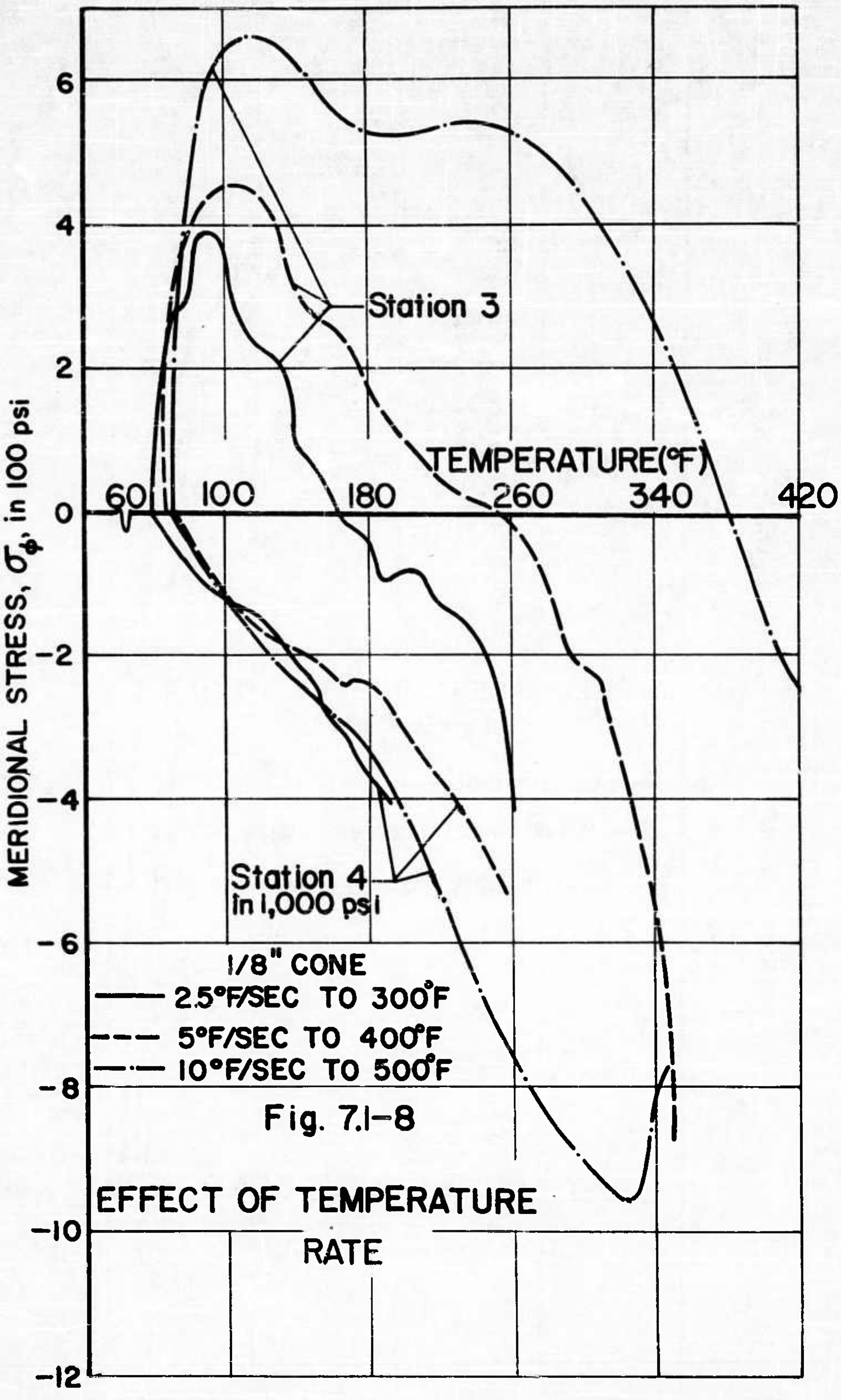

Fig. 7.1−8

EFFECT OF TEMPERATURE RATE

APPENDIX A

MATHEMATICAL DETAILS

Appendix A.1 Simplification of the Strain-displacement Relationship by the Order of Magnitude Consideration

The strain-displacement relationship for the general case are

$$\epsilon_{\phi\xi} = \frac{1}{\rho_1}\left(\frac{\partial v}{\partial \phi} - w\right) - \frac{1}{\rho_1}\frac{\partial}{\partial \phi}\left(\frac{v}{\rho_1} + \frac{\partial w}{\rho_1 \partial \phi}\right)\xi$$

$$\epsilon_{\theta\xi} = \frac{1}{\rho_2}\left(v \cot\phi - w\right) - \frac{\cot\phi}{\rho_2}\left(\frac{v}{\rho_1} + \frac{\partial w}{\rho_1 \partial \phi}\right)\xi$$

As applied to the conical shell

$$\rho_1 = \infty$$
$$\rho_1 \partial\phi = \partial \ell$$
$$r = \ell \sin\gamma$$
$$\rho_2 = \ell \tan\gamma$$

The strain-displacement relation becomes

$$\epsilon_{\phi\xi} = \frac{\partial v}{\partial \ell} - \xi \frac{\partial^2 w}{\partial \ell^2}$$

$$\epsilon_{\theta\xi} = \frac{1}{\ell}\left(v - w \cot\gamma\right) - \frac{\xi}{\ell}\frac{\partial w}{\ell}$$

Introduction of the dimensionless variables

$$v' = \frac{v}{\delta}$$
$$w' = \frac{w}{\delta}$$
$$\ell' = \frac{\ell}{\ell_0}$$
$$\xi' = \frac{\xi}{\delta}$$

gives for the strains

$$\epsilon_{\phi\xi} = \frac{\delta}{l_0}\left(\frac{\partial v'}{\partial l'}\right) - \left(\frac{\delta}{l_0}\right)^2 \frac{\partial^2 w'}{\partial l'^2}$$

$$\epsilon_{\theta\xi} = \frac{\delta}{l_0}\left(\frac{v' - w'\cot\gamma}{l'}\right) - \left(\frac{\delta}{l_0}\right)^2 \frac{\partial w'}{\partial l'}$$

Since for a thin shell $\frac{\delta}{l_0} < 1$

and $\left(\frac{\delta}{l_0}\right)^2 << \left(\frac{\delta}{l_0}\right) < 1$

it is obvious that the terms having the order of magnitude $\left(\delta/l\right)^2$ may be neglected. Therefore,

$$\epsilon_{\phi\xi} \doteq \frac{\delta}{l_0}\left(\frac{\partial v'}{\partial l'}\right)$$

$$\epsilon_{\theta\xi} \doteq \frac{\delta}{l_0}\left(\frac{v' - w'\cot\gamma}{l'}\right)$$

or

$$\epsilon_{\phi\xi} \doteq \frac{\partial v}{\partial l}$$

$$\epsilon_{\theta\xi} \doteq \frac{v - w\cot\gamma}{l}$$

Appendix A.2 Elastic Analysis of a Thin Conical Shell of Constant Thickness under Constant Pressure and Thermal Loads.

Equations of Equilibrium

$$\frac{d}{dl}(N_\phi l) = N_\theta$$

$$\frac{d}{dl}(Q_\phi l) + N_\theta \cot\gamma + pl = 0$$

$$\frac{d}{dl}(M_\phi l) - M_\theta - Q_\phi l = 0$$

$$N_\phi + \left(Q_\phi + \frac{pl}{2}\right)\tan\gamma = 0$$

Temperature Profile Across the Shell Thickness

$$T = T_t\left(\frac{1}{2} - \frac{\xi}{\delta}\right)$$

Stress-Strain Relation

$$N_\phi = N_l = \frac{E\delta}{1-\nu^2}\left[\frac{dv}{dl} + \frac{v - w\cot\gamma}{l} - (1+\nu)\alpha\frac{T_t}{2}\right]$$

$$N_\theta = \frac{E\delta}{1-\nu^2}\left[\frac{v - w\cot\gamma}{l} + \nu\frac{dv}{dl} - (1+\nu)\alpha\frac{T_t}{2}\right]$$

$$M_\phi = -\frac{E\delta^3}{12(1-\nu^2)}\left[\frac{d^2w}{dl^2} + \frac{\nu}{l}\frac{dw}{dl} - (1+\nu)\alpha\frac{T_t}{\delta}\right]$$

$$M_\theta = -\frac{E\delta^3}{12(1-\nu^2)}\left[\nu\frac{d^2w}{dl^2} + \frac{1}{l}\frac{dw}{dl} - (1+\nu)\alpha\frac{T_t}{\delta}\right]$$

Working Variables

$$W = Q_\phi l$$

$$\chi = \frac{dw}{dl}$$

Governing Equations

$$l\frac{d^2\chi}{dl^2}+\frac{d\chi}{dl}-\frac{\chi}{l}-(1+\nu)\frac{l}{\delta}\frac{d(\alpha T_t)}{dt}+\frac{12W(1-\nu^2)}{E\delta^3}=0$$

$$l\frac{d^2W}{dl^2}+\frac{dW}{dl}-\frac{W}{l}+\frac{3}{2}pl-E\delta\chi\cot^2\gamma-\frac{E\delta^2 l}{2\tan\gamma}\frac{d}{dl}(\alpha T_t)=0$$

Solutions

$$\chi=A_1\left(Z_1+\frac{2Z_2'}{y}\right)+A_2\left(Z_2-\frac{2Z_1'}{y}\right)+\frac{3}{2}\frac{p\tan\gamma}{E\delta}l$$

$$N_\phi=4E\delta\cot\gamma\left[A_1\left(-\frac{2Z_1'}{y^3}+\frac{Z_2}{y^2}\right)+A_2\left(-\frac{2Z_2'}{y^3}-\frac{Z_1}{y^2}\right)\right]-\frac{pl\tan\gamma}{2}$$

$$N_\theta=2E\delta\cot\gamma\left[A_1\left(\frac{Z_2'}{y}-\frac{2Z_2}{y^2}+\frac{4Z_1'}{y^3}\right)+A_2\left(-\frac{Z_1'}{y}+\frac{2Z_1}{y^2}+\frac{4Z_2'}{y^3}\right)\right]-pl\tan\gamma$$

$$M_\theta=-\frac{E\delta^2\cot\gamma}{\sqrt{12(1-\nu^2)}}\left\{A_1\left[\nu\frac{2Z_1'}{y}+(1-\nu)\left(\frac{4Z_1}{y^2}+\frac{8Z_2'}{y^3}\right)\right]+A_2\left[\nu\frac{2Z_2'}{y}+(1-\nu)\left(\frac{4Z_2}{y^2}-\frac{8Z_1'}{y^3}\right)\right]\right\}+\frac{E\delta^2\alpha T_t}{12(1-\nu)}-\frac{p\delta^2\tan^2\gamma}{8(1-\nu)}$$

$$M_\phi=-\frac{E\delta^2\cot\gamma}{\sqrt{12(1-\nu^2)}}\left\{A_1\left[\frac{2Z_1'}{y}(1-\nu)\left(\frac{4Z_1}{y^2}+\frac{8Z_2'}{y^3}\right)\right]+A_2\left[\frac{2Z_2'}{y}-(1-\nu)\left(\frac{4Z_2}{y^2}-\frac{8Z_1'}{y^3}\right)\right]\right\}+\frac{E\delta^2\alpha T_t}{12(1-\nu)}-\frac{p\delta^2\tan^2\gamma}{8(1-\nu)}$$

where $Z_1 = Z_1(y)$ and $Z_2 = Z_2(y)$ are ber and -bei functions of y respectively, and $y^2 = \frac{4\cot\gamma}{\delta}\sqrt{12(1-\nu^2)}\,l$. The values of A_1 and A_2 are to be determined by the edge conditions of the shell.

Appendix A.3 Geometrical Imperfections

In recent years, considerable discussions have been made to explain discrepancies between shell theories and experimental results. Many investigators feel that these discrepancies are due to the geometrical imperfections that exist in the models.

The present investigators made a preliminary study of the effect of geometrical imperfections on the behavior of spherical shells under normal pressure to obtain some understanding of their effects. The analysis is based on the axisymmetrical type imperfections.

As in the case of other investigations by Chen (6), Kaplan and Fung (15), Budiansky (5), it is found that axisymmetrical analysis could not account for the total difference between theory and experiment. The mode of collapse of the models in the present investigation gives evidence that the initial imperfections of the models were probably unsymmetrical. Experimental evidence obtained by Kaplan and Fung leads on to the conclusion that an investigation of the effect of geometrical imperfections should be based on unsymmetrical rather than axisymmetrical analysis.

However, for such an analysis to be meaningful, it must be an exhaustive study supported by a number of experimental tests. The study need not involve temperature. Such an investigation was not attempted as part of the present program.

Previous Investigations:

To the knowledge of the writers, only five studies have been made about the effect of initial imperfection on the behavior of thin shells. Four of the studies were concerned with spherical shells and one dealt with general thin shells. In chronological order the studies and their general results are as follows:

> Mushtari presented the equilibrium equations of the middle surface of a thin shell which have irregularities of the order of the shell thickness. The relations were applied to thin shells subjected to normal pressure.
>
> Klein used two parameters in connection with experimental data to provide a better correlation of analytical and experimental results. He attempted to show that by proper choice of the allowable collapse pressure, the effect of initial imperfections of the shell could be taken into account.
>
> Gerard and Becker using an empirical approach based on an "unevenness factor" proposed that the

geometrical portion of the initial imperfections governs the average behavior of the spherical plates which the residual stress and other factors may contribute to the scatter in the experimental data.

Chen considering the axisymmetric buckling under uniform pressure of a shallow portion of a spherical shell, carried out a Rayleigh-Ritz solution of the variational equation equivalent to the governing equations. He concluded that the buckling pressures may be appreciably affected by the presence of imperfection of the middle surface and that its effect depend not only on the magnitude but also on the location of the maximum imperfection and the mode of the imperfection.

Budiansky, treating the same problem as Chen, based his analysis on the integral-equation formulation. Budiansky found that P_{cr} appears to approach 1 in an oscillatory fashion as λ (geometrical parameters) increases. Comparing the variation buckling pressures of initially perfect and imperfect clamped shallow spherical shells, he found that both followed the same trend.

Comparison of these investigations show very little agreement of the results. Within a certain range of λ , say $\lambda = 4$ to $\lambda = 5$, fairly good agreement has been observed. Beyond this narrow range, the correct theoretical variation of P_{cr} with λ is questionable.

Method of Analysis

To study the possible causes for discrepancies which exist between the present analytical and experimental results, a simplified analysis was made of thin spherical shells with axisymmetrical imperfections.

For simplification, the study is restricted to the hemispherical shells subjected to pressure only. Following a method proposed by Budiansky, we consider the buckling of such shells whose deviated surface may be represented by

$$z_0 = H\left[1 - \left(\frac{r}{a}\right)^2 - \epsilon\, e(r)\right]$$

where e(r) is the shape of the imperfection, ϵ is the ratio of the downward initial displacement at the center of the shell to the rise H of the perfect shell.

For simplicity the shape of imperfection is taken as

$$e(r) = \left[1 - \left(\frac{r}{a}\right)^2\right]^2$$

By the aid of the geometrical parameter λ defined by

$$\lambda^4 = 48(1-\nu^2)\left(\frac{H}{t}\right)^2$$

and the non-dimensional variables

$$X = \frac{\lambda r}{a}$$

$$\theta = \left(\frac{\lambda a}{2H}\right)\beta$$

$$\Phi = \left[\frac{12(1-\nu^2)a}{\lambda E t^2}\right]\psi$$

where ψ is the stress function, $\beta = (dw/dr)$ is the rotation of an element of the shell, q_0 is the classical buckling pressure of a complete spherical shell having the same radius of curvature $R = a^2/2H$ as the given shallow spherical shell.

The non-dimensional equilibrium and compatibility equations for an initially perfect spherical shell are

$$(x\theta')' - \frac{\theta}{x} + x\Phi = -2px + \theta\Phi$$

$$(x\Phi')' - \frac{\Phi}{x} - x\theta = -\frac{1}{2}\theta^2$$

The prime denotes differentiation with respect to x and P. A non-dimensional pressure parameter p is defined as

$$p = \frac{q}{q_0}$$

where

$$q_0 = \frac{2E}{\sqrt{3(1-\nu^2)}}\left(\frac{t}{R}\right)^2$$

The non-dimensional boundary conditions appropriate for a clamped shell

$$\theta(\lambda) = 0$$

$$\lambda\Phi'(\lambda) - \nu\Phi(\lambda) = 0$$

the first condition states that the rotation at r = a is zero. The second boundary condition fulfills the requirement that the horizontal displacement at the shell edge must vanish.

For the initially imperfect shell, the basic equations take the form

$$(x\theta')' - \frac{\theta}{x} + x\Phi = -2px + \theta\Phi + \epsilon h\Phi$$

$$(x\Phi')' - \frac{\Phi}{x} - x\theta = -\frac{1}{2}\theta^2 - \epsilon h\theta$$

$$\text{where } h = \frac{\lambda^2}{2} e'$$

The boundary conditions, of course, are still valid.

The solution of these equations and the boundary conditions can be represented by two integral equations

$$\theta(x) = \gamma(x) + dA_1(x) + eA_2(x)$$

$$\Phi(x) = z(x) + dB_1(x) + eB_2(x) - 2px$$

where

$$\gamma(x) = \int_0^\lambda G(x,\xi)r(\xi)d\xi + \int_0^\lambda H(x,\xi)s(\xi)d\xi$$

$$z(x) = -\int_0^\lambda H(x,\xi)r(\xi)d\xi + \int_0^\lambda G(x,\xi)s(\xi)d\xi$$

$$r = \theta\Phi + \epsilon h\Phi$$

$$s = -\frac{1}{2}\theta^2 - \epsilon h\theta$$

$$e = -\gamma(\lambda)$$

$$d = 2p\lambda(1-\nu) - (1-\nu)z(\lambda) - \frac{1}{\lambda}\int_0^\lambda (x^2\gamma + \lambda s)dx$$

$$G(x,\xi) = \mathrm{bei}'x\,\mathrm{ker}'\xi + \mathrm{ber}'x\,\mathrm{kei}'\xi \qquad (0 \le x \le \xi)$$

$$= \mathrm{bei}'\xi\,\mathrm{ker}'x - \mathrm{ber}'\xi\,\mathrm{kei}'x \qquad (0 \le \xi \le x)$$

$$H(x,\xi) = \mathrm{ber}'x\,\mathrm{ker}'\xi - \mathrm{bei}'x\,\mathrm{kei}'\xi \qquad (0 \le x \le \xi)$$

$$= \mathrm{ber}'\xi\,\mathrm{ker}'x - \mathrm{bei}'\xi\,\mathrm{kei}'x \qquad (0 \le \xi \le x)$$

$$A_1(x) = -\frac{1}{D}(\mathrm{ber}'\lambda\,\mathrm{bei}'x - \mathrm{bei}'\lambda\,\mathrm{ber}'x)$$

$$B_1(x) = -\frac{1}{D}(\mathrm{ber}'\lambda\,\mathrm{ber}'x + \mathrm{bei}'\lambda\,\mathrm{bei}'x)$$

$$A_2(x) = -(1+\nu)B_1(x) - \frac{\lambda}{D}(\mathrm{ber}\,\lambda\,\mathrm{bei}'x - \mathrm{bei}\,\lambda\,\mathrm{ber}'x)$$

$$B_2(x) = (1+\nu)A_1(x) + \frac{\lambda}{D}(\mathrm{ber}\,\lambda\,\mathrm{ber}'\lambda + \mathrm{bei}\,\lambda\,\mathrm{bei}'\lambda)$$

$$D = (1+\nu)\left[(\mathrm{ber}'\lambda)^2 + (\mathrm{bei}'\lambda)^2\right] - \lambda(\mathrm{ber}\,\lambda\,\mathrm{bei}'\lambda - \mathrm{bei}\,\lambda\,\mathrm{ber}'\lambda)$$

The solution of the basic equations is obtained by iterative procedures in terms of matrix operations with the integrations being performed numerically on the basis of Simpson's rule. For the particular application under discussion, the following data are selected for comparison of the buckling stress of a perfect spherical shell with that of a geometrically imperfect spherical shell:

$$\lambda = 12$$

$$\epsilon = 0.05$$

$$\nu = 0.33$$

$$\Delta x = 0.25$$

where Δx is the invariant spacing of stations in the numerical integration.

The results of the calculation may be stated as follows for the critical pressure

$$q_{CR} = 0.75\, q_o$$

where q_{CR} is the local maximum pressure at which buckling occurs, q_o is the buckling pressure of a complete sphere without bending.

For a perfect spherical shell, one finds that

$$q_{CR} = 0.96\, q_o$$

In terms of stresses, one can write that

$$\sigma_{CR} = \frac{0.96E}{\sqrt{3(1-\nu^2)}}\left(\frac{t}{R}\right) \qquad \text{Perfect shell}$$

$$= \frac{0.75E}{\sqrt{3(1-\nu^2)}}\left(\frac{t}{R}\right) \qquad \text{Imperfect shell}$$

This means that the predicted buckling stress band on an "imperfect shell" analysis is approximately 80% of that given by the "perfect shell". This reduction is not sufficient to bring the analytical results within the range of available experimental results for elastic hemispherical shells.

However, a reduction of the analytical stresses obtained in the present viscoelastic analysis by a similar magnitude gives a more favorable comparison of analytical and experimental results for the hemispherical shell.

ADDITIONAL REFERENCES FOR APPENDIX A.3

(not stated in main grouping)

Mushtari, H. M. (in Russian), "On the Elastic Equilibrium of a Thin Shell with Initial Irregularities in the Form of the Middle Surface", Prikladnaia Matematika i Mekhanika, Vol. 15, pp. 743-750, 1951.

Klein, B., "Parameters for Predicting the Initial and Final Collapse Pressures of Uniformly Loaded Spherical Shells", Journal of the Aeronautical Sciences, Vol. 22, No. 1, pp. 69-70, 1955.

Gerard, G. and Becker, H., "Handbook of Structural Stability, Part III - Buckling of Curved Plates of Shells", U. S. N. A. C. A. TN 3783, pp. 59-65, August 1957.

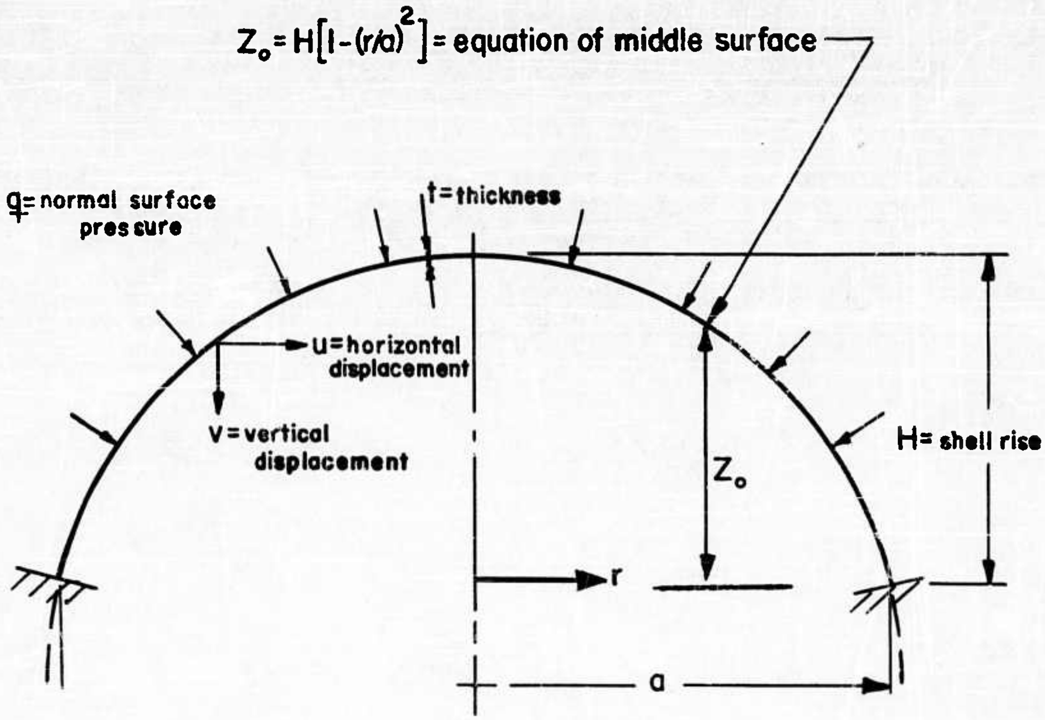

Fig. A.3-1
SHELL GEOMETRY

APPENDIX B

EXPERIMENTAL INVESTIGATION

B.1 Experimental Facility

(a) Heating System

The functional arrangement of the experimental facility is represented by the block diagram shown in Fig. B-1.

The radiant heating oven consists of a polished aluminum reflector with attached heating lamps. The heating lamps are the GE T3/CL quartz type. Thirty-two 2000 T3/CL lamps form the heating unit for Zone I; Zones II and III each consist of fifty-six 1000 T3/CL lamps (See Fig. B-2 for heating zones).

The maximum power dissipation of the entire unit is 478 KVA which can be increased by replacing the lamps of Zones II and III with 2000 T3/CL lamps. The capacity of the unit corresponds to 100 BTU/sq. ft/sec. The heat input to the model is less, depending upon a number of parameters including distance from model, model configuration, model surface, etc. The efficiency is estimated to be 50-85%.

The oven is equipped with polished aluminum heat shields to maintain zonal temperature control. Two sets are provided; one set for conical shells and the other for hemispherical shells.

The model SPG6266W three-phase temperature controller provides zonal control of temperature in the oven by proportioning the a-c heater power through ignitrons controlled by a closed-loop thermocouple feedback circuit. Temperatures may be automatically maintained to within 0.5% by employing precision potentiometric circuitry held in continuous calibration by a standard cell. The load power may also be manually varied from zero to full power by a front panel dial. The temperature controller is used to program temperature as a function of time by switching to the remote temperature programmer. The temperature controller can proportion a continuous load power of 390 KVA for the three phases with water-cooled ignitrons. Each load phase is controlled independently, thereby providing three separate zones.

The controller is a complete three-phase ignitron powered control unit combined with three d-c potentiometric circuits and high gain a-c amplifiers. Accurate specimen temperature control is accomplished by comparing a low level d-c potentiometer milli-voltage with the thermal electromotive force from the specimen thermocouple. Any positive error between these voltages is chopped and a-c amplified to a relatively high voltage level. The amplified a-c output voltage is converted back to d-c in a diode modulator circuit and used to control the firing angle of the ignitrons. The ignitrons, in turn, proportion the power to the oven to restore the termocouple to the set point temperature and to reduce the low level error to within the proportional band of control. Compensation for ambient temperature chances at the thermocouple cold junction is automatic.

(b) Temperature Programmer

The Research, Inc., Data-Trak function generator (FGE5035) provides an output proportional to the ordinate of the chosen temperature-time function. It is a curve follower in that two conducting lines bordering the desired curve generate a high electrostatic potential field so a null-seeking probe can be servo-driven to follow the zero potential line.

The temperature-time graph is fastened to each of three drums such that the abscissa (time) is the rotational position of the drum. The probe is mounted between two parallel slide bars beneath the drum. As the servo positions the probe, a flexible cable from the probe carriage rotates a precision potentiometer to provide an output voltage proportional to the translational position of the probe.

Since there is no contact between the conducting lines or the probe the system does not rely upon sensing current or a magnetic flux.

One can also regulate the drum cycle from 10 to 300 seconds providing a flexible time scale. In addition, by placing the generator in a "hold" condition a given situation can be maintained for as long as desired.

(c) Vacuum-Pressure System

The vacuum system is automatic with a capability of permitting a pressure difference across the shell to vary within ±1/8 inch of mercury. The mercury column is positioned by two pins, 1/4 inch apart, through the relay and the vacuum pump. The tank acts as a reservoir and a check valve while the relief valve allows the system to be opened to the atmosphere at will.

B.2 Instrumentation

Modified HT-600 strain gages, manufactured by the High Temperature Instruments Corporation are used. The gage is modified in that in addition to the HT-600 alloy, which has a negative coefficient of resistivity with temperature, an alloy with a positive coefficient is employed, thereby reducing the apparent strain. The gages are applied in a meridional and parallel direction at four stations along a meridian using Allen PBX cement (See Fig B-2). Obtaining a good bond between either the pre-coat and the aluminum surface or the second coat and the pre-coat was not always successful. As available testing time became short this dictated operation with less than full strain gage instrumentation. Each gage used a three wire connection to the bridge thereby negating effects of change in lead wire resistance. The signal is picked off a one gage bridge, recorded, and then corrected for temperature effects. Since the apparent strain versus temperature curves varied widely for different gages, each gage was provided with individual curves. Also, the nature of the curves changed with each temperature cycle thereby necessitating strain-temperature data not more than one cycle distant from the test run.

To calibrate the strain gage circuits, a decade resistance is shunted around the active gage and the resistance varied while the galvanometer deflection is recorded. Knowing the gage factor, one can interpret the resistance change as a strain and the deflection then calibrated in terms of micro-inches/inch/inch of deflection.

The temperature recording circuit is simply a measurement of the current induced by the potential difference between the hot and cold junctions. On later models differential thermocouples (Fig B-3) provided data on the temperature difference across the shell wall. One junction is a spot welded to the inner surface while the other, after being led through a small hole in the wall a distance from the measuring area, was cemented opposite to the previous junction. Since one junction had to be electrically insulated from the other, yet in good thermal contact with the outer surface, the mechanical bond of the copper oxide cement used often failed, providing only qualitative data on the temperature differential. An aluminum foil-backed tape shielded the outer junction from direct radiation while also sealing the hole in the shell wall. The calibration procedure is as follows: the hot and cold junctions are brought to the same temperature; a voltage is induced across the thermocouple resistance and the galvanometer by a precision millivolt potentiometer; with the aid of standard potential difference-temperature charts for the particular thermocouple, the circuit is calibrated for ^{o}F versus deflection.

All the instrumentation wiring in the model was supported by a brass center post bolted to the apex of the model. Brass rod branches from the center post supported leads to the individual gages.

A porcelain filter disk provided a means of passing the wiring through a pressure differential at high temperatures. The individual leads passed through the holes in the disk with the PBX cement acting as a potting agent. The disk was then bolted to the steel mounting plate atop a quad ring providing a pressure seal.

B.3 Test Specimens

The test specimens are shown in Figs B-4 and B-5. The specimen is attached to a 5/8 inch thick steel plate. A silicone rubber "Quad" ring is inserted around the specimen support to provide an adequate vacuum seal.

The specimens are coated with soot to increase the absorptivity and to provide a common surface for all tests.

B.4 Material Properties

Although the model manufacturer and Alcoa assured the investigators that soaking the models for a period of thirty minutes at $650^{o}F$ anneals the material and removes any residual stresses (produced in spinning), a series of supplementary tests were conducted to check certain important mechanical properties of the material.

Models were tested before and after soaking at room temperature under the action of a concentrated load. It was felt that this would

produce the desired biaxial stress condition without complicating the test program.

The tests were limited to the determination of the modulus of elasticity and of Poisson's Ratio. Because of the considerable scatter of test data, the investigators feel that these data are valueless to the investigation and are omitted.

The mechanical properties involved in the analysis are: shear modulus of elasticity, Poisson's ratio, coefficient of viscosity, and the coefficient of linear thermal expansion.

(a) Shear Modulus of Elasticity

The following approximate values for shear modulus are given:

Temperature (^{o}F)	75	212	300	400	500	600	700
G x 10^{-6} psi	3.8	3.7	3.6	3.4	3.0	2.6	1.5

(b) Poisson's Ratio

At elevated temperatures, Poisson's ratio is a multivaried function of elastic strain, plastic strain, creep strain (time dependent), and anisotropy (varies with strain). Poisson's ratio, therefore, is no longer a unique property. Tests conducted by the investigators show a range of values from 0.33 to 0.45. At elevated temperatures, it seems that the results are highly sensitive to the specimen geometry and test procedure, rather than a strong dependence on the properties of the material.

An attempt to eliminate such variables is useless without an exhaustive number of well controlled tests.

(c) Coefficient of Viscosity

No attempt was made to establish experimentally the coefficient of viscosity of the subject material. To the knowledge of the writers, no data exist of the variation of viscosity with temperature below the melting point for aluminum alloys. Although some attempts have been made to establish such a viscosity-temperature curve for pure aluminum, the use of the results for the present application is highly questionable.

It is agreed, however, that the viscosity-temperature curve for pure metal may be quite different from that of alloys. The alloy may show:

1. Different rate of decrease of viscosity with increase of temperature.

2. Different rate at which the slope of the viscosity-temperature curve increases as the liquid state is approached.

3. A greater coefficient of viscosity.

Based on tests conducted above the melting points (6), the results of pure aluminum and aluminum alloys indicate the following:

1. In all cases, the viscosity-temperature curve of the low per cent alloys (99% aluminum) is similar to that of the pure metal.

2. For higher per cent alloys (98% or less aluminum), the presence of the alloy had a characteristic effect.

Since the coefficient of viscosity is one of the principal parameters in the temperature-dependent viscoelastic analysis, an attempt is made to estimate the viscosity-temperature curve for the material of the present investigation. An expression of the form

$$\eta = CG \exp(H/RT)$$

Where C is a constant, G is modulus of rigidity (dynes/cm^2), H is heat of activation (calories/mole), R is the gas constant, and T is the absolute temperature (^{o}K), is used to represent the curve. This functional relationship is a typical form of the variation of viscosity with temperature for some polycrystalline solids and liquids.

In the present investigation, the empirical expression was taken as:

$$\eta = 1.819 \times 10^{-20} G \exp(18000/T)$$

the above expression is based on established values by Alcoa (2) at the temperature range for aluminum alloys.

The graph of this expression is shown in Fig. 2.1.3-1 together with the results obtained by Kê (16) for pure aluminum.

(d) <u>Coefficient of Thermal Expansion</u>

No attempt was made to investigate the coefficient of thermal expansion. The values used in the analysis are based on Reference 2 and communication with Alcoa.

Fig. 2.1.3-2 shows the variation of these properties with temperature for 6061 aluminum alloy.

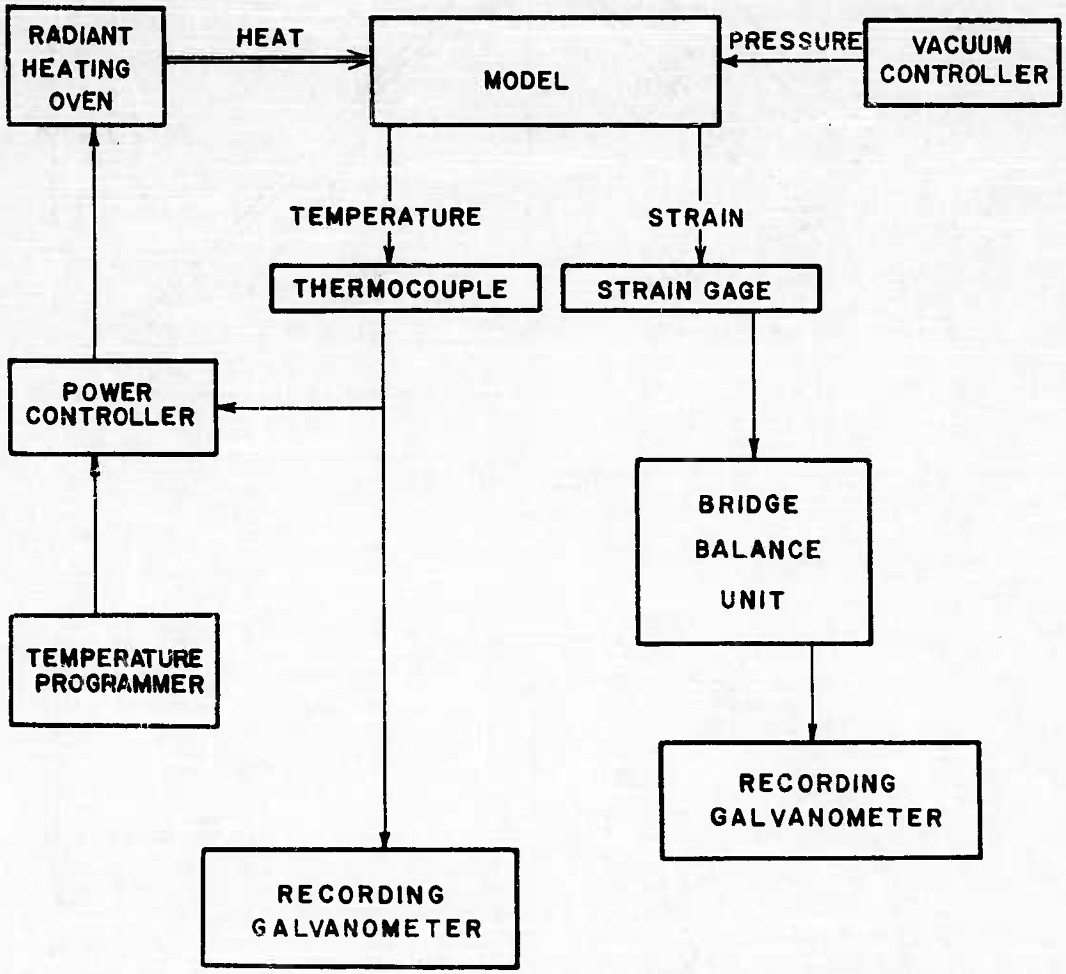

Fig. B-1
TESTING FACILITY BLOCK DIAGRAM

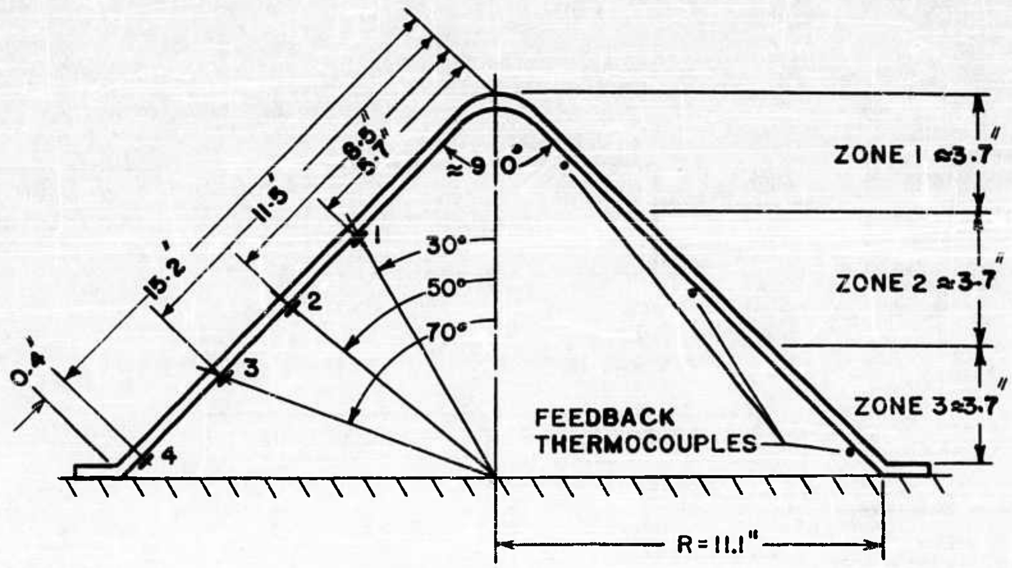

CONICAL MODEL

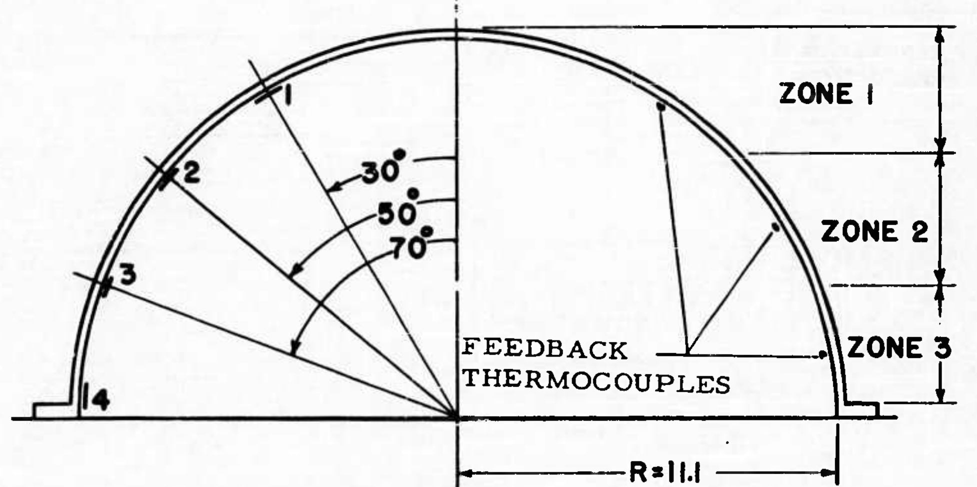

HEMISPHERICAL MODEL

FIG. B-2A

INSTRUMENTATION

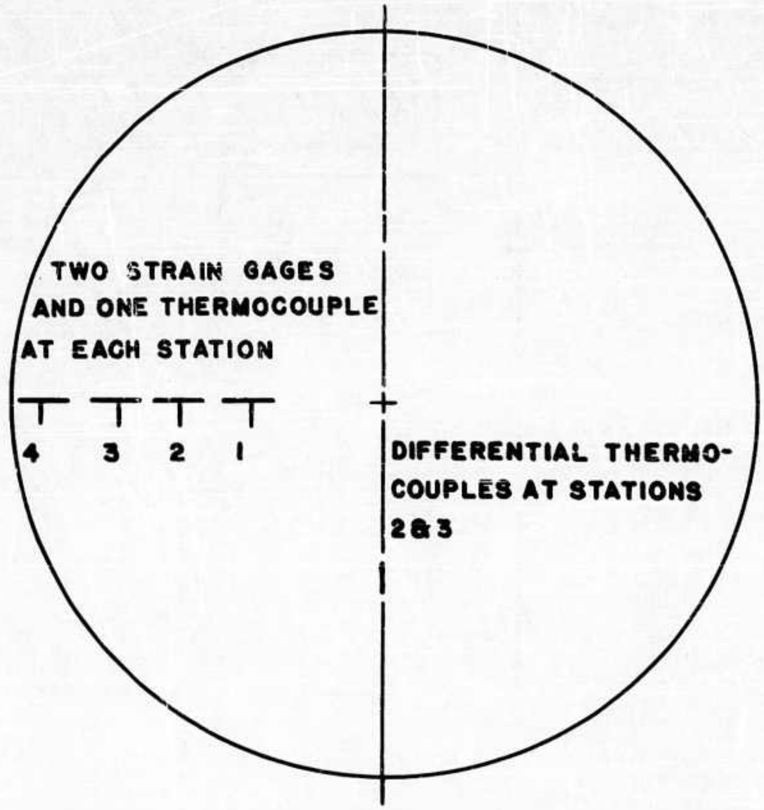

Fig. B-2B
INSTRUMENTATION

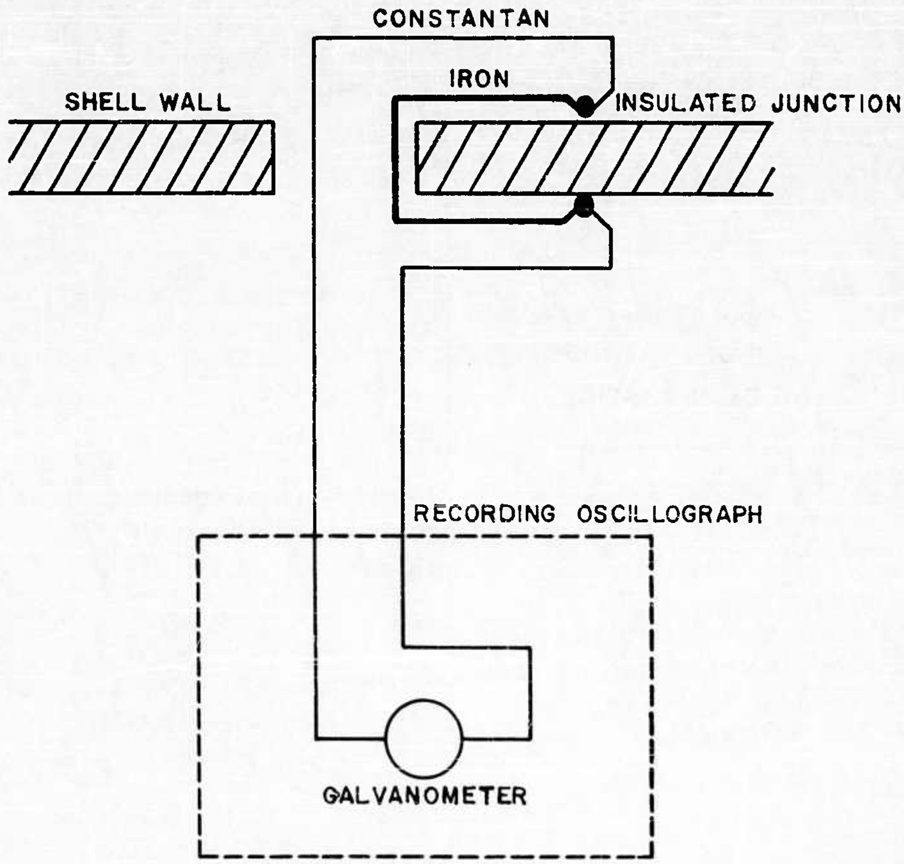

Fig. B-3
DIFFERENTIAL THERMOCOUPLE CIRCUIT

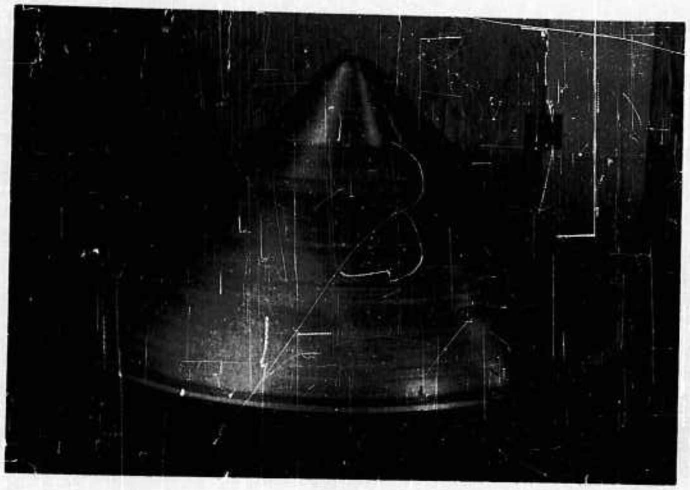

Fig. B-4 Conical Shell Model

Fig. B-5 Hemispherical Shell Model

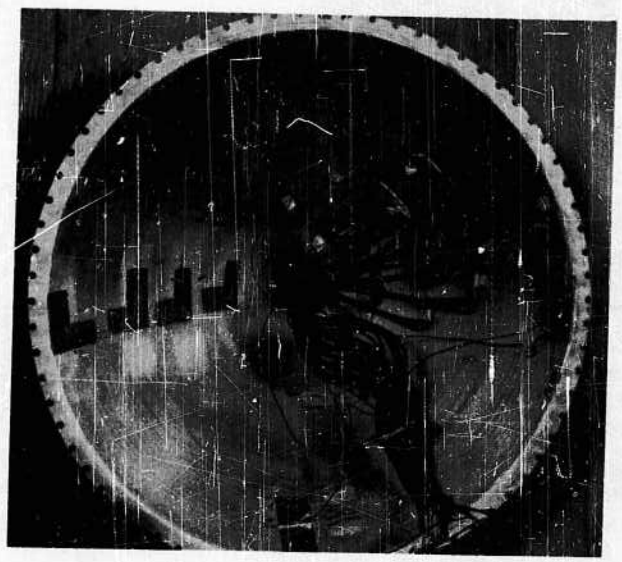

Fig. B-6 Instrumented Conical Shell Model

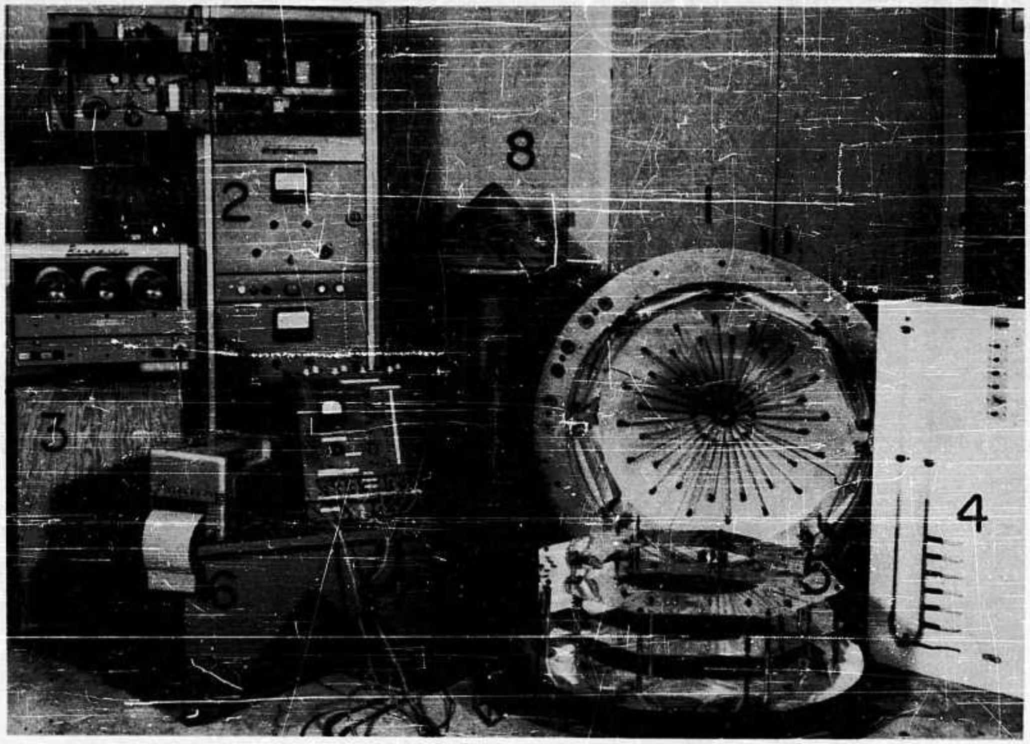

Fig. B-7 Experimental Facilities

LEGEND 1. Radiant Heating Oven, 2. Power Controller, 3. Temperature Programmer, 4. Vacuum Controller, 5. Zonal Heat Shields, 6. Oscillograph, 7. Bridge Balance Unit, 8. Model.

APPENDIX C

EXPERIMENTAL DATA

TABLE C-1 TEST PROGRAM

MODEL	STEADY STATE TEMPERATURE	RATE ($^{o}F/sec$)	PRESSURE
1/32" Cones	400°F	5	None
	400°F	10	None
	500°F	20	None
	(1) 400 (2) 300 (3) 200	(1) 10 (2) 5 (3) 2.5	None
1/16" Cones	300°F	2.5	None
	400°F	5	None
	500°F	10	None
	400°F	10	22" Hg
	500°F *	20	22" Hg
	(1) 500 (2) 400 (3) 300	(1) 50 (2) 40 (3) 30	22" Hg
1/8" Cones	300°F	2.5	None
	400°F	5	None
	500°F	10	None
	400°F	10	24" Hg
	500°F	20	23" Hg
	(1) 400 (2) 300 (3) 200	(1) 10 (2) 5 (3) 2.5	24" Hg
	(1) 400 (2) 300 (3) 200	(1) 20 (2) 10 (3) 5	23" Hg
	(1) 500 (2) 400 (3) 300	(1) 10 (2) 5 (3) 2.5	23" Hg
	(1) 500 (2) 400 (3) 300	(1) 20 (2) 10 (3) 5	23" Hg
	(1) 500 (2) 400 (3) 300	(1) 50 (2) 40 (3) 30	23" Hg
1/16" Hemispheres	400	5	None
	400	5	21" Hg
	500	10	None
	(1) 400 (2) 300 (3) 200	(1) 10 (2) 5 (3) 2.5	21" Hg
	(1) 500 (2) 400 (3) 300	(1) 10 (2) 5 (3) 2.5	21" Hg
	(1) 500 (2) 400 (3) 300	(1) 20 (2) 10 (3) 5	21" Hg
	(1) 500 (2) 400 (3) 300	(1) 50 (2) 40 (3) 30	18" Hg

* Repeated

TABLE C -2

Temperatures and Stresses in 1/32" Thick Cone for a Program of 5 °F/sec. to 400 °F.

TIME Sec.	STATION 1 Temp.	Stress M	C	STATION 2 Temp.	Stress M	C	STATION 3 Temp.	Stress M	C	STATION 4 Temp.	Stress M	C
0	73	0	0	73	0	0	73	0	0	73	0	0
5	89	- 10	20	80	284	- 91	76	324	162	78	- 284	- 274
10	117	+ 10	90	106	80	- 202	100	768	585	108	- 1120	- 1300
15	147	- 30	100	127	71	- 273	125	697	465	125	- 1760	- 1890
20	177	- 50	40	155	50	- 240	155	660	340	143	- 2410	- 2310
25	200	- 79	40	178	70	- 287	179	640	370	158	- 2880	- 2560
30	225	-108	29	201	- 70	- 396	207	831	495	177	- 3160	- 2740
35	251	-193	- 125	228	- 19	- 403	236	754	353	193	- 3690	- 3085
40	276	-261	- 125	250	- 68	- 438	267	912	446	210	- 3870	- 3120
45	301	-315	- 230	278	- 87	- 445	295	874	317	224	- 4250	- 3240
50	324	-378	- 265	301	-210	- 563	323	928	104	242	- 4420	- 3240
55	350	-409	- 251	326	-122	- 567	351	874	102	258	- 4680	- 3280
60	373	-524	- 248	352	-102	- 400	381	933	82	274	- 4950	- 3280
90	391	-445	- 246	407	36	- 108	438	149	201	274	- 4400	- 2625
120	397	-234	- 9	424	124	- 70	448	191	452	277	- 4265	- 2490
150	400	126	72	430	264	229	448	339	670	282	- 4200	- 2380
180	400	0	135	430	396	387	448	583	940	286	- 4175	- 2285
210	400	99	288	430	510	502	446	766	1140	286	- 4250	- 2275
240	400	108	315	430	581	563	446	783	1190	290	- 4100	- 2040
270	400	108	333	430	660	642	442	1045	1280	292	- 4000	- 2020
300	400	162	378	430	748	722	442	1140	1500	295	- 4000	- 1890
330	400	225	441	430	792	774	442	1140	1500	298	- 3980	- 1840
360	400	225	441	430	845	827	442	1200	1520	300	- 3840	- 1700
390	400	270	459	430	854	854	442	1260	1700	300	- 3840	- 1700
420	400	270	459	430	862	871	442	1260	1700	300	- 3840	- 1700

TABLE C - 3

Temperatures and Stresses in 1/32" Thick Cone for a Program of 10 °F/sec. to 400°F.

TIME	STATION 1			STATION 2			STATION 3			STATION 4		
	Temp.	Stress		Temp.	Stress		Temp.	Stress		Temp.	Stress	
Sec.		M	C		M	C		M	C		M	C
0	90	0	0	91	0	0	91	0	0	91	0	0
5	112	40	0	100	320	- 200	97	1400	1000	108	- 190	- 30
10	166	- 120	40	142	492	- 210	136	2650	1680	156	- 1630	- 2410
15	220	-305	- 108	186	80	- 458	186	2517	995	198	- 2653	- 3792
20	275	- 444	- 193	235	78	- 539	238	2560	980	232	- 4018	- 5086
25	326	- 510	- 425	285	96	- 538	294	2800	980	270	- 5170	- 6200
30	375	- 524	- 552	330	141	- 432	347	2740	567	301	- 6200	- 6952
35	326	- 364	- 546	360	-259	- 370	384	1146	-127	294	- 5683	- 6520
40	375	- 245	- 364	371	0	- 92	398	864	-135	288	- 5340	- 6130
45	389	- 73	- 164	380	37	- 27	410	823	- 54	288	- 5070	- 5880
50	388	- 9	- 90	387	146	63	418	640	-142	286	- 4990	- 5760
55	388	55	- 18	392	208	136	423	522	-177	286	- 4920	- 5640
60	388	145	46	396	235	235	428	610	- 35	286	- 4920	- 5540
90	391	428	228	414	347	356	432	580	35	288	- 4920	- 5540
120	393	610	320	424	549	610	442	802	540	290	- 4830	- 5540
150	393	720	410	424	673	788	442	872	750	290	- 4800	- 5400
180	393	837	491	424	761	823	442	942	977	298	- 4800	- 5400
210	393	900	555	424	903	1044	442	977	1080	300	- 4800	- 5400
240	391	992	646	424	1044	1200	438	970	1150	304	- 4560	- 5210
270	391	992	646	424	1090	1270	438	1000	1260	308	- 4550	- 5180

TABLE C - 4

Temperatures and Stresses in 1/32" Thick Cone for a Program of 20° F/sec. to 500° F.

TIME	STATION 1			STATION 2			STATION 3			STATION 4		
Sec.	Temp.	Stress		Temp.	Stress		Temp.	Stress		Temp.	Stress	
		M	C		M	C		M	C		M	C
0	66	0	0	66	0	0	66	0	0	66	0	0
2	66	0	0	66	0	0	66	0	0	66	0	0
4	99	81	121	74	131	-464	70	1116	639	84	-873	-560
6	146	50	150	102	121	-858	94	1654	913	133	-1650	-2050
8	190	-20	200	131	10	-970	124	1740	636	168	-3580	-3370
10	235	-127	127	167	-20	-1140	161	1870	620	200	-3600	-3930
12	276	-270	-97	202	-20	-1140	200	1980	535	250	-5000	-4740
14	321	-455	-275	243	225	-980	242	2050	333	262	-6270	-5710
16	362	-594	-417	275	290	-878	278	2180	241	289	-7080	-6200
18	404	-657	-603	314	390	-693	320	2230	-104	317	-7640	-6560
20	445	-617	-852	350	409	-595	358	2550	110	347	-7840	-6300
22	484	-768	-1085	387	455	-400	396	2880	154	369	-8200	-6210
24	512	-940	-1250	420	62	-542	435	2100	-240	383	-8220	-6210
26	515	-867	-1190	437	-385	-507	460	342	-1026	371	-8000	-6100
28	510	-745	-1150	447	-597	-631	476	-420	-1400	359	-7300	-5640
30	510	-704	-1030	455	-602	-507	487	-769	-1560	353	-7200	-5510
35	509	-526	-842	470	-304	-460	510	-	-	347	-6600	-5100
40	506	-300	-672	482	-234	-150	522	-	-	343	-6620	-5125
45	506	-194	-518	490	-215	-83	535	-	-	341	-6350	-4950
50	506	-113	-445	498	-238	-156	542	-	-	341	-6350	-4950
55	506	-57	-390	503	-230	-148	547	-	-	341	-6350	-4950
60	506	-16	-332	510	-186	-24	553	-	-	341	-6340	-4900
180	512	729	356	540	465	883	563	-1330	-444	363	-5880	-3920
300	515	826	526	540	907	1450	565	-1060	-37	377	-5200	-3210
420	515	1050	575	545	1050	1590	565	-791	200	386	-4940	-2940
540	515	1070	535	551	1140	1730	565	-1010	150	392	-4800	-2730
660	515	1134	591	551	1220	1875	565	-1010	150	400	-4530	-2550

TABLE C -5

Temperatures and Stresses in 1/32" Thick Cone for a Zonal Program:

Zone 1, 10 °F/sec. to 400°F; Zone 2, 5 °F/sec. to 300°F; Zone 3, 2.5 °F/sec. to 200°F.

TIME	STATION 1			STATION 2			STATION 3			STATION 4		
	Temp.	Stress		Temp.	Stress		Temp.	Stress		Temp.	Stress	
Sec.		M	C		M	C		M	C		M	C
0	93	0	0	93	0	0	93	0	0	93	0	0
5	104	-110	-50	93	225	125	93	250	220	93	50	10
10	142	-312	-161	93	313	-131	100	869	788	101	272	0
15	182	-478	-200	121	333	-90	109	1020	768	103	111	-141
20	219	-680	-424	142	260	-161	119	919	686	105	121	-191
25	258	-844	-601	160	190	-190	126	690	430	108	60	-252
30	298	-1050	-830	180	100	-209	136	670	420	113	151	-222
35	317	-1045	-893	200	-158	-198	152	970	620	126	-432	-774
40	328	-836	-695	217	-30	-285	168	970	680	134	-543	-985
45	335	-733	-639	238	-88	-225	184	650	480	139	-532	-1075
50	335	-677	-564	242	-98	-49	190	446	377	136	-442	-954
55	335	-677	-564	245	20	68	196	544	435	136	-600	-1000
60	335	-620	-545	245	39	127	200	653	653	134	-482	-924
90	333	-432	-253	248	205	283	204	713	752	134	-382	-754
120	330	-357	-188	250	331	409	206	683	831	134	-382	-754
150	330	-290	-132	250	341	458	206	683	831	134	-382	-754
180	328	-188	-85	250	390	526	206	683	831	134	-382	-754
210	326	-122	65	250	409	565	206	713	920	134	-382	-754
240	325	-56	56	250	478	614	206	732	980	138	-231	-704
270	325	9	94	250	517	653	206	732	980	138	-231	-704
300	325	9	94	250	565	663	206	881	1100	138	-221	-653
330	325	47	178	250	585	720	206	881	1100	138	-221	-653
360	325	47	178	250	585	720	206	881	1100	138	-221	-653

TABLE C - 6

Temperatures and Stresses in 1/16 " Thick Cone for a Program of 2.5 ^{o}F/sec. to 300^{o}F

TIME Sec.	STATION 1			STATION 2			STATION 3			STATION 4		
	Temp.	Stress		Temp.	Stress		Temp.	Stress		Temp.	Stress	
		M	C		M	C		M	C		M	C
0	69	0	0	67	0	0	67		0	67	0	0
5	75	- 51	71	69	172	142	69		0	69	- 19	- 15
10	85	- 112	30	83	223	274	83		- 485	89	- 1840	- 1630
15	99	- 91	10	96	303	354	98		- 395	102	- 2500	- 2460
20	112	- 151	- 81	111	263	283	114		- 232	115	- 2950	- 3140
25	125	- 91	- 10	126	323	364	128		- 364	126	- 3515	- 3900
30	139	- 81	- 30	140	293	354	144		- 331	138	- 3920	- 4435
35	151	- 121	- 81	152	271	331	161		- 320	150	- 4380	- 5040
40	164	- 80	- 40	166	280	400	176		- 349	161	- 4930	- 5720
45	177	- 112	- 80	181	279	389	193		- 427	172	- 5360	- 6190
50	191	- 69	- 40	195	228	337	208		- 386	183	- 5860	- 6760
55	203	- 59	- 59	208	178	307	224		- 355	194	- 6280	- 7230
60	215	- 109	- 59	222	226	325	239		- 372	205	- 6780	- 7781
65	230	- 20	88	234	156	293	253		- 507	216	- 7390	- 8260
70	241	- 98	10	248	175	331	269		- 398	227	- 7970	- 8760
75	252	- 49	49	262	251	367	283		- 394	237	- 8360	- 9130
80	266	- 125	- 212	276	321	347	299		- 430	248	- 8950	- 9600
85	279	38	125	289	297	374	314		- 405	258	- 9430	- 10700
90	287	125	163	302	171	307	327		- 387	265	- 9720	- 10280
120	304	286	267	325	47	113	344		- 300	260	- 8900	- 9590
150	313	352	361	336	131	216	346		- 271	260	- 8650	- 9250
180	320	492	540	341	225	291	346		- 159	260	- 8370	- 8940
210	324	595	652	343	310	319	344		- 75	260	- 8260	- 8830
240	328	680	775	343	375	413	342		37	260	- 8030	- 8580
270	330	737	832	343	469	450	340		- 9	258	- 8030	- 8540
300	330	737	832	343	497	535	338		47	258	- 7900	- 8370
330	331	784	888	343	563	553	337		103	256	- 7900	- 8330
360	331	822	954	342	638	610	336		112	256	- 7850	- 8270
390	331	851	954	342	685	675	335		140	255	- 7770	- 8160
420	331	879	973	342	722	694	334		168	255	- 7700	- 8050

TABLE C - 7

Temperatures and Stresses in 1/16" Thick Cone for a Program of 5 ^{o}F/sec. to 400^{o}F

TIME Sec.	STATION 1 Temp.	STATION 1 Stress M	STATION 1 Stress C	STATION 2 Temp.	STATION 2 Stress M	STATION 2 Stress C	STATION 3 Temp.	STATION 3 Stress M	STATION 3 Stress C	STATION 4 Temp.	STATION 4 Stress M	STATION 4 Stress C
0	80	0	0	80	0	0	80		0	80	0	0
5	94	20	223	89	102	284	92		- 70	103	- 1310	- 1310
10	119	0	141	117	788	616	124		- 151	133	- 3150	- 3160
15	144	80	180	147	752	591	151		- 280	153	- 4230	- 4200
20	170	60	140	172	680	580	180		- 50	173	- 5450	- 5220
25	193	- 20	- 30	199	663	525	209		- 405	193	- 6450	- 6130
30	219	69	158	225	600	520	238		- 382	216	- 7490	- 6960
35	244	78	215	249	673	497	267		- 350	236	- 8580	- 7900
40	269	49	116	275	704	463	296		- 470	255	- 10400	- 8640
45	293	77	115	303	696	496	326		- 482	277	- 10100	- 9254
50	318	133	209	328	650	490	355		- 567	297	- 10800	- 9800
55	343	- 28	- 103	353	577	409	385		- 582	315	- 11500	- 10200
60	368	- 221	- 626	378	487	367	414		- 543	333	- 12060	-10750
65	381	- 311	- 1043	398	270	216	433		- 616	339	- 11900	-10600
70	385	- 328	- 1201	408	171	45	440		- 513	335	- 11300	-10200
75	388	- 346	- 1265	412	117	27	447		- 441	331	- 11000	- 9900
80	388	- 382	- 1356	417	106	9	450		- 441	331	- 10800	- 9770
85	393	- 364	- 1430	424	159	44	454		- 435	331	- 10800	- 9770
90	395	- 362	- 1475	426	80	18	456		- 413	331	- 10600	- 9600
120	407	- 261	- 1460	443	174	70	461		- 215	331	- 10200	- 9320
150	415	- 62	- 1370	449	294	173	461		- 68	331	- 10000	- 9090
180	420	9	- 1415	452	536	389	461		85	331	- 9770	- 8850
210	423	97	- 1340	452	666	450	458		188	331	- 9570	- 8670
240	426	185	- 1260	452	822	554	454		250	331	- 9500	- 8530
270	426	273	- 1180	452	960	666	452		325	334	- 9320	- 8360
300	428	273	- 1180	452	1020	683	451		328	334	- 9220	- 8230
330	428	273	- 1180	452	1100	770	450		380	334	- 9200	- 8175
360	430	343	- 1117	450	1140	780	447		458	335	- 9000	- 7900
390	432	370	- 1110	451	1160	790	446		485	335	- 8970	- 7900
420	435	378	- 1065	451	1160	790	446		485	335	- 8970	- 7900

TABLE C - 8

Temperatures and Stresses in 1/16" Thick Cone for a Program of 10 ^{o}F/sec. to 500^{o}F

TIME Sec.	STATION 1 Temp.	STATION 1 Stress M	STATION 1 Stress C	STATION 2 Temp.	STATION 2 Stress M	STATION 2 Stress C	STATION 3 Temp.	STATION 3 Stress M	STATION 3 Stress C	STATION 4 Temp.	STATION 4 Stress M	STATION 4 Stress C
0	66	0	0	66	0	0	66		0	66	0	0
5	76	71	223	70	528	426	73		- 183	83	- 1560	- 1070
10	121	- 353	- 181	115	626	757	123		- 1313	142	- 5310	- 4960
15	175	- 289	- 70	166	860	1140	178		- 1400	188	- 7800	- 7650
20	224	- 315	- 216	220	955	1014	233		- 1480	233	- 10090	- 9900
25	274	- 251	- 106	273	1030	1050	293		- 1330	276	- 1190	- 11570
30	325	- 480	- 453	327	888	936	354		- 1380	320	- 13880	- 13280
35	378	- 660	- 761	380	576	714	414		- 1270	360	- 15780	- 14860
40	427	- 628	- 584	433	510	580	471		- 1280	400	- 16690	- 15380
45	470	- 726	- 701	482	300	359	528		- 1300	436	- 17310	- 15890
50	482	- 670	- 770	504	- 300	- 138	554		- 1200	431	- 16040	- 14930
55	487	- 616	- 757	515	- 536	- 264	563		- 1100	420	- 15050	- 14190
60	491	- 589	- 805	525	- 537	- 284	571		- 1070	420	- 14840	- 14040
90	507	- 235	- 575	556	- 574	- 250	591		- 768	418	- 13790	- 13300
120	517	128	- 272	568	- 377	- 52	591		- 451	418	- 13200	- 12830
150	523	329	- 88	573	- 88	146	588		- 291	418	- 12820	- 12470
180	528	569	245	575	146	350	583		- 57	420	- 12970	- 12200
210	529	717	355	575	300	438	580		64	420	- 12400	- 12000
240	530	812	473	575	467	569	576		146	420	- 12250	- 11800
270	530	906	527	575	518	628	574		191	422	- 12100	- 11660
300	533	905	562	575	620	708	572		213	422	- 11970	- 11500
330	535	811	546	575	723	781	570		257	425	- 11800	- 11320
360	538	1045	694	575	737	825	570		375	425	- 11770	- 11200
390	542	1046	760	575	759	832	568		434	426	- 11750	- 11150
420	542	1085	775	575	854	883	565		456	426	- 11550	- 10930

TABLE C - 9

Temperatures and Stresses in 1/16" Thick Cone for a Program of 10 ^{o}F/sec. to 400^{o}F

with 22" Hg Differential Pressure.

TIME Sec.	STATION 1			STATION 2			STATION 3			STATION 4		
	Temp.	Stress		Temp.	Stress		Temp.	Stress		Temp.	Stress	
		M	C		M	C		M	C		M	C
0	67	-264	-528	66	-508	-1066	65		-903	66	3880	-1180
5	93	-374	-405	80	102	-254	76		-1210	92	1230	-3070
10	141	-551	-521	129	171	71	124		-2210	149	-2800	-6300
15	191	-645	-556	178	259	220	176		-2315	196	-5560	-8590
20	240	-666	-530	228	294	294	226		-2350	237	-7440	-9050
25	289	-586	-336	278	318	309	284		-2180	276	-8890	-11130
30	338	-770	-573	326	142	161	336		-2130	316	-10000	-12000
35	377	-1110	-1120	371	-294	-138	389		-2250	347	-10900	-12660
40	384	-1130	-1301	388	-855	-710	414		-2260	338	-9570	-11660
45	390	-1100	-1280	395	-1095	-996	425		-2240	332	-8820	-11100
50	393	-1150	-1440	404	-1200	-1070	436		-2260	330	-8460	-10800
55	395	-1070	-1390	409	-1226	-1100	443		-2180	330	-8180	-10610
60	397	-1090	-1460	414	-1282	-1080	446		-2240	327	-7914	-10440
90	410	-850	-1230	437	-1320	-1190	458		-2150	325	-7350	-10050
120	416	-694	-1100	450	-1100	-1040	458		-2050	325	-7144	-9860
150	422	-573	-890	454	-886	-920	456		-1950	325	-6871	-9640
180	426	-336	-540	455	-714	-774	453		-1860	325	-6730	-9440
210	430	-246	-396	455	-568	-671	453		-1800	326	-6650	-9280
240	430	-194	-334	455	-464	-610	450		-1750	326	-6530	-9240
270	430	-132	-282	455	-344	-482	446		-1770	329	-6320	-9052
300	430	-123	-246	455	-301	-525	446		-1770	329	-6251	-9000
330	433	-44	-141	455	-250	-464	446		-1700	329	-6170	-8840
360	435	-35	-97	455	-163	-396	443		-1700	329	-6080	-8770
390	438	9	44	455	-163	-396	443		-1650	329	-5940	-8550
420	440	35	44	455	-163	-396	443		-1650	329	-5940	-8550

TABLE C - 10

Temperatures and Stresses in 1/16" Thick Cone for a Program of

20 °F/sec. to 500°F with 22" Hg Differential Pressure

TIME Sec.	STATION 1 Temp.	STATION 1 Stress M	STATION 1 Stress C	STATION 2 Temp.	STATION 2 Stress M	STATION 2 Stress C	STATION 3 Temp.	STATION 3 Stress M	STATION 3 Stress C	STATION 4 Temp.	STATION 4 Stress M	STATION 4 Stress C
0	81	- 524	- 524	80	- 661	- 1090	82		- 741	85	4090	125
2	124	- 675	68	107	- 1026	- 1070	97		- 1400	108	2340	- 891
4	166	- 1013	- 280	140	- 1230	- 1380	140		- 1600	150	- 678	- 4150
6	205	- 1320	- 514	179	- 1210	- 1320	174		- 1940	183	- 2576	- 6350
8	248	- 1390	- 585	217	- 1225	- 1290	214		- 2050	216	- 4540	- 8300
10	286	- 1600	- 885	253	- 1200	- 1260	253		- 2020	243	- 6460	- 9790
12	330	- 2020	- 1340	293	- 1290	- 1345	297		- 1930	277	- 8140	- 11160
14	368	- 2570	- 1855	330	- 1440	- 1480	334		- 2130	307	- 9750	- 12300
16	407	- 2660	- 2050	364	- 1640	- 1570	372		- 2300	332	- 11680	- 13730
18	444	- 2610	- 1820	395	- 1780	- 1690	410		- 2330	360	- 13300	- 15000
20	480	- 2830	- 1870	430	- 1630	- 1630	450		- 2300	390	- 14400	- 15900
25	490	- 2620	- 2245	462	- 1910	- 1940	495		- 2580	384	- 12400	- 14400
30	490	- 2360	- 2090	470	- 1890	- 2000	515		- 2620	378	- 11300	- 13650
35	490	- 2250	- 2040	478	- 1890	- 2090	523		- 2590	375	- 10760	- 13000
40	490	- 2120	- 1980	483	- 1850	- 2030	530		- 2630	375	- 10470	- 13000
45	490	- 1980	- 1900	487	- 1870	- 2040	536		- 2550	375	- 10300	- 13000
50	490	- 1825	- 1825	493	- 1860	- 2000	540		- 2570	375	- 10300	- 13000
55	490	- 1750	-1790	495	- 1860	- 2000	544		- 2620	375	- 10300	- 13000
60	490	- 1600	- 1640	500	- 1840	- 1970	545		- 2620	375	- 10000	- 12800
90	490	- 1100	- 1260	512	- 1600	- 1800	545		- 2460	375	- 9790	- 12700
120	490	- 807	- 940	515	- 1270	- 1510	542		- 2420	380	- 9600	- 12600
150	490	- 553	- 697	515	- 970	- 1260	540		- 2320	380	- 9600	- 12600
180	490	- 276	- 310	515	- 564	- 960	540		- 2320	380	- 9600	- 12600
210	490	- 66	- 55	515	- 426	- 852	536		- 2290	383	- 9320	- 12350
240	490	66	110	515	- 266	- 680	536		- 2290	385	- 9440	- 12400
270	490	144	200	515	- 75	- 618	533		- 2310	385	- 9320	- 12400
300	490	254	332	515	- 53	- 575	530		- 2260	385	- 9260	- 12300
600	490	553	697	510	160	- 437	530		- 2690	406	- 7600	- 10900
900	490	686	818	510	266	- 383	525		- 3220	412	- 6670	- 10200
1140	490	752	918	510	372	- 330	520		- 2120	417	- 6000	- 9600

TABLE C - 11

Temperatures and Stresses in 1/16" Thick Cone for a Program of 20 °F/sec. to 500°F with 22" Hg. Differential Pressure, **with collapse**

TIME Sec.	STATION 1 Temp.	STATION 1 Stress M	STATION 1 Stress C	STATION 2 Temp.	STATION 2 Stress M	STATION 2 Stress C	STATION 3 Temp.	STATION 3 Stress M	STATION 3 Stress C	STATION 4 Temp.	STATION 4 Stress M	STATION 4 Stress C
0	84	-524	-456	84	-752	-935	84	-1070	-1780	84	2300	-1000
5	194	-1090	-179	167	316	-294	171	-1240	-2020	180	-2970	-6640
10	294	-1730	-853	258	90	-440	269	-1300	-2170	262	-7700	-10230
16.4	416	-2740	-1860	372	291	-31	396	-1500	-2400	356	-12140 / -11300	-12978
20	486	-3260	-2410	440	49	-522	474	-1840	-2920	410	-11900	-13300
25	490	-3000	-2930	472	-725	-1200	513	-1900	-2950	395	-10000	-12020
30	490	-2830	-2880	480	-693	-1310	531	-2080	-3050	386	-9200	-11440
35	490	-2700	-2830	490	-686	-1430	543	-2200	-3130	383	-8760	-11100
40	490	-2640	-2820	497	-735	-1490	552	-2370	-3230	380	-8530	-11000
45	490	-2530	-2770	500	-745	-1530	557	-2470	-3340	380	-8360	-10940
50	490	-2460	-2780	505	-754	-1550	563	-2570	-3350	380	-8190	-10800
55	490	-2360	-2750	510	-820	-1600	565	-2500	-3330	380	-8090	-10750
60	490	-2320	-2700	512	-839	-1590	565	-2430	-3370	380	-8010	-10700
120	492	-1670	-2200	525	-392	-1390	565	-1820	-2880	386	-7620	-10550
180	492	-1220	-1720	527	125	-1070	565	-1350	-2670	400	-7750	-10700
240	492	-1030	-1500	525	384	-910	560	-1220	-2690	400	-7150	-10080
300	492	-987	-1330	522	634	-740	550	-990	-2570	400	-7420	-10080
332.5	490	-930	-724	522	295	-920	550	-1250	-3070	400	-6710	-9670
332.5	490	-959	-526	522	384	-670	550	-1230	-2950	400	-6700	-9620
360	490	-1580	-733	515	36	-693	535	-2290	-4070	393	-6320	-9530
390	487	-2850	-1650	515	-567	-1290	533	-3770	-6000	390	-6180	-9660
420	487	-3730	-2250	510	-990	-1930	530	-5900	-9360	390	-6040	-9700

TABLE C - 12

Temperatures and Stresses in 1/16" Thick Cone for a Zonal Program with 22" Hg Differential Pressure

Zone 1, 50 ^{o}F/sec. to 500^{o}F; Zone 2, 40 ^{o}F/sec. to 400^{o}F; Zone 3, 30 ^{o}F/sec. to 300^{o}F.

TIME	STATION 1			STATION 2			STATION 3			STATION 4		
Sec.	Temp.	Stress M	Stress C	Temp.	Stress M	Stress C	Temp.	Stress M	Stress C	Temp.	Stress M	Stress C
0	72	-325	-274	72	-690	-842	72	-487	-436	72	2550	-1350
1	78	-264	-91	72	-487	-750	72	-740	-1420	75	2590	-1167
2	130	-61	1421	89	670	477	80	-640	-1110	90	1680	-2260
3	169	-540	610	117	438	122	103	-1090	-1580	120	20	-4370
4	219	-1560	108	153	456	-50	137	-1550	-2030	155	-1780	-5880
5	257	-2050	115	184	278	-260	165	-1580	-2150	177	-3500	-7000
6	303	-1920	-296	214	158	-325	194	-1640	-2140	198	-4820	-7840
7	346	-2340	-850	248	-68	-520	226	-1820	-2300	225	-6530	-8930
8	391	-2750	-1200	280	-212	-595	258	-1940	-2400	248	-7700	-9680
9	433	-3300	-1725	313	-142	-360	290	-2230	-2750	264	-8500	-10290
10	457	-4025	-2870	345	-914	-765	312	-2530	-3080	262	-8250	-9950
11	455	-3900	-3290	360	-1380	-1050	320	-2300	-2980	254	-7780	-9390
12	453	-3600	-3230	364	-1380	-1000	323	-2000	-2800	246	-7460	-9050
13	450	-3340	-3030	365	-1290	-932	325	-1800	-2600	241	-7050	-8700
14	449	-3180	-2900	365	-1140	-830	325	-1650	-2380	240	-6800	-8440
15	449	-3070	-2820	367	-1040	-800	327	-1580	-2330	240	-6770	-8440
20	448	-2840	-2670	370	-892	-708	340	-1420	-2140	230	-6130	-7950
25	447	-2770	-2640	372	-874	-780	350	-1400	-2120	229	-5840	-7750
30	447	-2790	-2670	374	-782	-754	354	-1400	-2120	227	-5620	-7540
60	440	-2480	-2570	381	-773	-745	363	-1420	-1980	230	-5400	-7390
90	440	-2270	-2380	380	-613	-613	360	-1270	-1830	230	-5180	-7320
120	440	-2000	-2060	380	-393	-460	360	-1120	-1740	230	-5180	-7320
150	436	-1850	-1940	380	-192	-285	357	-1020	-1650	232	-5180	-7320
180	435	-1700	-1820	380	-20	-175	357	-930	-1550	233	-5180	-7320
210	435	-1620	-1630	378	120	-55	355	-865	-1490	235	-5160	-7270
240	435	-1520	-1560	378	247	35	355	-865	-1490	235	-5160	-7270
270	435	-1470	-1510	378	330	73	355	-810	-1420	235	-5160	-7270
300	435	-1430	-1430	378	366	120	355	-770	-1390	235	-5160	-7270
330	435	-1420	-1450	378	412	137	352	-745	-1310	235	-5160	-7270
360	435	-1380	-1320	378	457	156	352	680	-1300	235	-5160	-7270

TABLE C - 13

Temperatures and Stresses in 1/8 "Thick Cone for a Program of 2.5 °F/sec. to 300 °F.

TIME Sec.	STATION 1 Temp.	STATION 1 Stress M	STATION 1 Stress C	STATION 2 Temp.	STATION 2 Stress M	STATION 2 Stress C	STATION 3 Temp.	STATION 3 Stress M	STATION 3 Stress C	Station 4 Temp.	Station 4 Stress M	Station 4 Stress C
0	60	0	0	58	0	0	57	0	0	58	0	0
5	78	- 211	- 70	74	- 244	- 81	66	255	233	62	- 222	- 377
10	91	- 189	- 24	87	- 322	- 111	78	300	455	74	- 616	- 1309
15	101	- 422	- 22	99	- 433	- 144	88	389	488	82	- 867	- 2031
20	115	- 440	- 33	110	- 484	- 99	103	297	352	91	- 1064	- 2453
25	126	- 462	- 0	123	- 484	- 99	115	231	110	98	- 1243	- 3058
30	136	- 451	- 11	134	- 429	- 88	127	220	198	106	- 1342	- 3685
35	148	- 352	0	146	- 418	- 77	138	99	242	113	- 1375	- 4020
40	160	- 294	32	157	- 360	- 66	150	55	209	120	- 1507	- 4697
45	172	- 196	32	170	- 349	- 120	162	0	218	129	- 1837	- 5313
50	183	- 131	55	184	- 283	- 98	175	- 33	153	135	- 2090	- 5819
55	194	- 174	32	195	- 305	- 101	187	- 98	131	143	- 2309	- 6314
60	207	- 108	54	206	- 292	- 97	199	- 76	108	152	- 2596	- 6897
65	218	- 151	43	219	- 322	- 108	211	- 119	858	161	- 2907	- 7458
70	230	- 173	43	230	- 301	- 97	226	- 151	- 11	168	- 3212	- 8019
75	241	- 194	32	241	- 301	- 97	236	- 162	- 43	175	- 3586	- 8613
80	253	- 213	21	255	- 352	- 118	249	- 256	- 96	184	- 3850	- 9262
85	261	- 245	- 32	263	- 406	- 96	256	- 363	- 161	187	- 4026	- 9427
90	262	- 266	- 21	266	- 309	- 64	259	- 299	- 128	183	- 3894	- 3141
95	264	- 244	53	268	- 331	- 64	260	- 395	- 202	181	- 3795	- 8965
100	265	- 193	64	270	- 331	- 64	259	- 438	- 224	179	- 3696	- 8668
105	267	- 171	64	270	- 331	- 64	259	- 502	- 245	178	- 3616	- 8450
110	268	- 161	86	272	- 320	- 64	259	- 502	- 245	178	- 3637	- 8565
115	270	- 139	86	273	- 320	- 64	259	- 470	- 245	179	- 3692	- 8602
120	270	- 139	107	274	- 309	- 43	260	- 502	- 245	179	- 3670	- 8527
125	270	- 128	139	274	- 309	- 43	260	- 502	- 245	179	- 3659	- 8450
300	265	- 86	171	270	- 256	- 234	260	- 341	- 299	193	- 4026	- 9170

TABLE C - 14

Temperatures and Stresses in 1/8" Thick Cone for a Program of 5° F/sec. to 400°F.

TIME Sec.	STATION 1 Temp.	STATION 1 Stress M	STATION 1 Stress C	STATION 2 Temp.	STATION 2 Stress M	STATION 2 Stress C	STATION 3 Temp.	STATION 3 Stress M	STATION 3 Stress C	STATION 4 Temp.	STATION 4 Stress M	STATION 4 Stress C
0	66	0	0	66	0	0	66	0	0	66	0	0
5	66	0	0	66	0	0	66	0	0	66	0	0
10	80	-45	57	77	-57	-23	69	296	285	68	-68	-205
15	105	-136	23	102	-194	-68	93	445	536	92.5	-934	-2340
20	129	-205	23	126	-160	-57	120	433	433	109	-1500	-4000
25	153	-262	0	150	-147	-45	143	285	376	130	-1850	-5415
30	175	-342	-46	173	-11	11	168	228	285	148	-2080	-6500
35	198	-136	0	196	-124	-34	192	123	213	165	-2400	-7700
40	222	-148	-34	219	-113	-11	216	56	179	180	-2400	-8160
45	244	-330	-160	242	-79	23	239	0	-22	193	-2840	-9800
50	265	-422	-216	264	-121	-22	264	-33	-44	208	-3400	-11000
55	288	-479	-296	290	-165	-99	288	-173	-259	224	-3900	-12100
60	311	-558	-365	313	-270	-140	312	-267	-353	239	-4600	-13200
65	334	-695	-490	335	-353	-193	333	-466	-530	252	-5130	-12900
70	348	-718	-536	352	-382	-212	349	-693	-777	256	-5200	-14100
75	349	-661	-467	354	-378	-200	349	-777	-777	250	-4800	-13400
80	349	-615	-410	356	-346	-158	349	-872	-840	243	-4600	-13000
85	351	-535	-330	357	-346	-168	347	-872	-840	240	-4570	-12600
90	353	-478	-240	358	-336	-136	349	-892	-819	242	-4540	-12800
95	353	-410	-194	360	-304	-126	350	-913	-798	242	-4500	-12700
100	353	-353	-125	362	-262	-115	350	-892	-735	242	-4500	-12700
105	353	-273	-84	362	-273	-136	350	-871	-672	242	-4500	-12660
110	353	-252	-31	362	-220	-115	351	-871	-672	243	-4560	-12800
115	353	-190	10	363	-220	-115	351	-871	-672	245	-4520	-12840
120	354	-178	42	364	-220	-115	351	-735	-567	245	-4520	-12840

TABLE C - 15

Temperatures and Stresses in 1/8" Thick Cone for a Program of 10 °F/sec. to 500 °F.

TIME Sec.	STATION 1 Temp.	STATION 1 Stress M	STATION 1 Stress C	STATION 2 Temp.	STATION 2 Stress M	STATION 2 Stress C	STATION 3 Temp.	STATION 3 Stress M	STATION 3 Stress C	STATION 4 Temp.	STATION 4 Stress M	STATION 4 Stress C
0	68	0	0	68	0	0	68	0	0	68	0	0
5	116	- 91	125	110	- 307	- 63	107	661	752	112	- 1680	- 4000
10	163	45	170	155	- 227	- 37	157	554	600	155	- 2780	- 7540
15	207	- 123	78	199	- 178	76	202	526	605	189	- 3850	- 10120
20	253	- 264	- 132	242	- 302	11	251	540	583	224	- 5780	- 12980
25	301	- 507	- 380	289	- 359	- 109	301	432	389	258	- 7620	- 15800
30	349	- 714	- 588	335	- 393	- 141	351	210	126	293	- 8870	- 18200
35	397	- 989	- 836	383	- 463	- 181	399	- 133	- 122	322	- 9600	- 20200
40	440	- 1250	-1240	425	- 451	- 107	446	- 406	- 386	352	- 9830	- 22000
45	449	- 1230	-1170	438	- 443	- 208	457	- 908	- 821	339	- 9340	- 21600
50	450	- 1140	-1090	442	- 411	- 185	458	- 1170	- 985	326	- 8740	- 20500
55	453	- 940	- 900	444	- 313	- 147	458	- 1275	-1010	324	- 8300	- 19550
60	452	- 873	- 873	447	- 313	- 147	460	- 1275	-1060	320	- 8140	- 19100
90	455	- 300	- 310	454	- 171	6	466	- 1290	- 965	322	- 8000	- 19000
120	456	- 30	- 116	454	132	170	466	- 954	- 625	326	- 7910	- 18950
150	456	78	87	454	359	296	466	- 742	- 382	333	- 7770	- 18800
180	456	165	145	454	501	419	466	- 456	- 138	339	- 7750	- 18100
210	456	223	243	454	634	463	466	- 297	85	339	- 7920	- 19430
240	456	272	252	454	691	478	466	- 74	274	345	- 7760	- 19200
270	456	291	310	452	624	539	466	- 42	285	345	- 7760	- 19200
300	456	340	330	452	624	539	463	0	410	350	- 7760	- 19200
330	456	310	320	452	624	615	463	0	410	350	- 7760	- 19200
360	456	370	398	452	851	644	463	52	483	358	- 7700	- 19000
390	456	370	398	452	860	644	463	242	578	358	- 7630	- 19000
420	456	320	380	452	860	660	463	242	578	360	- 7650	- 19000
450	456	320	380	452	908	660	463	284	620	362	- 7650	- 19000
480	456	320	380	452	908	660	463	357	640	362	- 7700	- 19000

TABLE C - 16

Temperatures and Stress in 1/8" Thick Cone for a Program of 10° F/sec. to 400°F with 24" Hg Differential Pressure

TIME Sec.	STATION 1 Temp.	STATION 1 Stress M	STATION 1 Stress C	STATION 2 Temp.	STATION 2 Stress M	STATION 2 Stress C	STATION 3 Temp.	STATION 3 Stress M	STATION 3 Stress C	STATION 4 Temp.	STATION 4 Stress M	STATION 4 Stress C
0	82	-342	-240	83	-467	-536	82	-627	-810	82	3900	22
5	108	-524	-240	104	-490	-479	103	182	0	105	3160	-3110
10	155	-407	-283	151	-350	-373	153	237	23	149	2700	-6000
15	199	-463	-350	196	-314	-325	199	403	67	185	2170	-8280
20	244	-717	-560	241	-418	-451	247	781	143	218	421	-10600
25	288	-935	-737	286	-518	-670	296	734	22	249	638	-12200
30	333	-1560	-1130	333	-710	-900	339	392	-297	278	-218	-13900
35	357	-1650	-1300	360	-742	-909	366	73	-572	281	-120	-14000
40	359	-1430	-1220	362	-742	-900	368	-312	-760	268	430	-13100
45	359	-1350	-1140	364	-752	-961	367	-593	-967	257	792	-12300
50	361	-1220	-1060	366	-752	-961	367	-750	-1020	254	891	-12000
55	361	-1220	-1060	367	-697	-936	368	-790	-1060	253	1030	-11850
60	361	-1150	-1000	368	-676	-926	368	-853	-1080	253	1030	-11850
100	365	-763	-920	377	-487	-829	370	-760	-1000	256	1090	-11800
140	363	-491	-606	377	-280	-725	370	-572	-780	260	1140	-11750
180	365	-470	-533	377	-124	-622	370	-406	-676	267	1080	-12000
220	365	-440	-523	374	-104	-550	368	-312	-562	272	1230	-12000

TABLE C - 17

Temperatures and Stresses in 1/8" Thick Cone for a Program of 20 °F/sec. to 500°F with 23" Hg Differential Pressure

TIME Sec.	STATION 1 Temp.	STATION 1 Stress M	STATION 1 Stress C	STATION 2 Temp.	STATION 2 Stress M	STATION 2 Stress C	STATION 3 Temp.	STATION 3 Stress M	STATION 3 Stress C	STATION 4 Temp.	STATION 4 Stress M	STATION 4 Stress C
0	86	-213	-456	85	-213	-598	86	-425	-861	85	2806	-213
2.5	122	-223	-384	109	121	-313	111	182	-222	128	2328	-3306
5	169	-310	-450	160	200	-260	165	490	-40	175	718	-7475
10	257	-601	-669	248	205	-263	255	953	369	258	-1028	-12842
15	346	-1221	-1137	340	-28	-385	348	1042	391	324	-3225	-16880
20	436	-1658	-1508	430	-229	-607	435	711	272	387	-3604	-20575
25	455	-1875	-1686	458	-377	-719	407	-187	-451	373	-1983	-19219
30	455	-1823	-1668	458	-291	-693	467	-510	-638	350	-1107	-17856
35	456	-1737	-1600	460	-317	-710	467	-850	-850	334	-639	-17052
40	456	-1686	-1557	462	-295	-685	469	-969	-893	332	-535	-16845
100	461	-1221	-1127	476	84	-455	477	-739	-655	340	-37	-16565
480	462	-812	-675	475	749	42	475	8	34	360	603	-16620
660	463	-778	-573	476	926	194	473	235	286	372	1316	-16201
840	464	-718	-530	478	985	286	474	344	344	378	1598	-15846
1020	464	-658	-462	476	1069	354	472	294	504	384	2202	-15051
1200	464	-650	-462	476	1145	413	475	227	487	388	2475	-14578
1380	462	-616	-385	478	1162	429	476	168	512	392	2603	-14424
1560	462	-581	-351	478	1162	429	475	118	563	396	2812	-14041
1740	463	-596	-333	478	1204	455	474	109	596	397	2876	-13940

TABLE C - 18

Temperatures and Stresses in 1/8" Thick Cone for a Zonal Program with 24" Hg Differential Pressure

Zone 1, 10 ^{o}F/sec. to 400^{o}F; Zone 2, 5 ^{o}F/sec. to 300^{o}F; Zone 3, 2.5 ^{o}F/sec. to 200^{o}F.

TIME Sec.	STATION 1			STATION 2			STATION 3			STATION 4		
	Temp.	Stress		Temp.	Stress		Temp.	Stress		Temp.	Stress	
		M	C		M	C		M	C		M	C
0	79	-296	-250	77	-467	-535	77	-661	-912	77	3200	140
5	124	-433	-433	97	-570	-627	85	-445	-640	83	2200	-445
10	166	-531	-554	126	-588	-655	96	-445	-801	84	2140	-638
15	204	-706	-773	149	-723	-791	106	-456	-775	86	2190	-798
20	247	-1043	-1090	175	-870	-802	118	-445	-801	90	2280	-946
25	285	-1380	-1340	199	-830	-830	140	-486	-848	104	2280	-1960
30	315	-1850	-1690	219	-921	-866	155	-520	-880	110	2350	-2280
35	337	-2130	-1850	241	-1160	-1030	165	-520	-860	112	2500	-2220
40	353	-2140	-1780	266	-1450	-1220	179	-610	-960	115	2630	-2270
45	356	-2100	-1730	274	-1600	-1290	184	-784	-1110	115	2710	-2280
50	354	-2070	-1720	274	-1550	-1280	188	-795	-1165	115	2820	-2250
55	350	-2000	-1660	273	-1490	-1250	190	-851	-1180	115	2840	-2230
60	350	-1940	-1640	274	-1450	-1240	191	-828	-1100	115	2860	-2220
90	346	-1600	-1370	275	-1260	-1120	200	-896	-1140	121	2940	-2500
120	346	-1490	-1250	275	-1160	-1080	205	-840	-1120	125	2980	-2700
150	346	-1340	-1123	275	-1060	-1050	207	-830	-1075	128	2950	-2840
180	346	-1270	-1040	275	-992	-1000	207	-817	-1040	130	3000	-2890
210	346	-1220	-960	275	-937	-981	207	-817	-1040	132	2950	-3090
240	346	-1220	-960	277	-905	-937	209	-638	-940	134	2980	-3170
270	346	-1200	-890	277	-872	-926	209	-638	-940	136	3000	-3170
300	346	-1160	-820	278	-818	-915	211	-616	-874	138	3080	-3210
330	346	-1120	-810	278	-818	-915	211	-616	-874	140	3080	-3210

TABLE C - 19

Temperatures and Stresses in 1/8" Thick Cone for a Zonal Program with 23" Hg Differential Pressure

Zone 1, 20 °F/sec. to 400 °F; Zone 2, 10 °F/sec. to 300 °F; Zone3, 5 °F/sec. to 200 °F.

TIME	STATION 1			STATION 2			STATION 3			STATION 4		
	Temp.	Stress		Temp.	Stress		Temp.	Stress		Temp.	Stress	
Sec.		M	C		M	C		M	C		M	C
0	70	-239	-580	71	-410	-787	72	-513	-980	70	3520	-182
5	117	-148	-400	97	-547	-775	78	-46	-501	74	3430	-167
10	191	-426	-750	147	-588	-814	105	148	-433	91	2950	-1650
15	262	-924	-1220	192	-773	-918	136	147	-440	108	2630	-2720
20	323	-1890	-1830	240	-910	-1090	164	23	-463	122	2520	-3530
25	351	-2230	-2000	273	-1210	-1240	188	-113	-644	128	2500	-3920
30	349	-2150	-1920	273	-1200	-1300	193	-437	-795	124	2740	-3630
35	349	-2150	-1920	273	-1180	-1300	198	-493	-885	122	2870	-3470
40	347	-2080	-1840	273	-1180	-1300	201	-560	-907	122	2990	-3300
45	345	-2020	-1820	273	-1140	-1290	201	-594	-918	122	3030	-3240
50	348	-2020	-1820	276	-992	-1230	205	-571	-896	122	3100	-3210
55	346	-2000	-1750	276	-981	-1200	206	-604	-907	122	3100	-3210
60	346	-1900	-1700	275	-990	-1170	206	-672	-930	122	3110	-3250
90	347	-1650	-1520	276	-883	-1110	209	-616	-874	126	3160	-3330
120	349	-1520	-1370	279	-784	-1050	212	-594	-806	126	3110	-3470
150	349	-1450	-1280	279	-676	-970	212	-549	-762	129	3160	-3500
180	349	-1380	-1200	280	-610	-915	212	-504	-717	129	3160	-3500
210	349	-1350	-1140	280	-578	-905	212	-504	-717	129	3140	-3550
240	349	-1320	-1130	280	-501	-828	212	-481	-650	132	3120	-3590
270	349	-1320	-1130	280	-501	-828	212	-481	-650	134	3240	-3570

TABLE C - 20

Temperatures and Stresses in 1/8" Thick Cone for a Zonal Program with 23" Hg Differential Pressure

Zone 1, 10 °F/sec. to 500°F; Zone 2, 5 °F/sec. to 400°F; Zone 3, 2.5 °F/sec. to 300°F.

TIME Sec.	STATION 1 Temp.	STATION 1 Stress M	STATION 1 Stress C	STATION 2 Temp.	STATION 2 Stress M	STATION 2 Stress C	STATION 3 Temp.	STATION 3 Stress M	STATION 3 Stress C	STATION 4 Temp.	STATION 4 Stress M	STATION 4 Stress C
0	66	- 262	- 559	63	- 353	- 707	64	- 479	- 969	64	3550	0
5	92	- 560	- 650	76	- 456	- 707	69	- 285	- 752	66	3480	- 194
10	133	- 638	- 707	103	- 581	- 752	78	- 171	- 592	70	3430	- 342
15	174	- 859	- 994	129	- 661	- 912	92	- 34	- 388	79	3240	- 1050
20	213	- 1050	- 1100	151	- 667	- 893	110	- 23	- 422	87	3020	- 1710
25	251	- 1420	- 1410	175	- 712	- 892	124	- 91	- 581	90	3000	- 1880
30	292	- 1800	- 1790	200	- 773	- 974	137	- 147	- 508	96	2920	- 2170
35	333	- 2120	- 2010	223	- 910	- 1090	151	- 214	- 508	103	2610	- 2500
40	371	- 2550	- 2410	246	- 990	- 1120	164	- 226	- 576	106	2990	- 2700
45	403	- 3090	- 2670	268	- 1140	- 1230	178	- 271	- 588	108	3060	- 2800
50	421	- 3240	- 2720	290	- 1320	- 1330	189	- 336	- 616	111	3090	- 2920
55	436	- 3114	- 2560	314	- 1570	- 1430	203	- 202	- 604	114	3100	- 3040
60	452	- 3100	- 2500	341	- 1810	- 1580	216	- 325	- 683	119	3030	- 3410
70	466	- 2860	- 2300	370	- 2240	- 1840	240	- 462	- 814	125	3120	- 3630
80	460	- 2700	- 1990	370	- 1980	- 1770	256	- 583	- 858	139	2970	- 4490
90	456	- 2430	- 1950	372	- 1790	- 1640	276	- 616	- 864	156	2730	- 5450
120	447	- 1940	- 1580	372	- 1425	- 1400	289	- 670	- 842	163	2810	- 5710
150	445	- 1760	- 1430	375	- 1270	- 1290	291	- 616	- 767	166	2750	- 5820
180	445	- 1680	- 1380	375	- 1110	- 1190	291	- 530	- 680	168	2770	- 5900
210	446	- 1610	- 1230	375	- 1030	- 1130	292	- 508	- 616	171	2810	- 5920
240	446	- 1520	- 1170	375	- 936	- 1040	292	- 486	- 550	171	2810	- 5920
270	446	- 1450	- 1100	375	- 915	- 1040	292	- 475	- 518	173	2900	- 5980
300	446	- 1410	- 1060	375	- 915	- 1040	292	- 388	- 432	175	2830	- 6000
330	446	- 1390	- 990	376	- 820	- 946	292	- 292	- 367	177	2830	- 6000
360	446	- 1390	- 990	376	- 820	- 946	293	- 280	- 335	177	2800	- 6010
390	446	- 1360	- 980	376	- 780	- 936	293	- 270	- 302	179	2840	- 6000
420	446	- 1360	- 980	376	- 707	- 832	293	- 270	- 302	179	2840	- 6000

TABLE C — 21

Temperatures and Stresses in 1/8" Thick Cone for a Zonal Program with 23" Differential Pressure

Zone 1, 20 ^{o}F/sec. to 500^{o}F; Zone 2, 10 ^{o}F/sec. to 400^{o}F; Zone 3, 5 ^{o}F/sec. to 300^{o}F.

TIME	STATION 1			STATION 2			STATION 3			STATION 4		
	Temp.	Stress		Temp.	Stress		Temp.	Stress		Temp.	Stress	
Sec.		M	C		M	C		M	C		M	C
0	84	- 239	- 490	87	- 342	- 730	86	- 501	- 1040	87	3690	46
5	94	- 11	- 353	87	- 342	- 730	86	- 501	- 1040	98	3690	46
10	168	- 239	- 791	127	- 182	- 604	101	- 102	- 798	97	3680	- 559
15	247	- 726	-1120	175	- 192	- 667	133	- 11	- 912	120	3420	- 2000
20	322	- 1370	-1780	221	- 422	- 810	160	46	- 718	131	3120	- 2820
25	391	- 2480	-2550	268	- 638	- 935	188	23	- 660	144	3070	- 3570
30	430	- 2880	-2690	311	- 995	-1170	214	78	- 660	154	3020	- 4100
35	460	- 2910	-2530	359	- 1420	-1470	241	22	- 721	161	3020	- 4430
40	461	- 2780	-2430	368	- 1570	-1560	258	- 308	- 968	167	3070	- 4780
45	458	- 2740	-2430	368	- 1270	-1460	276	- 414	- 970	182	2860	- 5720
50	455	- 2560	-2280	368	- 1070	-1340	291	- 400	- 983	194	2690	- 6450
55	450	- 2490	-2180	368	- 1000	-1310	284	- 464	- 994	192	2840	- 6150
60	447	- 2360	-2090	368	- 1000	-1310	296	- 529	- 1015	188	2980	- 5940
90	441	- 1790	-1650	371	- 852	-1150	299	- 594	- 1025	184	3160	- 5540
120	442	- 1700	-1560	374	- 707	-1080	299	- 518	- 972	187	3170	- 5670
150	442	- 1540	-1370	374	- 540	- 946	299	- 497	- 907	188	3200	- 5660
180	442	- 1430	-1310	374	- 468	- 925	300	- 475	- 842	190	3240	- 5640
210	442	- 1290	-1130	374	- 374	- 832	300	- 389	- 767	192	3240	- 5640
240	444	- 1290	-1180	376	- 322	- 821	300	- 302	- 680	194	3280	- 5790
270	444	- 1270	-1120	376	- 270	- 800	301	- 302	- 680	197	3280	- 5790
300	444	- 1260	-1090	376	- 250	- 738	301	- 227	- 594	198	3280	- 5790
330	444	- 1260	-1090	376	- 250	- 738	301	- 227	- 594	198	3280	- 5790

TABLE C = 22

Temperatures and Stresses in 1/8" Thick Cone for a Zonal Program with 23" Hg Differential Pressure

Zone 1, 50 °F/sec. to 500°F; Zone 2, 40 °F/sec. to 400°F; Zone 3, 30 °F/sec. to 300°F.

TIME Sec.	STATION 1 Temp.	STATION 1 Stress M	STATION 1 Stress C	STATION 2 Temp.	STATION 2 Stress M	STATION 2 Stress C	STATION 3 Temp.	STATION 3 Stress M	STATION 3 Stress C	STATION 4 Temp.	STATION 4 Stress M	STATION 4 Stress C
0	62	- 285	- 536	61	-342	- 672	60	- 490	- 912	60	3260	68
1	67	- 57	- 330	61	-171	- 524	60	- 342	- 832	60	3240	- 23
2	102	- 68	- 114	78	-217	- 388	68	364	- 57	72	3120	- 741
3	141	- 147	- 271	112	-285	- 365	89	900	581	95	2540	- 2630
4	178	- 283	- 260	144	-296	- 388	112	1120	684	125	1800	- 4830
5	224	- 377	- 421	185	-450	- 565	149	1190	667	158	870	- 7180
6	260	- 627	- 660	219	-667	- 723	174	1360	880	184	123	- 8840
7	302	- 983	- 940	257	-748	- 704	208	1490	930	210	-650	- 10800
8	345	- 1180	- 1140	291	-864	- 756	237	1590	1040	234	-1220	- 12090
9	383	- 1470	- 1420	327	-1110	- 933	264	1560	902	249	-1800	- 13230
10	404	- 2150	- 2000	356	-1290	- 1220	285	1170	462	253	-1850	- 13380
11	411	- 2360	- 2160	364	-1340	- 1270	293	950	280	249	-1630	- 13050
12	414	- 2480	- 2240	364	-1300	- 1260	297	712	108	243	-1310	- 12600
13	415	- 2540	- 2260	364	-1250	- 1240	300	648	86	240	-1130	- 12300
14	417	- 2600	- 2280	364	-1200	- 1220	301	530	43	234	- 877	- 11800
15	419	- 2660	- 2350	363	-1140	- 1210	302	356	- 65	232	- 655	- 11520
20	426	- 2810	- 2380	362	- 1010	- 1190	307	0	- 238	216	112	- 10340
25	430	- 2840	- 2470	363	- 1020	- 1220	312	- 262	- 432	205	570	- 9520
30	432	- 2820	- 2400	365	- 990	- 1200	312	- 432	- 518	197	896	- 8860
35	436	- 2790	- 2380	365	- 990	- 1200	312	- 540	- 583	192	1140	- 8490
40	436	- 2690	- 2300	368	- 1020	- 1220	310	- 583	- 659	188	1380	- 8030
45	436	- 2620	- 2200	368	- 1020	- 1220	307	- 616	- 680	184	1370	- 7860
50	439	- 2610	- 2200	368	- 1020	- 1220	306	- 583	- 670	181	1410	- 7640
55	439	- 2570	- 2160	368	- 1040	- 1230	304	- 605	- 734	177	1460	-7500
60	439	- 2510	- 2120	370	- 1040	- 1230	302	- 680	- 756	177	1560	- 7320
70	439	- 2440	- 2090	372	- 1040	- 1230	299	- 659	- 745	175	1670	- 7120
80	442	- 2320	- 2000	373	- 1050	- 1260	297	- 605	- 650	172	1790	- 6900
90	442	- 2270	- 1910	373	- 1020	- 1220	297	- 530	- 594	176	1740	- 7100
120	445	- 2100	- 1740	379	- 894	- 1140	298	- 464	- 486	177	1790	- 7070
150	445	- 1930	- 1530	379	- 822	- 1050	298	- 432	- 475	177	1860	- 7050
180	446	- 1870	- 1480	380	- 742	- 960	299	- 334	- 356	180	1970	- 7060
300	448	- 1790	- 1370	379	- 463	- 782	300	- 162	- 97	187	2170	- 7020
420	447	- 1700	- 1235	380	- 412	- 690	302	- 77	- 97	191	2230	- 7040
540	448	- 1620	- 1150	381	- 381	- 680	300	- 43	- 54	192	2420	- 6800
720	447	- 1600	- 1090	381	- 330	- 660	300	54	43	196	2430	- 6760
900	448	- 1510	- 1040	381	- 268	- 607	300	97	77	199	2530	- 6570
1080	449	- 1500	- 1000	383	- 258	- 577	300	140	118	201	2530	- 6480

TABLE C - 23

Temperatures and Stresses in 1/16" Thick Hemisphere for a Program 5 °F/sec. to 400°F

TIME Sec.	STATION 1 Temp.	STATION 1 Stress M	STATION 1 Stress C	STATION 2 Temp.	STATION 2 Stress M	STATION 2 Stress C	STATION 4 Temp.	STATION 4 Stress M	STATION 4 Stress C
0	77	0	0	77	0	0	77	0	0
5	98	-57	-182	105	-890	-786	97	114	-935
10	128	-125	-535	135	-1090	-1410	117	-1240	-2400
15	159	-55	-296	166	-780	-915	132	-2590	-3820
20	192	-34	-168	200	-619	-583	151	-3600	-5130
25	223	-178	-300	230	-664	-697	170	-4860	-6770
30	254	-132	-209	260	-836	-891	187	-7500	-8700
35	284	-206	-293	288	-1075	-1060	206	-7000	-9300
40	312	-226	-333	314	-1280	-1180	222	-8000	-10700
45	339	-180	-340	341	-1310	-1250	237	-9110	-12000
50	367	-10	-239	366	-1270	-1200	256	-10000	-13200
55	396	-62	-374	393	-1270	-1150	273	-10800	-15400
60	418	-483	-523	418	-1400	-1200	290	-	-
90	427	-110	-10	437	-673	-307	297	-	-
120	427	231	372	442	-226	295	305	-12200	-15900
150	427	473	594	442	70	670	307	-12300	-15900
180	427	583	684	442	393	1050	310	-12100	-15800
210	427	724	825	440	531	1240	314	-12200	-15700
240	425	775	885	440	747	1460	317	-12300	-15700
270	425	815	895	435	786	1307	320	-12400	-15700
300	422	796	885	433	934	1460	324	-12300	-15600
330	422	826	895	430	1090	1590	325	-12400	-15600
360	422	876	915	430	1170	1660	325	-12500	-15700
390	422	876	915	430	1220	1700	327	-12600	-15500
420	422	896	920	430	1290	1820	330	-12300	-15200
450	420	925	925	427	1350	1960	330	-12400	-15300
480	420	915	876	427	1410	1990	330	-12400	-15200
510	417	965	896	425	1500	2050	334	-12300	-15000
540	417	985	905	425	1570	2070	335	-12350	-15000

TABLE C - 24

Temperatures and Stresses in 1/16" Thick Hemisphere for a Program of 5 °F/sec. to 400°F

With 21" Hg Differential Pressure.

TIME	STATION 1			STATION 2			STATION 3			STATION 4		
	Temp.	Stress		Temp.	Stress		Temp.	Stress		Temp.	Stress	
Sec.		M	C		M	C		M	C		M	C
0	74	-707	-627	74	-445	-741	74		-604	74	125	-1130
5	82	-707	-627	100	-1265	-1390	107		-1070	96	-68	-2620
10	106	-958	-1050	126	-1360	-1820	132		-1182	107	-673	-3440
15	135	-978	-1125	151	-893	-1210	164		-1290	123	-1230	-4430
20	159	-1040	-1130	177	-655	-655	192		-1460	138	-1930	-5600
25	186	-1080	-1035	201	-403	-358	222		-1530	154	-2475	-6280
30	213	-1165	-1110	230	-278	-155	252		-1560	170	-3280	-7490
35	235	-1365	-1440	255	-363	-110	283		-1530	187	-3930	-8550
40	258	-1390	-1595	280	-356	43	313		-1700	202	-4590	-9300
45	281	-1620	-1840	307	-524	64	342		-1890	218	-5240	-10260
50	304	-1560	-1930	331	-752	0	372		-2110	235	-5870	-11180
55	326	-1530	-2040	357	-588	189	400		-2350	250	-6420	-12020
60	348	-1400	-2030	380	-525	216	428		-2580	264	-7120	-13100
90	375	-738	-1730	401	-173	337	459		-2460	277	-7900	-13600
120	384	-300	-1430	406	-337	163	464		-2350	284	-8000	-13700
150	384	-155	-1290	408	-296	173	464		-2060	290	-8100	-13800
180	384	-124	-1110	408	-153	224	461		-1970	294	-8190	-14000
210	382	-10	-999	408	-20	357	460		-1930	300	-8200	-14000
240	378	52	-874	406	112	428	460		-1740	302	-8300	-14000
270	378	83	-853	405	255	622	460		-1640	304	-8300	-14000
300	378	177	-749	405	398	785	455		-1715	306	-8500	-14200
330	378	198	-676	405	449	826	455		-1617	308	-8570	-14400
360	378	198	-676	405	510	847	450		-1670	310	-8560	-14300
390	378	239	-655	405	510	847	450		-1670	314	-8500	-14300
420	378	239	-655	405	510	847	450		-1670	314	-8600	-14300

TABLE C - 25

Temperature and Stresses in 1/16" Thick Hemisphere for a Program of 10 °F/sec. to 500°F

TIME Sec.	STATION 1 Temp.	STATION 1 Stress M	STATION 1 Stress C	STATION 2 Temp.	STATION 2 Stress M	STATION 2 Stress C	STATION 3 Temp.	STATION 3 Stress M	STATION 3 Stress C	STATION 4 Temp.	STATION 4 Stress M	STATION 4 Stress C
0	78	0	0	78	0	0	78		0	78	0	0
5	126	250	148	132	-114	-273	118		171	115	1320	-946
10	187	134	-146	195	-380	-930	175		-56	148	520	-2490
15	245	-33	-451	254	-759	-1500	232		-330	181	45	-4330
20	305	-162	-356	314	-1060	-1940	294		-326	217	-121	-5420
25	364	-530	-707	375	-1310	-2270	356		-567	250	-682	-7170
30	424	-726	-1024	430	-1550	-2380	416		-805	283	-810	-8430
35	480	-912	-1090	486	-1750	-2360	475		-922	317	-1100	-9880
40	529	-1330	-1380	538	-1820	-2320	531		-958	350	-1050	-10700
45	550	-1610	-1460	555	-1580	-1930	565		-945	357	-1650	-11370
50	550	-1560	-1220	560	-1030	-1440	575		-743	358	-1600	-11360
55	545	-1380	-1000	560	-755	-1150	580		-720	360	-1400	-11200
60	540	-1290	-835	560	-466	-907	585		-673	360	-1400	-11200
90	535	-633	-61	560	483	-16	585		-238	368	-938	-10830
120	531	-184	396	555	1000	493	580		119	368	-887	-10800
150	527	18	580	550	1530	1100	575		371	370	-683	-10740
180	522	286	884	547	1810	1440	570		455	374	-235	-10200
210	520	366	930	542	2030	1680	565		669	375	-204	-10100
240	516	515	1060	536	2360	1970	560		831	377	-153	-9980
270	512	560	1070	535	2500	2070	555		981	380	133	-9735
300	512	570	1030	530	2670	2200	553		1026	380	205	-9530
330	510	562	970	527	2730	2250	550		1080	380	340	-9120
360	505	695	1060	527	2760	2330	546		1200	380	380	-9000
390	505	723	1070	525	2790	2430	546		1260	380	380	-9000

TABLE C - 26

Temperatures and Stresses in 1/16" Thick Hemisphere for a Zonal Program with 21" Hg Differential Pressure

Zone 1, 10 °F/sec. to 400°F; Zone 2, 5 °F/sec. to 300°F; Zone 3, 2.5 °F/sec. to 200°F.

TIME Sec.	STATION 1 Temp.	STATION 1 Stress M	STATION 1 Stress C	STATION 2 Temp.	STATION 2 Stress M	STATION 2 Stress C	STATION 3 Temp.	STATION 3 Stress M	STATION 3 Stress C	STATION 4 Temp.	STATION 4 Stress M	STATION 4 Stress C
0	94	-454	- 545	87	-387	- 650	86		- 501	87	250	- 980
5	143	-567	- 386	125	11	- 320	108		216	98	1880	250
10	192	-549	- 515	155	- 124	- 316	125		376	106	2280	11
15	240	-575	- 520	186	- 157	- 393	141		306	111	1675	- 125
20	289	-759	- 542	217	- 257	- 549	162		465	122	2245	296
25	332	-842	- 634	246	- 189	- 696	181		452	130	1820	- 409
30	357	-628	- 533	267	- 324	- 702	198		439	135	1670	- 648
35	362	- 544	- 512	287	- 454	- 540	219		333	143	1590	- 851
40	360	- 408	- 460	297	- 454	- 324	236		222	151	1616	--1017
45	360	- 335	- 376	297	- 302	- 86	245		276	153	1330	- 1290
50	359	- 303	- 356	297	- 194	- 22	248		331	153	1280	- 1300
55	359	- 200	- 303	297	- 194	- 22	248		331	153	1280	- 1300
60	358	- 146	- 251	298	- 194	- 22	250		331	155	1280	- 1300
90	357	- 31	- 94	298	- 194	- 22	252		442	158	1410	- 1330
120	357	115	52	299	- 184	22	252		552	160	1590	- 1200
150	357	220	115	299	- 162	86	252		690	160	1510	- 1320
180	357	303	167	299	- 76	259	250		684	161	1450	- 1380
210	357	439	261	299	- 22	346	248		762	163	1680	- 1100
240	357	481	313	298	22	367	248		806	164	1660	- 1160
270	357	492	366	298	32	400	248		861	165	1620	- 1160
300	357	533	429	296	130	486	248		883	166	1770	- 1020
330	357	575	470	296	162	497	248		927	167	1720	- 1040
360	357	628	492	296	216	550	246		883	169	1780	- 842
390	357	628	492	296	227	605	246		883	169	1780	- 842
420	357	628	492	296	227	605	246		938	169	1780	- 842

TABLE C - 27

Temperatures and Stresses in 1/16" Thick Hemisphere for a Zonal Program with 21" Hg Differential Pressure.

Zone 1, 10 °F/sec. to 500°F; Zone 2, 5 °F/sec. to 400°F; Zone 3, 2.5 °F/sec. to 300°F.

TIME Sec.	STATION 1 Temp.	STATION 1 Stress M	STATION 1 Stress C	STATION 2 Temp.	STATION 2 Stress M	STATION 2 Stress C	STATION 3 Temp.	STATION 3 Stress M	STATION 3 Stress C	STATION 4 Temp.	STATION 4 Stress M	STATION 4 Stress C
0	71	- 587	- 452	69	- 330	- 627	71		- 456	70	- 137	- 1015
5	144	- 418	- 23	92	- 160	- 513	79		- 855	75	- 285	- 1450
10	159	- 1000	- 881	123	- 433	- 798	97		- 490	83	- 912	- 2140
15	205	- 1390	- 1140	153	- 542	- 791	115		- 353	90	- 650	- 1980
20	249	- 1350	- 1130	183	- 698	- 900	134		- 307	99	- 216	- 1760
25	291	- 1310	- 1100	209	- 840	- 1280	153		- 192	106	- 524	- 2040
30	340	- 1380	- 1070	240	- 873	- 1410	170		- 34	113	- 365	- 1860
35	385	- 1285	- 1275	270	- 1070	- 1660	191		- 168	122	- 320	- 2020
40	427	- 1290	- 1390	298	- 1275	- 1640	209		- 168	128	- 513	- 2270
45	446	- 1307	- 1445	317	- 1470	- 1780	226		- 211	136	- 531	- 2330
50	445	- 1270	- 1400	334	- 1470	- 1660	246		- 355	142	- 655	- 2640
55	445	- 1120	- 1320	351	- 1600	- 1760	266		- 344	149	- 632	- 2830
60	445	- 1040	- 1290	370	- 1670	- 1760	289		- 259	157	- 600	- 3000
90	445	- 707	- 953	393	- 1210	- 1110	363		- 312	204	- 1040	- 4730
120	446	- 570	- 796	400	- 1000	- 908	376		- 146	212	- 1280	- 4800
150	448	- 432	- 580	403	- 806	- 724	376		- 104	218	- 1290	- 5000
180	448	- 285	- 442	403	- 704	- 580	376		83	222	- 1040	- 4920
210	448	- 245	- 344	403	- 571	- 510	374		208	225	- 1060	- 5060
240	448	- 108	- 187	403	- 377	- 235	372		312	227	- 910	- 4940
270	448	- 98	- 167	400	- 326	- 245	370		301	230	- 700	- 4770
300	448	- 49	- 108	400	- 143	- 92	368		364	230	- 810	- 4800
330	448	- 39	- 59	398	- 153	- 143	368		468	230	- 977	- 4860
360	448	- 9	9	398	- 122	- 133	367		416	231	- 977	- 4860
390	448	20	50	397	- 51	10	364		364	233	- 890	- 4740
420	448	20	50	395	- 61	- 40	364		447	233	- 920	- 4750

TABLE C – 28

Temperatures and Stresses in 1/16" Thick Hemisphere for a Zonal Program with 21" Hg Differential Pressure:

Zone 1, 20 °F/sec. to 500°F; Zone 2, 10 °F/sec. to 400°F; Zone 3, 5 °F/sec. 300°F.

TIME	STATION 1			STATION 2			STATION 3			STATION 4		
	Temp.	Stress		Temp.	Stress		Temp.	Stress		Temp.	Stress	
Sec.		M	C		M	C		M	C		M	C
0	76	-616	-560	76	-327	-621	76		-502	76	80	-741
5	193	-1340	-896	153	-361	-723	116		-490	94	307	-1220
10	275	-1280	-1020	207	-560	-974	149		-584	110	376	-1560
15	364	-1510	-1260	265	-946	-1470	185		-600	125	308	-2030
20	437	-1540	-1430	316	-1740	-2040	220		-583	139	477	-1920
25	455	-1290	-1620	352	-1700	-2060	256		-575	152	260	-2340
30	455	-1063	-1420	386	-1870	-2110	296		-653	165	158	-2840
35	451	-934	-1350	391	-1590	-1640	322		-710	180	90	-3015
40	450	-806	-1270	394	-1120	-1020	341		-567	194	90	-3416
45	450	-784	-1210	395	-1120	-1020	358		-504	204	-571	-4030
50	450	-773	-1160	395	-989	-969	363		-494	205	-1110	-4450
55	450	-720	-1150	395	-918	-908	367		-525	206	-1220	-4440
60	450	-666	-1130	395	-877	-857	371		-416	209	-1160	-4300
90	450	-418	-890	400	-602	-612	375		-218	214	-1160	-4500
120	450	-183	-494	400	-480	-480	375		-31	219	-1050	-4550
150	450	-21	-322	400	-334	-334	375		135	223	-1060	-4540
180	450	75	-161	400	-204	-214	372		146	225	-1160	-4660
210	450	128	-97	398	-122	-102	370		156	228	-1200	-4640
240	450	215	0	398	10	10	368		291	230	-1065	-4600
270	450	257	54	398	102	81	368		416	231	-1170	-4630
300	450	344	160	396	194	163	367		468	233	-1270	-4650
330	450	344	160	395	184	143	365		562	235	-1020	-4400
360	450	376	172	395	200	179	364		593	236	-1050	-4400
390	450	387	225	395	262	242	363		603	236	-966	-4350
420	450	408	236	395	284	305	363		624	236	-966	-4350

TABLE C - 29

Temperatures and Stresses in 1/16" Thick Hemisphere for a Zonal Program with 18" Hg Differential Pressure:

Zone 1, 50 ^{o}F/sec. to 500^{o}F; Zone 2, 40 ^{o}F/sec. to 400^{o}F; Zone 3, 30 ^{o}F/sec. to 300^{o}F.

TIME Sec.	STATION 1 Temp.	STATION 1 Stress M	STATION 1 Stress C	STATION 2 Temp.	STATION 2 Stress M	STATION 2 Stress C	STATION 3 Temp.	STATION 3 Stress M	STATION 3 Stress C	STATION 4 Temp.	STATION 4 Stress M	STATION 4 Stress C
0	70	-467	-422	68	-308	-560	70		-553	70	-102	-809
1	126	-456	-342	123	114	-524	84		-640	80	-250	-1250
2	166	-915	-859	156	-56	-768	103		-274	96	46	-1500
3	207	-1360	-1310	190	-293	-1250	129		-388	116	1700	-992
4	251	-1810	-1840	227	-178	-966	161		-350	134	2740	-990
5	300	-2170	-2130	264	-176	-1100	191		-34	151	3420	-1090
6	340	-2400	-2360	299	-140	-1180	220		-377	166	3670	-1390
7	390	-2490	-2520	338	138	-1070	252		-375	183	3360	-2280
8	433	-2800	-2780	374	11	-1360	281		-356	195	2480	-3320
9	460	-3100	-3170	394	-775	-1800	310		-756	195	1160	-4420
10	467	-2760	-3050	400	-1000	-1430	327		-856	194	314	-4700
11	469	-2620	-2950	402	-867	-1300	333		-795	193	-280	-4760
12	472	-2400	-2750	404	-683	-950	336		-551	193	-627	-4550
13	472	-2290	-2690	406	-581	-867	337		-223	193	-874	-4540
14	472	-2100	-2540	406	-460	-735	339		74	193	-1050	-4600
15	472	-2070	-2530	406	-388	-622	341		180	193	-1230	-4650
30	468	-2020	-2320	406	-296	-592	360		840	196	-1380	-4640
45	465	-2020	-2320	406	-204	-480	366		1070	199	-850	-4410
60	464	-1720	-1830	406	-102	-326	367		1200	201	-493	-4300
360	447	-980	-1070	387	1040	896	346		1750	219	544	-3230
660	446	-882	-892	389	1150	1030	341		1800	228	355	-3470
960	447	-784	-725	388	1180	1060	340		1760	234	-297	-3560
1260	448	-696	-637	389	1280	1150	340		1640	240	121	-3310
1560	449	-666	-540	390	1350	1200	336		1700	242	-121	-3340
1860	447	-588	-343	390	1410	1290	336		1720	244	253	-3000
2160	447	-559	-362	388	1420	1320	333		1750	247	143	-2780
2400	447	-500	-314	388	1420	1320	333		1800	248	99	-2800

APPENDIX D

ENERGY ANALYSIS

ENERGY APPROACH TO ANALYSIS OF LINEAR VISCOELASTIC SHELLS OF REVOLUTION

L. Albert Scipio II

and

Mansa Singh

ABSTRACT

A variational equation based on energy principles has been developed for thin hemispherical shells. The behavior of the shell is assumed to be characterized by a viscoelastic material with temperature dependent properties.

The Ritz method is applied by assuming that the shell displacements are functions of the curvilinear shell coordinates and that their unknown coefficients are functions of time.

A system of six ordinary differential equations of order two is developed. These equations result from operations on the variational equation.

TABLE OF CONTENTS

LIST OF SYMBOLS

$a_{\alpha\beta}$	Metric tensor of surface coordinates
E	Modulus of elasticity
e_{ij}	Components of strain deviatoric tensor
F	Free energy
f	Energy density/unit volume
G	Shear modulus
g_{ij}	Metric tensor
K	Kinetic energy
S_{ij}	Components of stress deviatoric tensor
T	Temperature field of the shell
t	Time
u^i, u_i	Displacement components
W	Work integral
x^i	Rectangular coordinates of the shell
y^i	Curvilinear coordinates of the shell

GREEK LETTERS

α	Coefficient of thermal expansion
β_1, β_2	Coefficients (functions of time)
δ	First variation
ϵ_{ij}	Components of strain tensor
γ_1, γ_2	Coefficients (functions of time)
η	Coefficient of viscosity
ρ	Density of the material/unit volume
ρ_1, ρ_2	Coefficients (functions of time)
σ_{ij}	Components of stress tensor

SUBSCRIPTS AND SUPERSCRIPTS

i, j	Refer to numbers 1, 2, 3
o	Refer to datum value, middle surface reference
α, β, γ	Refer to number 1, 2, 3
DOT $(\cdot)$	represents differentiations with respect to time.

D.1 Introduction

A number of investigations have been directed towards determining the thermoelastic behavior of shell structures. In recent years several investigators[1,2,3,4,5,8,9] have used variational methods to treat problems of thermoelasticity and certain linear thermoviscoelastic problems.

This report extends some of these results toward determining the viscoelastic behavior of shells of revolution under uniform pressure and thermal gradients. Although certain restrictions are made concerning the coupling of heat conduction and the viscoelastic phenomena, the analysis has general applicability.

The use of generalized coordinates and variational calculus leads to concepts of generalized forces of the Lagrangian type which are applicable to mechanical (static and dynamic) and thermal (with material property variations) problems.

First, the general three-dimensional thermoviscoelasticity formulation of the variational equation is presented in curvilinear coordinates. The energy and work integrals, including the material properties, are expanded into powers of the normal coordinate. This permits the introduction of thermal effects on the material properties.

The general equations are specialized to thin shells. For the thin shell analysis, the shell thickness is allowed to approach zero and only terms of shell thickness of unit power are retained. An example of a hemispherical shell is given to illustrate the procedure of analysis.

D.2 Mathematical Formulation

D.2.1 Variational Equation

The transient response of a shell to mechanical and thermal loadings can be investigated by standard energy methods without the complications connected with the analytical solution of the partial differential equations of equilibrium.

If the shell is subjected to simultaneous mechanical and thermal loading, according to Hamilton's principle the energy formulation is given by the variational equation

$$\delta \int_{t_0}^{t_1} (K + F - W)\, dt \qquad \text{(D.2.1-1)}$$

where

δ is the first variation and integration with respect to time performed between the limits t_o and t_1

K is kinetic energy

F is free energy (potential energy in isothermal analysis)

W is work integral

The function (K + F - W) is identical to the Lagrangian function. In the following paragraphs, the proper form of equation D.2.1-1 is developed for application to the viscoelastic analysis of shell structures.

D.2.1.1 Energy and Work Integrals

The coupling between thermoelasticity and dynamics is expressed by the inclusion of the acceleration term in equilibrium equation, thus forming the usual equations of motion

$$\sigma_{ij,j} = \rho \ddot{u}_i \qquad \text{(D.2.1-2)}$$

where σ_{ij} and u_i are the unknown field variables. This leads to the Lagrangian formulation, expressed in terms of kinetic energy

$$K = \frac{1}{2}\int_V \rho (\dot{u}_i)^2 dV \qquad \text{(D.2.1-3)}$$

where ρ is the density of the material and ρdV represents the mass of the element which independent of time t, u_i is the covarient displacement vector, and σ_{ij} is the stress tensor, the dot represents differentiation with respect to time t. It is assumed that the variation of the density with time is negligible.

The Helmholtz free energy expression to be used as the potential energy form in the variational formulation is

$$F = \int_V f dV \qquad \text{(D.2.1-4)}$$

where f is the energy density per unit volume. Equation D.2.1-4 can be expressed in terms of the stress and strain tensors as follows

$$F = \frac{1}{2}\int_V \sigma_{ij} \epsilon_{ij} dV \qquad \text{(D.2.1-5)}$$

Now let us introduce the stress-strain relations. The material is assumed to that of a Kelvin body with temperature dependent properties, in which case the following function for the stress tensor is chosen.

$$S_{ij} = 2Ge_{ij} + 2\eta\dot{e}_{ij}{}^{*} \quad \Big\} \qquad \sigma_{ii} = 3K\epsilon_{ii} + 3\rho\dot{\epsilon}_{jj} \tag{D.2.1-6}$$

where α is linear thermal expansion coefficient, η is coefficient of viscosity, G is shear modulus, K is bulk modulus. The strain-displacement relations are

$$\epsilon_{ij} = \frac{1}{2}\left(u_{i;j} + u_{j;i}\right) \quad \text{AND} \quad \epsilon_{ii} = u_{i;i}$$

Substitution of the stress-strain and strain displacement relations into the free energy expression yields

$$F = \int_V \left[G\left\{u_{i;j}u_{i;j} - 3\alpha^2 T^2\left(1 - \frac{2(1+\nu)}{1-2\nu}\right)\right\} + \eta\left\{u_{i;j}u_{i;j} - 3\alpha^2 T\dot{T}\left(1 - \frac{3\rho}{2\eta}\right)\right\}\right] dV \tag{D.2.1-7}$$

To include the effects of static or transient external loading, it is necessary to express the work done on the mass of material by the body forces. The work integral may be written as

$$W = \int_V \rho F_i u^i dV \tag{D.2.1-8}$$

where F_i is the body force per unit mass acting on the material. Or, in terms of the displacement vector u^i and/the unit pressure intensity, we find

$$W = \int_V P_i u^i dV \tag{D.2.1-9}$$

It is assumed that the only external force acting on the shell is that of external normal pressure, P_3. Therefore the work may be written as a two-dimensional integral, where now P_3 is a function of the curvilinear coordinates y^1 and y^2.

$$W = \int_S P_3 u^3 ds \tag{D.2.1-10}$$

Combining equations (D.2.1-4), (D2.1-8) and (D2.1-10) we may now write equation (D2.1-1) as follows

$$\delta\int_{t_0}^{t_1}\left[\frac{\rho}{2}\int_V (\dot{u}_i)^2 dV - \int_V \left[G\left\{u_{i;j}u_{i;j} - 3\alpha^2 T^2\left(1 - \frac{2(1+\nu)}{1-2\nu}\right)\right\} + \eta\left\{u_{i;j}u_{i;j} - 3\alpha^2 T\dot{T}\left(1 - \frac{3\rho}{2\eta}\right)\right\}\right] dV + \right.$$

$$\left. + \int_S P_3 u^3 ds\right] dt = 0 \tag{D.2.1-11}$$

D.2.2 Geometrical Relations in Curvilinear Coordinates

General formulation of the variational equation appropriate to shell theory expressed in curvilinear y^i coordinate system requires the characterization of the middle-surface geometry. Let y^i represent an orthogonal curvilinear coordinates which are single-valued functions of the Cartesian coordinates x^i

$$y^i = y^i(x^i) \tag{D.2.2-1}$$

We may represent any point on the mean-surface by $y^1 y^2$, with y^3 as the local normal as shown in Figure D.2.1.

The volume element, dV, in the y^i coordinate system is given by

$$dV = \sqrt{|g_{ij}|}\, dy^1 dy^2 dy^3 \; ; \; g_{ij} = 0, \; i \neq j \tag{D.2.2-2}$$

and the element of area, dS on the y^i surface is

$$ds = \sqrt{|a_{\alpha\beta}|}\, dy^1 dy^2 \tag{D.2.2-3}$$

where $\sqrt{|g_{ij}|}$ is the square root of determinant of the metric tensor. In equation (2.2-2) $g_{ij} = g_{ij}(y^1, y^2, y^3)$ while in (2.2-3) $a_{\alpha\beta} = a_{\alpha\beta}(y^1, y^2)$.

For specific examples $\sqrt{|a_{\alpha\beta}|}$ has taken the following forms:

Hemispherical Shells: $\sqrt{|a_{\alpha\beta}|} = r^2 \sin y^2$ (D.2.2-4)

Conical Shells: $= y^2 \sin^2 \gamma$ (D.2.2-5)

(vertical height is unity) where γ is one-half the apex angle.

D.2.3 Deformation of a Shell and Its Middle Surface

The expressions for the components of displacement of an arbitrary point of the shell in terms of displacement of the corresponding point of the middle surface are

$$\left.\begin{aligned} u^1 &= u_0^1 + u_1^1 y^3 \\ u^2 &= u_0^2 + u_1^2 y^3 \\ u^3 &= u_0^3 \end{aligned}\right\} \tag{D.2.3-1}$$

where u_0^i and u_1^α are functions of y^1 and y^2 only. The strain displacement relations in curvilinear coordinates can be expressed as

$$\eta_{ij} = \frac{1}{2}\left(a_{ir}\xi^{r}_{,j} + a_{jr}\xi^{r}_{,i}\right) \qquad \text{(D.2.3-2)}$$

where

η_{ij} convarient components of strain tensor

$\xi^{r}_{,j}$ convarient differential coefficient of contravarient displacement vector ξ^{r} with respect to the curvilinear coordinates y^i

a_{ir} metric tensor

Making use of the assumption that the normals to middle surface before bending remain normal after bending, we get

$$\eta_{\alpha 3}\Big|_{y^3=0} = \frac{1}{2}\left(a_{\alpha\delta}\xi^{\delta}_{,3} + a_{3\delta}\xi^{3}_{,\alpha}\right)$$
$$= \frac{1}{2}\left[\xi_{\alpha,3} + \xi_{3,\alpha}\right]\Big|_{y^3=0} = 0 \qquad \text{(D.2.3-3)}$$

After performing covarient differentiation, simplification, and substituting the following expression

$$u_\alpha = u^\alpha = \xi_\alpha\sqrt{a^{\alpha\alpha}} = \frac{\xi_\alpha}{\sqrt{a_{\alpha\alpha}}}$$

or $$\xi_\alpha = u^\alpha\sqrt{a_{\alpha\alpha}} \qquad \text{(D.2.3-4)}$$

we obtain

$$u^\alpha_{1} = -\left(\sqrt{E^{\alpha\alpha}}\,\frac{\partial u^3_0}{\partial y^\alpha} + L^\alpha_\alpha u^\alpha_0\right) \qquad \text{(D.2.3-5)}$$

where $$a_{\alpha\alpha}\Big|_{y^3=0} = E_{\alpha\alpha}\,, \quad E^{\alpha\alpha} = \frac{1}{E^{\alpha\alpha}}$$

$$\frac{\partial a_{\alpha\alpha}}{\partial y^3}\Big|_{y^3=0} = -2L_{\alpha\alpha} \qquad \text{(D.2.3-6)}$$

no summation on α .

and

$$L^\alpha_\alpha = E^{\alpha\alpha}L_{\alpha\alpha}$$

D.3 Variational Equation in Terms of the Displacement of the Middle Surface of the Shell.

D.3.1 Expression of General Displacements in Terms of the Displacements of the Middle Surface

Consider now the general displacements. Employing the results of paragraph D.2.3, we can write that

$$\dot{u}^i\dot{u}^i = (\dot{u}^1)^2 + (\dot{u}^2)^2 + (\dot{u}^3)^2$$

$$\begin{aligned}
&= (\dot{u}_0^1)^2 + (\dot{u}_0^2)^2 + (\dot{u}_0^3)^2 - 2y^3\Big[2\dot{u}_0^1\Big\{\sqrt{E^{11}}\frac{\partial \dot{u}_0^3}{\partial y^1} + L_1^1\dot{u}_0^1\Big\} + \\
&\quad + 2\dot{u}_0^2\Big\{\sqrt{E^{22}}\frac{\partial \dot{u}_0^3}{\partial y^2} + L_2^2\dot{u}_0^2\Big\}\Big] + \\
&\quad + (y^3)^2\Big\{E^{11}\Big(\frac{\partial \dot{u}_0^3}{\partial y^1}\Big)^2 + 2\sqrt{E^{11}}\frac{\partial u_0^3}{\partial y^1}L_1^1\dot{u}_0^1 + \big(L_1^1\dot{u}_0^1\big)^2\Big\} + \\
&\quad + (y^3)^2\Big\{E^{22}\Big(\frac{\partial \dot{u}_0^3}{\partial y^2}\Big)^2 + 2\sqrt{E^{22}}\frac{\partial u_0^3}{\partial y^2}L_2^2\dot{u}_0^2 + \big(L_2^2\dot{u}_0^2\big)^2\Big\}
\end{aligned} \qquad \text{(D.3.1-1)}$$

$$u_{i;j}u_{i;j} = (u_{1,1})^2 + (u_{1,2})^2 + (u_{1,3})^2 + (u_{2,1})^2 + (u_{2,2})^2 + (u_{2,3})^2 + (u_{3,1})^2 + (u_{3,2})^2 + (u_{3,3})^2 \qquad \text{(D.3.1-2)}$$

From equation (D.2.3-5) we have

$$u_\alpha = u_0^\alpha - y^3\Big(\sqrt{E^{\alpha\alpha}}\frac{\partial u_0^3}{\partial y^\alpha} + L_\alpha^\alpha u_0^\alpha\Big)$$

$$u_3 = u_0^3$$

Differentiating and substituting above result we can express equation (D3.1-2) as follows:

$$\begin{aligned}
u_{i;j}u_{i;j} &= \Big(\frac{\partial u_0^1}{\partial y^1} - y^3 A\Big)^2 + \Big(\frac{\partial u_0^1}{\partial y^2} - y^3 B\Big)^2 + (C)^2 + \Big(\frac{\partial u_0^2}{\partial y^1} - y^3 D\Big)^2 + \\
&\quad + \Big(\frac{\partial u_0^2}{\partial y^2} - y^3 F\Big)^2 + (H)^2 + \Big(\frac{\partial u_0^3}{\partial y^1}\Big)^2 + \Big(\frac{\partial u_0^3}{\partial y^2}\Big)^2
\end{aligned} \qquad \text{(D.3.1-3)}$$

where

$$
\left.\begin{aligned}
A &= \frac{\partial}{\partial y^1}\left(\sqrt{E^{11}}\,\frac{\partial u_0^3}{\partial y^1} + L_1^1 u_0^1\right)\\
B &= \frac{\partial}{\partial y^2}\left(\sqrt{E^{11}}\,\frac{\partial u_0^3}{\partial y^1} + L_1^1 u_0^1\right)\\
C &= \sqrt{E^{11}}\,\frac{\partial u_0^3}{\partial y^1} + L_1^1 u_0^1
\end{aligned}\right| \qquad \text{(D.3.1-4)}
$$

$$
\left.\begin{aligned}
D &= \frac{\partial}{\partial y^1}\left(\sqrt{E^{22}}\,\frac{\partial u_0^3}{\partial y^2} + L_2^2 u_0^2\right)\\
F &= \frac{\partial}{\partial y^2}\left(\sqrt{E^{22}}\,\frac{\partial u_0^3}{\partial y^2} + L_2^2 u_0^2\right)\\
H &= \sqrt{E^{22}}\,\frac{\partial u_0^3}{\partial y^2} + L_2^2 u_0^2
\end{aligned}\right| \qquad \text{(D.3.1-5)}
$$

D.3.2 Variational Equation for a General Shell of Revolution

By making use of equations (D.2.1-11), (D.2.2-2), (D.3.1-1) and (D.3.1-3), we can write the variational equation for a general shell of revolution (shell of general geometry) in the following form:

$$
\begin{aligned}
&\int_{t_0}^{t_1}\Bigg[\iiint_V \frac{\rho}{2}\sqrt{|g_{ij}|}\left\{(\dot u_0^1)^2+(\dot u_0^2)^2+(\dot u_0^3)^2+(y^3)^2\left[(C)^2+(H)^2\right]-2y^3\left[C u_0^1+H u_0^2\right]\right\}dy^1dy^2dy^3+\\
&+\iiint_V G\sqrt{|g_{ij}|}\left\{\left(\frac{\partial u_0^1}{\partial y^1}-y^3A\right)^2+\left(\frac{\partial u_0^1}{y^2}-y^3B\right)^2+C^2+\left(\frac{\partial u_0^2}{\partial y^1}-y^3D\right)^2+\left(\frac{\partial u_0^2}{\partial y^2}-y^3F\right)^2+H^2+\left(\frac{\partial u_0^3}{\partial y^1}\right)^2+\left(\frac{\partial u_0^3}{\partial y^2}\right)^2\right\}dy^1dy^2dy^3-\\
&-\iiint_V G\sqrt{|g_{ij}|}\,3\alpha^2T^2\left\{1-\frac{2(1+\nu)}{1-2\nu}\right\}dy^1dy^2dy^3+\iiint_V \eta\sqrt{|g_{ij}|}\left\{\left(\frac{\partial u_0^1}{\partial y^1}-y^3A\right)\left(\frac{\partial \dot u_0^1}{\partial y^1}-y^3\dot A\right)+\right.\\
&\quad+\left(\frac{\partial u_0^1}{\partial y^2}-y^3B\right)\left(\frac{\partial \dot u_0^1}{\partial y^2}-y^3\dot B\right)+C\dot C+\left(\frac{\partial u_0^2}{\partial y^1}-y^3D\right)\left(\frac{\partial \dot u_0^2}{\partial y^1}-y^3\dot D\right)+\left(\frac{\partial \dot u_0^2}{\partial y^2}-y^3F\right)\left(\frac{\partial \dot u_0^2}{\partial y^2}-y^3\dot F\right)+H\dot H+\\
&\left.+\frac{\partial u_0^3}{\partial y^1}\frac{\partial \dot u_0^3}{\partial y^1}+\frac{\partial u_0^3}{\partial y^2}\frac{\partial u_0^3}{\partial y^2}\right\}dy^1dy^2dy^3-\iiint_V \eta\sqrt{|g_{ij}|}\,3\alpha T\dot T\left(1-\frac{3\rho}{2\eta}\right)dy^1dy^2dy^3-\iint_S P u_3\sqrt{|g_{ij}|}\,dy^1dy^2\Bigg]dt=0
\end{aligned}
$$

(D.3.2-1)

D.3.3 Variational Equation for a Hemispherical Shell

Now we expand equation (D.3.2-1) for application to hemispherical shells in terms of middle surface deformations.

From Equations (D.2.3-1) and (D.2.3-5) we have that

$$
\left.
\begin{aligned}
&u^{\alpha} = u_0^{\alpha} - y^3\left(\sqrt{E^{\alpha\alpha}}\,\frac{\partial u_0^3}{\partial y^{\alpha}} + E^{\alpha\alpha} L_{\alpha\alpha}\, u_0^{\alpha}\right) \\
&u^3 = u_0^3 \\
&E_{\alpha\alpha} = a_{\alpha\alpha}\Big|_{y^3=0} \quad , \quad -2L_{\alpha\alpha} = \frac{\partial a_{\alpha\alpha}}{\partial y^3}\Big|_{y^3=0}
\end{aligned}
\right| \qquad \text{(D.3.3-1)}
$$

$$
\left.
\begin{aligned}
&E_{11} = a_{11}\Big|_{y^3=0} = r^2 \sin^2\phi \quad , \quad E^{11} = \frac{1}{E_{11}} = \frac{1}{r^2\sin^2\phi} \quad , \quad L_{11} = -r\sin^2\phi \\
&E_{22} = a_{22}\Big|_{y^3=0} = r^2 \quad , \quad E^{22} = \frac{1}{E_{22}} = \frac{1}{r^2} \quad , \quad L_{22} = -r
\end{aligned}
\right| \qquad \text{(D.3.3-2)}
$$

From the above two sets of equations we can write that

$$u^1 = u_0^1 + \frac{y^3}{r}\left(u_0^1 - \frac{1}{\sin\phi}\frac{\partial u_0^3}{\partial\theta}\right) \qquad \text{(D.3.3-3)}$$

$$u^2 = u_0^2 + \frac{y^3}{r}\left(u_0^2 - \frac{\partial u_0^3}{\partial\phi}\right) \qquad \text{(D.3.3-4)}$$

The functions A, B, C, D, F and H take the following forms:

$$C = \frac{1}{r}\left(u_0' - \frac{1}{\sin\phi}\frac{\partial u_0^3}{\partial\theta}\right)$$

$$H = \frac{1}{r}\left(u_0' - \frac{\partial u_0^3}{\partial\phi}\right)$$

$$A = \frac{\partial C}{\partial\theta} = \frac{1}{r}\left(\frac{\partial u_0'}{\partial\theta} - \frac{1}{\sin\phi}\frac{\partial^2 u_0^3}{\partial\theta^2}\right)$$

$$B = \frac{\partial C}{\partial\phi} = \frac{1}{r}\left(\frac{\partial u_0'}{\partial\phi} - \frac{1}{\sin\phi}\frac{\partial^2 u_0^3}{\partial\phi\,\partial\theta} + \frac{\partial u_0^3}{\partial\theta}\cot\phi\,\mathrm{cosec}\,\theta\right)$$

$$D = \frac{\partial H}{\partial\theta} = \frac{1}{r}\left(\frac{\partial u_0'}{\partial\theta} - \frac{\partial^2 u_0^3}{\partial\phi\,\partial\theta}\right)$$

$$F = \frac{\partial H}{\partial\phi} = \frac{1}{r}\left(\frac{\partial u_0'}{\partial\phi} - \frac{\partial^2 u_0^3}{\partial\phi^2}\right)$$

Also for a hemispherical shell

$$\sqrt{|a_{\alpha\beta}|} = \sqrt{\begin{vmatrix} r^2 \sin^2\phi & 0 \\ 0 & r^2 \end{vmatrix}} = \sqrt{r^4 \sin^2\phi} = r^2 \sin\phi$$

After putting these values in (D.3.2-1), simplifying the expression and integrating with respect to y^3 through the thickness of the shell, we get the following variational equation for a hemispherical shell.

Variational equations for the hemispherical shell

$$\delta \int_{t_0}^{t_1} \Bigg[\iint_S \frac{\rho}{2} \sin^2\phi \Bigg\{ h\left[(\dot{u}_0^1)^2 + (\dot{u}_0^2)^2 + (\dot{u}_0^3)^2 \right] + \frac{h^3}{12 r^2} \left[\left(\dot{u}_0^1 - \frac{1}{\sin\phi} \frac{\partial \dot{u}_0^3}{\partial \theta} \right)^2 + \left(\dot{u}_0^2 - \frac{\partial \dot{u}_0^3}{\partial \phi} \right)^2 \right] \Bigg\} d\phi\, d\theta +$$

$$+ \iint_S G r^2 \sin\phi \Bigg\{ h\left[\left(\frac{\partial u_0^1}{\partial \theta}\right)^2 + \left(\frac{\partial u_0^1}{\partial \phi}\right)^2 + \left(\frac{\partial u_0^2}{\partial \theta}\right)^2 + \left(\frac{\partial u_0^2}{\partial \phi}\right)^2 + \left(\frac{\partial u_0^3}{\partial \theta}\right)^2 + \left(\frac{\partial u_0^3}{\partial \phi}\right)^2 \right] + \frac{h}{r^2} \left[\left(u_0^1 - \frac{1}{\sin\phi} \frac{\partial u_0^3}{\partial \theta} \right)^2 + \left(u_0^2 - \frac{\partial u_0^3}{\partial \phi} \right)^2 \right] +$$

$$+ \frac{h^3}{12 r^2} \left[\left(\frac{\partial u_0^1}{\partial \theta} - \frac{1}{\sin\theta} \frac{\partial^2 u_0^1}{\partial \theta^2} \right)^2 + \left(\frac{\partial u_0^1}{\partial \phi} - \frac{1}{\sin\phi} \frac{\partial^2 u_0^1}{\partial \theta \partial \phi} + \frac{\partial u_0^1}{\partial \theta} \cot\phi \operatorname{cosec}\phi \right)^2 + \left(\frac{\partial u_0^2}{\partial \theta} - \frac{\partial^2 u_0^3}{\partial \phi \partial \theta} \right)^2 + \left(\frac{\partial u_0^2}{\partial \phi} - \frac{\partial^2 u_0^3}{\partial \phi^2} \right)^2 \right] \Bigg\} d\phi\, d\theta +$$

$$+ \iint_S \eta r^2 \sin\phi \Bigg\{ h\left[\left(\frac{\partial u_0^1}{\partial \theta} \frac{\partial \dot{u}_0^1}{\partial \theta} + \frac{\partial u_0^1}{\partial \phi} \frac{\partial \dot{u}_0^1}{\partial \phi} + \frac{\partial u_0^2}{\partial \theta} \frac{\partial \dot{u}_0^2}{\partial \theta} + \frac{\partial u_0^2}{\partial \phi} \frac{\partial \dot{u}_0^2}{\partial \phi} + \frac{\partial u_0^3}{\partial \theta} \frac{\partial \dot{u}_0^3}{\partial \theta} + \frac{\partial u_0^3}{\partial \phi} \frac{\partial \dot{u}_0^3}{\partial \phi} \right] +$$

$$+ \frac{h}{r^2} \left[\left(u_0^1 - \frac{1}{\sin\phi} \frac{\partial u_0^3}{\partial \theta} \right) \left(\dot{u}_0^1 - \frac{1}{\sin\phi} \frac{\partial \dot{u}_0^3}{\partial \theta} \right) + \left(u_0^2 - \frac{\partial u_0^3}{\partial \phi} \right) \left(\dot{u}_0^2 - \frac{\partial \dot{u}_0^3}{\partial \phi} \right) \right] + \frac{h^3}{12 r^2} \left[\left(\frac{\partial u_0^1}{\partial \theta} - \frac{1}{\sin\phi} \frac{\partial^2 u_0^3}{\partial \theta^2} \right) \left(\frac{\partial \dot{u}_0^1}{\partial \theta} - \right. \right.$$

$$\left. - \frac{1}{\sin\phi} \frac{\partial^2 \dot{u}_0^3}{\partial \theta^2} \right) + \left(\frac{\partial u_0^1}{\partial \phi} - \frac{1}{\sin\phi} \frac{\partial^2 u_0^3}{\partial \theta \partial \phi} + \frac{\partial u_0^3}{\partial \theta} \cot\phi \operatorname{cosec}\phi \right) \left(\frac{\partial \dot{u}_0^1}{\partial \theta} - \frac{1}{\sin\phi} \frac{\partial^2 \dot{u}_0^3}{\partial \theta \partial \phi} + \frac{\partial \dot{u}_0^3}{\partial \theta} \cot\phi \operatorname{cosec}\phi \right) +$$

$$+ \left. \left(\frac{\partial u_0^2}{\partial \theta} - \frac{\partial^2 u_0^3}{\partial \theta \partial \phi} \right) \left(\frac{\partial \dot{u}_0^2}{\partial \theta} - \frac{\partial^2 \dot{u}_0^3}{\partial \theta \partial \phi} \right) + \left(\frac{\partial u_0^2}{\partial \phi} - \frac{\partial^2 u_0^3}{\partial \phi^2} \right) \left(\frac{\partial \dot{u}_0^2}{\partial \phi} - \frac{\partial^2 \dot{u}_0^3}{\partial \phi^2} \right) \right] \Bigg\} d\phi\, d\theta + \iint_S N_1 \left(G \alpha^2 T_s^2 \right) r^2 \sin\phi\, d\phi\, d\theta +$$

$$+ \iint_S N_2 \left(\eta \alpha^2 T_s \dot{T}_s \right) r^2 \sin\phi\, d\phi\, d\theta + \iint_S p u_0^3 r^2 \sin\phi\, d\phi\, d\theta \Bigg] dt = 0$$

WHERE $\quad N_1 = \frac{3}{4} h \left(1 + \frac{h}{3}\right) \left[1 - \frac{2(1+\nu)}{1-2\nu} \right] , \quad N_2 = \frac{3}{4} h \left(1 + \frac{h}{3}\right) \left[1 - \frac{3\rho}{2\eta} \right]$

$T_s = T_s(t)$ IS SURFACE TEMPERATURE

where

$$N_1 = \frac{3}{4}h\left(1+\frac{h}{3}\right)\left[1-\frac{2(1+\nu)}{1-2\nu}\right]$$

$$N_2 = \frac{3}{4}h\left(1+\frac{h}{3}\right)\left[1-\frac{3\rho}{2\eta}\right]$$

$T_s = T_s(t)$ is surface temperature

D.4 Integration of the Variational Equation for Thin Hemispherical Shell

D.4.1 Boundary Conditions

Consider a hemispherical shell which is clamped at the edge, $\phi = \frac{\pi}{2}$ (See Fig. D.4.1). At $\phi = \pi/2$ [10] and $0 \leqslant \theta \leqslant 2\pi$, the deformations u, v, w and the rotation ψ become

$$u = v = w = 0$$

$$\psi = -\frac{1}{A_2}\frac{\partial w}{\partial \alpha_2} + \frac{v}{r} = 0$$

In case of a hemispherical shell we have that

$$u = u^1 = u_0^1 + \frac{y^3}{r}\left(u_0^1 - \frac{1}{\sin\phi}\frac{\partial u_0^3}{\partial \theta}\right)$$

$$v = u^2 = u_0^2 + \frac{y^3}{r}\left(u_0^2 - \frac{\partial u_0^3}{\partial \phi}\right)$$

$$w = u^3 = u_0^3 \qquad \alpha_1 \sim \theta\,, \quad \alpha_2 \sim \phi$$

and

$$A_2^2 = r_{,\phi} \cdot r_{,\phi} = r^2 \qquad \text{or} \qquad A_2 = r$$

Considering now the boundary conditions, we can write that

$$u^1\Big|_{\phi=\frac{\pi}{2}} = 0 = u_0^1\Big|_{\phi=\frac{\pi}{2}} + \frac{y^3}{r}\left(u_0^1 - \frac{\partial u_0^3}{\partial \theta}\right)\Big|_{\phi=\frac{\pi}{2}} = \left[u_0^1 + \frac{y^3}{r} - \left(u_0^1 - \frac{\partial u_0^3}{\partial \theta}\right)\right]\Big|_{\phi=\frac{\pi}{2}} - \frac{1}{r}\frac{\partial u_0^3}{\partial \phi} +$$

$$+ \frac{1}{r}\left\{u_0^2 + \frac{y^3}{r}\left(u_0^2 - \frac{\partial u_0^3}{\partial \phi}\right)\right\}\Big|_{\phi=\frac{\pi}{2}} = 0$$

$$u^2\Big|_{\phi=\frac{\pi}{2}} = \left[u_0^2 + \frac{y^3}{r}\left(u_0^2 - \frac{\partial u_0^3}{\partial \phi}\right)\right]\Big|_{\phi=\frac{\pi}{2}}\,, \qquad u^3\Big|_{\phi=\frac{\pi}{2}} = u_0^3\Big|_{\phi=\frac{\pi}{2}}$$

which can be written as

$$u_o^1 + \frac{y^3}{r}\left(u_o^1 - \frac{\partial u_o^3}{\partial \theta}\right) = 0 \tag{D.4.1-1}$$

$$u_o^2 + \frac{y^3}{r}\left(u_o^2 - \frac{\partial u_o^3}{\partial \phi}\right) = 0 \tag{D.4.1-2}$$

$$u_o^3 = 0 \tag{D.4.1-3}$$

$$u_o^2 + \frac{y^3}{r}\left(u_o^2 - \frac{\partial u_o^3}{\partial \phi}\right) - \frac{\partial u_o^3}{\partial \phi} = 0 \tag{D.4.1-4}$$

From equations (D.4.1-2) and (D.4.1-4)

$$\frac{\partial u_o^3}{\partial \phi} = 0$$

Hence

$$u_o^1 + \frac{y^3}{r} u_o^1 = 0$$

$$\text{OR} \quad u_o^1\left(1 + \frac{y^3}{r}\right) = 0$$

Therefore $\quad u_o^1 = 0$

Similarly $\quad u_o^2 = 0$

And from equations (D.4.1-3) $\quad u_o^3 = 0$

Thus we have the following boundary conditions:

$$\left.\begin{array}{l} u_o^1 = u_o^2 = u_o^3 = 0 \\ \dfrac{\partial u_o^3}{\partial \phi} = 0 \end{array}\right\} \text{ AT } \phi = \frac{\pi}{2} \text{ AND } 0 \leq \theta \leq 2\pi$$

Also the functions u_1, u_2, u_3 must be periodic with respect to θ with a period 2π.

D.4.2 Expression of Displacements in Terms of Functions ϕ and θ

It is necessary to represent u_o^1, u_o^2, u_o^3 in terms of functions of ϕ and θ whose coefficients are unknown functions of t. These functions must satisfy the boundary conditions and should be periodic with respect to θ with a period of 2π. These conditions are fulfilled by the following functions:

$$u_0^1 = \beta_1 \cos\phi + \beta_2 \cos\phi \sin^2\theta$$

$$u_0^2 = \gamma_1 \cos\phi + \gamma_2 \cos\phi \sin^2\theta$$

$$u_0^3 = \left(\frac{\pi}{2} - \phi\right)\left(\rho_1 \cos\phi + \rho_2 \cos\phi \sin^2\theta\right)$$

These functions or their derivatives are substituted in the variational equation for a thin hemispherical shell and integration is performed with respect to ϕ and θ over the given boundaries.

D.4.3 Integration of the Variational Equation for Thin Hemispherical Shell

For the hemispherical shell the integration has been carried out over the limits of $0 \leq \phi \leq \frac{\pi}{2}$ and $0 \leq \theta \leq \frac{\pi}{2}$. But as we must take the limits for as $0 \leq \theta \leq 2\pi$ i.e. go around the circle, a factor of 4 will be common in all integrations. Since it is a common factor, it will not affect our results. Some of the integrations have been carried out numerically. A singularity occurs at the apex and in one of the integrations an approximate value has been taken numerically a surface making an angle of $\phi = 0°30'$ with the axis. Thus the results of this analysis cannot be applied to the apex and a separate analysis will be needed from this region of the shell.

After having carried out the integration over the middle surface of the shell, we reduce the variational equation to functions of time only. This equation is shown as follows: (See next page).

Variational Equation for a Thin Hemispherical Shell

$$
\begin{aligned}
\delta\int_{t_0}^{t_1}\Big[\frac{\rho r^2 h}{2}\Big\{&0.524\dot\beta_1^2+0.524\dot\beta_1\dot\beta_2+0.196\dot\beta_2^2+0.524\dot\gamma_1^2+0.524\dot\gamma_1\dot\gamma_2+0.196\dot\gamma_2^2+0.478\dot\rho_1^2+0.478\dot\rho_1\dot\rho_2+0.179\dot\rho_2^2\Big\}+\\
&+Gr^2h\Big\{0.261\beta_2+1.047\beta_1^2+1.047\beta_1\beta_2+0.393\beta_2^2+0.261\gamma_2^2+1.047\gamma_1^2+1.047\gamma_1\gamma_2+0.393\gamma_2^2+\\
&+0.239\rho_2^2+0.445\rho_1^2+0.445\rho_1\rho_2+0.167\rho_2^2\Big\}+Gh\Big\{0.524\beta_1^2+0.524\beta_1\beta_2+0.196\beta_2^2+\\
&+6.837\rho_2^2-1.734\beta_1\rho_2+0.867\beta_2\rho_2+0.524(\gamma_1^2+2\gamma_1\rho_1+\rho_1^2)+0.524(\gamma_1^2+\gamma_1\rho_1+\rho_1\rho_2+\rho_1\gamma_2)+\\
&+0.196(\gamma_2^2+2\gamma_2\rho_2+\rho_2^2)-(0.776\rho_1^2+0.776\rho_1\rho_2+0.291\rho_2^2)+0.698(\rho_1^2+\rho_1\gamma_1)+\\
&+0.349(\rho_1\gamma_2+2\rho_1\rho_2+\rho_2\gamma_1)+0.262(\rho_2^2+\rho_2\gamma_2)\Big\}+\eta r^2h\Big\{0.261\beta_1\dot\beta_2+1.047\beta_1\dot\beta_1+0.524(\beta_1\dot\beta_2+\\
&+\dot\beta_1\beta_2)+0.393\beta_2\dot\beta_2+0.261\gamma_2\dot\gamma_2+1.047\gamma_1\dot\gamma_1+0.524(\gamma_1\dot\gamma_2+\dot\gamma_1\gamma_2)+0.393\gamma_2\dot\gamma_2+0.239\rho_2\dot\rho_2+\\
&+0.445\rho_1\dot\rho_1+0.263(\rho_1\dot\rho_2+\dot\rho_1\rho_2)+0.167\rho_2\dot\rho_2\Big\}+\eta h\Big\{0.524\beta_1\dot\beta_1+0.262(\beta_1\dot\beta_2+\dot\beta_1\beta_2)+\\
&+0.196\beta_2\dot\beta_2+6.837\rho_2\dot\rho_2-0.867(\beta_1\dot\rho_2+\dot\beta_1\rho_2)+0.434(\beta_2\dot\rho_2+\dot\beta_2\rho_2)+0.524(\gamma_1\dot\gamma_1+\gamma_1\dot\rho_1+\dot\gamma_1\rho_1+\rho_1\dot\rho_1)+\\
&+0.262(\gamma_1\dot\gamma_2+\gamma_2\dot\gamma_1)+0.262(\gamma_1\dot\rho_2+\dot\gamma_1\rho_2)+0.262(\rho_1\dot\rho_2+\dot\rho_1\rho_2)+0.262(\rho_1\dot\gamma_2+\dot\rho_1\gamma_2)+0.196(\gamma_2\dot\gamma_2+\\
&+\gamma_2\dot\rho_2)+0.196(\dot\gamma_2\rho_2+\rho_2\dot\rho_2)-0.776\rho_1\dot\rho_1-0.388(\rho_1\dot\rho_2+\dot\rho_1\rho_2)-0.291\rho_2\dot\rho_2+0.698\rho_1\dot\rho_1+\\
&+0.349(\rho_1\dot\gamma_1+\gamma_1\dot\rho_1)+0.176(\rho_1\dot\gamma_2+\dot\rho_1\gamma_2)+0.349(\rho_1\dot\rho_2+\dot\rho_1\rho_2)+0.175(\rho_2\dot\gamma_1+\dot\rho_2\gamma_1)+\\
&+0.262\rho_2\dot\rho_2+0.131(\rho_2\dot\gamma_2+\dot\rho_2\gamma_2)\Big\}+\\
&+1.571r^2N_1G\alpha^2T_s^2+1.571r^2N_2\eta\alpha^2T_s\dot T_s+Pr(1.854\rho_1+0.926\rho_2)\Big]dt=0
\end{aligned}
$$

(D.4.3-1)

where $N_1=\frac{3}{4}h\left(1+\frac{h}{3}\right)\left[1-\frac{2(1+\nu)}{1-2\nu}\right]$, $N_2=\frac{3}{4}h\left(1+\frac{h}{3}\right)\left[1-\frac{3\rho}{2\eta}\right]$

T_s is surface temperature and function of t only.

D.5. Development of Differential Equations for Thin Hemispherical Shell

D.5.1 Functional of the Variational Equation

The variational equation can be represented in the following form:

$$\delta\int_{t_0}^{t_1} F\left(\beta_1, \beta_2, \gamma_1, \cdots, \dot\beta_1, \dot\beta_2, \dot\gamma_1, \cdots, t\right) dt = 0 \qquad \text{(D.5.1-1)}$$

The integrand F is known as functional. It consists of independent variable t and other known and unknown functions of t e.g. $\beta_1, \beta_2, \dot\beta_1, \eta, T$ etc. Expression for the functional F is shown as follows:

Functional F of the Variational Equation is

$$
\begin{aligned}
F = \frac{\rho r^2 h}{2}\Big\{ & 0.524\dot\beta_1^2 + 0.524\dot\beta_1\dot\beta_2 + 0.196\dot\beta_2^2 + 0.524\dot\gamma_1^2 + 0.524\dot\gamma_1\dot\gamma_2 + 0.196\dot\gamma_2^2 + 0.478\dot\rho_1^2 + 0.478\dot\rho_1\dot\rho_2 + 0.179\dot\rho_2^2\Big\} + \\
& + G r^2 h\Big\{0.261\beta_2^2 + 1.047\beta_1^2 + 1.047\beta_1\beta_2 + 0.393\beta_2^2 + 0.261\gamma_2^2 + 1.047\gamma_1^2 + 1.047\gamma_1\gamma_2 + 0.393\gamma_2^2 + 0.239\rho_2^2 + 0.445\rho_1^2 + \\
& + 0.445\rho_1\rho_2 + 0.167\rho_2^2\Big\} + G h\Big\{0.524\beta_1^2 + 0.524\beta_1\beta_2 + 0.196\beta_2^2 + 6.837\rho_2^2 - 1.734\beta_1\rho_2 + 0.867\beta_2\rho_2 + 0.524\gamma_1^2 + \\
& + 1.048\gamma_1\rho_1 + 0.524\rho_1^2 + 0.524(\gamma_1\gamma_2 + \gamma_1\rho_2) + 0.524(\rho_1\rho_2 + \rho_1\gamma_2) + 0.196(\gamma_2^2 + 2\gamma_2\rho_1) + 0.196\rho_2^2 - 0.776\rho_1^2 - \\
& - 0.776\rho_1\rho_2 - 0.291\rho_2^2 + 0.698(\rho_1^2 + \rho_1\gamma_1) + 0.349(\rho_1\gamma_2 + 2\rho_1\rho_2 + \rho_2\gamma_1) + 0.262(\rho_2^2 + \rho_2\gamma_2)\Big\} + \\
& + \eta r^2 h\Big\{0.261\beta_2\dot\beta_2 + 1.047\beta_1\dot\beta_1 + 0.524(\beta_1\dot\beta_2 + \dot\beta_1\beta_2) + 0.393\beta_2\dot\beta_2 + 0.261\gamma_2\dot\gamma_2 + 1.047\gamma_1\dot\gamma_1 + 0.524(\gamma_1\dot\gamma_2 + \dot\gamma_1\gamma_2) + \\
& + 0.393\gamma_2\dot\gamma_2 + 0.239\rho_2\dot\rho_2 + 0.445\rho_1\dot\rho_1 + 0.223(\rho_1\dot\rho_2 + \rho_2\dot\rho_1) + 0.167\rho_2\dot\rho_2 + \eta h\Big\{0.524\beta_1\dot\beta_1 + 0.262(\dot\beta_1\beta_2 + \beta_1\dot\beta_2) + \\
& + 0.196\beta_2\dot\beta_2 + 6.837\rho_2\dot\rho_2 - 0.867(\beta_1\dot\rho_2 + \beta_1'\rho_2) + 0.434(\beta_2\dot\rho_2 + \dot\beta_2\rho_2) + 0.524\gamma_1\dot\gamma_1 + 0.524(\gamma_1\dot\rho_1 + \dot\gamma_1\rho_1) + \\
& + 0.524\rho_1\dot\rho_1 + 0.262(\gamma_1\dot\gamma_2 + \dot\gamma_1\gamma_2 + \gamma_1\dot\rho_2 + \dot\gamma_1\rho_2) + 0.262(\rho_1\dot\rho_2 + \dot\rho_1\rho_2 + \rho_1\dot\gamma_2 + \dot\rho_1\gamma_2) + 0.196(\gamma_2\dot\gamma_2 + \gamma_2\dot\rho_2 + \dot\gamma_2\rho_2) + \\
& + 0.196\rho_2\dot\rho_2 - 0.776\rho_1\dot\rho_1 - 0.388(\rho_1\dot\rho_2 + \dot\rho_1\rho_2) - 0.291\rho_2\dot\rho_2 + 0.698(\rho_1\dot\rho_1) + 0.349(\rho_1\dot\gamma_1 + \gamma_1\dot\rho_1) + \\
& + 0.349(\rho_1\dot\rho_2 + \rho_2\dot\rho_1) + 0.175(\rho_1\dot\gamma_2 + \dot\rho_1\gamma_2) + 0.175(\gamma_1\dot\rho_2 + \dot\gamma_1\rho_2) + 0.262\rho_2\dot\rho_2 + 0.131(\rho_2\dot\gamma_2 + \dot\rho_2\gamma_2)\Big\} + \\
& + 1.571 N_1 r^2 G \alpha^2 T_s^2 + 1.571 N_2 r^2 T_s \dot T_s + P_r(1.854\rho_1 + 0.926\rho_2)
\end{aligned}
$$

where $\beta_1, \beta_2, \gamma_1, \gamma_2, \rho_1, \rho_2, G, \eta, T_s$ are functions of time

D.5.2 Euler Lagrange Equations for the Thin Hemispherical Shell

We assume that value of functional F vanishes at both the time $t = t_0$ and $t = t_1$. It is on this assumption that we can make use of Euler-Lagrange equations for expression of the results in form of differential equations. The Euler-Lagrange equations for the functional F with unknowns $\beta_1, \beta_2, \gamma_1, \gamma_2, \rho_1, \rho_2$ and their time derivatives can be expressed in the following form.

$$\frac{d}{dt}\left(\frac{\partial F}{\partial \dot{\beta}_1}\right) - \frac{\partial F}{\partial \beta_1} = 0 \qquad \text{(D.5.2-1)}$$

$$\frac{d}{dt}\left(\frac{\partial F}{\partial \dot{\beta}_2}\right) - \frac{\partial F}{\partial \beta_2} = 0 \qquad \text{(D.5.2-2)}$$

$$\frac{d}{dt}\left(\frac{\partial F}{\partial \dot{\gamma}_1}\right) - \frac{\partial F}{\partial \gamma_1} = 0 \qquad \text{(D.5.2-3)}$$

$$\frac{d}{dt}\left(\frac{\partial F}{\partial \dot{\gamma}_2}\right) - \frac{\partial F}{\partial \gamma_2} = 0 \qquad \text{(D.5.2-4)}$$

$$\frac{d}{dt}\left(\frac{\partial F}{\partial \dot{\rho}_1}\right) - \frac{\partial F}{\partial \rho_1} = 0 \qquad \text{(D.5.2-5)}$$

$$\frac{d}{dt}\left(\frac{\partial F}{\partial \dot{\rho}_2}\right) - \frac{\partial F}{\partial \rho_2} = 0 \qquad \text{(D.5.2-6)}$$

The Euler-Lagrange Equations are

$$\begin{aligned}\rho n^2\ddot{\beta}_1 + 0.5\rho n^2\ddot{\beta}_2 - (4n^2+2)G\beta_1 - (2n^2+1)G\beta_2 + 3.31G\rho_2 + (2n^2+1)\dot{\eta}\beta_1 + \\ + (n^2+0.5)\dot{\eta}\beta_2 - 1.655\dot{\eta}\rho_2 = 0\end{aligned} \qquad \text{(D.5.2-7)}$$

$$\begin{aligned}\rho n^2\ddot{\beta}_1 + 0.75\rho n^2\ddot{\beta}_2 - (4n^2+2)G\beta_1 - (5n^2+1.5)G\beta_2 - 3.31G\rho_2 + (2n^2+1)\dot{\eta}\beta_1 + \\ + (2.5n^2+0.75)\dot{\eta}\beta_2 + 1.655\dot{\eta}\rho_2 = 0\end{aligned} \qquad \text{(D.5.2-8)}$$

$$\begin{aligned}\rho n^2\ddot{\gamma}_1 + 0.50\rho n^2\ddot{\gamma}_2 - (4n^2+2)G\gamma_1 - (2n^2+1)G\gamma_2 - 3.34G\rho_1 - 1.666G\rho_2 + (2n^2+1)\dot{\eta}\gamma_1 + \\ + (n^2+0.5)\dot{\eta}\gamma_2 + 1.67\dot{\eta}\rho_1 + 0.834\dot{\eta}\rho_2 = 0\end{aligned} \qquad \text{(D.5.2-9)}$$

$$\begin{aligned}\rho n^2\ddot{\gamma}_1 + 0.75\rho n^2\ddot{\gamma}_2 - (4n^2+2)G\gamma_1 - (5n^2+1.5)G\gamma_2 - 2.0G\rho_1 - 2.5G\rho_2 + (2n^2+1)\dot{\eta}\gamma_1 + \\ + (2.5n^2+0.75)\dot{\eta}\gamma_2 + 1.67\dot{\eta}\rho_1 + 1.24\dot{\eta}\rho_2 = 0\end{aligned} \qquad \text{(D.5.2-10)}$$

$$\begin{aligned}\rho n^2h\ddot{\rho}_1 + 0.5\rho n^2h\ddot{\rho}_2 - (1.86n^2+1.86)Gh\rho_1 - (0.93n^2+0.93)Gh\rho_2 - 3.68Gh\gamma_1 - 1.83Gh\gamma_2 - \\ - 3.88\rho n + (0.93n^2+0.93)\dot{\eta}h\rho_1 + (0.46n^2+0.46)\dot{\eta}h\rho_2 + \\ + 1.83\dot{\eta}h\gamma_1 + 0.92\dot{\eta}h\gamma_2 = 0\end{aligned} \qquad \text{(D.5.2-11)}$$

$$\begin{aligned}\rho n^2h\ddot{\rho}_1 + 0.75\rho nh\ddot{\rho}_2 - (1.86n^2+4.79)Gh\rho_1 - (3.40n^2+58.61)Gh\rho_2 + 7.26Gh\beta_1 - 3.63Gh\beta_2 - \\ - 3.50Gh\gamma_1 - 2.74Gh\gamma_2 + (0.93n^2+0.93)\rho_1 + (1.70n^2+29.31)\dot{\eta}h\rho_2 - \\ - 3.63\dot{\eta}h\beta_1 + 1.82\dot{\eta}h\beta_2 + 1.83\dot{\eta}h\gamma_1 + 1.37\dot{\eta}h\gamma_2 - 3.81\rho n = 0\end{aligned} \qquad \text{(D.5.2-12)}$$

D.5.3 Discussion

The general variational equation for the investigation of the visco-elastic behavior of shells of revolution subjected to uniform pressure and thermal gradients are developed. The development is based on the assumption that the material behaves as a Kelvin body with temperature dependent properties. The equation is applied to a shell of general geometry.

By making use of the geometrical relations for a hemispherical shell, the general equation is specialized for application to thin hemi-spherical shells. This is accomplished by neglecting all higher order terms. The respective geometrical relations for conical shells are presented for a similar application.

The boundary conditions applied in the investigation are based on a clamped shell. The Ritz method is applied by assuming that the dis-placement functions which satisfy the boundary conditions and their respective coefficients are dependent on time. Other boundary conditions can be incorporated by an appropriate choice of the displacement func-tions.

Integration of the variational equation (now a function of the dis-placements and their respective functions) over the limits governed by the shell geometry, results in an equation of unknown functions of t.

From the variational equation a system of Euler Lagrange equation is developed. In the specific problem we have a system of six ordinary differential equations of order two. The coefficients of the unknown functions are various functions of time. The equations are assumed to be continuous and that their values vanish at $t = t_o$.

A solution of this system of equations, which determines the un-known functions, must be made numerically by digital computer. The solution is based on the time interval $t_o \leq t \leq t_1$.

REFERENCES

1. Biot, M. A.: "Variational Principles in Irreversible Thermodynamics" with Application to Viscoelasticity". The Physical Review, Vol. 97, No. 6, pp. 1463-1469, March 15, 1955.

2. Biot, M. A.: "Thermoelasticity and Irreversible Thermodynamics". Journal of Applied Physics, Vol. 27, No. 3, pp. 240-253, 1956.

3. Biot, M. A.: "Linear Thermodynamics and the Mechanics of Solids". Cornell Aeronautical Laboratory, Inc., Report No. SA-987-S-6, June 1958.

4. Chu, Boa-Teh: "Thermodynamics of Elastic and of Some Visco-elastic Solids and Non-linear Thermoelasticity". Nour 562(20)1, July 1957.

5. Chu, Boa-Teh: "Deformation and Thermal Behavior of Linear Visco-elastic Materials, II". Division of Applied Mathematics, Brown University, Technical Report 2, Nord-17838/2, June 1958.

6. Freudenthal, A. M.: The Inelastic Behavior of Materials and Structures. John Wiley and Sons, New York, 1950.

7. Green, A. E. and Zerna, W.: Theoretical Elasticity. Oxford University Press, 1954.

8. Lane, F.: "Analysis of Radome Shell Structures under Pressure, Thermal and Vibratory or Dynamic Loading". Scientific Report No. 2, Gruen Applied Science Lab., Inc., July 1957. CONFIDENTIAL

9. Langhaar, H. L. and Boresi, A. P.: "A General Investigation of Thermal Stress in Shells". TAM Report No. 124, University of Illinois, October, 1957.

10. Novozhilov, V. V., The Theory of Thin Shells. P. Noordhoff ltd.- Gorningen-The Netherlands. 1959.

11. Scipio, L. A. and Chang, C. S.: "Recent Developments in Inelasticity". WADC TN 58-342, ASTIA Document No. AD 206261, November 1958.

12. Scipio, L. A. and Chien, S. F.: "Viscoelastic Behavior of Surfaces of Revolution under Combined Mechanical and Thermal Loads". ARL TR 60-305, November 1960.

13. Shaw, F. S.: "Linear Theories of Shells". Polytechnic Institute of Brooklyn, PIBAL Report No. 247, July 1953.

14. Sokolnikoff, I. S.: Mathematical Theory of Elasticity. McGraw-Hill Book Company, Inc., New York, 1946.

15. Sokolnikoff, I. S.: Tensor Analysis, John Wiley and Sons, Inc., New York, 1951.

16. Timoshenko, S.: Theory of Plates and Shells. McGraw-Hill Book Company, Inc., New York, 1940.

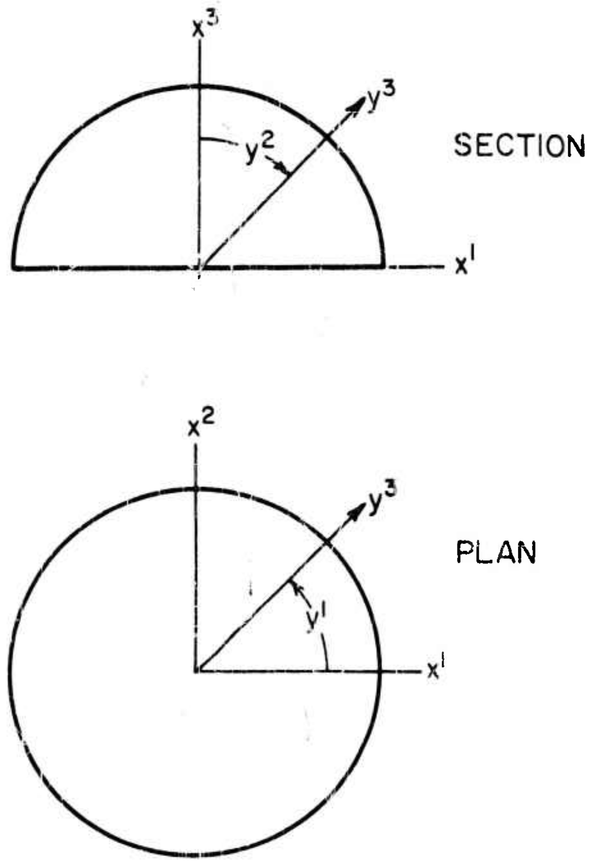

Fig. D-2.1

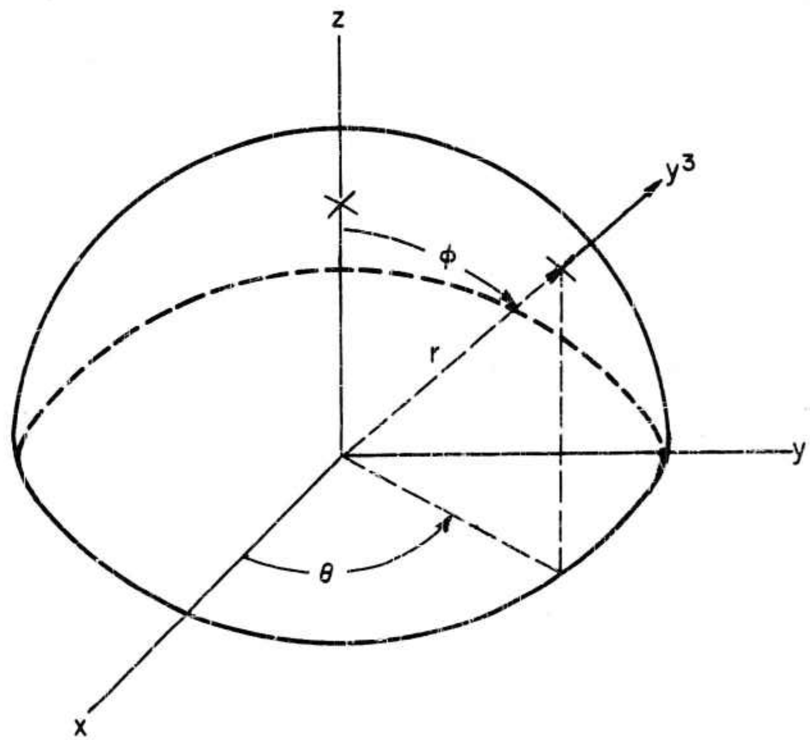

Fig. D-4.1

HEMISPHERICAL SHELL

University of Minnesota, Minneapolis, Minnesota. VISCOELASTIC BEHAVIOR OF SURFACES OF REVOLUTION UNDER COMBINED MECHANICAL AND THERMAL LOADS, by L. Albert Scipio II, Sze-Foo Chien, James A. Moses, Mansa Singh. May 1961. 168 p. incl. illus. and tables. (Project 7063; Task 70524)(ARL TR 60-305)
Unclassified Report

This paper presents the results of an analytical and experimental study of thin conical and hemispherical shells subjected to combined mechanical and thermal loads.
The analytical solutions are applicable for shells constructed from a linear viscoelastic material with temperature dependent properties.
Experimental models were subjected to

(over)

UNCLASSIFIED

UNCLASSIFIED

University of Minnesota, Minneapolis, Minnesota. VISCOELASTIC BEHAVIOR OF SURFACES OF REVOLUTION UNDER COMBINED MECHANICAL AND THERMAL LOADS, by L. Albert Scipio II, Sze-Foo Chien, James A. Moses, Mansa Singh. May 1961. 168 p. incl. illus. and tables. (Project 7063; Task 70524)(ARL TR 60-305)
Unclassified Report

This paper presents the results of an analytical and experimental study of thin conical and hemispherical shells subjected to combined mechanical and thermal loads.
The analytical solutions are applicable for shells constructed from a linear viscoelastic material with temperature dependent properties.
Experimental models were subjected to

(over)

UNCLASSIFIED

UNCLASSIFIED

various constant radiant heating rates to various steady-state temperatures. In some cases a constant normal pressure was combined with the thermal load.
Theoretical values for the meridional and circumferential stress distributions based on a viscoelastic analysis (both temperature independent and temperature dependent material properties) and the elastic analysis are compared with experimental results for typical time intervals during the transient and steady-state periods.

UNCLASSIFIED

UNCLASSIFIED

various constant radiant heating rates to various steady-state temperatures. In some cases a constant normal pressure was combined with the thermal load.
Theoretical values for the meridional and circumferential stress distributions based on a viscoelastic analysis (both temperature independent and temperature dependent material properties) and the elastic analysis are compared with experimental results for typical time intervals during the transient and steady-state periods.

UNCLASSIFIED

UNCLASSIFIED

University of Minnesota, Minneapolis, Minnesota. VISCOELASTIC BEHAVIOR OF SURFACES OF REVOLUTION UNDER COMBINED MECHANICAL AND THERMAL LOADS, by L. Albert Scipio II, Sze-Foo Chien, James A. Moses, Mansa Singh. May 1961. 168 p. incl. illus. and tables. (Project 7063; Task 70524)(ARL TR 60-305)
Unclassified Report

This paper presents the results of an analytical and experimental study of thin conical and hemispherical shells subjected to combined mechanical and thermal loads.

The analytical solutions are applicable for shells constructed from a linear viscoelastic material with temperature dependent properties.

Experimental models were subjected to

(over)

UNCLASSIFIED

UNCLASSIFIED

various constant radiant heating rates to various steady-state temperatures. In some cases a constant normal pressure was combined with the thermal load.

Theoretical values for the meridional and circumferential stress distributions based on a viscoelastic analysis (both temperature independent and temperature dependent material properties) and the elastic analysis are compared with experimental results for typical time intervals during the transient and steady-state periods.

UNCLASSIFIED

UNCLASSIFIED

University of Minnesota, Minneapolis, Minnesota. VISCOELASTIC BEHAVIOR OF SURFACES OF REVOLUTION UNDER COMBINED MECHANICAL AND THERMAL LOADS, by L. Albert Scipio II, Sze-Foo Chien, James A. Moses, Mansa Singh. May 1961. 168 p. incl. illus. and tables. (Project 7063; Task 70524)(ARL TR 60-305)
Unclassified Report

This paper presents the results of an analytical and experimental study of thin conical and hemispherical shells subjected to combined mechanical and thermal loads.

The analytical solutions are applicable for shells constructed from a linear viscoelastic material with temperature dependent properties.

Experimental models were subjected to

(over)

UNCLASSIFIED

UNCLASSIFIED

various constant radiant heating rates to various steady-state temperatures. In some cases a constant normal pressure was combined with the thermal load.

Theoretical values for the meridional and circumferential stress distributions based on a viscoelastic analysis (both temperature independent and temperature dependent material properties) and the elastic analysis are compared with experimental results for typical time intervals during the transient and steady-state periods.

UNCLASSIFIED

UNCLASSIFIED

UNCLASSIFIED

University of Minnesota, Minneapolis, Minnesota. VISCOELASTIC BEHAVIOR OF SURFACES OF REVOLUTION UNDER COMBINED MECHANICAL AND THERMAL LOADS, by L. Albert Scipio II, Sze-Foo Chien, James A. Moses, Mansa Singh. May 1961. 168 p. incl. illus. and tables. (Project 7063; Task 70524)(ARL TR 60-305)
Unclassified Report

This paper presents the results of an analytical and experimental study of thin conical and hemispherical shells subjected to combined mechanical and thermal loads.

The analytical solutions are applicable for shells constructed from a linear viscoelastic material with temperature dependent properties.

Experimental models were subjected to

(over)

UNCLASSIFIED

UNCLASSIFIED

various constant radiant heating rates to various steady-state temperatures. In some cases a constant normal pressure was combined with the thermal load.

Theoretical values for the meridional and circumferential stress distributions based on a viscoelastic analysis (both temperature independent and temperature dependent material properties) and the elastic analysis are compared with experimental results for typical time intervals during the transient and steady-state periods.

UNCLASSIFIED

UNCLASSIFIED

University of Minnesota, Minneapolis, Minnesota. VISCOELASTIC BEHAVIOR OF SURFACES OF REVOLUTION UNDER COMBINED MECHANICAL AND THERMAL LOADS, by L. Albert Scipio II, Sze-Foo Chien, James A. Moses, Mansa Singh. May 1961. 168 p. incl. illus. and tables. (Project 7063; Task 70524)(ARL TR 60-305)
Unclassified Report

This paper presents the results of an analytical and experimental study of thin conical and hemispherical shells subjected to combined mechanical and thermal loads.

The analytical solutions are applicable for shells constructed from a linear viscoelastic material with temperature dependent properties.

Experimental models were subjected to

(over)

UNCLASSIFIED

UNCLASSIFIED

various constant radiant heating rates to various steady-state temperatures. In some cases a constant normal pressure was combined with the thermal load.

Theoretical values for the meridional and circumferential stress distributions based on a viscoelastic analysis (both temperature independent and temperature dependent material properties) and the elastic analysis are compared with experimental results for typical time intervals during the transient and steady-state periods.

UNCLASSIFIED

University of Minnesota, Minneapolis, Minnesota. VISCOELASTIC BEHAVIOR OF SURFACES OF REVOLUTION UNDER COMBINED MECHANICAL AND THERMAL LOADS, by L. Albert Scipio II, Sze-Foo Chien, James A. Moses, Mansa Singh. May 1961. 168 p. incl. illus. and tables. (Project 7063; Task 70524)(ARL TR 60-305)
Unclassified Report

This paper presents the results of an analytical and experimental study of thin conical and hemispherical shells subjected to combined mechanical and thermal loads.
The analytical solutions are applicable for shells constructed from a linear viscoelastic material with temperature dependent properties.
Experimental models were subjected to

(over)

UNCLASSIFIED

UNCLASSIFIED

various constant radiant heating rates to various steady-state temperatures. In some cases a constant normal pressure was combined with the thermal load.
Theoretical values for the meridional and circumferential stress distributions based on a viscoelastic analysis (both temperature independent and temperature dependent material properties) and the elastic analysis are compared with experimental results for ... time intervals during the

UNCLASSIFIED

University of Minnesota, Minneapolis, Minnesota. VISCOELASTIC BEHAVIOR OF SURFACES OF REVOLUTION UNDER COMBINED MECHANICAL AND THERMAL LOADS, by L. Albert Scipio II, Sze-Foo Chien, James A. Moses, Mansa Singh. May 1961. 168 p. incl. illus. and tables. (Project 7063; Task 70524)(ARL TR 60-305)
Unclassified Report

This paper presents the results of an analytical and experimental study of thin conical and hemispherical shells subjected to combined mechanical and thermal loads.
The analytical solutions are applicable for shells constructed from a linear viscoelastic material with temperature dependent properties.
Experimental models were subjected to

(over)

UNCLASSIFIED

UNCLASSIFIED

UNCLASSIFIED

various constant radiant heating rates to various steady-state temperatures. In some cases a constant normal pressure was combined with the thermal load.
Theoretical values for the meridional and circumferential stress distributions based on a viscoelastic analysis (both temperature independent and temperature dependent material properties) and the elastic analysis are compared with experimental results for ... time intervals during the

UNCLASSIFIED